

University of Southampton

**SEDIMENTOLOGY AND GEOCHEMISTRY OF FINE-
GRAINED SEDIMENTS IN THE SOLENT ESTUARINE
SYSTEM**

by

A. Oya Algan (B.Sc., M.Sc.)

A thesis submitted to the University of Southampton in fulfilment of the
requirements for the degree of Doctor of Philosophy

August 1993

DEPARTMENT OF OCEANOGRAPHY

UNIVERSITY OF SOUTHAMPTON

ABSTRACT

FACULTY OF SCIENCE

OCEANOGRAPHY

Doctor of Philosophy

SEDIMENTOLOGY AND GEOCHEMISTRY OF FINE-GRAINED SEDIMENTS
IN THE SOLENT ESTUARINE SYSTEM

by A. Oya Algan

Grain size distributions, clay mineralogy and trace metal distributions associated with fine-grained sediments are used to define the prevailing sedimentological conditions and to trace sediment transport pathways in the Solent Estuarine System. Grain size distributions are determined to define the variations in energy conditions throughout the System. The clay mineralogy of the samples analyzed (by XRD) indicates the presence mainly of illite, smectite, and kaolinite, with trace amounts of chlorite. Clay mineral ratios are calculated from their peak heights. The relative abundance of the clay minerals provides evidence of two sources of supply of sediment into the area: one is high in smectite, whilst the other is high in illite. It is likely, therefore, that the distribution pattern of the clay mineral ratios is consistent with the mixing of fine-grained sediments from two sources (a smectite-rich riverine source and a smectite-poor marine source) throughout Southampton Water and the East Solent. The effect of the mixing of the different sources is detected by decreases in the S/I and S/(K+C) ratios.

Trace metal analysis are undertaken on total (bulk) samples and for the different grain size fractions. An association is identified between the concentrations of Co, Cr, Ni and Mn, and the fine-grained size fraction; they increase as the proportion of the clay-sized fraction increases. The concentrations of Cu, Pb and Zn are shown to be independent of grain size. Al is used to normalize the trace metal concentrations, in order to compensate for the natural variability of trace metals in the sediments and to undertake an intercomparison of sediments from the different localities. Normalization indicates that Cu, Pb and Zn are enriched anthropogenically in the upstream sections of the Rivers Itchen, Test and Hamble

and in the bay-head locations of the harbours. The distribution pattern of total trace metal concentrations suggests, once again, physical mixing of two sources (riverine, with higher metal contents, with the lower marine contents), decreasing from landward to seaward. Irregular variations in the normalized metal/Al ratios are attributable to changes in the mixing ratio of marine and fluvial-derived sediments.

Finally, a conceptual model is proposed for the supply and mixing of fine-grained sediments within the Solent Estuarine System.

LIST OF CONTENTS

ABSTRACT	i
LIST OF CONTENTS	iii
LIST OF FIGURES	vii
LIST OF PLATES	xiii
LIST OF TABLES	xiv
ACKNOWLEDGEMENTS	xvi
 CHAPTER 1	 1
INTRODUCTION	1
1.1. Background to the Study	1
1.2. Aims of the Study	2
1.3. Thesis Outline	3
 CHAPTER 2	 4
ENVIRONMENTAL CONSIDERATIONS	4
2.1. Grain Size Distributions	4
2.2. Clay Mineralogy	8
2.3. Trace Metal Concentrations & Phase Associations	12
2.3.1. Grain Size Effect on Trace Metal Concentrations	13
2.3.2. Trace Metal Containing Phases	14
2.3.3. Mobilization	17
2.3.4. Organic Carbon	18
2.3.5. Trace Metals in Estuaries	19
2.3.6. Distinguishing the Natural and Anthropogenic Influences	22

CHAPTER 3	25
AREA UNDER INVESTIGATION	25
3.1. Solent Estuarine System	25
3.2. Geological Setting	25
3.3. Oceanographical Setting	30
3.4. Coastal Forms of the Solent Estuarine System	35
3.5. Inlets of the Solent Estuarine System	37
3.5.1. The River Test	37
3.5.2. The River Itchen	37
3.5.3. The River Hamble	38
3.5.4. The River Beaulieu	39
3.5.5. The River Lymington	39
3.5.6. Estuaries of the Isle of Wight	39
3.5.7. Harbours	40
3.6. Seabed Configuration and Sediment Types	41
3.7. Recent Sedimentation and Sediment Transport	44
3.8. Reclamation and Dredging	47
3.9. Effluent Discharges	47
CHAPTER 4	49
METHODS & TECHNIQUES	49
4.1. Sample Collection/Field Sampling	49
4.2. Analytical Methods	51
4.2.1. Analysis of Grain Size	51
4.2.2. Analysis of Clay Minerals	52
4.2.3. Analysis of Trace Metals	54
4.2.4. Analysis of Organic Carbon	61
CHAPTER 5	63
RESULTS : Sedimentological Investigations	63
5.1. Grain Size Distributions of Surface Sediments	63
5.1.1. The General Classification	67

5.1.2. Distribution Pattern of Sediment Types	69
5.1.2. Frequency Distributions - Histograms	71
5.1.3. Grain Size Textural Parameters	78
5.1.4. Scatterplots of Textural Parameters	93
5.1.5. Grain Size Distributions: Concluding Remarks	95
5.1.6. Trend Vector Analysis	96
5.2. The Distribution of Clay Minerals within Surface Sediments	99
5.2.1. Proportional Abundance of Clay Minerals	101
5.2.2. Spatial Distribution of Clay Minerals	103
5.2.3. Clay Mineral Ratios	107
5.2.4. Clay Mineral Distributions: Concluding Remarks	109
 CHAPTER 6	 115
RESULTS : Geochemical Investigations	115
6.1. Trace Metal Distribution of Surficial Sediments	115
6.1.1. Total Metal Concentrations	115
6.1.2. The Range in Total Metal Concentrations	116
6.1.3. Spatial Distribution of Total Metals	123
6.1.4. Grain Size Dependency of Metal Concentrations	133
6.1.5. Trace Metal Concentrations in the Different Size Fractions	135
6.1.6. Normalization of Data	153
6.1.7. The Source and Transportation of Metals	157
6.2. Metal Fractionation in Geochemical Phases	164
6.2.1. Vertical Distribution of Metals	172
6.2.2. Organic Carbon Content association With Trace Metals	172
6.2.3. Fe and Metals Relationships	180
6.2.4. Trace Metal Distributions: Concluding Remarks	182
 CHAPTER 7	 189
DISCUSSION AND CONCLUSIONS	189
7.1. Recent Sedimentation	189

7.2. Sources and Transportation of Sediment	191
7.3. Geochemical Factors and Anthropogenic Inputs	194
7.4. Future Studies	194
REFERENCES	196
APPENDICES	214
APPENDIX A : Analytical Techniques	214
A1. CORE SAMPLING	214
The Craib Corer	214
A2. FINE-GRAINED SEDIMENT SIZE ANALYSIS	221
SediGraph	221
A3. DETERMINATION OF CLAY MINERALS	227
X-Ray Diffraction	227
Identification of Clay Minerals by XRD	228
A4. DETERMINATION OF ELEMENTS	232
Atomic Absorption	232
A5. ANALYSIS OF ORGANIC CARBON	237
APPENDIX B : Tables and Diagrams	241
B1. REFERENCE TABLES	241
B2. CUMULATIVE CURVES	243
B3. CHEMICAL DATA TABLES	254

LIST OF FIGURES

Figure 3.1 : The Solent Estuarine System (after Tubbs, 1980).	26
Figure 3.2 : Reconstruction of the Solent River, at a time of lowered sea level (after Melville & Freshney, 1982).	27
Figure 3.3 : The buried channel of the Solent River showing the sub-Pleisto- cene surface in meters below Ordnance datum (after Dyer, 1975; West, 1980).	28
Figure 3.4 (a) : Geological Map of the region around the Solent System (from West, 1980)	29
Figure 3.4 (b) : Vertically exaggerated, transverse section of strata beneath the Southampton Water and the East Solent (from West, 1980).	30
Figure 3.5 : Mean tidal ranges over the study area (from Webber, 1980).	31
Figure 3.6 : Refraction patterns of waves from SW, to the east of the Isle of Wight (from Webber, 1979).	33
Figure 3.7 : Longitudinal distribution of salinity in Southampton Water (from Webber, 1980).	34
Figure 3.8 : Coastal types in the Solent region (after SHELL, 1985).	36
Figure 3.9 : The Rivers, Test, Itchen and Hamble.	38
Figure 3.10 : Isle of Wight and the Rivers Beaulieu and Lymington.	40
Figure 3.11 : Portsmouth, Langstone and Chichester Harbours.	41
Figure 3.12 : Generalized bathymetric chart of the Solent region (based upon BGS, 1988): contours in meters.	42
Figure 3.13 : Recent sediments and sediment circulation in the Solent (from SHELL, 1985).	44
Figure 3.14 : Sediment transport patterns (bed load) in the Solent (after Dyer, 1980).	46
Figure 3.15 : Effluent discharges into Southampton Water and its estuaries (from Webber, 1980).	48

Figure 4.1.: Sample Locations. Core sample (denoted by prefix 'X')	
locations are illustrated by lines A-A' and B-B'.	50
Figure 5.1 : Sampling Locations.	63
Figure 5.2 : Trilinear Diagram - Classification of samples (after Dyer,	
1986).	68
Figure 5.3 : Geographical distribution of the different grain size categories. . .	70
Figure 5.4 : Histograms showing the Grain Size Distribution of Samples	
(continued on following pages).	71
.	72
Figure 5.4 (continued): Histograms showing the Grain Size Distribution of	
Samples.	72
Figure 5.4 (continued): Histograms showing the Grain Size Distribution of	
Samples.	73
Figure 5.4 (continued) : Histograms showing the Grain Size Distribution of	
Samples.	74
Figure 5.4 (continued) : Histograms showing the Grain Size Distribution of	
Samples.	75
Figure 5.4 (continued): Histograms showing the grain size distribution of	
samples.	76
Figure 5.4 (continued): Histograms showing the Grain Size Distribution of	
Samples.	77
Figure 5.4 (continued): Histograms showing the Grain Size Distribution of	
Samples.	78
Figure 5.5 : The distribution pattern of mean grain size of surficial sediment	
samples.	84
Figure 5.6 : Variation of Grain size parameters within the River Test (for	
sample locations, see Figure 5.1).	87
Figure 5.7 : Variations of Grain size parameters within the River Itchen (for	
locations, see Figure 5.1).	87
Figure 5.8 : Variation of Grain size parameters in Southampton Water (for	
sample locations, see Figure 5.1).	88
Figure 5.9 : Variation of Grain size parameters in the northern part of the	

East Solent (for sample locations, see Figure 5.1).	89
Figure 5.10 : Variation of Grain size parameters in southern part of the East Solent (for sample locations, see Figure 5.1).	89
Figure 5.11 : Variation of Grain size parameters within the River Hamble . . .	91
Figure 5.12 : Variation of Grain size parameters within the River Beaulieu (for sample locations, see Figure 5.1).	91
Figure 5.13 : A plot of kurtosis against mean grain size, for all the surficial sediment samples.	92
Figure 5.14 : A plot of sorting against mean grain size (r is presented on the basis of rejection of the outlying samples).	94
Figure 5.15 : A plot of skewness against mean grain size (r's are presented as two separate trends).	94
Figure 5.16 : Sediment transport vectors as determined by the Gao approach (1992, 1993) (i.e. modified 'McLaren technique').	98
Figure 5.17 : Ternary diagram of clay minerals.	102
Figure 5.18 : The distribution of illite in the surface sediments of the Solent. .	104
Figure 5.19 : The distribution of smectite in the surface sediments of the Solent.	105
Figure 5.20 : The distribution of K+C in the surface sediments of the Sol- ent.	106
Figure 5.21 : The distribution pattern of the S/I ratio in the surficial sediments of the Solent.	108
Figure 5.22 : The distribution pattern of the (K+C)/I ratio in the surficial sediments of the Solent.	108
Figure 5.23 : Distribution pattern of clay mineral ratios from landward to seaward (for sample locations, see Figure 5.1).	111
Figure 5.24 : A plot of smectite percentage against mean grain size, for all the surficial sediment samples.	113
Figure 6.1 : The distribution of total Co in the surficial sediments of the Solent Region.	124
Figure 6.2 : The distribution of total Cr in the surficial sediments of the Solent Region.	125

Figure 6.3 : The distribution of total Cu in the surficial sediments of the Solent Region.	126
Figure 6.4 : The distribution of total Mn in the surficial sediments of the Solent Region.	127
Figure 6.5 : The distribution of total Ni in the surficial sediments of the Solent Region.	128
Figure 6.6 : The distribution of total Pb in the surficial sediments of the Solent Region.	129
Figure 6.7 : The distribution of total Zn in the surficial sediments of the Solent Region.	130
Figure 6.8 : The distribution of total Al in the surficial sediments of the Solent Region.	131
Figure 6.9 : The distribution of total Fe in the surficial sediments of the Solent Region.	132
Figure 6.10 : Correlations between total metal content and percentage of clay (continued on next page).	134
Figure 6.10 (continued): Correlations between total metal content and percentage of clay.	135
Figure 6.11 : Metal content of the sand, silt and clay fractions (continued on following pages).	136
Figure 6.11 (continued): Metal content of the sand, silt and clay fractions. . . .	137
Figure 6.11 (continued): Metal content of the sand, silt and clay fractions. . . .	138
Figure 6.11 (continued): Metal content of the sand, silt and clay fractions. . . .	139
Figure 6.11 (continued): Metal content of the sand, silt and clay fractions. . . .	140
Figure 6.11 (continued): Metal content of the sand, silt and clay fractions. . . .	141
Figure 6.11 (continued): Metal content of the sand, silt and clay fractions. . . .	142
Figure 6.11 (continued): Metal content of the sand, silt and clay fractions. . . .	143
Figure 6.11 : Metal content in the sand, silt and clay fractions.	144
Figure 6.12 : The distribution of Co in the clay fraction of surficial sediments throughout the area of study.	147
Figure 6.13 : The distribution of Cr in the clay fraction of surficial sediments throughout the area of study.	148

Figure 6.14 : The distribution of Cu in the clay fraction of surficial sediments throughout the area of study.	149
Figure 6.15 : The distribution of Ni in the clay fraction of surficial sediments throughout the area of study.	150
Figure 6.16 : The distribution of Pb in the clay fraction in surficial sediments throughout the area of study.	151
Figure 6.17 : The distribution of Zn in the clay fraction of surficial sediments throughout the area of study.	152
Figure 6.18 : Correlations between total trace metal and Al concentrations for the surficial sediments (continued on next page).	154
Figure 6.18 (continued): Correlations between trace metal and Al concentrations for the surficial sediments.	155
Figure 6.19 : Correlations between Cu, Pb, Zn and Al concentrations for the surficial sediments, after rejection of outlying samples (sig.level= $=0.00$).	156
Figure 6.20 : The location of samples contain anomalous populations of Cu, Pb and Zn in the surficial sediments.	156
Figure 6.21 : Metal concentrations in the various size fractions of the surficial sediments, along a transect from the River Test to seaward.	158
Figure 6.21 (continued): Metal concentrations in the various size fractions of the surficial sediments, along a transect from the River Test to seaward.	159
Figure 6.21 (continued): Metal concentrations in the various size fractions of the surficial sediments, along a transect from the River Test to seaward.	160
Figure 6.22 : Variations in the mean grain size of the surficial sediments, along the same transect as in Figure 6.21.	161
Figure 6.23 : Metal/Al ratios in the surficial sediments, along the same transect as in Figure 6.21 (continued on next page).	162
Figure 6.23 (continued): Metal/Al ratios in the surficial sediments, along the same transect as in Figure 6.21.	163
Figure 6.24 : Core samples locations in Southampton Water.	164

Figure 6.25 : The phase association of metal concentrations in Core X1 (phase 3=reducible, phase 4= organic, phase 5=residual).	166
Figure 6.25 (continued): The phase association of metal concentrations in Core X1 (phase 3=reducible, phase 4=organic, phase 5=residual). . .	167
Figure 6.25 (continued) : The phase association of metal concentrations in Core X1 (phase 3=reducible, phase 4=organic, phase 5=residual). . .	168
Figure 6.26 : The phase association of metal concentrations in Core X5 (phase 3=reducible, phase 4=organic, phase 5=residual).	169
Figure 6.26 (continued) : The phase association of metal concentrations in Core X5 (phase 3=reducible, phase 4=organic, phase 5=residual). . .	170
Figure 6.26 (continued) : The phase association of metal concentrations in Core X5 (phase 3=reducible, phase 4=organic, phase 5=residual). . .	171
Figure 6.27 : Vertical variations of metal concentrations in the three extrac- tion phases in core X1.	173
Figure 6.28 : Vertical variations of metal concentrations in the three extrac- tion phases in core X5.	174
Figure 6.29 : The distribution of organic carbon in surficial samples in the Solent Region.	179
Figure 6.30 : Correlations between trace metals and Fe, in the surficial sediments of the Solent.	181
Figure 6.31 : Correlations between Cu, Pb, Zn and Fe after rejection of outlier samples (sig.level=0.00).	182
Figure 6.32 : Changes in Metal/Al ratios and carbonate carbon in the surfi- cial sediments, from the River Test to seaward (continued on next page).	186
Figure 6.32 (continued): Changes in metal/Al ratio and carbonate carbon in the surficial sediments, from the River Test to seaward.	187
Figure 7.1 : A conceptual model for fine-grained sediment transportation in the Solent.	193
Figure A1 : Details of the Sampler.	217
Figure A2 : Vertical section of the sampler (upper) and the ball closing mechanism (lower).	218

Figure A3 : The coring tube and housing assembly.	219
Figure A4: Tabular output of a sample run within size range of 63 to $2\mu\text{m}$. . .	223
Figure A5 : Tabular output of the same sample as Figure A4, but run within a size range of 63 to $0.18\mu\text{m}$	223
Figure A6 : Graphic outputs of the same sample of Figure A4 (upper) and Figure A5 (lower).	224
Figure A7 : Cumulative frequency curves of the same sample.	225
Figure A8 : Representative XRD output of a Solent sediment sample ($< 2\mu\text{m}$).	231
Figure A9 : Example of the Output from the Carlo Erba E.H. 1108 of a Standard, acetanilide.	238
Figure A10 : Example of the Output from the Carlo Erba E.H. 1108 of an Unacidified Sample.	239
Figure A11 : Example of the Output of the Carlo Erba E.H. 1108 of the Acidified Sample (i.e. the same sample as in Figure A10).	240

LIST OF PLATES

Plate 1 : The Craib Corer, shown on the deck of the research vessel.	216
Plate 2 : The sampler being brought up on deck (upper) and the core tube showing a sample collected (some 10 cm in length), with overlying waters (lower).	220

LIST OF TABLES

Table 4.1 : Total digestion of 5 replicate samples.	57
Table 4.2 : Total digestion within the different size fractions of a duplicate sample.	57
Table 4.3 : The sequential extraction of a duplicate sample.	60
Table 4.4 : Total digestion of 4 replicates of the reference material (CRM 277).	61
Table 5.1 : The % of modal size class in each sample (continued on next pages).	64
Table 5.1 (continued): The % of modal size class in each sample.	65
Table 5.1 (continued) : The % of modal size class in each sample.	66
Table 5.2 : Definition of parameters, and the descriptive terms applied to various ranges of parameters (from Folk & Ward, 1957).	80
Table 5.3 : Textural Parameters of all the Samples (continued on the following pages).	81
Table 5.3 (continued) : Textural Parameters of all the Samples.	82
Table 5.3 (continued) : Textural Parameters of all the Samples.	83
Table 5.4 : Proportional abundances and ratios of clay minerals in the surface sediments (continued on following pages).	99
Table 5.4 (continued) : Proportional abundances and ratios of clay minerals in the surface sediments.	100
Table 5.4 (continued) : Proportional abundances and ratios of clay minerals in the surface sediments.	101
Table 6.1 : Total metal concentrations within all the samples analysed - units are ppm (continued on following pages).	117
Table 6.1 (continued): Total metal concentrations within all the samples analysed - units are ppm.	118
Table 6.1 (continued) : Total metal concentrations within all the samples	

analysed - units are ppm.	119
Table 6.1 (continued) : Total metal concentrations within all the samples analysed - units are ppm.	120
Table 6.1 (continued) : Total metal concentrations within all the samples analysed - units are ppm.	121
Table 6.2 : Average metal concentrations of near shore muds (after Chester, 1990).	122
Table 6.3 : The organic carbon content of surficial samples in the Solent Region (continued on following pages).	176
Table 6.3 (continued) : The organic carbon content of surficial samples in the Solent Region.	177
Table 6.3 (continued) : The organic carbon content of surficial samples in the Solent Region.	178
Table A1 : Comparison of statistical parameters of the samples analysed in the SediGraph over different size intervals.	226
Table A2 : Basal Spacings of Clay Minerals (after Brown & Brindley, 1980).	229
Table A3 : Standard Solutions used in the investigation.	234
Table A4 : Accuracy and Precision of the Various Standard Solutions.	235
Table A5 : Operating Conditions for the Determination of Various Elements by AAS.	236
Table B1 : Size classification of Sediment Grains (after Leeder, 1982).	241
Table B2 : Settling Times used in the Clay Minerals and Grain Size Separation for Trace Metal Analysis (after Galehouse, 1971).	242
Table B3 : Total and 'sum' metal concentrations for all the samples.	255
Table B4 : Metal concentrations in various size fractions.	259
Table B5 : Metal concentrations in various geochemical phases.	267

ACKNOWLEDGEMENTS

I am gratefully indebted to my supervisors, Prof. M. B. Collins and Dr. M. Tranter, for their guidance and also for their continuous encouraging support, without which this thesis would not have been possible.

I would like to thank Mr. T. Clayton (Department of Geology) for his help and his valuable advise, particularly in the field of clay mineralogy.

Furthermore, all the technical staff of the Department of Oceanography, especially Mr. D. Hutchison and Mr. K. Padley, for assisting me in the compilation of field sampling, and Dr. P. Ovenden, Mr. P. Riddy, Mr. J. Gibbs and Mr. P. Gooddy, and also Mr. Akabari from Department of Geology, for their technical help are gratefully acknowledged.

I would also like to thank all my friends, supporting me from home and those friends of many nationalities whom I met in this country, for giving me the moral support I needed.

I am also grateful for the endless support given by my parents.

Last, but most deeply, I thank to my dearest friend and husband Melih, for his understanding and support from miles away.

This thesis was supported by funding from the University of Istanbul, Institute of Marine Sciences and Geography (Turkey).

CHAPTER 1

INTRODUCTION

1.1. Background to the Study

This research programme is concerned with an examination of the geochemistry of fine-grained sediments of the Solent Estuarine System and their relationships with sediment sources and transport pathways. The distribution of grain size, clay mineralogy and trace metal will be examined, in order to establish the general pattern of fine-grained sediment transport and the associated movement of pollutants. Further, a conceptual transportation model will be developed; this will encompass the controls on the composition of fine-grained sediments in the Solent Estuarine System.

Particles smaller than 63 μm are considered generally to be "fine-grained" and composed mainly of clay minerals. Fine-grained sediments move in suspension, in response to the residual flow of water; they may be deposited and re-eroded, however, in tidally-dominated areas. Fine-grained sediment movement and accumulation depends upon a variety of factors, such as the type of estuary, the amount of the river (freshwater) discharge, the extent of urbanization and the tidal range (Dyer, 1979). Such particles may undergo substantial changes in their chemical content and are considered to be efficient scavengers of trace metals (Buller & McManus, 1979).

Estuaries are mixing places of two principal components, river and sea water, by the action of tidal motions, by waves on the sea surface and by the river discharge forcing its way to the sea (Dyer, 1986). Each of these components can exhibit appreciable seasonal variations (Whitfield *et.al*, 1981). In these systems, marine and fluvial sediments combine and are mixed by hydrodynamic forces

(Salomons & Eysink, 1981). The most important sedimentological function of estuaries is that they provide a natural basin for the storage of sediment supplied from both the land and the sea; they are subjected to the combined action of waves and tidal currents which control erosion, transport and deposition (Avoine, 1986). Scientific investigations into the ability of estuaries to remove and to conserve sediments contributes to estuarine pollution and management problems such as: the accumulation of contaminants in sediments; the dredging and disposal of dredged material; nutrient enrichment; degradation and loss of benthic habitat; and the loss of submerged aquatic vegetation (Schubel & Kennedy, 1984).

Schubel & Hirschberg (1981) have defined the parameters necessary for the study of long-term accumulation of fine-grained sediments in estuaries: (i) the sources of sediment, their locations and intensities; (ii) the character of the sediment introduced, its size distribution, composition and associated contaminants; (iii) the routes and rates of sediment transport, including the transient repositories; (iv) the sites of final accumulation within the estuary, and the rates at which sediments and associated contaminants are accumulating; (v) the masses of sediment and contaminants discharged to the ocean; and (vi) changes in the patterns of accumulation of fine-grained sediments and particle-associated contaminants, as a result of man's activities.

1.2. Aims of the Study

The major objective of the study was to establish the characteristics of fine-grained sediments in the Solent Estuarine System and to investigate sediment transport pathways by natural tracers such as grain size distribution, clay mineralogy and trace metal content. From this point of view, a sampling strategy based upon the abundance of fine-grained sediments was undertaken in Southampton Water, the East Solent and the various tidal inlets and tributaries of the System. The grain size distribution pattern was determined, to define the sedimentological characteristics of the environment. Clay mineralogy was determined to define the

source of the fine-grained sediment. The spatial distribution of trace metals was determined, to investigate the sources and movement of sediments and their associated contaminants (Leoni *et al.*, 1991). Cores were collected, in order to obtain information on the vertical sedimentological and geochemical changes throughout the sediment column.

1.3. Thesis Outline

The thesis consists of 7 chapters and Appendices. The background and aims of the study is presented above. A literature review of the natural tracers used throughout the investigation is presented in Chapter 2. Previous studies relating to the geological, oceanographical and sedimentological characteristics of the Solent Estuarine System are presented then in Chapter 3; this is followed by the methodology used during this research (Chapter 4). The results of study are presented in Chapter 5 and 6. Finally, an overall discussion and the conclusions are given in Chapter 7. Appendix A includes the technical details of the methods and the related equipment used in the study. Appendix B contains a number of Tables and Figures not used within the main part of the text, together with a full tabulation of the data obtained during the investigation.

CHAPTER 2

ENVIRONMENTAL CONSIDERATIONS

The aim of the present study is to examine the geochemistry of fine-grained sediments of the Solent region and their relationships with sediment transport pathways and sources. To this end, it is necessary to examine the grain size distribution and clay mineralogy of the sediments, together with their trace metal contents.

2.1. Grain Size Distributions

Grain size distribution is a fundamental textural characteristics of all fragmentary deposits and their lithified equivalents. The texture of bottom sediments is a response to geological, hydrological and bathymetric conditions of the sedimentary environment, as well as a response to transportational and depositional processes. It is not possible to distinguish, however, depositional environments in ancient deposits on the basis of grain size criteria alone. Systematic variations in grain size parameters (*i.e.* mean grain size, standard deviation, skewness and kurtosis) may be detectable within a local or regional context; they may be related to sediment dynamics or the supply of material to a particular areas (McManus, 1988).

Various methods are available for measuring grain size distribution and include mechanical, settling, and electronic techniques; these depend, to a certain extent, on the range in grain sizes present. Once the size of sediment particles has been measured, such data may be used to derive statistical parameters which describe the nature of the grain size distribution in the sediment sample. Histograms and frequency/ cumulative curves are the most common means of presenting these

data. Bi-variate scattergrams of statistical parameters have been used also to characterise depositional environments (Miola & Weiser 1968; Hubert, 1964; Jones, 1971; Freidman, 1979; Folk & Ward, 1957; Allen, 1971; Nordstorm, 1977).

Sediments are composed generally of a combination of grain size sub-populations, rather than consisting of a single overall population. Each sub-population may be defined on the basis of dynamic considerations, or sediment supply. In the natural environment, individual sub-populations may be present in varying proportions between sampling locations. Hence, it may be possible to trace material from a specific source, using its modal size and particle distributions, by noting the increase and decrease in its contribution to local materials (McManus *et al.*, 1980).

Fine-grained material tends to move more readily and is transported more rapidly than coarser grains. The fine fraction is transported in suspension whilst the coarser fraction is transported on or near the bed (as bed or saltation load). As the distance from the source increases and where the currents are lower, most of the coarser material in a particular population will have been deposited. Consequently, the mean sediment grain size will decrease with distance from the source, the so-called 'fining down the transport path' (Dyer, 1986) (although this pattern is not always the case (Gao & Collins, 1992)). A brief literature survey, presented below, should exemplify the interpretation of grain size distributions and the interrelationships between grain size parameters and sediment transport studies.

In an investigation of surface sediments of the continental shelf of the northwestern Gulf of Mexico, size frequency curves were dissected into the different distributions of individual components. It was suggested that, since many natural sediments consist of several components mixed in varying proportions, individual components tend to retain their own characteristics except when systematically modified by processes causing transportation and mixing (Curry, 1961). Passega (1964) devised two parameters: C, the coarsest one percentile, and M, the median diameter. CM diagrams were produced which reflected the characteristics of a depositional environment. Visher (1969) differentiated log-normal sub-popula-

tions, defined by distinct breaks within the complete size range of the sandstones, into various transport components. Three modes of transportation were reflected by the sub-populations, namely (1) suspension, (2) saltation and (3) surface creep or rolling. This investigator suggested that a number of processes (current, swash and backwash, wave, tidal channel, fallout from suspension, turbidity current and aeolian (dune) are reflected distinctively in the log-probability curves representing the grain size distributions of sand and sandstones. Glaister & Nelson (1974) have concluded that the most reliable approach to grain size analysis was that of graphic analysis of log-probability plots, which show details of the entire size distribution. This approach can constitute a valuable aid in facies identification. However, Christiansen *et al.* (1984) have argued that the traditional interpretation of segmented curves on probability paper was unjustified, suggesting that grain size distributions are better regarded as log-hyperbolic rather than log-normal. Previously, Bagnold & Barndorff-Nielsen (1980) introduced hyperbolic distributions, to recognize the pattern of natural size distributions, instead of log-normal distributions. Barndorff-Nielsen *et al.* (1982) applied this method to define the variation in the grain size distribution of a dune. Folk & Ward (1957), examining Brazos River Bar, emphasized the importance of skewness and kurtosis in distinguishing the genesis of sediments; they concluded that both skewness and kurtosis indicate the bimodality of a distribution, even when the modes are not apparent. In this way, the mixing of two populations (*i.e.* bimodal), in variable proportions, was identified. It was suggested also that skewness, kurtosis and sorting (associated with transport) are simple functions of the ratio between the two modes of the sediment distribution.

Friedman (1961) has distinguished between beach and river sediments by plotting skewness against sorting. Grain size distributions of dune sands are, for the most part, positively skewed; in comparison, those of beach sands are negatively skewed. Wind and river transportation is associated with unidirectional flow, which may be responsible for the general positive skewness of the dune and river sands. On a beach, sand is exposed to forces of unequal strength which act in opposite

directions; incoming waves and outgoing swash remove fine-grained particles. Such winnowing is considered to be characteristic of a beach environment. Hence, the frequency distribution curve of a winnowed sand lacks the "tail" at the fine-grained end of the curve and is negatively skewed. In the same way, Duane (1964) recognized that skewness is environmentally sensitive and that the winnowing action produced by a fluid medium is the mechanism producing negative skewness. Negatively skewed curves are indicative of areas of erosion or non-deposition, whereas positively skewed curves indicate deposition.

Allen (1971), studying the relationship between grain size parameters distribution and current patterns in the Gironde estuary, has pointed out that the degree of sorting is inversely proportional to tidal current energy. Sediments found in tidally dominated areas are characteristically coarser, less well sorted, and negatively skewed than sediments from wave dominated areas which are characterized by finer grained, well sorted and positively skewed material. Nordstrom (1977), studying the beach sediment of Sandy Hook Bay, concluded that changes in grain size parameters are related to the specific energy-mobility category of the beach. Latterly, McLaren (1981) has developed a model that distinguished three different sedimentary processes, by using intercomparisons between mean grain size, sorting and skewness. The relative textural changes between a deposit and its source were interpreted on the basis of three assumptions: i) that a deposit is the product of a single sediment source; ii) the probability of transport processes moving fine (light) grains is greater than the probability of moving coarse (heavy) grains; and iii) that there is a greater probability of coarse grains being deposited from sediment in transport, than fine grains. From this point of view, if a sediment deposit is eroded, with the resultant transported sediment being deposited completely, then the deposit must be finer, better sorted and more negatively skewed than the source. The lag remaining after erosion, on the other hand, must be relatively coarser and, better/ more positively skewed with respect to the original deposit (McLaren & Bowles, 1985).

Sediment in transport may become finer or coarser, depending upon the

action of the transporting agent; it may also become better sorted. If it becomes finer, the skewness must become more negative, whereas if it becomes coarser the skewness must become more positive (McLaren & Little, 1987). Exceptions to these trends may occur, for example, in the presence of more than one sediment source and during flocculation of fine sediments; both of these may change the sediment size distribution during transport (McLaren, 1981).

Gao & Collins (1991) have re-examined the model defined by McLaren & Bowles (1985) and argued that other cases may also occur during transportation. In the direction of transport successive deposits can become coarser and more negatively skewed due to transport processes themselves. A statistical procedure has been suggested to determine grain-size trends caused by net sediment transport (Gao & Collins, 1992). This technique examines grain-size trends which defines 'transport' vectors for a grid of sampling sites, in a shallow marine environment.

On the basis of this brief outline, the importance of the grain size distribution of sediments can be clearly identified. However, the interpretation of the grain size analyses of mud must be undertaken with caution, when attempting to determine the hydrological regime during deposition. Statistical parameters obtained for fine-grained sediments (*i.e.* fine silt and clay) may have little significance considering the physical character of samples, which are disaggregated prior to grain size analysis; these may be different from that in the environment of deposition (Lindholm, 1987). Clays commonly settle as 'flocs' and/or in association with faecal pellets; hence, they may respond to hydrological conditions differently than if they existed as individual particles.

In this study, grain size distributions of the surface samples will be examined on the basis of their frequency distribution and grain size statistical parameters.

2.2. Clay Mineralogy

Clay mineralogy is a useful technique to be applied to the identification of sedimentary provenance, and the tracing of transport pathways (Chamley,

1989; Hardy & Tucker, 1988; Weaver, 1989; Irion & Zölmer, 1990). Riverborne and marine sources of sediment can be distinguished often from an examination of the clay mineralogy of the sediments. The primary clay mineral character of recent river, delta and shallow marine sediments is controlled by detrital clay material derived from land (Weaver, 1959; Griffin *et al.*, 1968).

Hathaway (1972) has examined some 400 samples from the rivers, estuaries and continental margin of the east coast of the United States and has identified two major clay mineral facies. The reworking of older sediments on the continental shelf and shoreline erosion were identified as contributing clay-sized material to the estuarine sediments. Similarly, Pinet & Morgan (1979) have pointed out that the erosion of coastal outcrops supplies a large amount of clay to Sapelo Sound, a tidal water body receiving minor freshwater discharge. Elsewhere, Kolla *et al.* (1980) have demonstrated that high concentrations of illite and chlorite in the northern part of the Phillipine Sea are derived from the islands of eastern China, Taiwan and Japan. Smectite is associated with volcanoclastic material and is abundant in the southern regions of the Phillipine Basin. Shaw (1978) has defined four main clay mineral provinces for the NE Mediterranean, each with a characteristic clay assemblage. The origins of the assemblages are from rivers draining/coastal erosion of the southern Turkish coastline and from the NW coast of Cyprus. Six distinct clay mineral assemblages were identified by Rao (1991) for the eastern continental shelf of India, once again reflecting their source. Johns & Grimm (1958), investigating the clay mineral composition of recent sediments from the Mississippi River Delta concluded that the offshore decreasing trend of montmorillonite (accompanied with increasing kaolinite and illite) was due to diagenetic formation of the latter two minerals from the montmorillonite during contact with seawater.

For estuaries, a number of studies have shown that clay mineral (*i.e.* smectite, illite and kaolinite) ratios are reasonable indicators of land- or marine-derived material (Dyer, 1986). Therefore, spatial variations in clay mineral ratios may indicate transport pathways (at least, to some extent). Gibbs (1977) has argued that spatial variation in clay mineral ratios can be explained by three possible

mechanisms: (i) chemical alteration; (ii) differential flocculation; and (iii) size segregation. Chemical alteration of clay minerals refers to the transformation to a more stable phase of detrital clay minerals. Differential flocculation is a mechanism suggested by Whitehouse *et al.* (1960); it is based upon the dissimilar aggregation of different clay minerals in waters of varying salinity. Illite and kaolinite flocculate with only small incremental changes in salinity, whereas montmorillonite (smectite) flocculates over a much wider salinity range. The third mechanism, size segregation is based upon physical sorting by size. Smectite has the smallest particle size, whereas illites and kaolinites consist of relatively coarser-grained material. Hence, illite and kaolinite are deposited closer to a particular source, whilst smectite remains preferentially in suspension (Gibbs, 1977).

Several processes or factors contradict the interpretation of clay mineral ratios described below. Edzwald & O'Melia (1975) have suggested that diagenesis (*i.e.* chemical alteration of clay minerals) is important only for deep sea sediments, but is negligible for surface sediments. Chamley (1989), in a review of earlier studies, concluded that the chemical effect on clay mineral distributions is restricted usually to ion exchange in the surface and inter-layer positions. Similarly, Scafe & Kunze (1971) have reported no evidence of differential settling of clay minerals from an examination of sediment cores in the Gulf of Mexico. Feuillet & Fleischer (1980), examining bottom sediments of the James River estuary, identified estuarine dynamics as being the cause of the upstream transport of sediments, governing the clay mineral distribution: in contrast, differential settling, flocculation and diagenesis appeared to have no effect on the distribution of the clay minerals. Although the roles of the flocculation and differential settling processes are indistinct, they maintain the smectite in suspension and enhance transport towards the marine environment *i.e.* without settling in estuaries. Chamley (1989) emphasized also the importance of specific environmental conditions, such as river influx and tidal range, in controlling clay mineral distributions. For example, estuaries characterized by an important river influx (as opposed to a medium tidal range) support appropriate conditions for differential settling; others, where river and

marine particle influx are opposed to each other in comparable proportions under medium to high tidal ranges, support source mixing. It is believed that estuarine circulation plays the dominant role in the control of clay minerals distributions (Chamley, 1989).

Shaw (1973) found no significant variation in the relative proportions of clay minerals in the modern intertidal flat sediments of the Wash embayment, eastern England. Erosion and re-deposition of the intertidal flat material was believed there to be an important source of clay-grade sediments. Aoki *et al.* (1974), studying the recent sediments of the sea of Japan, concluded that the dispersal pattern of clay minerals is influenced strongly by the supply of fine-grained material from the rivers and is related also to the Tsushima Warm Current. Karlin (1980) identified that the main dispersal pattern of clay minerals is controlled by seasonal, meteorological and oceanic factors, such as: periodic peak river discharge, winter storms and summer coastal upwelling along the continental margin of Oregon, U.S. Elsewhere, in the southeastern U.S., Neihsel & Weaver (1967) have examined the clay mineralogy of the Piedmont Province, where kaolinite is the dominant clay mineral: montmorillonite and illite are the major clay minerals in the coastal plain and continental shelf sediments, respectively. In the rivers and estuaries, the kaolinite/montmorillonite ratio serves to identify the relative proportion of clay-sized sediment derived from the two source areas. These investigators concluded that mineral dispersal patterns are governed by hydraulic parameters, such as salinity, velocity and the Coriolis force in the estuary. The Coriolis force causes the salinity slope of the boundary layer to be tilted downward to the left (or west) in the northern hemisphere. Hence, water on the eastern side of an estuary is more dense than its western side. Pevear (1972) studied the origins of clays in the same study area. The main source of river clays was from weathered feldspar, derived from metamorphic rocks of the Piedmont Province. The estuarine clays were derived partly from the rivers, but erosion of local Pleistocene outcrops and landward transport from the shelf appear to be equally important sediment sources. It was concluded that the clay mineral distributions support the hypothesis that the estu-

aries of the southeastern U.S. are in a state of equilibrium, with respect to the influx and outflow of sediments.

Wright (1974) has studied the major and minor elements of the clay fraction of surface and sub-surface sediments from the southwestern Barent Sea. There is considerable variation in the relative content of the principal mineralogical components, and (3) distinct petrographic provinces could be identified. Park *et al.* (1986), studying the suspended particulate matter in the Keum estuary and the adjacent continental shelf of southeastern Yellow Sea, found that the major dispersal directions of suspended matter derived from Keum River are westward and southwestward. Investigation of the clay mineralogy and the trace metal content of the bottom sediments in the same study area confirmed that the bulk of the fine-grained sediment was derived from the Keum River and that the dominant direction of transport is southwestward. Subsequent and sporadic westward and northwestward transport could also occur. Irion & Zölmer (1990) identified a transport path in estuaries of the Inner German Bight (North Sea), to the Skagerrak, utilizing clay mineral ratios and the Zn content of the sediment; the latter showed a similar trend to the smectite/kaolinite ratio.

The hydrodynamic conditions in estuaries are complex, due to the effects of independent factors such as tide, river discharge, wind and the density difference between water masses (Salomons & Eysink, 1981). Mixing of river and sea water (resulting in variable water salinities and current velocities) can give rise to "selective transportation and deposition of clay minerals". The high and low tidal phases (still stands) allow smectite to settle, which accumulates on the surface sediments as a 'mud cream' that can be reworked easily during the subsequent flood or ebb phase (Chamley, 1989).

2.3. Trace Metal Concentrations & Phase Associations

The concentration of trace elements in riverine and estuarine sediments reflects both the occurrence and abundance of certain rocks or mineralized

deposits in the drainage area of the river and, since the rivers are used for the disposal of domestic and industrial wastes, the anthropogenic input of certain heavy metals into the environment. The latter often equals or exceeds the amount released by natural weathering processes. A large part of the anthropogenic discharge of heavy metals into the environment becomes incorporated into the fine-grained sediment and suspended particulate material (Boldrin *et al.*, 1989). The natural concentrations of heavy metals are associated or combined structurally with a limited number of detrital aluminosilicate minerals, secondary clay minerals, secondary oxides of Fe and Mn, and in the discrete particles of detrital metal oxides, sulphides and carbonates. Organic material is also a carrier of heavy metals; it is not a predominant contributor to total metal levels, however, because of its low abundance in most sediments (Loring, 1991). Elevated concentrations of Zn, Pb, Cu are believed to reflect anthropogenic influences. The most constant and/or conservative elements are usually the rare earths, Si, Al, Fe, Ti, Sc and U (Förstner, 1989).

2.3.1. Grain Size Effect on Trace Metal Concentrations

Estuarine sediments are a mixture of inorganic and organic material, with a wide range of grain sizes (Loring, *op.cit.*). Metal-particle interactions are related to properties of the particulate matter, such as grain size, mineralogy, specific surface area and organic or metal oxyhydroxide coatings. Fine-grained particulates, with large specific surface areas and elevated organic matter contents, accumulate heavy metals onto their surfaces, either by adsorption or by incorporation into organic coatings (Cauwet, 1987; Boldrin *et al.*, *op.cit.*). Ackermann *et al.* (1983) suggested the separation of the $<20\ \mu\text{m}$ size fraction for the monitoring of trace metal in sediments. Mudroch & Duncan (1986) determined the major and trace elements in six size fractions ($<13\ \mu\text{m}$, $13\text{--}19\ \mu\text{m}$, $19\text{--}27\ \mu\text{m}$, $27\text{--}40\ \mu\text{m}$, $40\text{--}54\ \mu\text{m}$, and $54\text{--}150\ \mu\text{m}$) of bottom sediments collected at 8 stations along the Niagara River, suggesting that the $<13\ \mu\text{m}$ size can accumulate a high concentra-

tion of trace elements. Horowitz & Elrick (1987) investigated the interrelationship between grain size, surface area and *operationally-defined* geochemical phases on the trace metal distribution of 17 geographically and hydrologically diverse stream bed sediments. The strongest correlation between trace metals and grain size occurred within the < 63 or $< 125 \mu\text{m}$ size fraction. Thus, as the proportion of these size fractions increases, the trace metal concentration also increases. The same correlations occur for bulk sediment chemistry, surface area and grain size and surface area. Grain size correction procedures are necessary, therefore, to facilitate inter-sample comparisons and for the elucidation of spatial or temporal trends (Horowitz & Elrick, *op.cit.*; Loring & Rantala, 1990). Förstner (1989) discussed the controversies surrounding the selection of certain grain size fractions for the tracing of pollution sources. The following issues arise from this review: (i) since the larger sediment fractions are less affected by transport, they are more likely to reflect the impact of urbanization on the distribution of heavy metals over an extended period of time at a given location; (ii) the fine sand fraction is of particular interest for the differentiation of natural and pollutant metal transport, because it comprises most of the total sediment; and (iii) the silt and clay fractions ($< 63 \mu\text{m}$) are the predominant carriers for both natural and anthropogenic compounds and are almost equivalent to the material carried in suspension (by far the most important transport mode of sediments). Therefore, the $< 63 \mu\text{m}$ fraction (*i.e.* silt and clay) is the size separation most recommended for the determination of trace metals.

2.3.2. Trace Metal Containing Phases

Broadly, two types of natural minerals occur, namely detrital and authigenic minerals (Engler *et al.*, 1977). Detrital materials include: (a) mineral grains and rock fragments; (b) organic materials; and (c) anthropogenic components, derived from agricultural run-off and industrial waste discharges. Authigenic materials include aquatic organisms, shell material and some organic products of

anaerobic or aerobic changes.

It is convenient to make a fundamental distinction between those trace elements held in lattice positions within detrital minerals and those held on surface and in inter-sheet positions. The metals held in the latter non-lattice positions are susceptible to processes involving reactions between dissolved and particulate forms. Metals introduced anthropogenically into the aquatic systems exist usually in relatively unstable chemical associations; they are predominantly available, therefore, for biological uptake (Förstner, 1989). The geochemical fractionation of heavy metals in a sediment depends upon several factors, such as source materials, weathering processes, sediment transport and dissolution and redox reaction kinetics (Filipek & Owen, 1978).

The geochemical phases which may contain trace metals can be *operationally* defined, as follows:

- 1) exchangeable (absorbed as surface coatings);
- 2) bound to the carbonates fraction;
- 3) bound to Fe and Mn oxides fraction;
- 4) bound to the organic matter fraction; and
- 5) the residual fraction (*i.e.* a lattice of crystalline minerals).

A particular trace metal or major element can be present or can occur in several phases. Commonly, the trace metals are found in all phases, namely adsorbed on mineral surfaces, associated with hydrous Fe and Mn oxides and hydroxides (which can exist as surface coatings or discrete particles), adsorbed or adsorbed with organic matter, and in the lattice of crystalline minerals or the inter-layer positions of clay minerals. These locations represent also a range extending from stable components in the mineral interior, which are essentially insoluble, to soluble compounds loosely-bounded to the sediment, which are readily mobile (Engler *et al.*, 1977). Metals in exchangeable positions are generally authigenic and are relatively mobile and readily available for biological uptake. Trace metals in the carbonate fraction of sediments may be either detrital or authigenic, because many metals have carbonate species which are stable under natural pH and Eh conditions

(Filipek & Owen, 1978). Trace metals associated with Fe and Mn oxides are co-precipitated or adsorbed onto pre-existing oxide coatings. These processes are very sensitive to changes in redox potential. Trace metals associated with organic matter, through biological uptake, are related to adsorption with subsequent incorporation into resistant organic degradation products (such as humic substances). Under oxidizing conditions in natural waters, organic matter can be degraded, leading to a release of soluble trace metals (Tessier *et al.*, 1979). The concentration of trace metals in the lithogeneous (residual) fraction of sediments is controlled almost exclusively by the mineralogy of the land-derived detrital materials; it is not affected by anthropogenic inputs (Filipek & Owen, *op.cit.*). Possible applications of the selective extraction results include the evaluation of the effects of dredging operations and the prediction of trace metal behaviour in the estuarine system (Tessier *et al.*, *op.cit.*).

There are a large number of studies regarding trace metal-phase associations. Gibbs (1973) distinguished the main partitioning of trace metals in the Amazon and Yukon rivers, as follows: Cu and Cr were transported as crystalline solids, Mn as coatings on particulate material and Fe, Ni and Co were distributed equally between precipitated metallic coatings and crystalline solids. Förstner & Patchineelam (1980) studied highly polluted Rhine River sediments with a 5 step extraction sequence. Fe, Ni and Co were found to be associated mainly with the residual (lithogeneous or detrital) fractions, which are less affected by man's activities. Pb, Cu and Cr were found to be associated with the Fe-Mn hydroxide phases. Salomons & Förstner (1984) found an increase in the relative amount of metal existing in the residual fraction for less polluted river sediments from different parts of the world. Skei & Paus (1979) observed significantly higher non-detrital fractions of Cu, Pb, Mn, and Zn in the upper part of sediment cores from northern Norway. This enrichment corresponded to sediments deposited since 1900, when mining activities started in the area. These investigators suggested that Cu, Zn and Pb increases were related to the mining activities, whilst Mn was enriched in the surface due to migration of dissolved Mn and precipitation in the oxic surface

layer. Filipek & Owen (1978) examined sediments from Lake Michigan and pointed out that Fe and Cr were concentrated mainly in the residual fraction, Cu and Zn were associated with the organic fraction and carbonate-exchangeable fraction, respectively, and Mn was present in detrital carbonate or as amorphous oxides. Kitano *et al.* (1980) found that Cu, Zn and Mn contents of sulphide, carbonate and organic fractions vary with depth in the sediment column in Tokyo Bay, whereas the metal contents in the residual fraction were almost constant with depth.

2.3.3. Mobilization

The mobilization of metals arises from either dissolution and/or migration in pore waters, due to variations in the physical-chemical properties of the water and sediment column (Kemp *et al.*, 1976). Changes in physico-chemical parameters, such as pH, Eh and ionic strength, all of which occur throughout the estuarine system, affect the extent of metal-particle interactions (Aston & Chester, 1976). The solubility, mobility and bioavailability of metals bound to sediments can be increased by 4 major factors; (i) the lowering of pH; (ii) the changing of redox conditions; (iii) the formation of organic complexes and (iv) increasing salinity. The first 2 factors are particularly important for on-land deposition of dredged materials, whilst salinity influences re-suspended Cd-rich sediment in estuaries (Förstner *et al.*, 1986). Lowering pH and changes in redox potential affect the exchangeable, carbonate and Fe-Mn oxides fractions. In anoxic environments, complexation with organic materials may occur. It is also thought that most metals are co-precipitated with abundant sulphide forms (Luoma, 1990). Aeration of anoxic sediments can both increase and decrease the mobility of metals. De Groot & Allersma (1975) found that large differences among several metals in their degree of mobilization in the Rhine estuary, North Sea and Wadden Sea, induced by intensive decomposition of organic matter in sediments from the fresh water tidal area. Cd, Hg, Cu, Zn, Pb, Cr and As, were strongly subject to mobilization. Ni has showed an intermediate level of mobilization, whilst Sm, Sc, La and Mn

were not mobilized. El Ghobary & Latouche (1986) examined the surficial sediments of the Aquitaine Coast and have found that a high percentage of the mobile fraction of metals was associated with oxides and, to a lesser extent, with carbonates. Cu, Mn, Ni and Fe were found in association with sulphides. The enrichment of Cu, Zn and Pb in the surficial sediments was believed to be the result of the high anthropogenic flux of these metals during recent years. On the basis of a study of sediment cores in the northwestern Mediterranean, Fernex *et al.* (1986) concluded that 30-50 % of Cu is released during sediment transport and after deposition, under oxic conditions; Mn is largely remobilized under reducing conditions.

2.3.4. Organic Carbon

Organic matter in estuarine sediments is derived from 2 sources: (i) allochthonous plant detritus, derived from soils and carried to the coast by rivers; and (ii) autochthonous plant and animal detritus derived from indigenous organisms and industrial effluents located in the vicinity of the estuary or along rivers (Folger, 1972). Most of the organic matter in recent marine sediments is in a firmly bound and/or adsorbed state. The adsorption of organic matter begins in the water column, where there is usually a significant amount of suspended particulate material, in addition to dissolved organic matter (Bordovsky, 1965). Suspended matter in estuarine waters has a high degree of surface uniformity with respect to its electrical properties and controls the surface electrical state (Hunter & Liss, 1982). The surface coatings of metals and surface-active organic matter onto suspended matter is believed to be result of this surface film.

Organic carbon concentrations in the bottom sediments of relatively unpolluted estuaries (*e.g.* Pedscot Bay, Apalachicola Bay, Florida) are <5 %. Values are commonly higher where biogenic material is abundant, or where bottom waters are anaerobic (Folger, *op.cit.*). Concentrations of organic matter increase generally with a decrease in grain size. Hence, the clay fraction contains more organic matter than the sands. This association is the result of a number of factors, including the

settling characteristics of the particles, the permeability of the sediment and the chemistry and microbiology of the interstitial water (Folger, 1972). Clay minerals may adsorb 50-60 % of the dissolved organic matter formed by the decomposition of phytoplankton. Since organic matter is precipitated from water as particles of various sizes, its distribution is influenced greatly by hydrodynamic conditions (Bordovsky, 1965).

Organic matter plays an important role in the chemical behaviour of trace metals and their deposition and transportation in estuaries, since it is able to bind or chelate trace metals and take part in diagenetic processes after deposition (Salomons & Förstner, 1984). Metals associated with organic matter can comprise a large fraction of the total concentrations. Some trace metals show remarkable enrichment in the organic matter of certain sediments (Bewers & Yeats, 1981; Krauskopf, 1967). Rosental *et al.* (1986) found a well-established correlation between metal concentration (except for Pb) and the organic matter content of sediments in False Bay (South Africa). It has also been observed that organic matter could be an important sink for dissolved metals during estuarine mixing (Boldrin *et al.*, 1989; El Ghobary & Latouche, 1986; Martin *et al.*, 1987; Sholkovitz, 1976). Finally, Nissenbaum & Swaine (1976) have found that humic substances contain a sizeable proportion of the Cu, Mo and Zn found in the sediments, but are less important for Ni, Co and Pb; it is insignificant for Mn, V and Fe. Any metals are believed to be introduced into the humates during their diagenetic formation in the sediment.

2.3.5. Trace Metals in Estuaries

Estuaries act as trace element traps and reflect the mean heavy metal concentrations of a water body (Chester, 1975; Burton & Liss, 1976; Duinker & Nolting, 1976; Boldrin *et al.*, *op.cit.*; Ackermann *et al.*, 1983). Trace metals are introduced into estuaries in two principal forms; those associated with solid and colloidal material and those in solution (Aston & Chester, 1976). The transportation and depositional behaviour of coarse-grained particles is governed largely by

hydrodynamic factors, whereas the behaviour of silt- and clay-sized suspended materials may be modified by processes such as the disaggregation of flocculated material (Burton, 1976). In general, river waters contain clay particles which flocculate in the saline waters of estuaries. The increase in total ionic strength tends to decrease the thickness of the electrical double layer surrounding the clay particles, with flocculation occurring below a critical thickness. When the flow velocity slackens, coarser-grained particles and aggregates will settle, especially in estuaries and harbours. However, fine-grained particles have low settling velocities and may remain in suspension for long periods of time and, hence, be transported over large distances. There is an additional source of trace elements to the waters within the estuary: ions are desorbed from particulate matter reaching the estuarine environment (Aston & Chester, 1976). These trace elements may be removed from solution by processes such as re-adsorption onto inorganic and organic detritus and by incorporation into estuarine biota. The formation of iron oxide coatings on clay particles is one of the important adsorption mechanisms active during estuarine mixing (Aston & Chester, *op.cit.*). Adsorption may occur both physically and chemically (Salomons & Förstner, 1984). Physical adsorption occurs on the external surface of a particulate and is based on Van der Waals forces of relatively weak ion-dipole or dipole-dipole interactions. Chemical adsorption is characterized by the formation of chemical associations between ions or molecules from solution and the surface particles. Balistrieri & Murray (1984) observed experimentally the absorption of 13 trace metals from seawater onto sediment from Guatemala Basin. The adsorption data indicate a long equilibration time for most metals (~20 day). Factors such as increasing pH and particle concentration increase the adsorption ability. It has been observed also that biogenic particles tend to bind most metals more strongly than lithogenic or authigenic particles. Li *et al.* (1984) observed that Co, Mn, Cs, Cd, Zn and Ba were desorbed from riverine suspended particles, whilst significant fractions of dissolved Fe, Sn, Bi, Ce and Hg were coagulated during estuarine mixing. Brüggman (1988), studying dissolved and particulate trace metals in the Baltic Sea, concluded that dispersal patterns of trace metals are

influenced by the redox state of the water column. Under anoxic conditions, the dissolved fraction of some elements increases (Mn, Co and Fe), whereas others are diminished significantly (Cu, Cd, Zn and Pb) or behave more conservatively (Ni and Hg). Boldrin *et al.* (1989) observed the scavenging of metals during estuarine mixing in the Adige River. Increasing pH and salinity favours the adsorption of dissolved metals onto particle surfaces. High concentrations of Cr in the organic phase were believed to be indicative of anthropogenic influence.

The processes affecting trace metal concentrations in the depositional environment differ from those during transportation; they include chemical mobilization and the physical mixing of contaminated riverine sediments with marine or riverine sediments which have a lower heavy metal content (De Groot *et al.*, 1976). The latter process gives rise to a decrease in the heavy metal content of estuarine sediments, in a seaward or landward direction. Information on the mixing ratios of marine and fluvial material is necessary for an understanding of transport processes, as well as for assessing the balance of riverine mud and particulate metals in the estuarine environment (Salomons & Eysink, 1981). In long-term transport studies, natural tracers, such as differences in mineralogy, chemistry and isotopic composition, may be used to trace the source and transport pathways. A decrease in the trace metal concentration of estuarine sediments in the seaward direction may be caused by mixing of uncontaminated marine sediments with contaminated riverine sediments, and/or adsorption, precipitation and mobilization. To distinguish between these processes, the mixing ratio of marine to riverine sediments must be known. If so, it is possible to calculate the concentration of trace metals behaving conservatively. Computed values exceeding those actually observed would indicate mobilization processes and lower values would suggest precipitation or adsorption processes (Salomons & Eysink, *op.cit.*). Salomons & Mook (1977) studied the isotopic composition of fluvial and marine sediments in the Rhine and Ems rivers. The trace metal concentration of marine sediments is lower compared to those of riverine sediments with mixing causing a decrease in the downstream metal content. These investigators observed good agreement between the metal content, calculated

from the measured mixing ratio concluding that conservative mixing processes govern mainly the trace metal concentrations in these estuaries.

It is important to consider also the processes which occur within the sediment column, since these may result in relocation of metals. As a result of (early) diagenesis, heavy metals may become enriched in pore waters and diffuse to the surface; hence, the distribution patterns for the metals could be attributed mistakenly to enhanced pollutant input. The enrichment of heavy metals in pore waters alters dramatically the partition between dissolved and particulate phases from that found in the estuarine water column; this may have implications for metal uptake by organisms (Elderfield & Hepworth, 1975). High concentrations of metals can build up in the pore waters of estuarine sediments. These concentrations exceed the background levels of the elements in unpolluted natural waters. If they exceed the levels in the overlying estuarine water column then a concentration gradient is present between the pore water and the estuarine water; this may allow the metals in the pore water to diffuse upwards until a new chemical environment is reached which sets different limits on their solubility. This new environment may be just below the water-sediment interface, in which case the measured levels of metals in surface estuarine sediments will reflect not only the immediate input by natural and pollutant sources, but also the long term diagenetic recycling of metals through the sediment column. Alternatively, metals may diffuse out of the sediment environment into the overlying water column, with the result that the soluble load of metals in estuarine waters will reflect both present-day sources and also the diagenetic input (Elderfield & Hepworth *op.cit.*).

2.3.6. Distinguishing the Natural and Anthropogenic Influences

There are several procedures to discern natural and anthropogenic influences: (i) identifying the pollutant (non-residual) phase; (ii) the definition of baseline or background concentrations; and (iii) establishment of comparability among sediments (Luoma, 1990).

Experimental procedures that extract the non-residual fraction of the total metal from sediments aim to estimate "potentially" reactive metals, in terms of their sediment/water mobility and bioavailability (Luoma, 1990). Contaminant metal is considered to be present in the sediment, if the relationship between non-residual and total metals is hyperbolic rather than linear.

A baseline or background may be established by several approaches (Luoma, *op.cit.*). Dating of the sediment cores is one of the widely-used methods (Bruland *et al.*, 1974; Durham & Joshi, 1984; Skei & Paus, 1979; Smith & Walton, 1980). Dating of the sediment column helps to decipher the sedimentary record of both natural and (the addition of) anthropogenic fluxes. Natural or baseline fluxes are determined from the older parts of the sedimentary column, assuming sediment stability and the lack of significant diagenetic redistribution of metals. Background levels can be estimated also by direct measurements of metal concentrations in recent texturally- and mineralogically-equivalent sediments from a known pristine region (Loring & Rantala, 1990).

Comparability among sediments, in terms of uniformity in grain size, composition and origin, can be achieved by several different methods (Luoma, *op.cit.*; Förstner, 1989): (i) separation and analysis of a certain grain size- the $<63\ \mu\text{m}$ fraction (*i.e.* silt and clay) is the most commonly recommended size separation (this size fraction is carried in suspension and is the most important transport mode); (ii) extrapolation from the regression of metal concentration plotted against grain size or concentration versus specific surface area (this technique requires a relatively large number of samples and is not always very accurate); (iii) comparison or normalization with respect to conservative elements, such as Al, Fe and Li. This latter method seems to be the most useful for the reduction of grain size effects (Loring & Rantala, *op.cit.*; Loring, 1991). In particular, Loring (*op.cit.*) suggested that Li is superior to Al for the normalization of trace metal concentrations from the glacial sediments. Analysis of the metal concentration of the $<63\ \mu\text{m}$ size fraction is effective, since this fraction has higher metal concentrations and is usually homogeneous in composition.

Normalizing metal concentrations to a textural or compositional parameter assumes a baseline regression between a given variable and non-pollutant metal concentrations (Luoma, 1990). The influence of the baseline may then be removed by normalising with respect to the baseline regression.

Calculation of an enrichment factor relative to the earth's crust may be employed normalising the metal concentrations against background values;

$$EF = (M_x / Al_x) / (M_c / Al_c)$$

where, M_x and Al_x are metal and aluminum concentrations in the sample and M_c and Al_c are metal and aluminum concentrations in the crust (Luoma, *op.cit.*). Sinex & Helz (1981) compared the enrichment factors of trace metals in Susquehanna River and Chesapeake Bay sediments, and found that riverine sediments have higher metal values relative to average crustal values, while bay sediments have enrichment factors dropping rapidly to unity, except for Zn, Cd, and Pb.

CHAPTER 3

AREA UNDER INVESTIGATION

3.1. Solent Estuarine System

The Solent Estuarine System includes the Solent, Spithead, Southampton Water, the harbours of Portsmouth, Langstone and Chichester, together with numerous inlets in the area (Figure 3.1). The system extends for a distance of 30 km from Ryde-Gilkicker in the east, to Hurst Castle in the west; its width is ~ 4 km in its western part and ~ 5.5 km over much of the eastern part (Webber, 1980), with the narrowest part being at Hurst Castle (1 km). The largest estuary in the region is Southampton Water which has a width, at high water, of about 2 km and a length of 9 km. The western shore of Southampton Water consists of salt-marshes and extensive mudflats, whereas the eastern shore consist of a steep beach which is affected by wind and wave action. The tributary estuaries of Southampton Water are the Hamble, Test and Itchen. Other estuaries within the Solent are Beaulieu and Lymington in the west, and the Western Yar, Newtown, Medina, and Wootton Creek on the Isle of Wight.

3.2. Geological Setting

The Solent lies along the axis of the syncline of the Hampshire Basin separating the Isle of Wight from the Hampshire mainland. Sedimentary deposition within the area commenced during the Jurassic, when a series of shallow water marine shales, limestones, mudstones and dolomites were formed (Melville & Freshney, 1982). Towards the end of the Jurassic, the sea retreated and a thin layer of non-marine deposits developed.

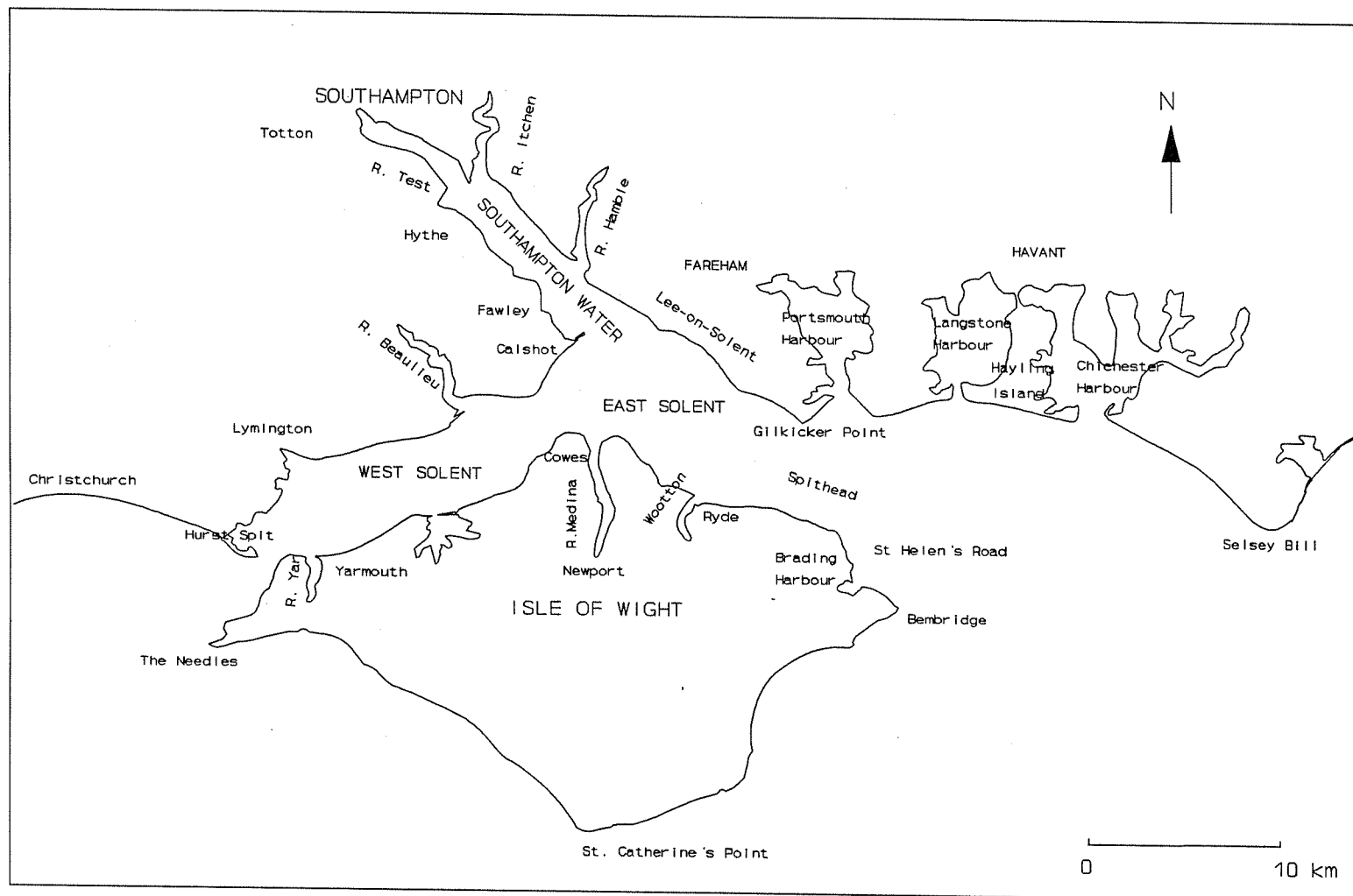


Figure 3.1 : *The Solent Estuarine System (after Tubbs, 1980).*

The Cretaceous era was characterised by the successions of (brightly coloured) marls, shallow marine sands, muds and chalks; some of these extend up to 500 m in thickness. The Jurassic and Cretaceous deposits are not exposed in the area. At the beginning of the Tertiary, the Hampshire Basin was formed.

The present configuration of the system has been derived from the post-glacial Flandrian Marine transgression, into the previously extensive Tertiary and Quaternary Solent river systems (Figure 3.2). During the glacial phase of the Pleistocene, the valleys of the local rivers were excavated below present sea-level before they were flooded during the transgression (West, 1980).

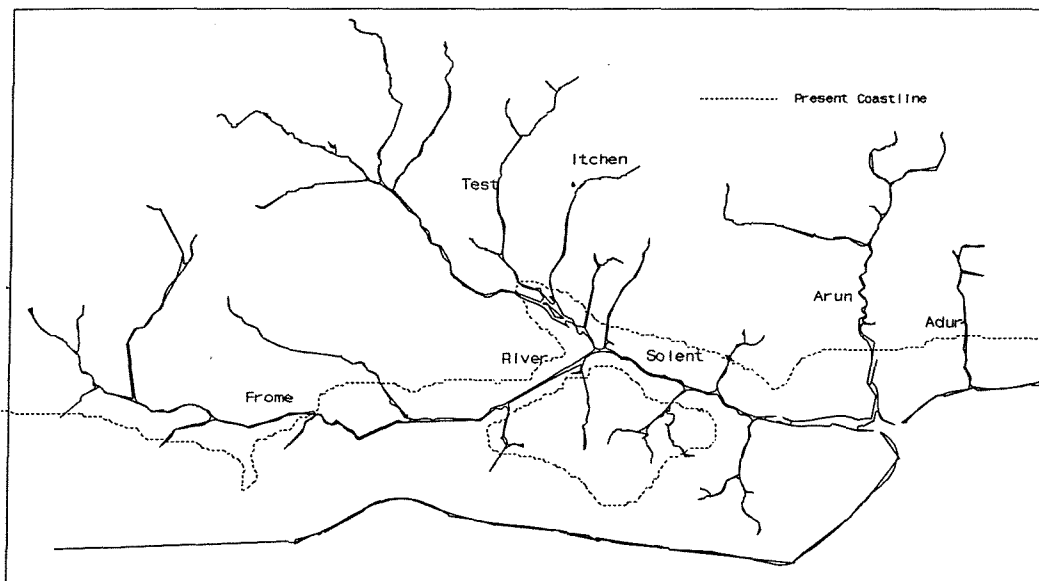


Figure 3.2 : *Reconstruction of the Solent River, at a time of lowered sea level (after Melville & Freshney, 1982).*

On the basis of an examination of the gravel terraces, Nicholls (1987) has concluded that the Solent River migrated south during the Pleistocene. Likewise, Dyer (1975) has suggested that the Solent River System was incised to a base level of at least -46 m O.D; it flowed to the east, determining the location of the buried channels of the Solent (Figure 3.3). The Flandrian transgression separated the Isle of Wight from the mainland and drowned the lower reaches of the tributary streams, which are the Keyhaven, Lymington, Beaulieu, Test, Hamble, Yar, and

Medina Rivers and Wootton Creek. Portsmouth, Langstone, Brading and Newtown harbours were produced, by the drowning of broad and unconfined valleys. The region is underlain, therefore, by extensive Eocene, Oligocene, Pleistocene and Holocene sediments (Figure 3.4 (a) and (b)).

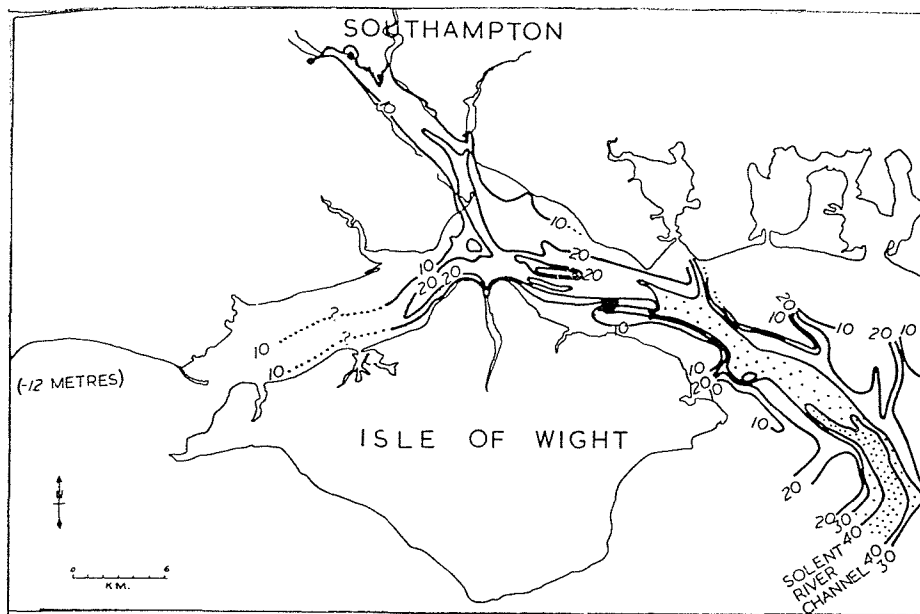


Figure 3.3 : *The buried channel of the Solent River showing the sub-Pleistocene surface in meters below Ordnance datum (after Dyer, 1975; West, 1980).*

Pre-Pleistocene Strata

The Upper Chalk is the oldest unit underlying an extensive area of Portsmouth, Langstone and Chichester Harbours. Reading and London Clay Formations are the successive series exposed at Alum Bay; they underlie both Langstone and Chichester Harbours. The Bagshot Formation comprises sand and pebble beds and succeeds the London Clay Formation. The Bracklesham Formation underlies extensive areas of Southampton Water, the Solent and Spithead (West, 1980); it contains glauconitic and pyritic sands, sandy clays, clayey sands and molluscan remains. Above it is the Barton Clay Formation, a blue-grey illite and montmorillonite clay which is exposed at Fawley Power Station. The next member

of the depositional sequence is the Barton Sand Formation, which occurs under Spithead, the East Solent and the eastern part of the West Solent; it is exposed between Calshot Spit and Stone Point (West, 1980).

The overlying strata are largely marls, soft limestones and sands; these contain ostracod, mammal, reptile and fish remains and comprise the Headon, Osborne, Bembridge and Hamstead Formations. The deposits occur mainly beneath the shorelines of the mainland, but are exposed along the northern coastline of the Isle of Wight (West, *op.cit*).

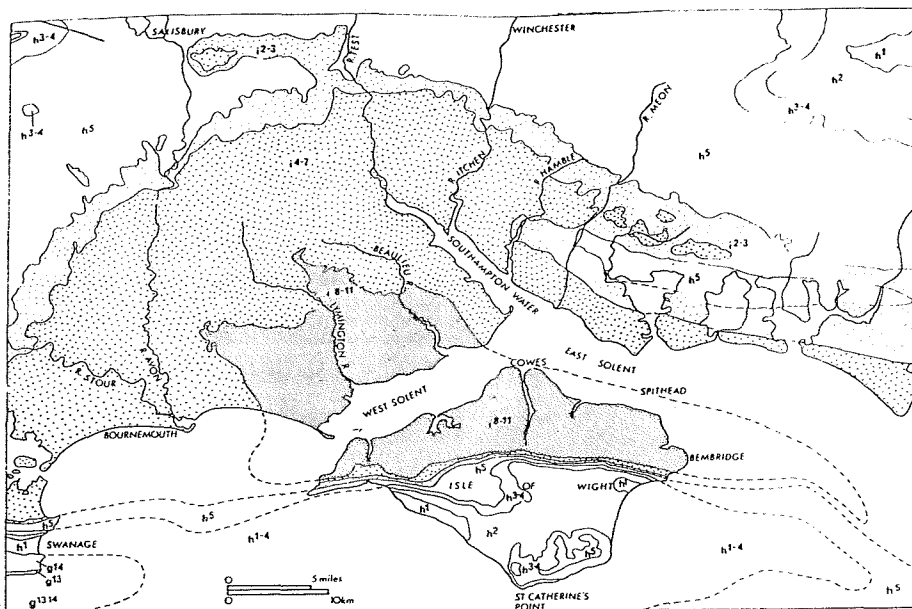


Figure 3.4 (a) : Geological Map of the region around the Solent System (from West, 1980) Symbols: g¹³⁻¹⁴ Portland Purbeck Groups; h¹ Wealden; h² Lower Greensand; h³ Chalk; i²⁻⁵ Reading Beds and London Clay; i⁴⁻⁷ Bagshot, Brackelsham and Barton Beds; and i⁸⁻¹¹ Headon Formation.

Pleistocene Deposits

The most common of the Pleistocene deposits are subangular flint pebbles in matrices of brown, limonite-stained, coarse sands. These deposits lie on a series of terraces around the estuaries (West, *op.cit*).

Interglacial mud and beach deposits surround the estuaries in the Portsmouth

and Chichester areas, and the Isle of Wight.

Holocene Deposits

Spithead, the East Solent and Calshot Spit are sites of extensive Holocene marine shingle and sand deposits. Hodson & West (1972) found that the deepest Holocene deposits lie beneath Calshot Spit, which is about 21 m below O.D; they are mainly blue-grey, pyritic clays with a high organic matter content. Within the more sheltered parts of the estuarine system, fine-grained, organic-rich sediments are developed.

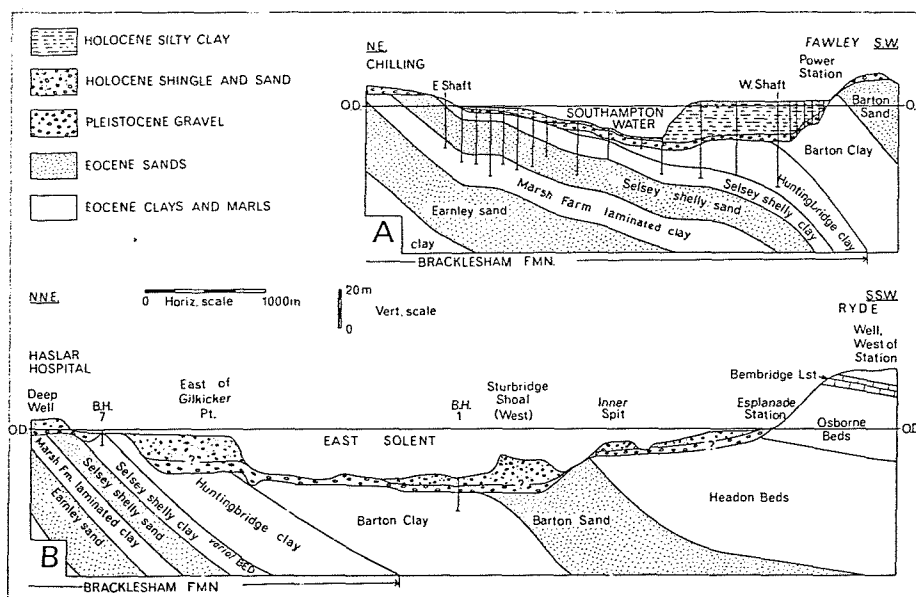


Figure 3.4 (b) : *Vertically exaggerated, transverse section of strata beneath the Southampton Water and the East Solent (from West, 1980).*

3.3. Oceanographical Setting

This section describes briefly the main water circulation patterns of the Solent Estuarine System.

The tidal features of the Solent are very complex and are controlled by the

tidal characteristics of the English Channel (Webber, 1980). Tidal currents in the West Solent are much faster (up to 3.9 knots - 2 ms^{-1}) than in the East Solent (up to 2.5 knots - 1.3 ms^{-1}) (Figure 3.5). These values attribute to the average current over a depth of about 9 m; surface currents should be higher. High and low water occur slightly earlier in the West Solent than in the East Solent and Southampton Water (SHELL 1985). There is a long period of "still stand" around high water, extending over about 3 hours. The ebb currents are faster than the corresponding flood currents; they provide, therefore, a mechanism for the flushing of silt and associated contaminants in a seaward direction.

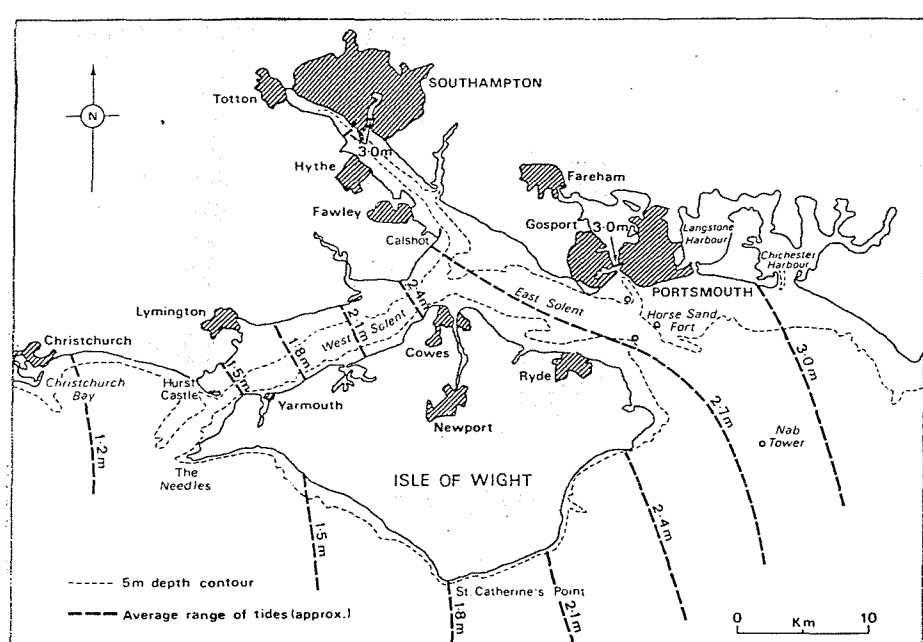


Figure 3.5 : Mean tidal ranges over the study area (from Webber, 1980).

The tidal prism of Southampton Water is $1.03 \times 10^8 \text{ m}^3$ and $5.31 \times 10^7 \text{ m}^3$ for spring and neap tides, respectively (Westwood, 1982). The amount of water entering and leaving the West Solent is $900 \times 10^6 \text{ m}^3$ (springs) and $550 \times 10^6 \text{ m}^3$ (neaps), whilst comparable values for the East Solent are $650 \times 10^6 \text{ m}^3$ (springs) and $430 \times 10^6 \text{ m}^3$ (neaps) (Webber, 1980). The net change in tidal volume is 540×10^6 on a spring tide and $270 \times 10^6 \text{ m}^3$ on a neap for the Solent (Webber, *op.cit*): 20% of

this total volume is contributed by Southampton Water. The volume of water entering and leaving is higher in the West Solent (Hurst Spit) than the East (Ryde-Gilkicker). There is, therefore, a considerable throughput of water (Webber, 1980). A westward-flowing current is present during the high water stand, with an eastward current over low water (Dyer & King, 1975). Overall, this causes a total transport of water towards the west throughout a tidal cycle. Dyer & King (*op.cit*) have suggested that the Solent flushes out intermittently towards the west on spring tides, and to the east on neaps. The flushing time has been calculated as 6.25 days, by dividing the total volume of the Solent ($27 \times 10^8 \text{ m}^3$) by the residual transport (5000 m^3). The flow is along the line of the central axis in the East Solent whereas, on the margins, eddies prevail at certain states of the tide and local flows occur in and out of the estuaries (Medina Estuary, Wootton Creek, Southampton Water and Portsmouth Harbour) (SHELL, 1985). In the West Solent, the tidal currents flow essentially parallel to the channel axis. The tidal currents flood towards the east and ebb towards the west, of the Solent Estuarine System. Recent alterations made to the environment, by reclamations and dredging have not changed the tidal prism (Webber, *op.cit*).

Wave regime is considerably variable, depending upon the geographical setting (Webber, *op.cit*); wave heights and periods decrease, in comparison to that outside of the Solent (SHELL, 1986). Southampton Water and most part of the Solent region are well sheltered by the presence of the Isle of Wight (Gao & Collins, 1991) (Figure 3.6). Significant wave heights (the "significant" wave height is the average of the highest third of the waves in any period of the record, usually about 20 min) within the Solent are generally less than 3 feet (0.9 m), whilst 6 feet (1.8 m) in the offshore (SHELL, 1986) and are of over 1.2 m in the vicinity of Lee-on-Solent during the autumn and winter months (Webber, *op.cit*). Local variations in wave climate occur in particular locations, such as sand banks in the East Solent, due to the varying degree of exposures. Wave-current interactions are more noticeable in the West Solent than the East Solent, on account of the strong tidal currents in the West Solent. In Christchurch Bay, southwesterly waves are domi-

nant. On the eastern side of the area, wave activity decreases in a westerly direction from Selsey Bill to Gilkicker Point (Gao & Collins, 1991). Southwesterly waves are refracted due to the presence of the Isle of Wight and then approach to Hayling Island from a more southerly direction (Whitcombe, 1991).

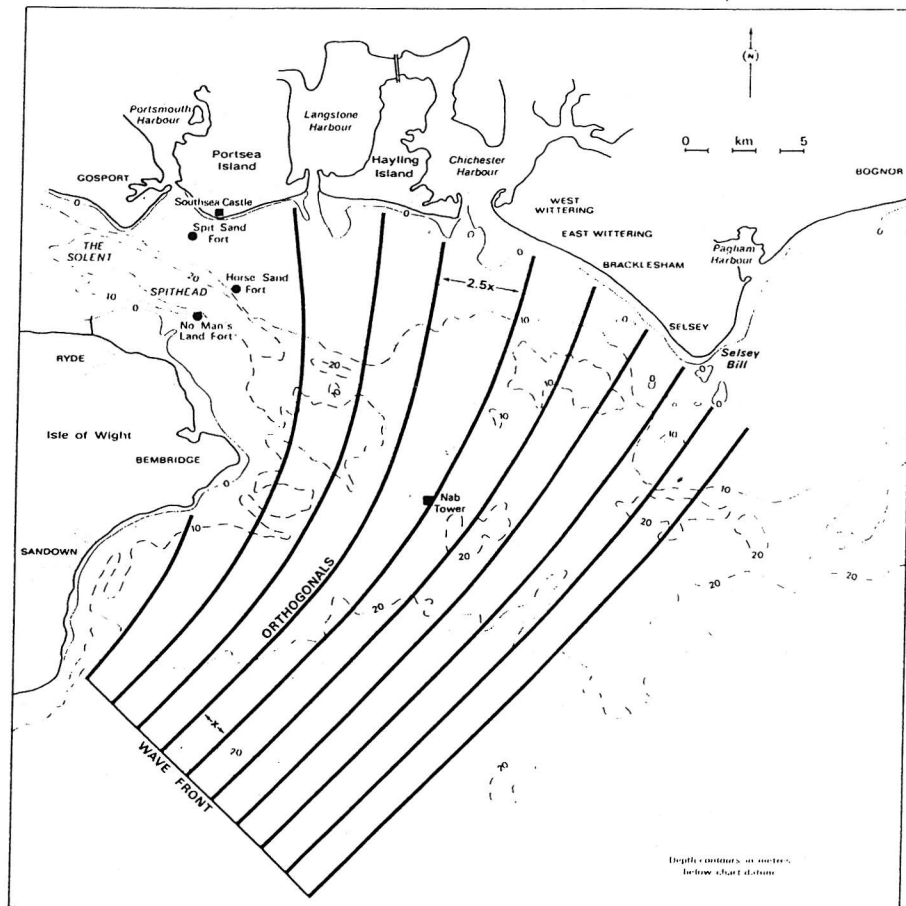


Figure 3.6 : *Refraction patterns of waves from SW, to the east of the Isle of Wight (from Webber, 1979).*

Measurements of salinity in the water column show there to be stratification in the upper reaches of the estuaries. In contrast, partially mixed and well mixed patterns occur in other areas of the system (Webber, 1980). The mean surface salinities are about 34.3 ‰, being slightly greater in the Spithead and western entrance, and slightly less in Southampton Water (Phillips, 1980) (Figure 3.7). The mixing of the Test and Itchen estuarine waters into Southampton Water is more

dependent upon fresh water discharge than tidal range (Ashraf, 1982). Itchen and Test rivers contribute 45 % of the total freshwater input of the Solent region to Southampton Water (Webber, 1980). Stratification is developed at the mouth of the Test, with surface salinities being lower on the west side at the confluence of the Test and Itchen. Salinities of less than 30 ‰ occur in the upper reaches of Southampton Water and in the most of the other tributary inlets within the area (Phillips, 1980). Iriarte (1991) has reported that the vertical distributions of salinity and temperature indicate the water column to be well mixed, at high tide at Calshot Spit. Spithead has a salinity in average of 34.5 ‰, more exposing to the open sea (Phillips, *op.cit*).

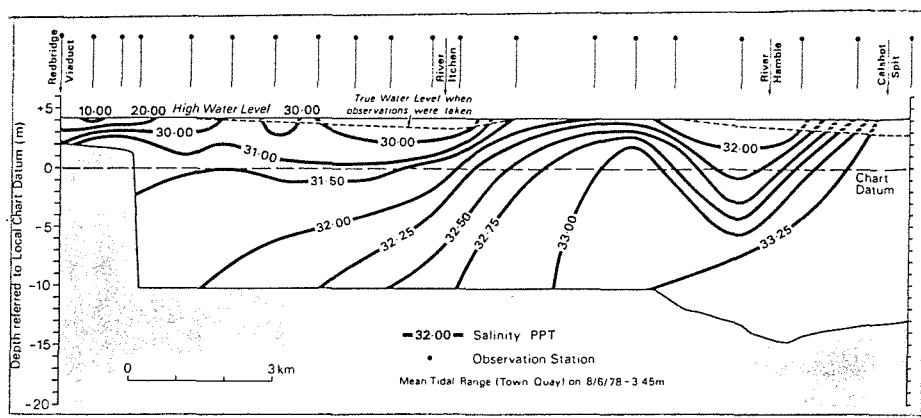


Figure 3.7 : Longitudinal distribution of salinity in Southampton Water (from Webber, 1980).

The temperature variations of the surface waters range from 14°C to 21°C, between summer and winter (Carr *et al.*, 1980). On average, Southampton Water is some 1°C warmer than the Solent. The mean water column temperature from January to October varies between 8.4°C and 20.8°C; it is always slightly higher at Netley than at Calshot Spit (Iriarte, *op.cit*).

The temperature distribution is homogeneous, with depth, throughout most of the year. The river waters are cooler than sea water in winter, and warmer in

summer. The river discharge influence is small, however, in relation to the spring tides in Southampton Water. Hence, in the deeper waters of the system, diurnal temperature variations are small, in the shallow waters, larger variations are produced by the drainage of heated or cooled water from intertidal mud flat areas (Carr *et al.*, 1980).

3.4. Coastal Forms of the Solent Estuarine System

The coastal forms of the Solent Estuarine System are varied, reflecting the different sediment types and energy levels along the coast (SHELL, 1985). The different coastal forms and their occurrence are outlined below and shown on Figure 3.8.

CLIFF COASTS: these are found along the western coastline (The Needles) and the eastern coastline (Culver Cliff) of the Isle of Wight.

BOULDER BEACHES: these occur between Lee-on-Solent and Langstone Harbour, from Newtown Creek to Wootton Creek on the northern coastline of the Isle of Wight, at Hurst Spit on the mainland, and to the east of Yarmouth on the Isle of Wight. Some of these boulder beaches are mobile, whilst others are inactive.

SAND and SHINGLE BEACHES: are exposed frequently between Hurst Spit and Chichester Harbour and from the River Yar to Wootton Creek on the Isle of Wight. This type of shoreline is exposed to high wave energy and is considered normally to be the most mobile of the coastal sediments present over the region.

SAND BEACHES: these occur from Portsmouth Harbour to Selsey Bill with the size range varying from fine- to coarse-grained sands.

INTERTIDAL MUDFLATS: which are located within the sheltered areas of the inlets or estuaries. Such areas include Southampton Water, Portsmouth, Langstone and Chichester Harbours, the Lymington and Beaulieu river inlets, and Newtown and Wootton creeks.

INTERTIDAL SALTMARSHES: these occur between Hurst Spit and Lymington, in the vicinity of the Beaulieu estuary, and within Langstone and

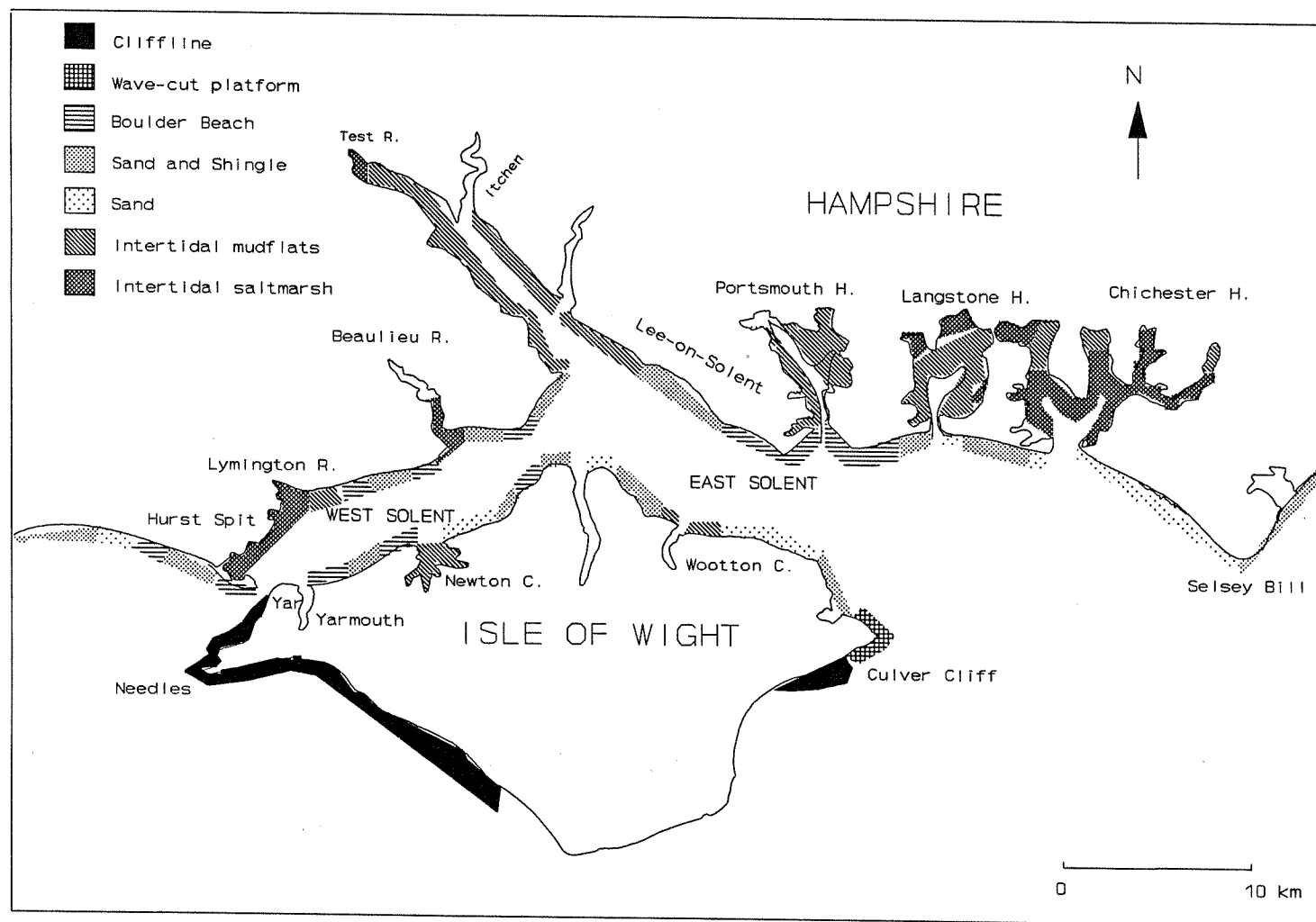


Figure 3.8 : Coastal types in the Solent region (after SHELL, 1985).

Chichester Harbours. They consist of intertidal flat deposits which are covered with vegetation. The two types of saltmarsh which are present in the Solent region are the *Spartina* marsh and the mixed saltmarsh (SHELL, 1985).

3.5. Inlets of the Solent Estuarine System

The total catchment area of the Solent drainage network is 3000 km², to which the Rivers Test and Itchen contribute 45% of the total inflow (Webber, 1980). The River Test discharges about 25 m³s⁻¹ in winter, and 6 m³s⁻¹ during summer. The flow of the River Itchen is about half that of the River Test, whereas the flow contributed from the River Hamble is negligible.

3.5.1. The River Test

The Test estuary is approximately 8 km in length (Figure 3.9) (Westwood, 1982). The average flow is ~ 12.8 m³s⁻¹ with a lowest flow is of 4.7 m³s⁻¹ (Wooley, 1973). The topography of the estuary has been altered in response to dredging activities and a large area of land has been reclaimed in the upper region (Romans, 1979). The 10 m dredged channel ends in the vicinity of Millbrook, and the mudflats at the side of the channel are exposed at low water; hence, runoff is confined to the channel at this state of the tide. The Test estuary is well mixed at its mouth, becoming partially mixed towards its head and with increasing stratification. Reduction in the width of the estuary restricts the movement of water in the deeper part of the channel, but the upper limit of the salt intrusion moved recently upstream.

3.5.2. The River Itchen

The River Itchen forms the northeastern tributary of Southampton Water (Figure 3.9); it is ~ 8 km in length and has a tidal limit at Woodmill

(Westwood, 1982). The river shape has been subjected to less modification than the Test (Phillips, 1980). The water column displays a more "natural" salinity regime, with fairly regular longitudinal salinity gradients. The average freshwater flow is $5.5 \text{ m}^3\text{s}^{-1}$ and the lowest flow is $2.7 \text{ m}^3\text{s}^{-1}$ (Wooley, 1973).

3.5.3. The River Hamble

The Hamble tributary enters Southampton Water along the eastern margin (Figure 3.9), approximately 2 km upstream of the estuary mouth (Westwood, *op.cit.*). The river is shallow and is floored by sand and gravel. The tidal limit is at Botley Mill, whilst the mouth of the Hamble is protected by a long shingle spit and shell banks (Dyer, 1969).

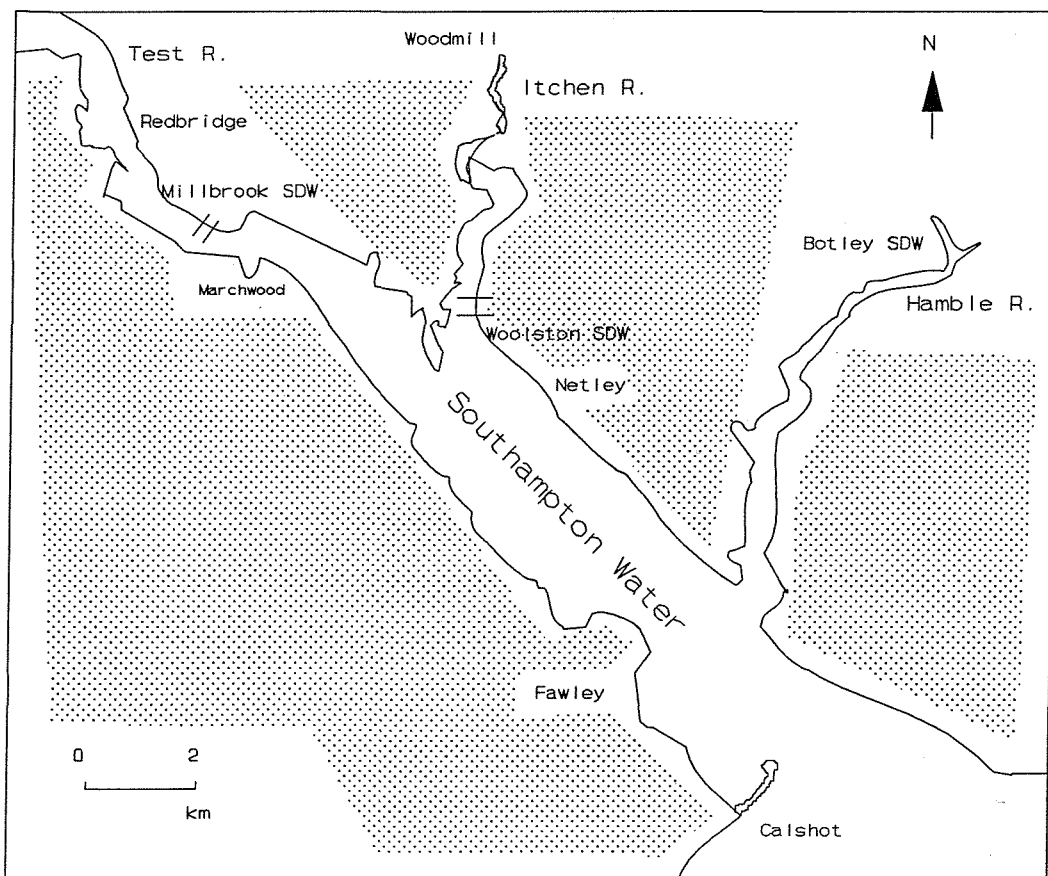


Figure 3.9 : The Rivers, Test, Itchen and Hamble.

3.5.4. The River Beaulieu

The river is situated in the southeastern part of the New Forest and flows into the West Solent (Figure 3.10). The upper part of the estuary varies in width from about 30 to 80 m, whilst the mouth, which connects it to the West Solent, is 3 km wide. The estuary is about 9 km long and is relatively shallow, with water depths in the channel ranging from about 1 m to 8 m. The upstream limit of salt intrusion can reach into the pond at Beaulieu at high tide (Sealey, 1987). The waters over much of the estuary are homogeneous and vertically mixed. However, at the head of the estuary, there is significant stratification in the waters.

3.5.5. The River Lymington

The River Lymington flows into the West Solent, opposite the western end of Isle of Wight (Figure 3.10). Average salinities at high water are ~ 30 ‰ (Phillips, 1980). The mouth of the estuary is covered by extensive areas of saltmarsh.

3.5.6. Estuaries of the Isle of Wight

Yarmouth is the most westerly of the estuaries, located on the northern coastline of the Isle of Wight. This estuary covers an area of 1.5 km and is tidal for a distance of some 3 km. whereas, Newtown estuary is situated between Yarmouth and Cowes; it has a narrow mouth, which broadens into a complex series of marshes and creeks. The Medina Estuary is located centrally on the Isle of Wight (Figure 3.10). It is ~ 7 km in length and has a width which varies from 0.5 km at its mouth, to less than 100 m within the upper reaches. Salinities throughout the water column vary from almost zero to 30 ‰, over the complete tidal cycle (Phillips, *op.cit.*). Wootton Creek is the most easterly of the estuaries of the Isle of Wight; it has a short inlet, some 2 km in length.

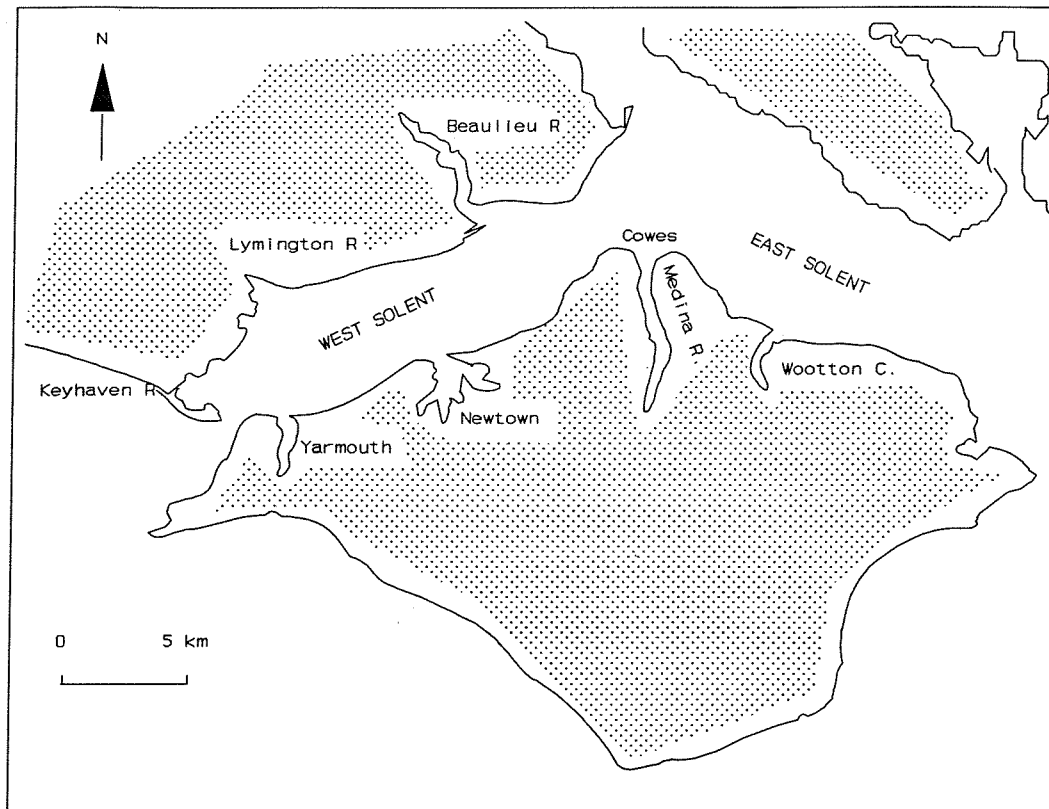


Figure 3.10 : *Isle of Wight and the Rivers Beaulieu and Lymington.*

3.5.7. Harbours

Portsmouth, Langstone and Chichester harbours are tidal inlets and consist essentially of extensive intertidal flats and saltmarshes (Figure 3.11). Portsmouth Harbour is used as a Naval Dockyard and receives a large discharge of sewage effluent (Soulsby *et al.*, 1978). The main concentration of sewage is confined to the western side of the Harbour. Reclamation here has caused a reduction of $\sim 6\%$ of the tidal prism (Westwood, 1982). Langstone and Chichester Harbours both have well developed tidal deltas at their mouths (Dyer, 1980).

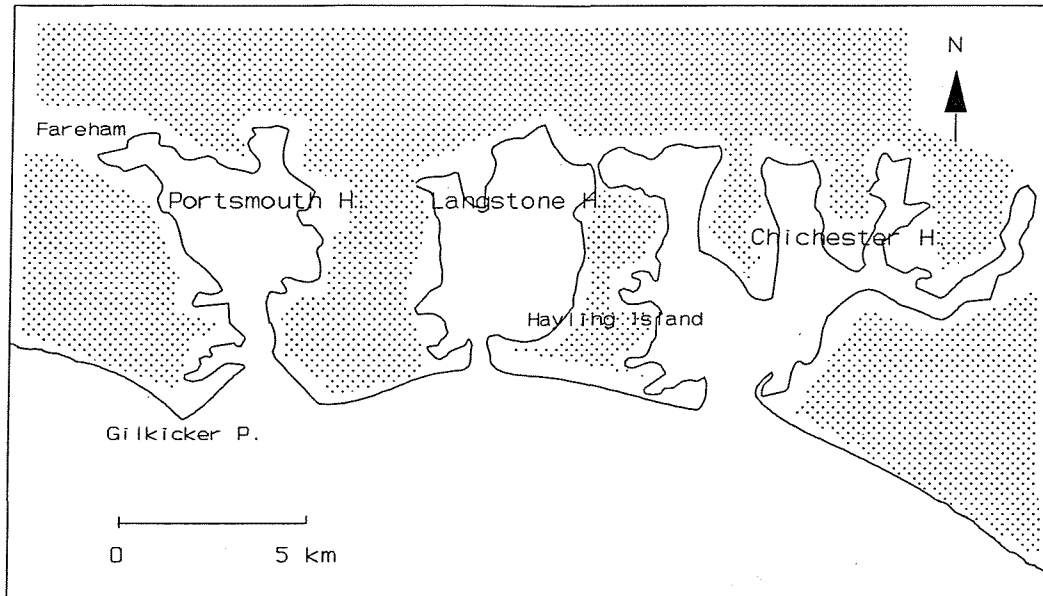


Figure 3.11 : *Portsmouth, Langstone and Chichester Harbours.*

3.6. Seabed Configuration and Sediment Types

Within the Solent, the water depths are generally about 15-25 m (Figure 3.12). The maximum depth, of more than 60 m, is located between Hurst Spit and the Isle of Wight (Dyer, 1969). The main channel of the Solent widens eastward, to a maximum of 2 km; it is bounded by the 12 m contour. The depth of the channel increases to 18-20 m towards the east; it remains about 2 km wide until just to the south of the Beaulieu River. The overall width between the Stansore and Egypt Points is 2.5 km, broadening to 6 km in the East Solent. The main channel to the east, which is bounded by the 10 m contour and runs north-west, is 2-2.5 km wide and 20 to 30 m deep as far as Gilkicker Point (Lonsdale, 1969). The channel divides to the northwest and shallows towards Portsmouth Harbour. At Gilkicker Point, the channel is constricted to 1.5-2 km between the headland and Sturbridge Shoal.

In the East Solent, the seabed configuration consists of hummocky dunes and narrow trains of sand and gravel waves on the edges of a series of banks (Dyer,

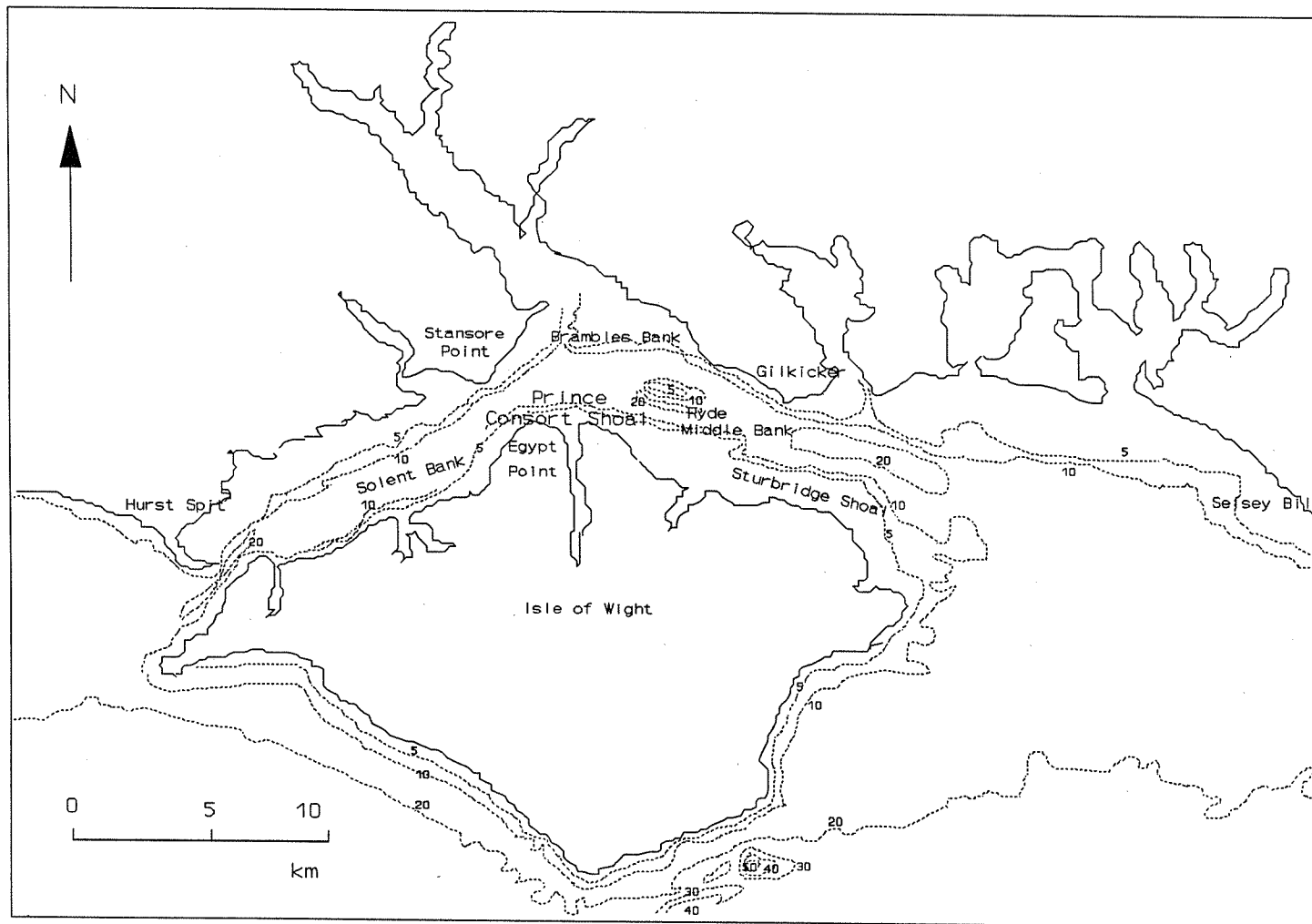


Figure 3.12 : *Generalized bathymetric chart of the Solent region (based upon BGS, 1988): contours in meters.*

1980). There are three main banks within the Solent; the Solent Bank in the West Solent; the Brambles Bank, at the confluence of the East and West Solent and Southampton Water; and the Ryde Middle Bank, to the south of the Brambles Bank (Dyer, *op.cit*). The Brambles Bank is situated to the north of the Cowes Roads and is exposed at low water spring tides. Ryde Middle Bank is a linear bank, to 4 km length by 800 m wide, rising to a height of 3 m above the surrounding sea bed. The bank is composed of Tertiary bedrock and is covered with a thin sediment layer, dipping towards the south; it may have a marked control on water circulation and sediment patterns in the East Solent (Dyer, *op.cit*). To the south of this bank, the channel is 1 km wide and its depth increases westwards from 15 to 25 m (Lonsdale, 1969). In the West Solent, low amplitude gravel waves and sand dunes (1-2 m high, 10-20 m long) have been observed (SHELL, 1985; Dyer, 1971). Dyer (*op.cit*) has reported that the sand dunes were moving in different directions, on opposite sides of the channel. Lonsdale (*op.cit*) and Dyer (1969) both described bedrock exposures on the seabed in the East Solent.

Summers (1983) has noted the presence of limestone boulders around Selsey Bill and has suggested that their origin was related to floating ice, during a post-glacial period. In Southampton Water, linear erosional furrows have developed as a result of current activities and secondary flows (Dyer, 1970). Powell (1977) considers that the furrows are positionally stable and are a widespread feature in Southampton Water. Fine-grained sediments with a high moisture content, clayey-silt to silty-clay, seems to be the type of sediment associated with the development of the furrows.

The sediments of Southampton Water and the East Solent consist mainly of sandy muds or muds with extensive patches of sand at the mouths of the estuaries and on some of the banks (SHELL, 1980). The recent sediments of Southampton Water are underlain by a continuous layer of Pleistocene Valley Gravel and, at some locations, a thin layer of peat deposited during the Tertiary or Pleistocene (Hodson & West 1972; Barton, 1979).

3.7. Recent Sedimentation and Sediment Transport

On the basis of seismic profiling in the Solent area, the thickness of recent sediment is less than 2 m (Dyer, 1980). The West Solent is floored predominantly by gravel, containing various proportions of coarse sand. An exception to this generalization lies at the northern side, where intertidal mud flats are present between Lymington and Hurst Spit (Figure 3.13).

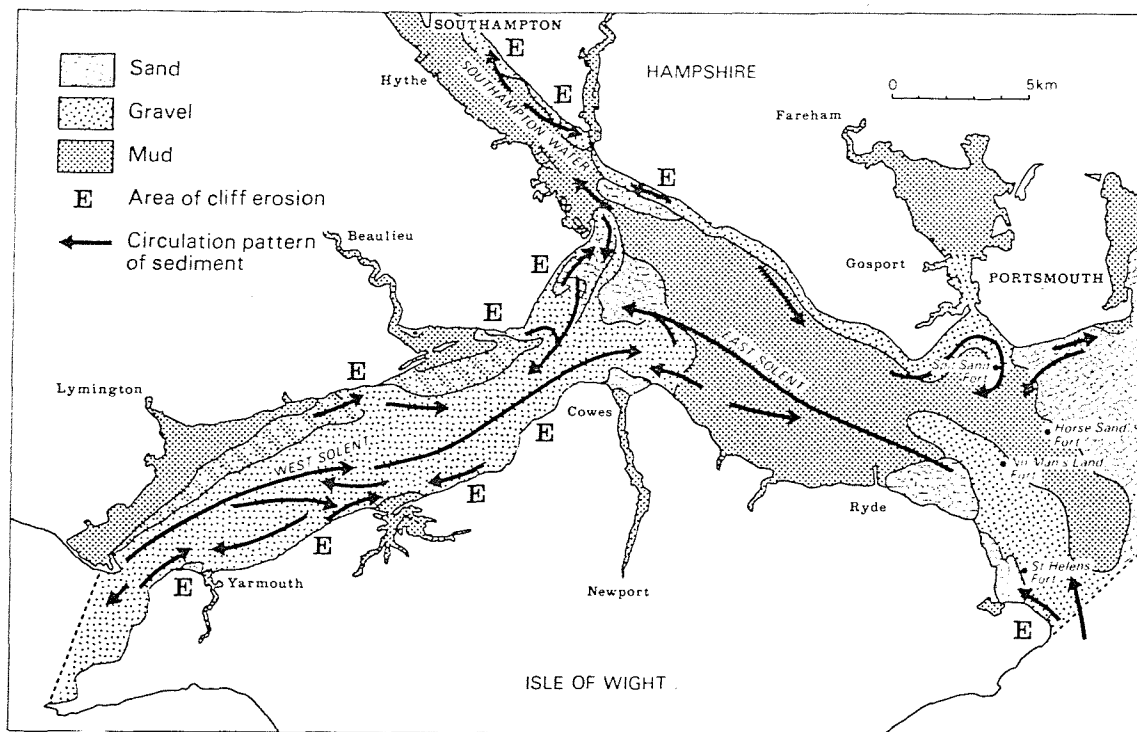


Figure 3.13 : *Recent sediments and sediment circulation in the Solent (from SHELL, 1985).*

The recent sediments of the East Solent and underlying most of Southampton Water are mud or sandy mud. The coarsest material occurs off Gilkicker and in the tidal channel of Portsmouth Harbour (Lonsdale, 1969). The main channel of Gilkicker Point is floored by silt. From Selsey Bill to Portsmouth Harbour, well-sorted sand and gravel are confined to the beaches, whilst poorly-sorted gravel and sand with some muddy material occur in the offshore area (Harlow, 1982). Chichester and

Langstone Harbours are covered mainly by muddy sediments. Sand and gravel are present near the harbour entrances, whereas Ryde Middle Bank consists of fine sand. Some of the mud in the inlets may be fluvially derived, but the greatest proportion has been derived probably from a seaward source, entering during estuarine circulation and exchange with marine waters (Dyer, 1980).

Sediment movement as bedload in the Solent is deduced on the basis of interference from either end of the system (Figure 3.14) (Dyer, *op.cit.*). The transport of sediments in suspension is relatively insignificant due to the low concentrations of suspended sediment present in the waters. However, seasonal fluctuation of the suspended sediment is very apparent; increasing in winter to a maximum of five times that of the summer (Srisaengthong, 1982). This is due to the minor influence of seasonal variables such as, river discharge, rainfall and wind. The probable source for suspended load might be in Christchurch Bay and the additional Needles Spoil Ground where sewage sludge and dredging spoil have been dumped every winter. Surface concentrations of suspended sediment distribution is the time dependence over a tidal cycle. The concentration is increased with tidal velocity and vice versa due to the effect of turbulent mixing of sediment into the upper layers from the lower. In the West Solent, sediment from the deeper part of the water column is brought up to the surface during the times of maximum flood and ebb streams. Whilst tides slacken, the surface sediment is allowed to settle deeper. The same process occurs in the East Solent, but since tidal streams are weaker, sediment might settle to the bottom. Srisaengthong (*op.cit.*) found 20-50 mg/l suspended material within the water column during October-February, with 5-25 mg/l during March-September in the West Solent.

Longshore transport of sediments is more intensive in the East Solent than in the West Solent. In the West Solent and on the northern side of the East Solent, the predominant longshore transport direction is towards the east (Dyer, *op.cit.*). Harlow (1979, 1982) has determined the net sediment transport along the coastline, between Selsey Bill and Gilkicker Point. This section is a self-contained coastal unit, dominated by westerly littoral drift; this is caused by the refraction of waves

approaching from the south-west, around the Isle of Wight. Within this general longshore transport pattern, variations associated with the tidal inlet systems are also significant. At the entrance of each of the tidal inlets, the longshore drift is directed towards the tidal basin on both sides, indicating that the westerly longshore drift is confined by the tidal inlet system. From the River Hamble to the entrance of Portsmouth Harbour, however, easterly littoral drift is dominant (Harlow, 1982).

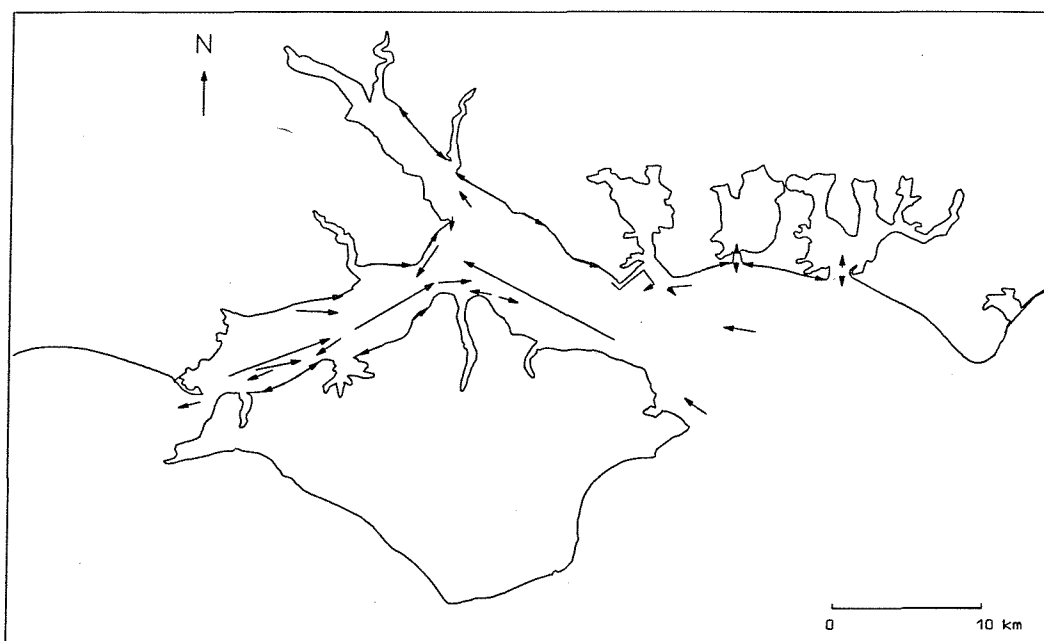


Figure 3.14 : *Sediment transport patterns (bed load) in the Solent (after Dyer, 1980).*

The main mode of sediment transport is as bedload, where a rate of 8×10^5 g cm⁻¹s⁻¹ has been calculated for Stansore Point (Dyer, 1980). From Christchurch Bay in the west, sand and gravel are transported to the east by recirculating eddies. Gravel transport ceases off Cowes. Coarse sand accumulates on Prince Consort Shoal, whereas medium sand accumulates on the Brambles Bank. Sand and mud entering from the east end of the region passes to the north.

The prevailing transport direction in the East Solent is from the southeast, towards the west (Lonsdale, 1969). Houghton (1986) has suggested a transport pathway similar to those of Dyer, on the basis of an examination of reworked

coccoliths. The mud deposited in the East Solent is carried into the estuaries during normal estuarine circulation, deposited during the long high water stand.

3.8. Reclamation and Dredging

Areas of mudflats and saltmarshes have been reclaimed from the sixteenth century until the beginning of the nineteenth century, mainly for agricultural purposes; this is a practice which continues today (Tubbs, 1980). Within Southampton Water, some 340 ha of mudflats have been reclaimed for development of the docks; approximately 350 ha on the western shore have been reclaimed, for Fawley Refinery and Calshot Power Station. Likewise, some 240 ha in Portsmouth and 72 ha in Langstone Harbours, respectively, have been reclaimed. There is little evidence that reclamation has affected the salinity regime of Southampton Water, although siltation may have been accelerated in some areas (Coughlan, 1979).

In Southampton Water, the rate of maintenance dredging is about $380,000 \text{ m}^3\text{y}^{-1}$ (Dyer, 1980). The approach channel to the docks has been dredged, for deepening (to 10 m) and widening (to 300 m) (Webber, 1980). The Test Estuary has also been dredged to a depth of 11.7 m. There are many commercial dredging activities for sand and gravel in the West Solent.

3.9. Effluent Discharges

Millbrook Sewage Works (for location, see Figure 3.15) is the largest input to Southampton Water (Wooley, 1973), discharging $0.84 \text{ m}^3\text{s}^{-1}$ into the Test estuary out of the Western Docks. Woolston Sewage Disposal Works discharges into the Itchen, at the mouth of the estuary, at a rate of about $0.16 \text{ m}^3\text{s}^{-1}$. Southampton Water and the West Solent receive thermal discharges from the Marchwood and Fawley Power Stations and the Esso Refinery at Fawley (Carr *et al.*, 1980). Portsmouth Harbour receives a discharge at Fareham Creek, from the Fareham sewage works. The present volume of this particular effluent discharge is

$0.2 \text{ m}^3\text{s}^{-1}$ (Soulsby *et al.*, 1978), but the main concentration of sewage effluent is confined to the western side of the Harbour.

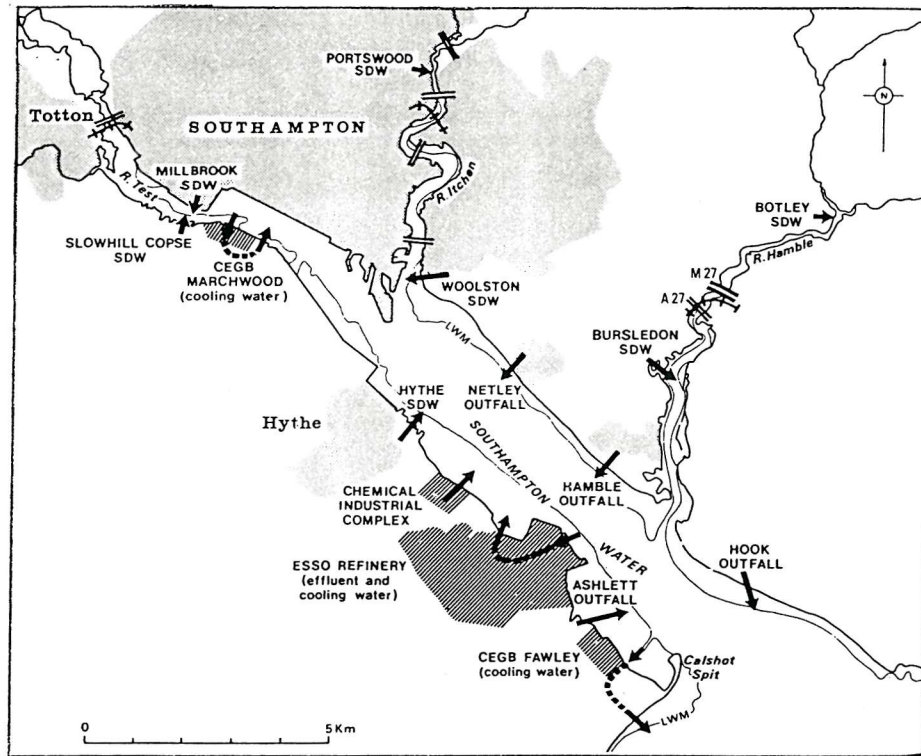


Figure 3.15 : Effluent discharges into Southampton Water and its estuaries (from Webber, 1980; Key; SDW: Sewage discharge water).

CHAPTER 4

METHODS & TECHNIQUES

4.1. Sample Collection/Field Sampling

Eighty-nine surficial sediment samples were collected from R.V. Labrax and R.V. Bill Conway, using a Van Veen grab sampler over a water depth of 3 to 20 m. The Van Veen grab sampler used in this study penetrates up to a depth of 15-20 cm of the bottom surface depending upon the texture of the sediments. A few samples were collected manually in the inlets and estuaries at low tide (*i.e.* samples H1, H8, H9, H14, H16, H19, H22, R1, R2, R3, R4 and R5). All the sampling locations are displayed on Figure 4.1. Sampling was carried out during April and August 1990, and June/July 1991. The sampling sites may be assembled into four groups:

- (i) the West Solent (Sample Nos. 1 to 3);
- (ii) Southampton Water (Sample Nos. 4 to 13);
- (iii) the East Solent (Sample Nos. 14 to 32);
- (iv) the inlets (Sample Nos. R1 to R35); and
- (v) the harbours (Sample Nos. H1 to H23)

Three supplementary samples were collected upstream within the Rivers Test (RT), Itchen (RI) and Beaulieu (RB). The location of RI ($1^{\circ}21' \text{ W}$, $50^{\circ}58' \text{ N}$), which was collected some way along the River Itchen (in the Barton River) is not shown on Figure 4.1. RT and RB were collected from Redbridge and King's Hot Cottage, respectively. In addition, 6 core samples were collected with a Craib Corer along two sections, A-A' and B-B' (Figure 4.1). The technical details of Craib Corer (Craib, 1965) used in the sampling programme is presented in Appendix A1.

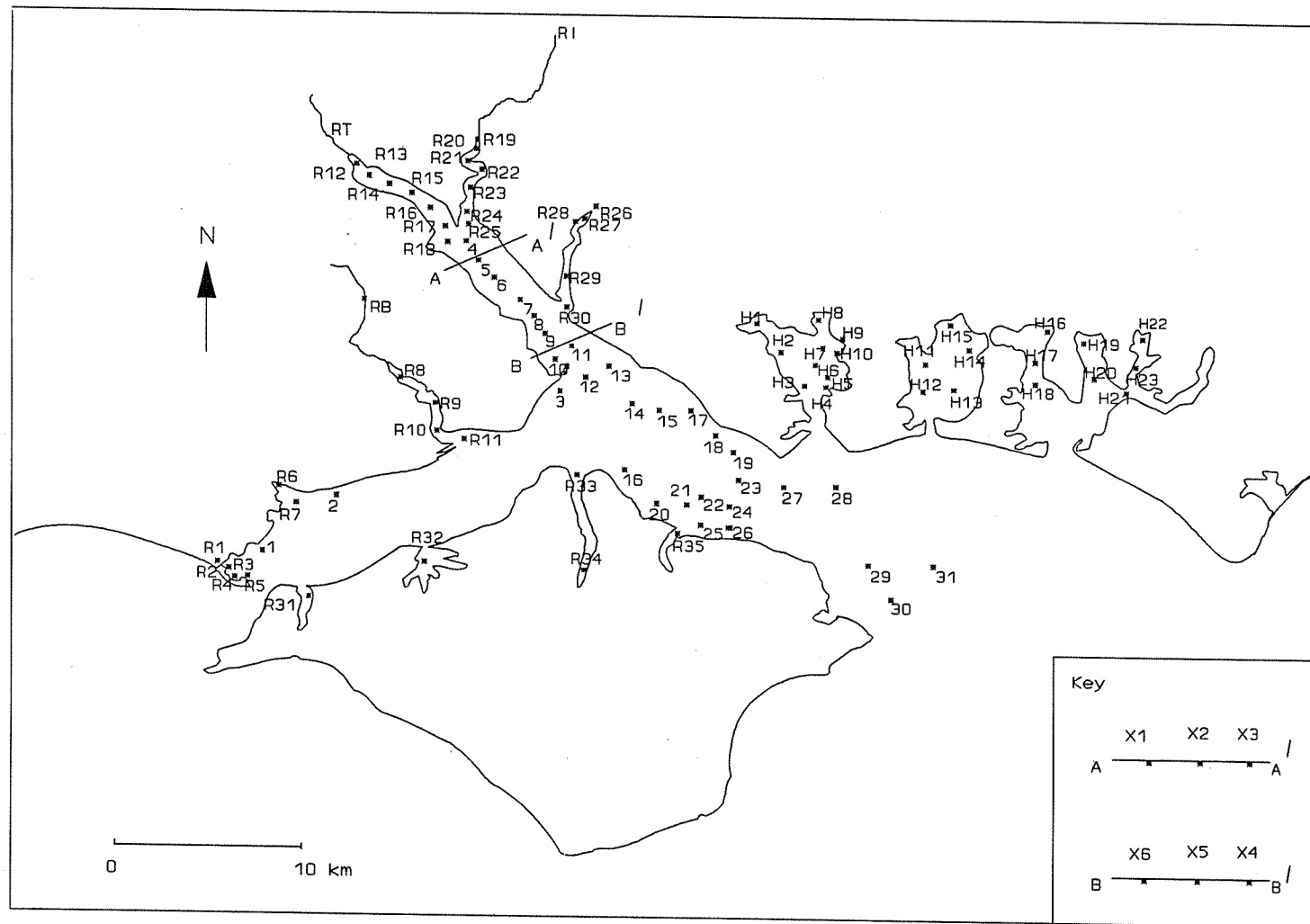


Figure 4.1.: *Sample Locations. Core sample (denoted by prefix 'X') locations are illustrated by lines A-A' and B-B'.*

The surficial sea bed samples were divided into sub-samples for the determination of grain size, clay mineralogy and the geochemical analyses. A 200g sample stored in a plastic bag, was used for grain size determination and clay mineralogy. A sample of $\sim 25 \text{ cm}^3$ ($\sim 12\text{g}$ dry weight) was taken, with a mini piston corer, extending to a depth of 10-12 cm, from the grab sampler for geochemical analysis.

Core samples were divided into 1 cm intervals. Each slice was placed in a separate plastic bag. All the samples were stored in a cold room, at 4°C .

Regional investigations of sediment characteristics are based often upon a grid pattern of sampling (Buller & McManus, 1979). For the present investigation, the sampling strategy was based upon an earlier description of muddy areas of the sea bed over the region, by Dyer (1980). This strategy was adopted on the basis of our interest in fine-grained sediment and its associated heavy metals, rather than other coarser sediments.

4.2. Analytical Methods

4.2.1. Analysis of Grain Size

Pretreatment of Samples

The majority of samples consisted of fine-grained material, silts and (mainly) clays. It was necessary to remove firstly the soluble salts, in order to achieve a well dispersed (homogeneous) mixture (Ingram, 1971; Galehouse, 1971; McManus, 1988). Salts cause the flocculation of clay-sized materials; thus, their presence might prevent the dispersion of the particles. To remove the salts, samples were agitated in distilled water, then allowed to settle. The clear supernatant was siphoned off and discarded. This procedure was repeated until the supernatant remained cloudy after standing for 24 hrs. Carbonates and organic matter were removed with 10-30% HCl and 10% H_2O_2 , respectively. These solutions were added to samples until effervescence had ceased (Ingram, *op.cit.*). Pretreatment was the most time-consuming part of the analysis, lasting over 5 to 6 days.

Dry and Wet Sieving

Pretreated samples were oven dried at 40°C, since it has been observed in many investigations that higher temperatures prevent subsequent dispersion (Ingram, 1971; Galehouse, 1971). Dried samples of between 20-50g were soaked in 0.1% Calgon for 24 hrs, to disperse the silt and clay materials. The sand and silt plus clay fractions of weighed samples were separated by wet sieving with a 63 μm sieve (Appendix B1). Analysis of the sand fraction was performed by dry sieving using standard A.S.T.M. sieves at $1/2 \phi$ intervals.

SediGraph

The fine fraction was analysed with the SediGraph Micromeritics 5100 Instrument, over the size range from 63 μm to 2 μm (*i.e.* 4 to 10 ϕ). The SediGraph determines the size distribution of particles dispersed in a liquid, assuming that Stokes' settling law holds for all particles (Stein, 1985). There are a number of publications addressing the use of the SediGraph in grain size analysis (*e.g.* Olivier *et al.*, 1970; Hendrix & Orr, 1970; Svarovsky & Allen, 1970; Welch *et al.*, 1979; Vitturi & Rabitti, 1980; Singer *et al.*, 1988; and Jones *et al.*, 1988). Technical details on the SediGraph are presented in Appendix A2.

The fine fraction was collected by wet sieving of a suspension at ~ 2 vol. % (*i.e.* $\sim 5\text{g}$ sediment per 100 ml liquid). Total dispersion was achieved by placing the solution in an ultrasonic bath for 10 mins, then mixing with a magnetic stirrer for 15 mins (Stein, *op.cit.*; Jones *et al. op.cit.*). This homogeneous solution was then poured into the mixing chamber of the SediGraph. The time required for the analysis of a sample was 3 mins. Precision of the measurements is $\pm 6\%$, as estimated from three replicate analysis of a sample.

4.2.2. Analysis of Clay Minerals

The clay mineralogy of the 92 surface samples was determined by X-ray diffraction (XRD), using the clay fraction ($< 2 \mu\text{m}$) of the samples, on a

Phillips PW 1130 instrument. Analytical details are presented in Appendix A3.

Pretreatment of samples

For good separation of the clay fraction, flocculation should be avoided (Hardy & Tucker, 1988; Brindley & Brown, 1980). Hence, samples were placed into 150 ml beakers and washed twice with distilled water. 1-2 ml of 10 % Calgon was added, in order to disperse the disaggregated clay particles. Samples were placed then into an ultrasonic bath for 10 mins. No attempt was made to remove carbonates and organic matter during the pretreatment of samples. The dispersed samples were allowed to settle for ~ 4 hrs (Appendix B1), in order to leave only the $< 2 \mu\text{m}$ fraction in suspension. Samples containing coarse material were wet sieved with a $63 \mu\text{m}$ sieve before sedimentation. The $< 2 \mu\text{m}$ fraction of all the samples was extracted by decantation; subsequently the suspension was centrifuged at 3400 rpm for 5 mins. A few ml of 10 % MgCl_2 were added to the solutions before centrifuging, in order to flocculate the clay particles. Excess MgCl_2 was removed by washing the solid in the centrifuge tube three times with deionised water. The clay slurry was removed from the centrifuge tube with a spatula and smeared onto three glass slides. Samples were examined as oriented smears, because clay minerals are generally platy and their basal reflections are enhanced in oriented mounts (Hardy & Tucker, *op.cit.*). The glass slides were air-dried and one of them was treated with ethylene glycol vapour for 24 hrs in a desiccator. The remaining slides were heated overnight, at either 375°C or 550°C .

X-Ray Diffraction

Samples were scanned from 2° to $40^\circ 2\theta$, at a speed of $1.2^\circ 2\theta$ per minute. Nickel-filtered Co K_α radiation was used. Peaks were identified from the XRD output by measuring the 2θ angle and converting onto lattice spacings by means of standard conversion tables. Smectite appears as a broad peak from 14 \AA to 15 \AA in the air-dried trace, which expands to $\sim 17 \text{ \AA}$ after glycolation. The presence of illite is shown by the 10 \AA peak, which is not affected by glycolation or

heating. Kaolinite is identified by a 7 Å reflection on the air-dried, glycolated and heated at 375°C traces. Heating at 550°C causes this peak to disappear. Chlorite was present in trace amounts and is identified on the basis of a ~ 14 Å peak, upon heating to 550°C. Heating to 375°C collapses the smectite to 10 Å, leaving the other clays unaffected. Heating to 550°C destroys the kaolinite and certain chlorites. The output of the glycolated traces were used for semi-quantitative determinations.

Semi-quantitative Analysis

Semi-quantitative analysis of the samples was based on the assumption that the four minerals constitute 100 percent of the clay fraction. The relative proportions of the clay minerals, illite, smectite, and the sum of kaolinite + chlorite, were estimated by comparing the peak areas of the basal reflections of the different clay minerals after glycolation of the specimen. Since chlorite was present in trace amount, no attempt was made to estimate separately. The estimation method utilised (Clayton, 1991) in this study was a modification of Biscayes (1965) method; smectite, illite and kaolinite were divided by factors of 2.5, 1, and 2, respectively (see Appendix 3). The precision of the method was $\pm 10\%$, as estimated from four replicate determinations of glycolated samples.

4.2.3. Analysis of Trace Metals

The analysis of certain major and trace metals was performed on total digestion extracts. Eighty (and four replicates) surficial sediments from Southampton Water, the East Solent, and the Rivers and Harbours were selected for total digestion. In addition, two core samples from Southampton Water were selected for sequential extraction. All sampling locations are displayed in Figure 4.1.

(a) Total Digestion Method

Total digestion was carried out to dissolve the silicate lattice and release all the associated metals. Elements such as Al, Fe and Li may be used for grain size normalisation of the data. The accuracy of the method can be assessed, by analysing reference materials certified for the total metal content. Intercomparable data, free from operationally-defined bias, can be obtained by careful analytical procedures (Loring & Rantala, 1989).

Pretreatment of Samples

All the apparatus was pre-cleaned by soaking in 50% HNO₃ for 24 hrs. Samples were extruded from the mini-piston core tubes and mixed with a plastic spatula in a glass mortar. A representative sub-sample was taken for subsequent total digestion, then dried. The remainder of the sample was used for grain size separation.

Grain Size Separation

Grain size separation was achieved by wet sieving with a nylon plankton net, of 63 μm mesh. Sand was collected on the sieve, transferred to a petri dish by washing with distilled water, and dried in an oven at $\sim 110^\circ\text{C}$. The 63 μm fraction was collected in a 300 ml beaker, washed with distilled water in order to remove salts, then placed in an ultrasonic bath for 15 mins to break up aggregates. Silt and clay fractions were separated by differential settling in distilled water, assuming that the settling particles obey Stokes' Law (Galehouse, 1971). After 3 hs 46 mins, the top 5 cm was siphoned off (Appendix B2). This mixture contained the clay fraction. Settling operation was not repeated until all the clay fraction siphoned off, and the remaining mixture was assumed to contain the silt fraction only. The silt fraction, therefore, contains some clay-sized material flocculated with silts. Both silt and clay mixtures were obtained by evaporating to dryness, in an oven at 110°C .

Total Digestion

All the dried samples were ground in a pre-cleaned agate mortar and 1 g was transferred to a teflon beaker. 10 ml of concentrated HNO_3 was added to the beaker and the mixture was warmed gently on a hot plate, for 30 mins. The HNO_3 has a pale colour when all organic material has been oxidised. After cooling, 5 ml of HF and 5 ml of HClO_4 were added. A teflon top was placed on the beaker and the solution was allowed to reflux on a hot plate for ~20 mins and stirred gently, on occasions. After observing dense white fumes, the cover was removed to allow the HClO_4 to evaporate. To further digest the resistant particles, 5 ml of HF was added and the mixture was allowed to reflux for a further 30 mins. The remaining solution was boiled to obtain a dry residue, which was redissolved with 10 ml of 1 M HCl, then diluted to 25 ml with 1 M HCl. This technique has been modified from that of Shaw *et al.* (1990).

Heavy metals (Cu, Ni, Zn, Cr, Pb, Co, Mn and Fe) were analyzed on a Pye Unicam SP9 Atomic Adsorption Spectrophotometer, by atomization with an air/acetylene flame- except for Al, which was determined by atomization with an N_2O /acetylene flame. The details of this technique are presented in Appendix A4. Sample concentrations were calculated as shown below:

$$\mu\text{g/g Metal} = \mu\text{g/ml Metal} \times \frac{\text{sample volume}}{\text{sample weight}}$$

Replicate samples were analysed, in order to establish the precision of the method. Additionally, a duplicate sample was separated into different grain sizes (sand, silt and clay) and, subsequently, totally digested (see Table 4.1 and 4.2).

The precision of the total digestion was 8-11 % (Table 4.1.), as determined from five replicates. However, the precision of the total digestion of the different grain sizes was variable; it was generally poor for the sand fraction (Table 4.2). The silt and clay-sized fractions were associated with precisions in the range of 2 to 20 % and 3 to 25 % respectively; for the sand-sized fraction, it was in the range of

1 to 140 %. Hence, determinations on the sand-size fraction were not reproducible for Co, Cu, Mn and Ni. A possible reason might be the presence of organic debris within the sand size fraction. This organic material (mainly plant debris) may be coated with metals and can cause the significant variations in metal content within the sand-sized fraction (Krumgalz, 1989).

Table 4.1 : Total digestion of 5 replicate samples.

Element	Mean and St.Deviation	Precision \pm (%)
Co	17 ± 1.8	11
Cr	36 ± 3.9	11
Cu	16 ± 1.8	11
Fe	33000 ± 3000	10
Mn	280 ± 30	11
Ni	35 ± 2.8	8
Pb	38 ± 3.4	9
Zn	120 ± 10	9
Al	48000 ± 5100	11

Table 4.2 : Total digestion within the different size fractions of a duplicate sample.

Element	Sand-sized Fraction		Silt-sized Fraction		Clay-sized Fraction	
	Mean and St.Dev.	Precis. \pm (%)	Mean and St.Dev.	Precis. \pm (%)	Mean and St. Dev.	Precis. \pm (%)
Co	6 ± 4.9	85	16 ± 0.3	2	40 ± 9.7	24
Cr	11 ± 2.2	20	60 ± 4.9	8	113 ± 3.4	3
Cu	23 ± 19	82	19 ± 3.6	20	76 ± 2.1	3
Fe	6200 ± 2600	42	35000 ± 2200	6	68000 ± 11000	16
Mn	5 ± 6.4	140	380 ± 16	4	240 ± 47	20
Ni	8 ± 8.4	100	35 ± 0.8	2	99 ± 24	25
Pb	20 ± 5.6	31	40 ± 8.1	20	91 ± 13	14
Zn	36 ± 0.5	1	84 ± 10.3	12	225 ± 36	16

(b) Sequential Extraction Method

Sequential (selective) extraction is used to simulate the various geochemical conditions to which the sediment may be subjected; also, to gain an appreciation of the potential mobility or bioavailability of the metals during diagenesis. Trace metals are distributed in various phases of the sediment, reflecting their origins, transport pathways and deposition mechanisms. The phases can be defined operationally as follows:

- 1) exchangeable or absorbed fraction;
- 2) bound to the carbonates fraction;
- 3) bound to Fe and Mn oxides (reducible) fraction;
- 4) bound to the organic matter (oxidizable) fraction; and
- 5) the residual fraction (mineral interiors)

In general, the most potentially reactive metals are found in the early fractions or phases, whilst the most inert are found in the residual fraction. The method adopted was that of Tessier *et al.* (1979). The first two steps of this analytical procedure, which determines the "exchangeable" and "carbonate bound" phase were discarded, assuming their contribution was not significant.¹ Three phases were, therefore, determined: the reducible phase (including fractions 1, 2 and 3 above); the organic fraction (4); and the residual fraction (5).

Sediment sample slices, stored formerly in the cold room at 4°C, were homogenised with a plastic spatula. A sub-sample of each slice was weighed to determine the wet weight, then dried in the oven at 110°C; this was subsequently re-weighed. This procedure was repeated until a constant weight was obtained. Consequently, the percentage dry weight of the sample (%D) was calculated as shown on the next page.

The main reason for making determinations on wet samples is that drying may alter the phase associations of the trace metal. Kersten & Förstner (1987)

¹. Numerous Undergraduate and Master research projects in the Oceanography Department have confirmed this assumption.

demonstrated that both oven drying and freeze drying affect metals bound originally to carbonate and to the sulfidic/organic fractions; easily oxidizable metals are transferred into the moderately reducible fraction.

$$\%D = \frac{Dw}{Ww}$$

Dw = dry weight of sample

Ww = wet weight of sample

Reducible Fraction. 2 g of wet sample was placed into a centrifuge tube, to which was added 20 ml of 0.04 M $\text{NH}_2\text{OH} \cdot \text{HCl}$ in 25 % HoAc . The mixture was heated in a water bath at $96 \pm 3^\circ\text{C}$, for 6 hrs. The supernatant was centrifuged and filtered with $0.45 \mu\text{m}$ filter membranes, then stored in a clean plastic bottle. The residue was washed three times, with Milli-Q water.

Organic Fraction. To the residue from the previous step, 3 ml of 0.02 M HNO_3 and 5 ml of 30 % H_2O_2 was added. The mixture was heated at $85 \pm 2^\circ\text{C}$ for 2 hrs in a water bath. A further 3 ml of H_2O_2 was then added and the sample was heated again, at the same temperature, for 3 hrs. After cooling, 5 ml of 3.2 M NH_4OAc in 20 % HNO_3 was added and the sample was agitated by a mechanical shaker, for 30 mins. The supernatant was removed and filtered after centrifugation. This solution was stored in a plastic bottle. The residue was washed three times with Milli-Q water.

Residual Fraction. The same procedure as used for total digestion was followed (see Section 4.2.3 (a)).

The precision of the selective extraction method is given in Table 4.3. The precision of the organic phase was the best of all the analyses, within the range of 2 to 9 %. The reducible and residual phases gave precisions in the range of 0.6 to 24 % and 2 to 27 %, respectively. The precisions for Al, Co, Ni, Pb and Zn are generally good in three phases. Cu and Mn gave low precision in the residual

phase, but improved in the organic and residual phases. Fe gave low precision in the reducible and residual phase.

Table 4.3 : The sequential extraction of a duplicate sample (ND=Not Detected).

Element	Reducible Phase		Organic Phase		Residual Phase	
	Mean and St.Dev.	Precis. \pm (%)	Mean and St.Dev.	Precis. \pm (%)	Mean and St. Dev.	Precis. \pm (%)
Al	7000 \pm 600	8	900 \pm 27	3	31000 \pm 700	2
Co	11 \pm 0.1	1	3 \pm 0.1	2	9.3 \pm 0.8	9
Cr	24 \pm 0.1	0.6	ND	-	32 \pm 8.7	27
Cu	1.8 \pm 0.4	21	4.9 \pm 0.4	4	5.9 \pm 0.2	3
Fe	9000 \pm 2000	24	3500 \pm 220	6	18000 \pm 3300	19
Mn	160 \pm 33	21	16 \pm 0.5	3	42 \pm 0.3	0.6
Ni	15 \pm 0.8	5	4.4 \pm 0.4	9	16 \pm 1	7
Pb	35 \pm 2.5	7	6.8 \pm 0.4	7	9.1 \pm 0.9	10
Zn	58 \pm 9.1	16	11 \pm 0.3	3	25 \pm 2.2	8

Additionally, to complete the precision and accuracy of all the trace metal analyses, the metal content of a certified reference estuarine sediment CRM 277 (BCR Information, 1988) was determined by total digestion. The comparisons of these values are shown in Table 4.4. The measured values of Co, Ni and Pb appear higher than the certified value, whereas Zn is lower. Cr, Cu, Fe and Mn are in agreement within $\sim 13\%$, whilst the percentage difference between the reference material and the measured value is 28 % for Al.

Table 4.4 : Total digestion of 4 replicates of the reference material (CRM 277).

Element	Reference Conc.(ppm) (CRM 277)	Measured		
		Mean and St.- Dev.	Precis. (%)	*Percentage Difference (%)
Al	4.7 (%)	6 % \pm 3‰	5	28
Co	19.8	30 \pm 1.6	5	53
Cr	192	217 \pm 11	5	13
Cu	101.7	117 \pm 5.2	5	14
Fe	4.5 (%)	5.2 % \pm 5‰	10	15
Mn	161	182 \pm 54	3	13
Ni	43.4	91 \pm 4.4	5	11
Pb	146	203 \pm 6.2	3	38
Zn	547	353 \pm 8.6	2	35

* Percentage difference is calculated as [(Measured-Ref.)/Ref] x 100%.

4.2.4. Analysis of Organic Carbon

A CARLO ERBA E.A. 1108 elemental analyzer was used to determine the total carbon, organic carbon and CaCO₃ content of the dry samples. The principle of the method is based upon the complete and instantaneous oxidation of the sample by "flash combustion"; this converts all the organic and inorganic substances into combustion products. The details of this technique are presented in Appendix A5.

Pretreatment of Sample

~2 g of wet sediment was split into two portions. One of the portions was acidified with 25 ml of dilute HCl (10 %), to remove inorganic carbon (*i.e.* carbonate carbon); it was washed then with distilled water. Both sediment portions were oven dried at 60°C (Verardo *et al.*, 1990). Dried samples were

ground in a pre-cleaned agate mortar and pestle, then stored in glass vials until further analysis.

Performing the Analysis

The analyzer was calibrated with three standards: acetanilide (C_8H_9NO) and three blank tin capsules. After calibration, a known amount of acetanilide was run as an unknown sample, in order to confirm the calibration and to check for drift. A known amount of dried and homogenized sample (~ 2 mg) was placed into a tin capsule, folded into a small spherical shape and then placed into the autosampler tray (Verardo *et al.*, 1990). Up to 50 samples can be run in one batch. The CHNOS analyzer gives the total amount of carbon present in the sample. The difference between the carbon content of the unacidified and the acidified subsample is defined operationally as the amount of inorganic or carbonate carbon. The amount of carbon in the acidified sample is defined operationally as the organic carbon content; this can be expressed simply as follows (Wilkinson, 1991):

$$C = 100C_a (1 - 0.0833C_b) / (100 - 8.33C_a)$$

C_a = wt% C of acid treated sample

C_b = wt% C of untreated sample

8.33 = atomic weights of $(CaCO_3)/C$

The above equation considers the fact that organic carbon will be concentrated in the acid treated samples, as a result of the dissolution of carbonate minerals; it assumes that any carbonate present is in the form of calcite, but the presence of other carbonates will make little difference (Wilkinson, *op.cit.*). The precision of the method was 12 %.

CHAPTER 5

RESULTS : Sedimentological Investigations

5.1. Grain Size Distributions of Surface Sediments

The sample locations are presented on Figure 5.1 (produced same as Figure 4.1), whilst the % contained within each modal size is given in Table 5.1.

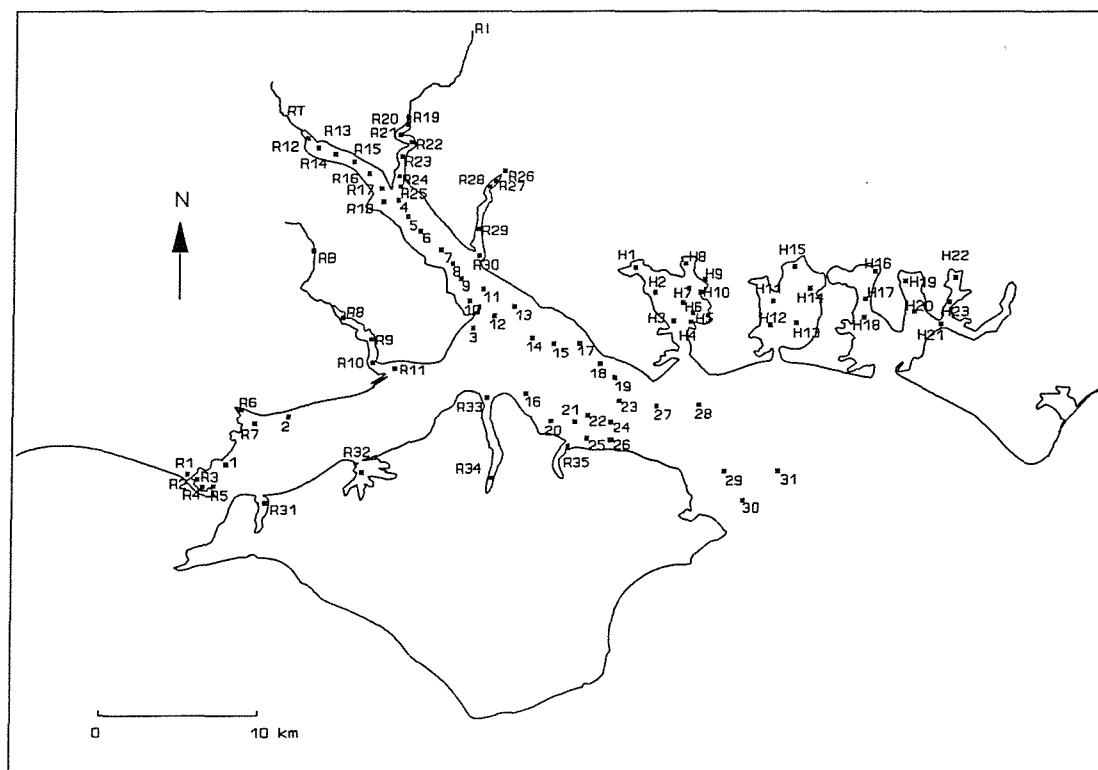


Figure 5.1 : Sampling Locations, within the Solent System.

Table 5.1 : The % of modal size class in each sample (continued on following pages).

Sample No	sand (%)	silt (%)	clay (%)
1	25	31	44
2	36	25	39
SOUTHAMPTON WATER			
3	16	35	49
4	12	21	67
5	1	32	67
6	3	32	65
7	5	43	52
8	20	12	68
9	9	24	67
10	25	42	33
THE EAST SOLENT			
12	31	12	57
13	44	9	47
14	59	17	24
15	47	15	38
16	51	7	42
17	26	8	66
18	20	33	47
19	63	3	34
20	71	5	24
21	34	10	56
22	45	10	45
23	47	11	42
24	21	12	67
25	27	17	56
26	27	13	60
28	59	15	26
29	76	7	17
30	41	10	49
31	80	5	15

Table 5.1 (continued): The % of modal size class in each sample.

Sample No	sand (%)	silt (%)	clay (%)
HARBOURS			
H1	24	25	51
H2	5	28	67
H3	6	24	71
H4	2	5	93
H5	8	13	79
H6	5	17	78
H7	7	16	77
H8	25	40	35
H9	42	27	31
H10	14	23	63
H11	62	9	29
H12	92	1	6
H13	17	19	64
H14	55	10	35
H15	54	9	37
H16	15	37	48
H17	44	16	40
H18	47	15	38
H19	31	12	57
H20	36	24	40
H21	64	12	24
H22	14	21	65
H23	53	15	32

Table 5.1 (continued) : The % of modal size class in each sample.

Sample No	sand (%)	silt (%)	clay (%)
RIVERS			
R1	90	2	8
R2	63	13	24
R3	75	5	20
R4	58	7	35
R5	51	9	40
R6	8	36	56
R7	8	41	51
R8	86	2	11
R9	14	16	70
R10	9	11	80
R11	24	13	63
R12	36	5	59
R13	17	30	54
R14	26	28	45
R17	6	7	87
R20	86	3	11
R21	24	23	53
R23	47	15	38
R24	67	11	21
R25	2	31	69
R26	59	21	20
R27	59	21	20
R28	10	36	55
R29	16	12	72
R30	65	6	29
R31	23	13	63
R32	50	6	44
R33	38	15	48
R34	26	45	29
R35	18	29	54

5.1.1. The General Classification

Sediments are composed generally of a combination of grain size sub-populations of sand, silt, and clay. The proportions of sand, silt and clay can be plotted on a trilinear diagram, to give rise to a comparative description based on grain size distribution (Dyer, 1986). Each apex represents 100 % of that particular modal size and the triangle is divided into a series of areas, such as sandy clay, silty sand etc. Figure 5.2 shows that most of the samples from the Solent region are concentrated around the sand and clay apexes. The percentage of sand varies from 2 to 90 %, whilst the silt percentage is confined to within narrower limits (2 to 45 %). Three main groups may be identified amongst the samples: silty clay, sandy clay and clayey sand. Some of the samples may be classified as clay, sand and sand-silt-clay.

Samples collected from the East Solent, which are shown with solid circles on the Figure 5.2, tend linearly trend from sand to sandy clay. At the same time, the percentage of silt does not vary significantly. The trend identified suggests a mixture of two sand and clay populations or end members. Samples 3 and 18 are two exceptions to this overall trend. Sample 18 is located close to Gilkicker Point and Sample 3 is located at the western entrance of Southampton Water. The highest percentage of sand occurs in Samples 29 and 31, obtained from the open (seaward) end of the East Solent.

The percentages of sand and silt in the Southampton Water samples are variable, whilst the clay percentage is almost constant. However, Sample 10, which is collected near to Calshot Spit, is placed in sand-silt-clay category.

The Harbour samples fall within two groups. The Langstone and Chichester samples appear largely within the clayey sand and silty clay categories, whereas most of the Portsmouth samples lie within the silty clay and clay categories. The exceptions are Samples H1, H8 and H9, which are sand-silt-clay. In general, therefore, the Portsmouth samples are finer-grained than those from Chichester and Langstone.

The riverine samples are not confined to a single category, showing variable proportions of sand, silt and clay.

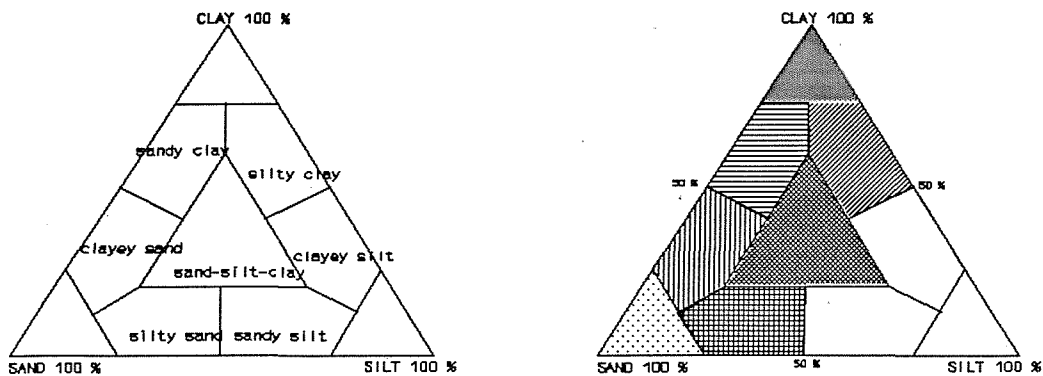
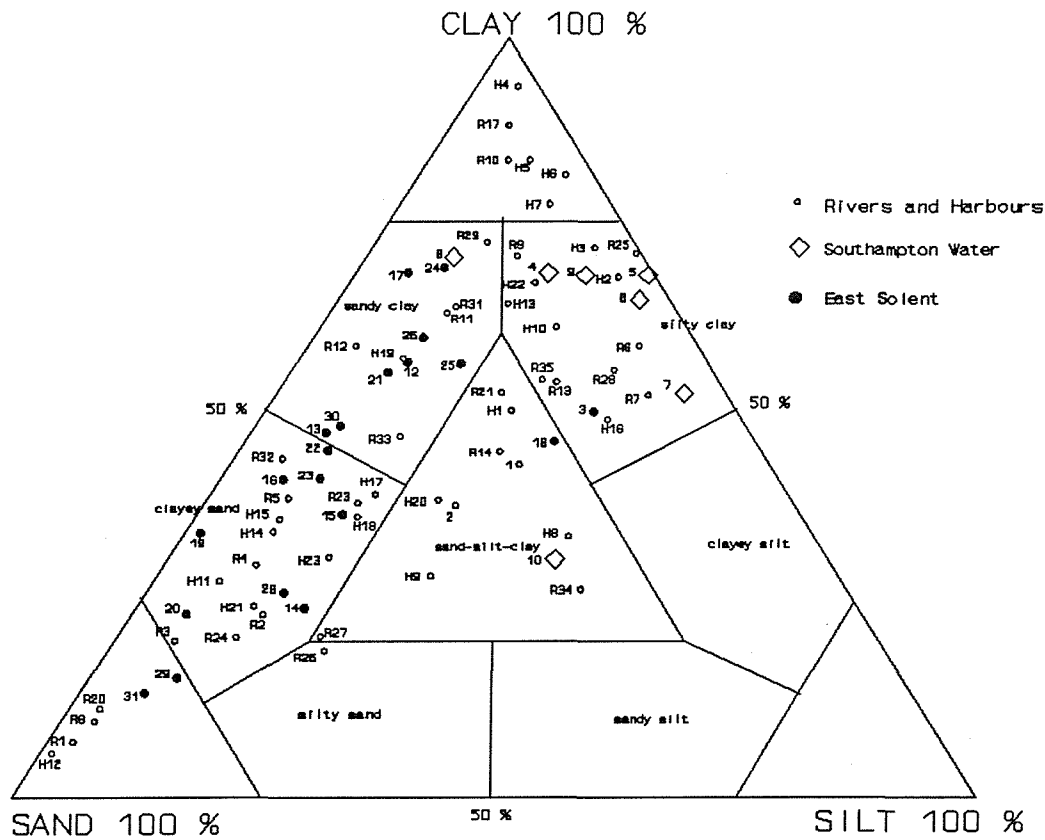


Figure 5.2 : Trilinear Diagram - Classification of samples (after Dyer, 1986).

5.1.2. Distribution Pattern of Sediment Types

The geographical distribution of sediment types is illustrated in Figure 5.3. Seven sediment types are used to classify most samples from Figure 5.2. Data for the offshore area and the West Solent were provided by BGS (1989).

The West Solent and the open (seaward) end of the East Solent consist of sand and gravel deposits. The coarser sediment on the western side is supplied by high velocity tidal currents from the open end of the West Solent (Dyer, 1980; Srisaengthong, 1982). From offshore to the eastern entrance of the Solent is dominated by wave activity (Whitcombe, 1991). The sand fraction (S) occurs mainly at the open end of the East Solent (St Helen's Road), at the entrance of the Langstone Harbour, within the upper part of Beaulieu River and on the intertidal flats between the Keyhaven and Lymington Rivers. The proportion of sand diminishes within the East Solent; this is reflected in the changing pattern from sand to clayey sand, alternating with sandy clay patches within the East Solent. Silty sand (SS) occurs locally upstream within the Hamble River. Sand-silt-clay (SSC) is present within the Medina, Hamble, Itchen, and Test Rivers, and in the bay-head of Portsmouth Harbour. It also exists within the intertidal flats from Keyhaven to Beaulieu, and occurs locally in the vicinity of Calshot Spit. Silty clay (SIC) occurs largely in Southampton Water and, locally, in Portsmouth Harbour, Wootton Creek and the Lymington River. Sandy clay (SC) is abundant in the East Solent, Sturbridge Shoal and Lee-on-Solent and, locally, at the mouths of the Beaulieu and Hamble Rivers, upstream of the Test, in Chichester Harbour, and at Cowes. Clayey sand (CS) is the prevailing sediment type in the East Solent, interrupted by sandy clay patches. It occurs largely in Langstone and Chichester Harbours and is, locally, abundant in Newtown Inlet and the River Itchen. Clay (C) is found mainly in Portsmouth Harbour and, locally, occurs in the River Beaulieu and at the mouth of the River Test.

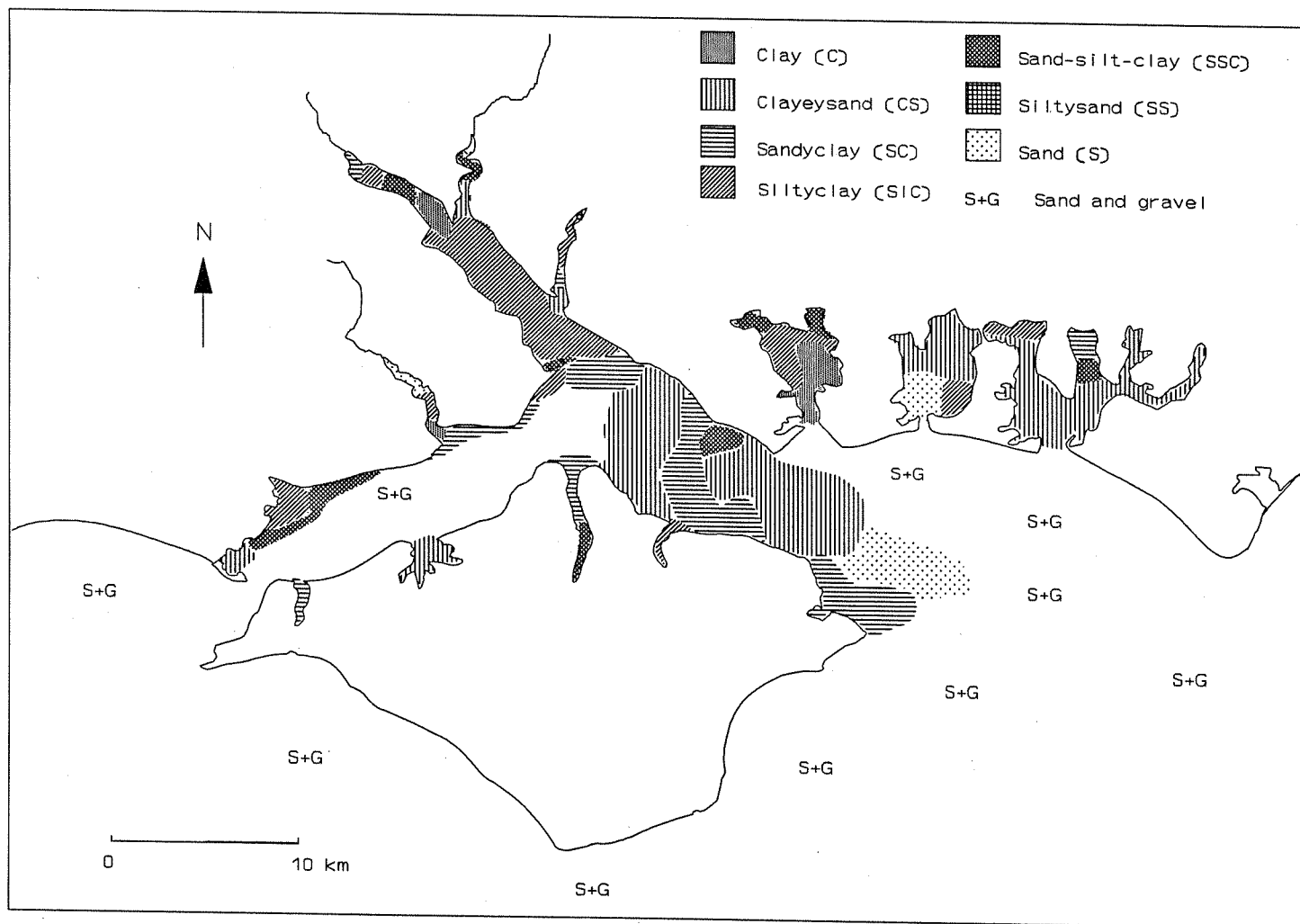


Figure 5.3 : *Geographical distribution of the different grain size categories of the surficial sediments.*

5.1.2. Frequency Distributions - Histograms

The simplest graphical method of presenting the data is by means of histograms (McManus, 1988). The independent variable used is grain size, whilst the dependent variable is the weight percentage. The number of columns depends upon the number of grades selected or calculated during the grain size determination and on the grain size spread of the sample (Buller & McManus, 1979). In this study, the grain size class was at 1 ϕ intervals, from -2 to 10 ϕ . The specific modal groups are displayed on Figure 5.4.

Southampton Water:

Samples 4, 5, 6, 7, 8 and 9 exhibit a fine-grained mode within the clay fraction. Sample 10 has a trimodal distribution of the fine sand, silt and clay sizes (near Calshot Spit), whilst Samples 12 and 13 (from the mouth of the estuary) have bimodal distributions of fine sand and clay, indicating mixing of the sand and clay components. Sample 3 (at the western approaches to the mouth of the estuary) has a trimodal distribution of fine sand, silt and clay.

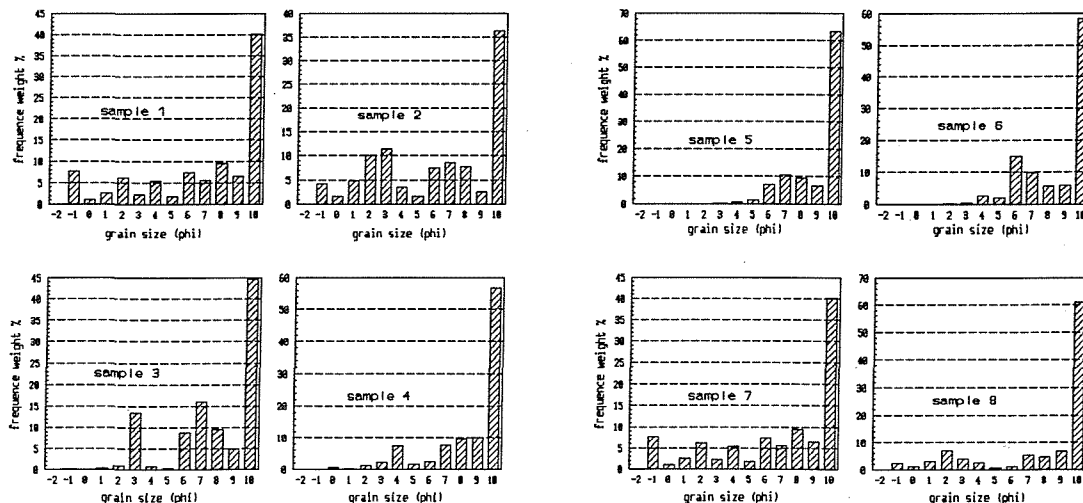


Figure 5.4 : *Histograms showing the Grain Size Distribution of Samples (continued on following pages).*

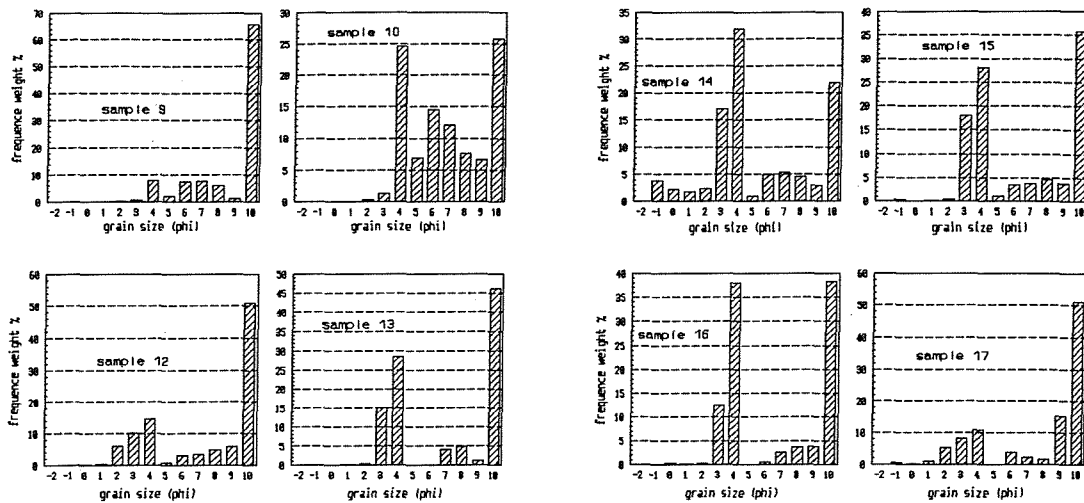


Figure 5.4 (continued): Histograms showing the Grain Size Distribution of Samples.

The East Solent:

Most of the samples from the East Solent have two modes, in fine sand and clay. Samples 14, 16, 29 and 31 are dominated by a coarser mode, whereas 15, 17, 18, 21, 22, 24, 25, 26 and 30 are dominated by a finer mode. Samples 19, 20, 23 and 28 have trimodal distributions.

Samples 1 and 2, collected from the tidal flats between Beaulieu and Keyhaven (West Solent), display a multimodal distribution; this may be an indication of the mixing of several components.

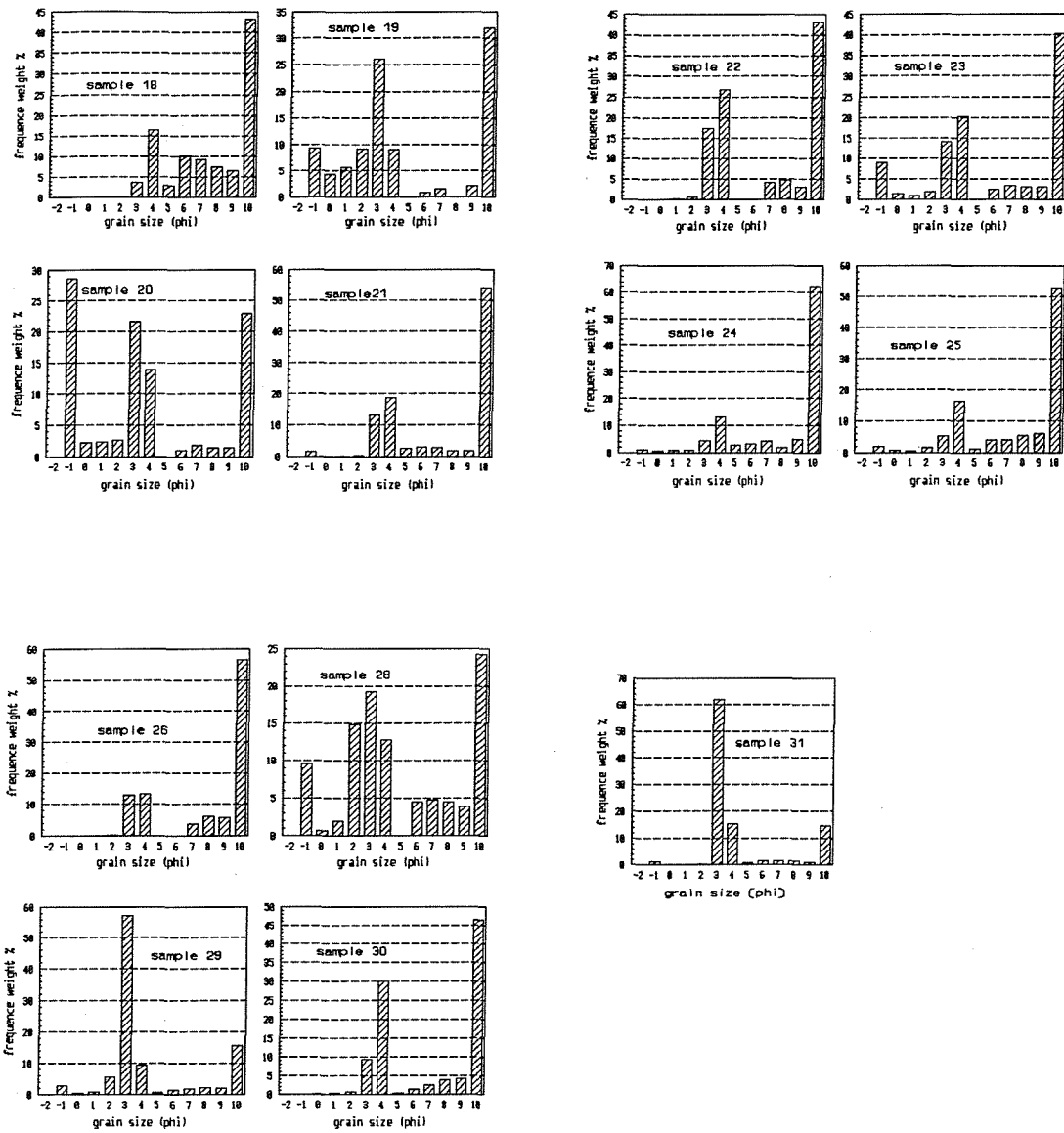


Figure 5.4 (continued): *Histograms showing the Grain Size Distribution of Samples.*

Harbours:

Portsmouth samples (H2, H3, H4, H5, H6, H7) have an almost unimodal distribution of clay, whereas samples H1, H8, H9 and H10 include modes in different size grades. For Langstone Harbour, H12 is distinctive because of its unimodal distribution of fine sand. This well sorted fine sand might be derived from the tidal delta. Within the Harbour, H11 shows a bimodal trend in fine sand clay, whereas H15 and H14 display a trimodal distribution. H13 has a bimodal distribution of mainly clay and fine sand. Chichester Harbour samples display multimodal distributions. H16, H19 and H22, located at the bay-head, are dominated by a fine-grained mode. These samples may reflect the composition of a fine-grained source material. However, the samples within the harbour have a distinct fine sand mode.

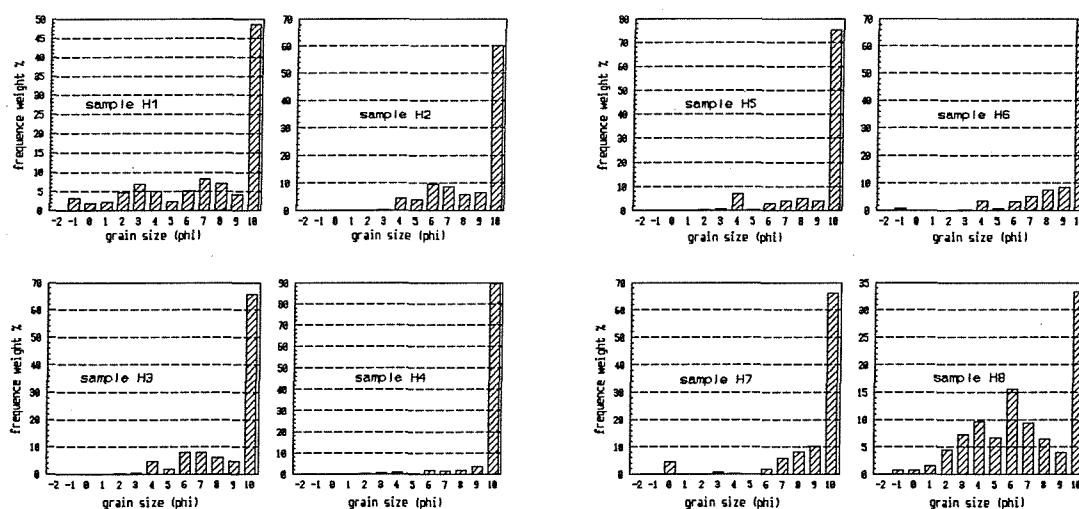


Figure 5.4 (continued) : *Histograms showing the Grain Size Distribution of Samples.*

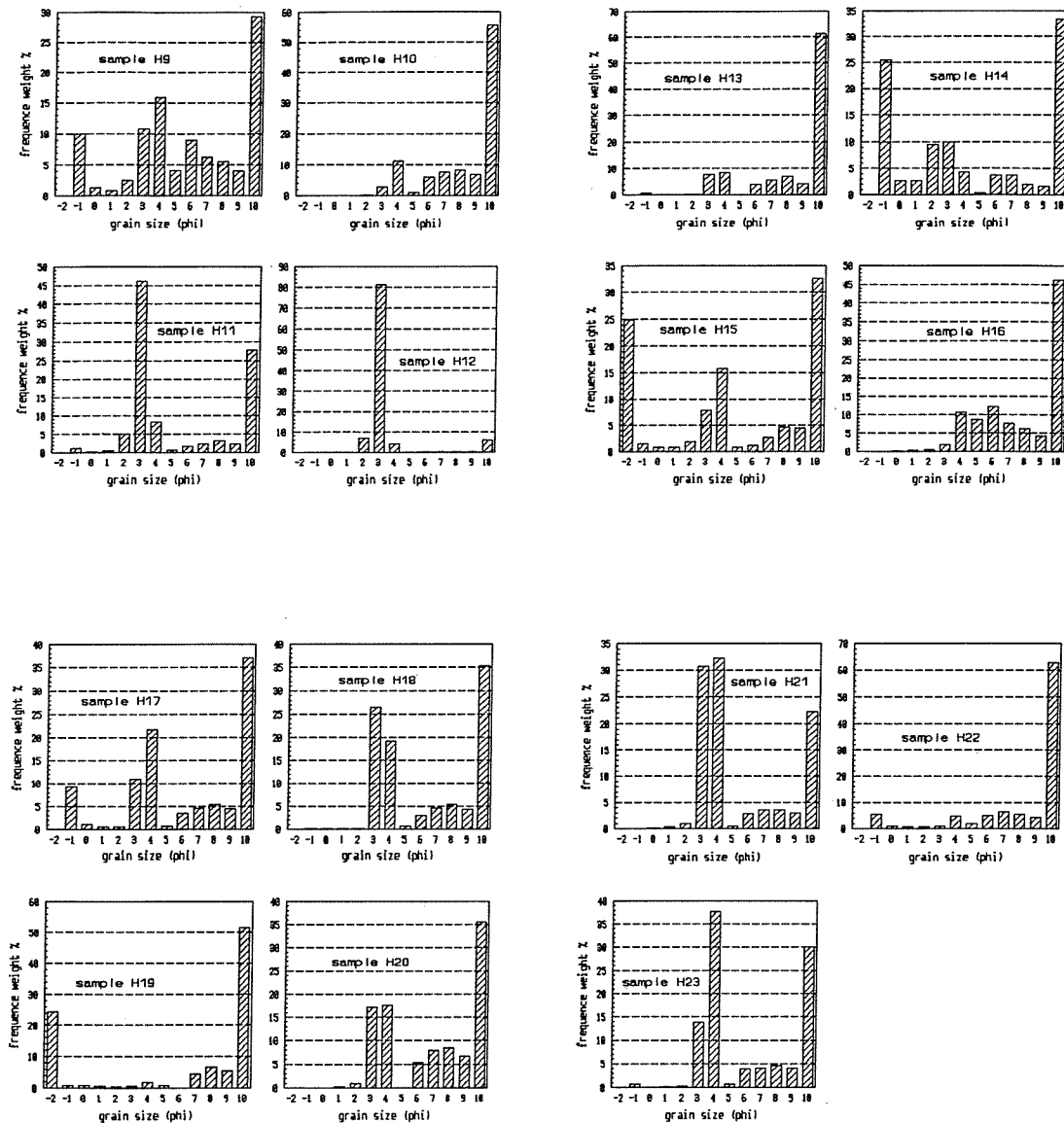


Figure 5.4 (continued) : *Histograms showing the Grain Size Distribution of Samples.*

Rivers:

Keyhaven samples (R1, R2, R3, R4, R5) are multimodal, and a coarse mode exists in all the samples. The Lymington samples, R6 and R7, have a bimodal distribution of silt and clay sizes. R8, the furthest collected upstream within the

River Beaulieu, consists mainly of pebbles. R9 has a multimodal distribution, dominated by a fine mode in clay. R10 and R11 have bimodal distributions in the fine sand and clay size ranges. The River Test samples (R12, R13, R14 and R17) also have two modes in fine sand and clay. Nearer the mouth of the river, the fine sand mode diminishes (R17). The River Itchen samples (R20, R21, R23, R24, R26) have multimodal distributions, with the exception of R25. The coarse mode dominates upstream and is replaced then with a fine (silt/clay) mode at the mouth of the river (R25). In the River Hamble, the fine sand mode dominates a bimodal distribution (R26, R27), whereas a clay size mode becomes dominant nearer the mouth of the river (R28, R29). Sample R30, which represents the mouth of the Hamble, has a bimodal distribution of sand and clay.

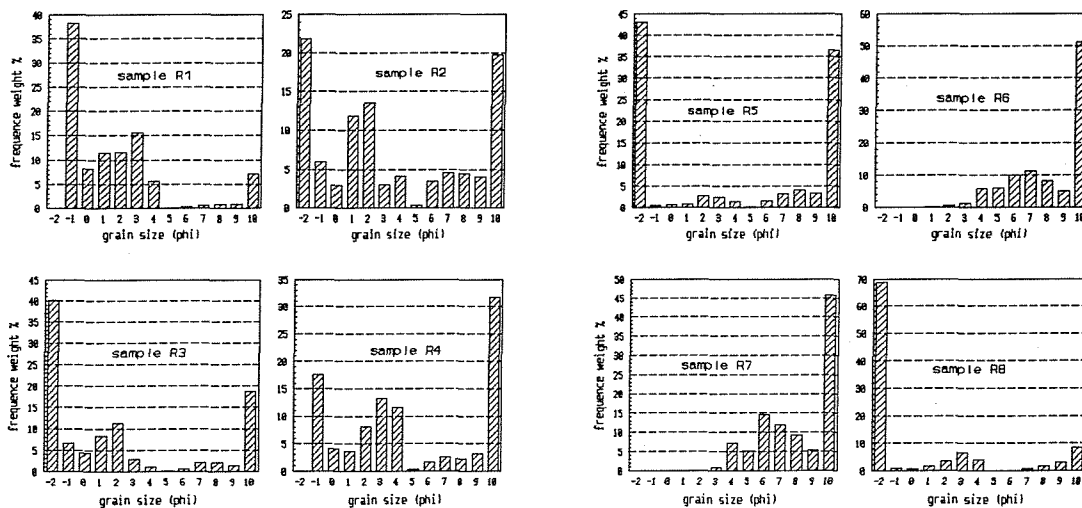


Figure 5.4 (continued): Histograms showing the grain size distribution of samples.

The samples from the Isle of Wight show similar features: R31 (the River Yar), R32 (Newtown Creek), R33 (the mouth of the River Medina), and R35 (Wootton Creek) have bimodal distributions in fine sand and clay. However, R34 (upstream in the River Medina) has a multimodal distribution.

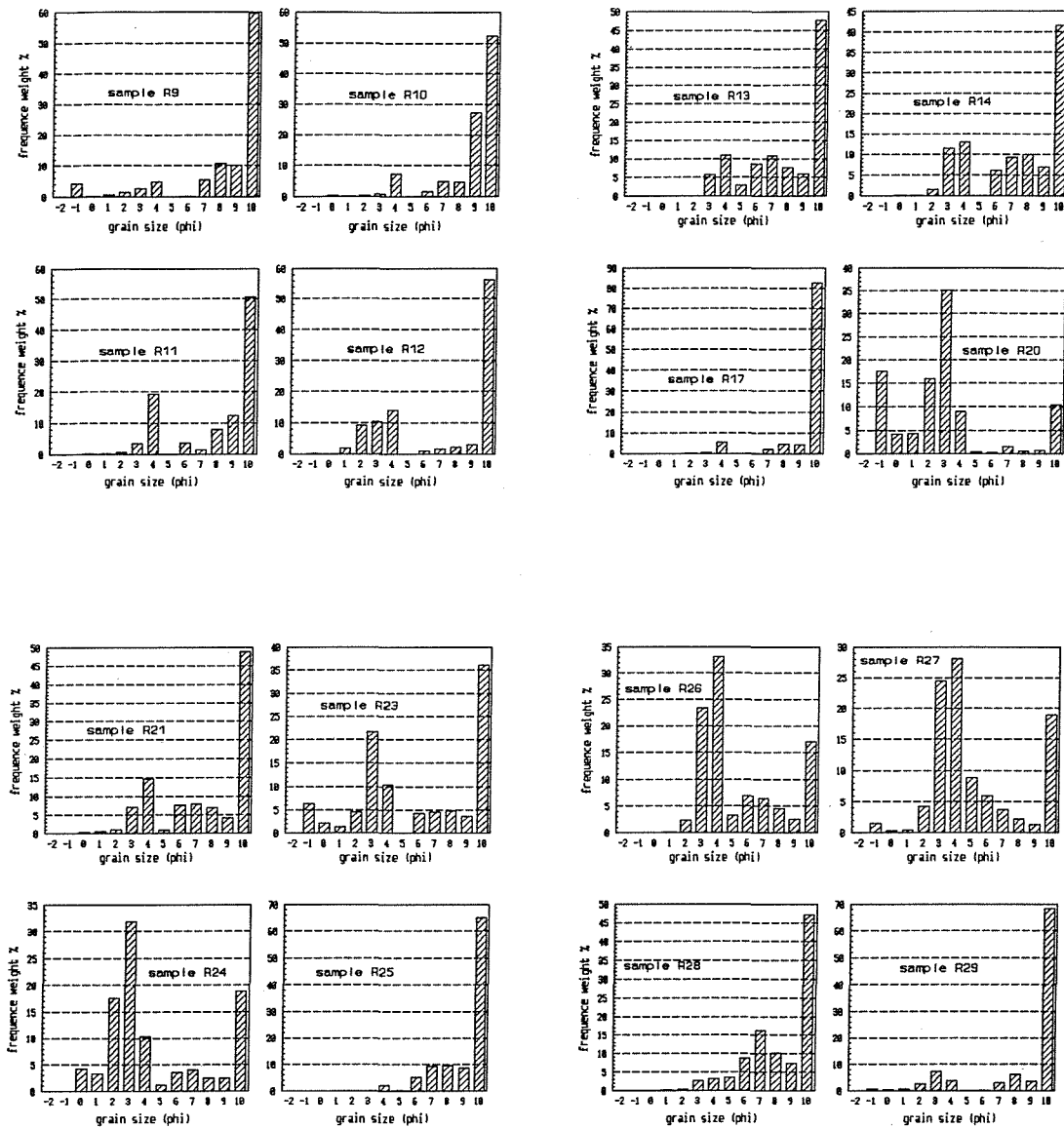


Figure 5.4 (continued): *Histograms showing the Grain Size Distribution of Samples.*

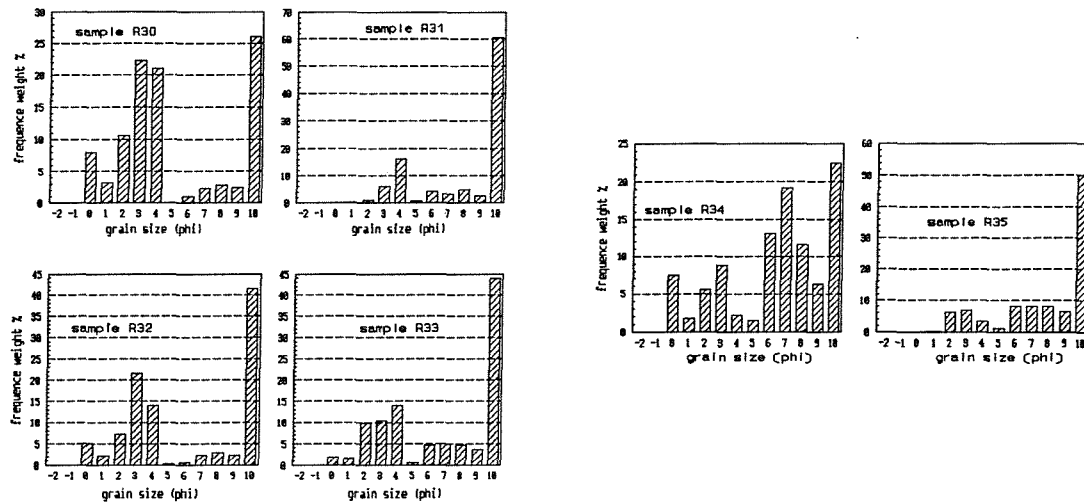


Figure 5.4 (continued): *Histograms showing the Grain Size Distribution of Samples.*

5.1.3. Grain Size Textural Parameters

Descriptive parameters are derived directly from the plotted cumulative curves (Folk, 1966). These parameters define the location of the distribution plot, its slope and the nature of any irregularities; this permits the curves to be characterised and compared (McManus, 1988). Cumulative frequency curves of the samples are presented in Appendix B2.

The parameters used for characterising the curves fall into four principal groups: (a) the average or mean grain size; (b) the spread of sizes about the average (sorting); (c) the asymmetry of any preferential spread to one side of the average (skewness); and (d) the degree of concentration of the grains around the central size (kurtosis). The definition of the parameters used in the present investigation are shown in Table 5.2. Sizes are expressed as ϕ values, defined as;

$$\phi = -\log_2 d$$

where d is the grain diameter in millimetres (McManus, *op.cit.*).

The mean reflects the average size of the sediment, and is influenced by both the source of sediment and the environment of deposition (Folk, 1966). Hence, it is a function of both the energy of the transporting medium and the size range of the available materials (Glaister & Nelson, 1974).

The mean grain size of fine-grained sediments in different regions of the Solent varies over a broad range, from 9 to 1 ϕ (Figure 5.5 and Table 5.3). Southampton Water and the East Solent samples have an almost constant mean grain size of 8-9 ϕ and 7 ϕ , respectively. In contrast, the Harbour and river samples show greater variability in their means. Along the main channel of Southampton Water, the mean grain size is 8-9 ϕ , coarsening to 6 ϕ at location 10. The middle section of the East Solent has a constant mean grain size of approximately 7 ϕ . Coarsening occurs at samples 14, 15, 16 (5, 6 and 5 ϕ respectively) located near to sand banks, and samples 28, 29, 31 (5, 5 and 4 ϕ respectively), which are located at the open (seaward) end of the system. The finest mean grain size, 8 ϕ , appears in the vicinity of the coast between Wootton Creek and Ryde on the Isle of Wight. Within the tidal inlet of Portsmouth Harbour, the mean grain size is fine, 8-9 ϕ . There is coarsening towards the bay-head, to 6-7 ϕ . Langstone and Chichester Harbour sediments are quite different, with a coarser and more variable mean grain size than at Portsmouth. The river samples display a general fine downstream, along the transport path. The River Test samples have a mean grain size of 7 ϕ upstream and 9 ϕ at the confluence with Southampton Water. The River Itchen samples show variability in the mean grain size distribution, although fining downstream is evident (7-9 ϕ). The mean grain size of the Hamble sediments is 5 ϕ upstream, becoming finer downstream (8-9 ϕ). At the confluence with Southampton Water, the grain size coarsens (5 ϕ). Within the upper estuary of the Beaulieu River, a high sand content gives rise to a mean size of -0.40 ϕ . The mean grain size decreases to 7 ϕ towards the mouth at the estuary. Keyhaven sediments are the coarsest sampled, with a range of 1 to 3 ϕ .

Table 5.2 : Definition of parameters, and the descriptive terms applied to various ranges of parameters (from Folk & Ward, 1957).

$$\text{mean } M_z = \frac{1}{3} (\phi 16 + \phi 50 + \phi 84)$$

$$\text{sorting } \sigma_1 = \frac{1}{2} \left(\frac{\phi 84 - \phi 16}{2} + \frac{\phi 95 - \phi 5}{3.3} \right)$$

$$\text{Skewness } Sk_1 = \left(\frac{\phi 16 + \phi 84 - 2\phi 50}{2(\phi 84 - \phi 16)} \right) + \left(\frac{\phi 5 + \phi 95 - 2\phi 50}{2(\phi 95 - \phi 5)} \right)$$

$$\text{Kurtosis } K_G = \frac{\phi 95 - \phi 5}{2.44(\phi 75 - \phi 25)}$$

ϕx = ϕ size of the x th. percentile

Sorting (σ_1)		Skewness (SK_1)		Kurtosis (K_G)	
Very well sorted	<0.35	Very positively skewed	+0.3 to +1.0	Very platykurtic	<0.67
Well sorted	0.35-0.50	Positively skewed	+0.1 to +0.3	Platykurtic	0.67-0.90
Moderately well sorted	0.50-0.70	Symmetrical	+0.1 to -0.1	Mesokurtic	0.90-1.11
Moderately sorted	0.70-1.00	Negatively skewed	-0.1 to -0.3	Leptokurtic	1.11-1.50
Poorly sorted	1.00-2.00	Very negatively skewed	-0.3 to -1.0	Very leptokurtic	1.50-3.00
Very poorly sorted	2.00-4.00			Extremely leptokurtic	>3.00
Extremely poorly sorted	>4.00				

Table 5.3 : Textural Parameters of all the Samples (continued on the following pages).

Sample No	mean (ϕ)	sorting	skewness	kurtosis
1	7	3.99	-0.51	0.78
2	6	3.24	-0.32	0.53
3	7	2.28	-0.45	0.91
SOUTHAMPTON WATER				
4	8	1.76	-0.86	1.24
5	9	1.71	-0.80	0.77
6	8	1.69	-0.78	0.67
7	8	2.13	-0.37	0.71
8	7	2.99	-0.91	1.38
9	9	2.18	-0.89	0.82
10	6	2.25	0.09	0.48
THE EAST SOLENT				
12	7	2.74	-0.89	0.55
13	7	2.98	-0.17	0.48
14	5	3.39	0.49	0.80
15	6	3.04	0.26	0.48
16	5	2.57	0.62	0.49
17	7	2.71	-0.89	0.60
18	7	2.97	-0.33	0.60
19	7	2.24	-0.14	0.83
20	4	4.61	0.32	0.56
21	7	2.64	-0.88	0.52
22	7	3.05	-0.16	0.48
23	6	3.79	-0.02	0.66
24	7	2.51	-0.89	0.77
25	8	2.99	-0.81	0.56
26	8	2.99	-0.88	0.52
28	5	3.94	0.39	0.67
29	5	3.02	0.75	2.53
30	7	3.00	-0.41	0.50
31	4	2.49	0.84	5.26

Table 5.3 (continued) : Textural Parameters of all the Samples.

Sample No	mean (ϕ)	sorting	skewness	kurtosis
PORTSMOUTH HARBOUR				
H1	7	3.45	-0.63	0.76
H2	8	1.73	-0.82	0.89
H3	8	1.74	-0.79	1.09
H4	9	0.50	-0.43	4.67
H5	9	1.46	-0.76	7.03
H6	9	1.31	-0.77	2.53
H7	9	1.71	-0.77	2.53
H8	7	3.12	0.00	0.62
H9	6	3.77	0.00	0.68
H10	8	2.00	-0.87	0.95
LANGSTONE HARBOUR				
H11	5	3.30	0.79	0.48
H12	3	1.29	0.37	5.49
H13	8	2.81	-0.89	0.90
H14	4	4.47	0.14	0.48
H15	4	4.76	-0.08	0.48
CHICHESTER HARBOUR				
H16	8	2.61	-0.35	0.60
H17	6	3.49	-0.09	0.60
H18	6	3.10	0.11	0.47
H19	5	4.74	-0.90	0.46
H20	7	3.05	-0.17	0.50
H21	5	3.05	0.72	0.61
H22	9	3.09	-0.88	1.27
H23	6	2.97	0.69	0.48

Table 5.3 (continued) : Textural Parameters of all the Samples.

sample	mean (ϕ)	sorting	skewness	kurtosis
RIVER KEYHAVEN				
R1	1	2.99	0.29	1.27
R2	3	4.69	0.29	0.55
R3	2	4.87	0.53	0.64
R4	4	4.29	0.10	0.57
R5	3	4.91	-0.04	0.45
RIVER LYMINGTON				
R6	8	1.92	-0.84	0.76
R7	8	1.89	-0.55	0.69
RIVER BEAULIEU				
R8	0	3.23	0.93	1.14
R9	7	2.06	0.72	1.78
R10	9	1.45	-0.75	2.46
R11	7	2.40	-0.84	0.69
RIVER TEST				
R12	7	2.95	-0.73	0.54
R13	7	2.31	-0.68	0.76
R14	7	2.93	-0.35	0.53
R17	9	1.06	-0.60	9.43
RIVER ITCHEN				
R20	7	2.45	-0.74	0.55
R21	2	3.03	-0.09	2.44
R23	6	3.77	0.01	0.63
R24	5	3.25	0.57	0.79
R25	9	1.55	-0.83	0.84
RIVER HAMBLE				
R26	5	2.71	0.61	0.77
R27	5	2.80	0.60	1.04
R28	8	1.92	-0.61	0.93
R29	9	2.36	-0.87	1.63
R30	5	3.47	0.36	0.62

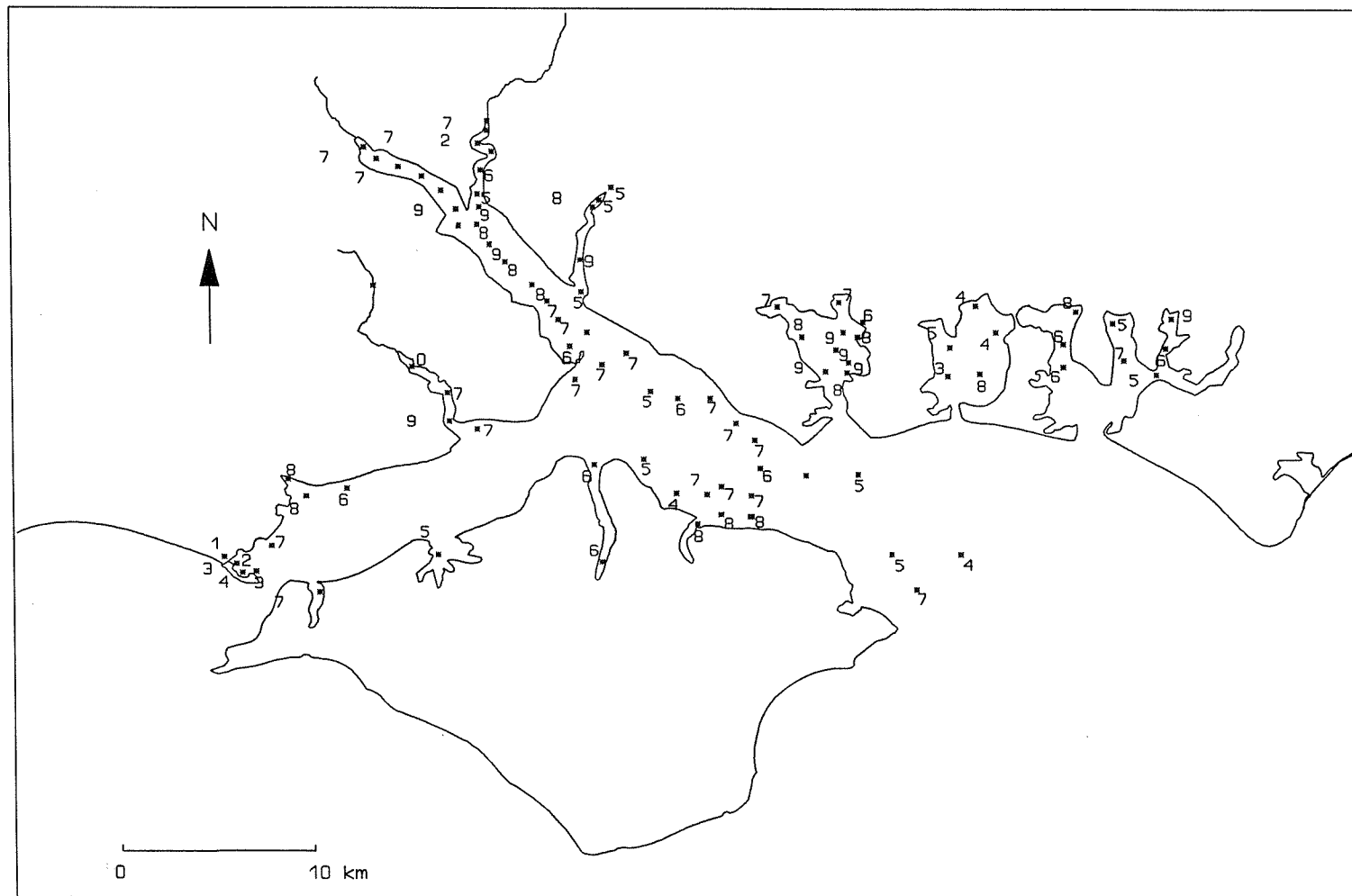


Figure 5.5 : *The distribution pattern of mean grain size (ϕ) of surficial sediment samples.*

Sorting or spread about the average depends upon the source of the material, the nature of the sedimentary processes (*e.g.* waves and current action) and the uniformity and persistence of energy conditions (Glaister & Nelson, 1974). The best sorted sediments approximate to a single grain size distribution and have low sorting values (McManus, 1988). Hence, sediments become finer-grained and better sorted in the direction of transport as a result of selective reworking (Glaister & Nelson *op.cit.*). The distribution of sorting values over the area is illustrated in Table 5.3. Sorting is generally better in the main channel of Southampton Water than those in the East Solent. Along the northern side of the East Solent, sorting ranges from 3.39 to 2.24, towards the east. It is nearly constant at around 2.5 on the southern side of the East Solent. Samples from the open end of the East Solent display close values (3) and become worse in the middle part of the East Solent. Portsmouth Harbour samples have better sorting values (2.3), in comparison to those of Langstone (3.4) and Chichester (~ 3).

Skewness (preferential spread) is a positive or negative dimensionless number, which lies within the range of -1 to +1. Skewness describes the tendency for a distribution to lean to one side of, or to deviate from, normality (McManus, *op.cit.*). According to Folk (1966), strongly skewed samples are obtained from zones of environmental mixing. Likewise, Allen (1971) has recognized that skewness reflects the degree of contamination of the sediments by coarse size grades, transported by strong tidal currents. If there is more material in the coarse tail (coarse skewed), the skewness is referred to as being negative. If there is more material in the fine tail (fine skewed), it is positive (Lindholm, 1987). The distribution of skewness values is shown in Table 5.3. In general, the samples display negative skewness. Skewness fluctuates around -0.80 to -0.90 within Southampton Water, but is remarkably variable in the East Solent (0.26 to -0.89). Positive values are found around the sand banks and at the open (seaward) end of the system.

McLaren (1981) has suggested that if a sediment deposit is eroded, the resultant sediment in transport must be finer, better sorted and more negatively skewed than the source, because there is a greater probability of moving fine (light)

grains than coarse (heavy) grains. The lag remaining after erosion, on the other hand, must be coarser, better sorted and more positively skewed than the original deposit. However, sediment in transport may become finer or coarser, depending upon the action of the transporting agent; if it becomes finer, the skewness must become more negative and, if it becomes coarser, the skewness must become more positive (McLaren & Little, 1987).

After considering the importance and the associations between mean grain size, sorting and skewness, it is necessary to examine the complementary variations in these grain size parameters. To this end, the parameters are shown on locations in order of distance (Figures 5.6 to 5.11). It should be noted that the sampling strategy of this study is not ideal to apply a complete 2-dimensional statistical sediment analysis, as in McLaren & Little (*op.cit.*). Therefore, the relative changes in grain size parameters are determined on possible transport paths with the assumptions of the two cases defined above *i.e.* sediment in transport becomes coarser and more positive or finer and more negative.

Within the Test River (Figure 5.6), sediment becomes finer, better sorted and less negatively skewed, from R12 to R17.

Within the Itchen River (Figure 5.7), however, the mean grain size is finer upstream (R20), becoming coarser and more poorly sorted downstream; this reflects an input of sediment to the river around the location of Sample R21. Sample R24, which is located downstream of the Itchen, is finer grained, very poorly sorted, but positively skewed. These variations might represent an additional (anthropogenic) input to the river. The sediments might have lost, therefore, their natural characteristics. At the confluence of the two rivers, the textural parameters of Sample 4 represent a mixture of River Test fine-grained sediment with River Itchen coarse-grained sediment. The mean size of Sample 4 reflects, however, the dominant influence of the Test River.

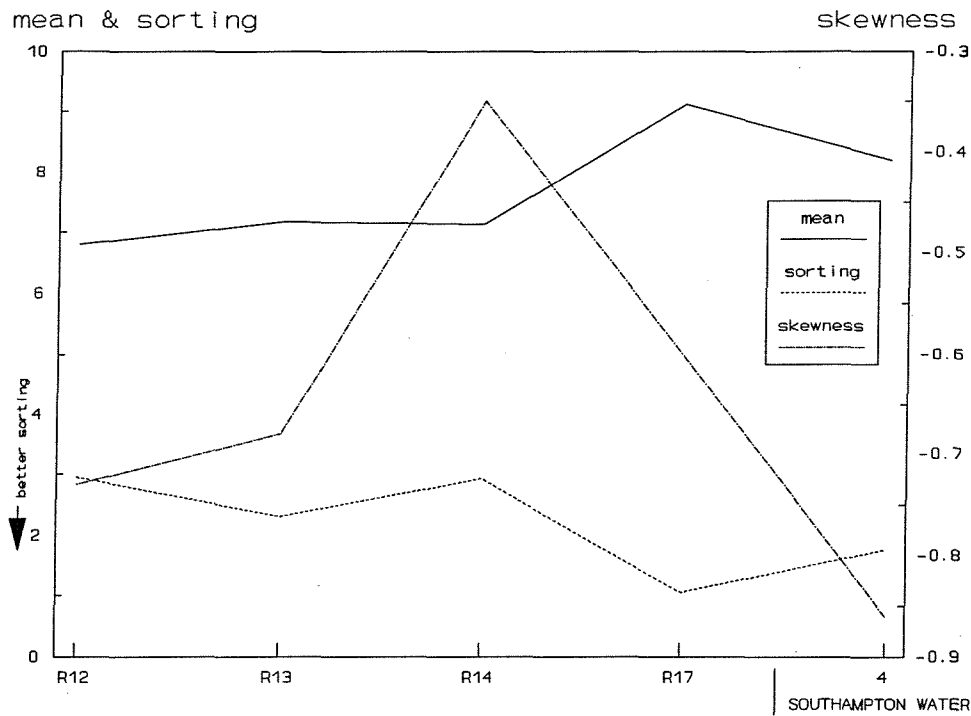


Figure 5.6 : Variation of Grain size parameters within the River Test (for sample locations, see Figure 5.1).

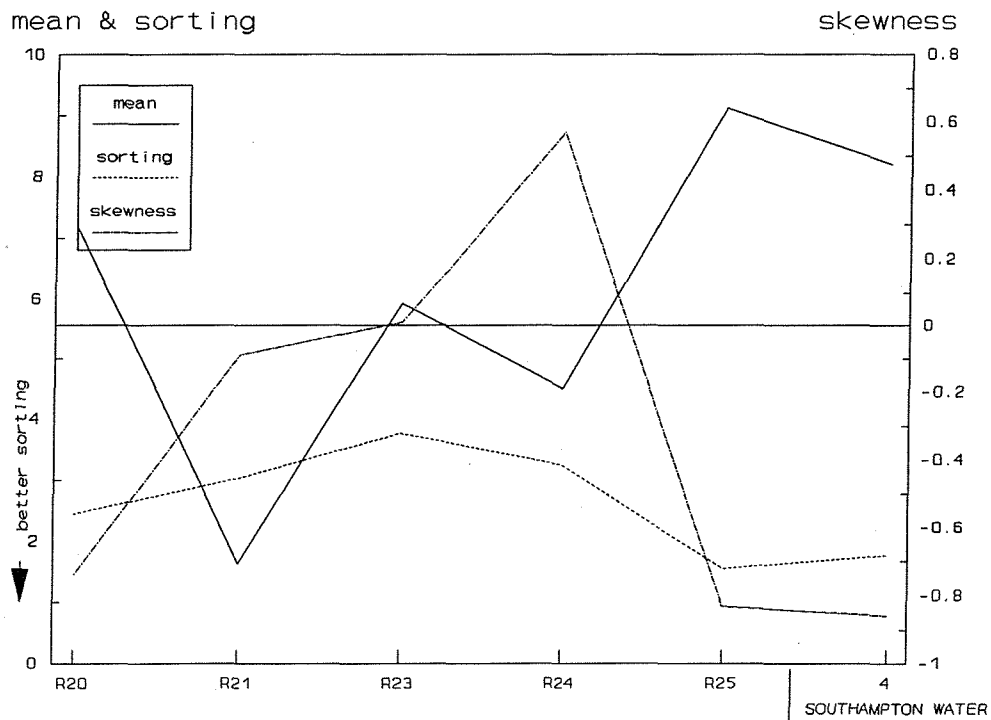


Figure 5.7 : Variations of Grain size parameters within the River Itchen (for locations, see Figure 5.1).

Sediment becomes coarser, poorer, and less negatively skewed in Southampton Water from Samples 4 to 7, possibly indicating a downstream transport direction (Figure 5.8). However, this trend is not obvious in the other locations (from 7 to 12). This changing pattern might be indicative of a changing transport direction or mixing with a material of different source, such as from Calshot Spit.

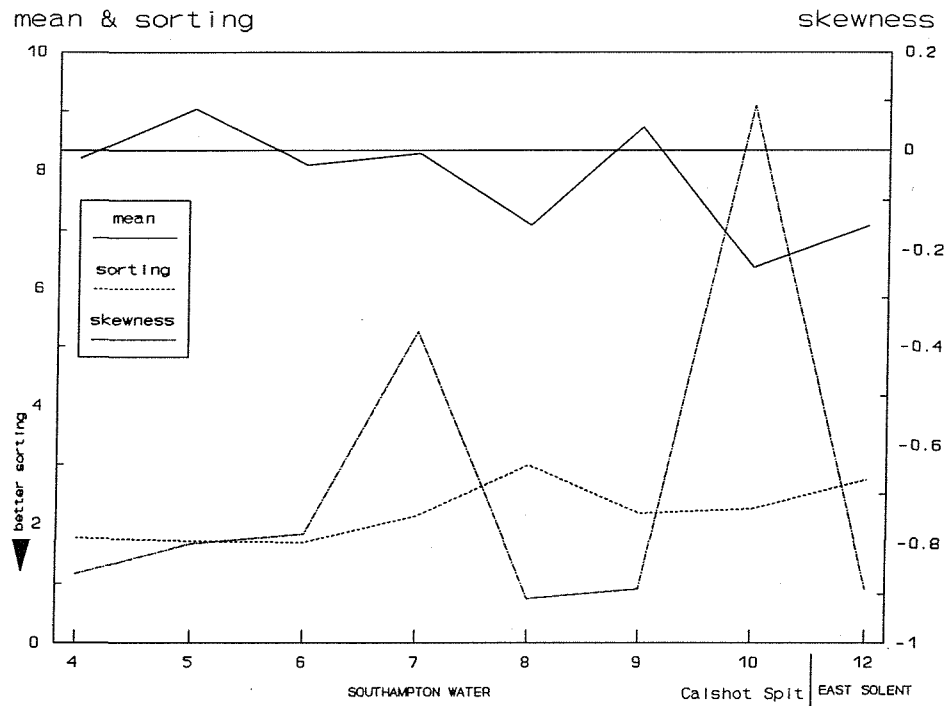


Figure 5.8 : Variation of Grain size parameters in Southampton Water (for sample locations, see Figure 5.1).

The East Solent samples can be examined in two groups, the one finer and negatively skewed; the other is coarser and positively skewed. Samples 3, 12, 13, 17, 18, 19, 21, 22, 23, 24, 25, 26 and 30 are finer and negatively skewed, whilst samples 14, 15, 16, 20, 28, 29 and 31 are coarse and positively skewed. Sediment movement is likely to proceed from the coarse sediment locations to those fine sediment locations. Variations in grain size parameters suggest two different transport paths in the northern part of the East Solent (Figure 5.9). Sediment becomes coarser, poorer sorted and more positively skewed from locations 17 to 31 with the exception of 30, suggesting a transport path from the open (seaward) end

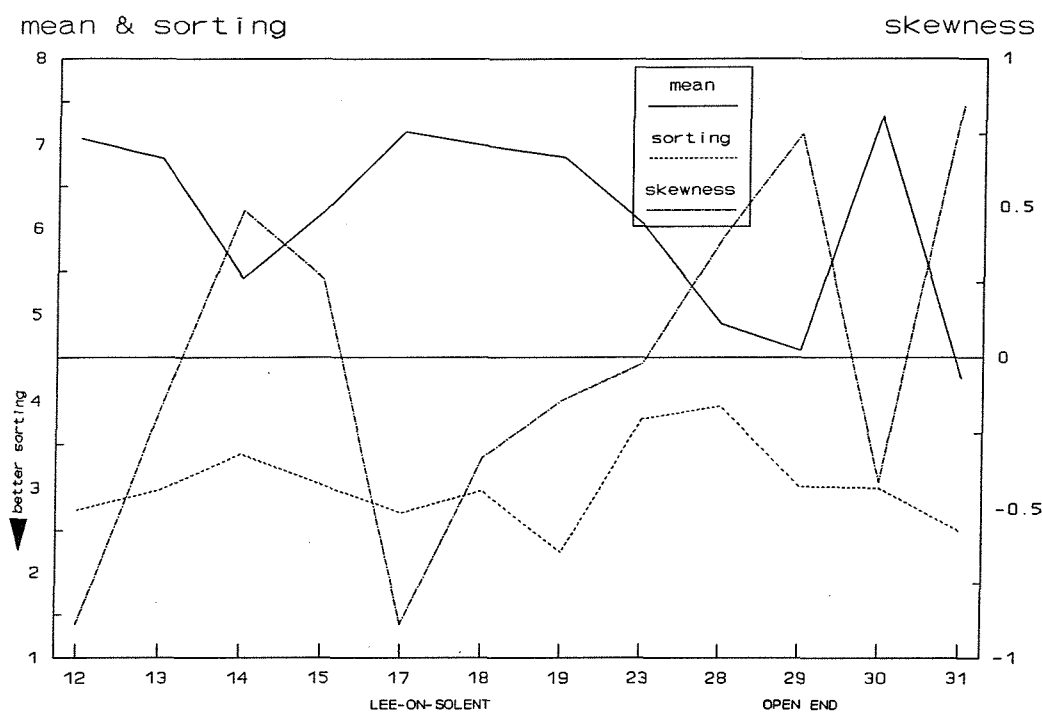


Figure 5.9 : Variation of Grain size parameters in the northern part of the East Solent (for sample locations, see Figure 5.1).

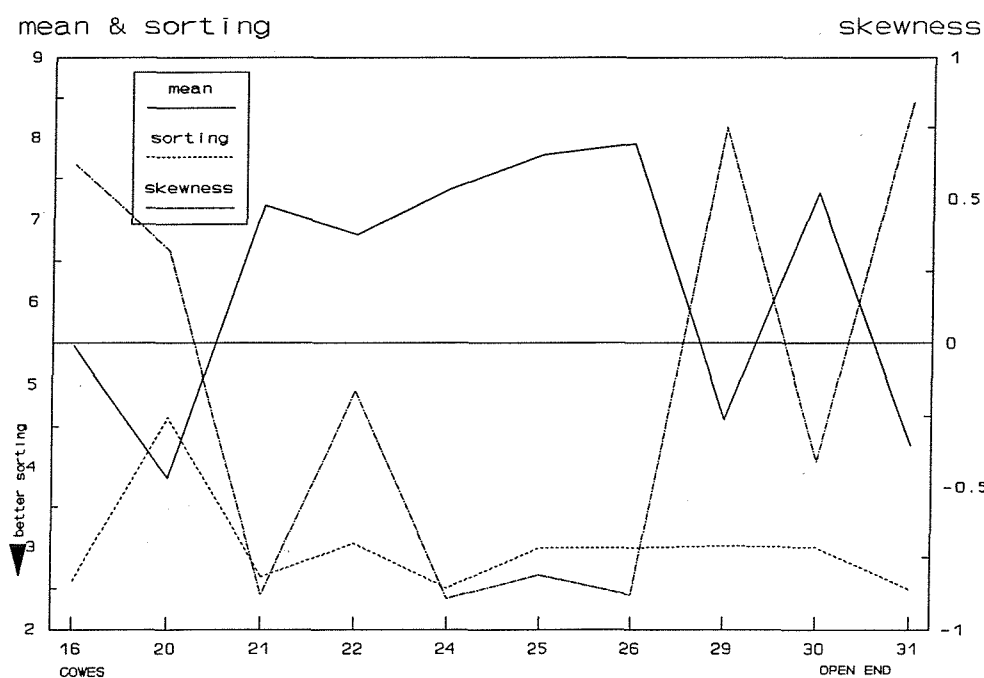


Figure 5.10 : Variation of Grain size parameters in southern part of the East Solent (for sample locations, see Figure 5.1).

of the system to Gilkicker Point. It becomes finer, better sorted and more negatively skewed from locations 14 to 17, suggesting another transport path in the eastward direction. In the southern part of the East Solent, where variations in grain size parameters do not show a clear transport path (Figure 5.10.). However, the sediment becomes finer, better sorted and more negatively skewed from locations 16 to 21. Sand associated with the small delta off Cowes is the probable source of the material, mixing with the pre-existing sediment, such as Sample 16. Hence, a transport path could be from Cowes eastward to Spithead.

Within the Hamble River, Samples R26 and R27 have similar textural parameters; they are very poorly sorted and consist of very positively skewed silt sized sediments. R28 is finer and better sorted than R26 and R27 and is negatively skewed (Figure 5.11). At the mouth of the Hamble, Sample R30 is coarser and more poorly sorted than Sample R28, and is positively skewed. This suggests possibly that longshore currents are transporting sand, which is deposited at the river mouth and is mixed with the original sediments of the River Hamble. The bimodal grain size distribution (Figure 5.4) supports this interpretation. Beaulieu samples (R8, R9, R10, R11) show the effects of downstream transportation, with respect to their decreasing grain size, improved sorting and negatively skewed (Figure 5.12).

Portsmouth Harbour samples are negatively skewed and are better sorted, compared with those from the inlets and the East Solent samples. Sengupta (1979) has pointed out that suspended sediment is, in every case, finer, better sorted and more negatively skewed than bed material. Hence, the unimodal Portsmouth samples (Figure 5.4) might have settled from suspension under prevailing quiescent conditions. Langstone and Chichester Harbour samples are coarse, poor and very poorly sorted, and some are positively skewed. The positively skewed samples are located at the entrance of Langstone and Chichester Harbours. Samples collected from the upper reaches of the harbours show negative skewness. This pattern might indicate the boundary between two sources: a marine-derived coarse fraction and a land-derived fine fraction. It is possible that coarse sediment exchange occurs

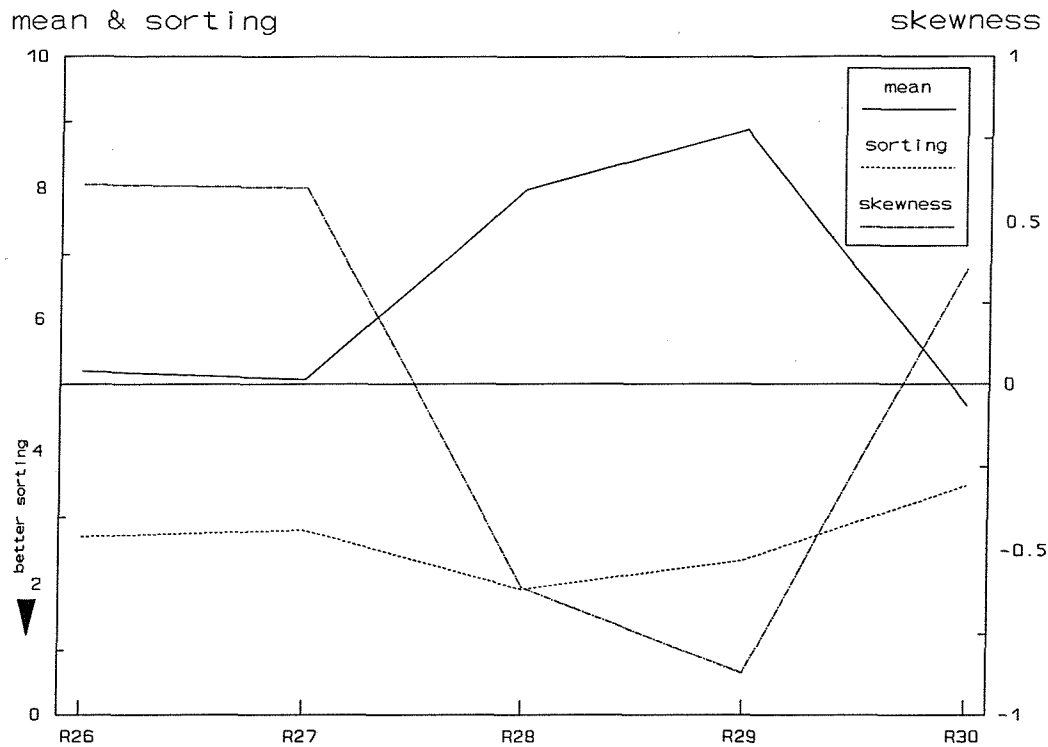


Figure 5.11 : Variation of Grain size parameters within the River Hamble (for sample locations, see Figure 5.1).

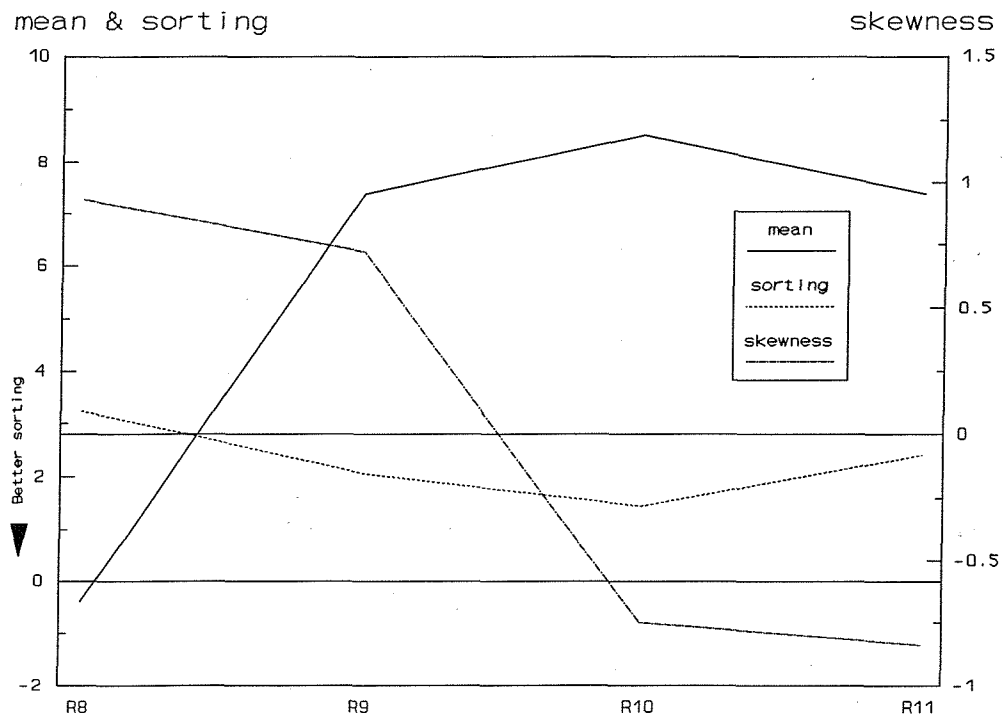


Figure 5.12 : Variation of Grain size parameters within the River Beaulieu (for sample locations, see Figure 5.1).

within Langstone and Chichester Harbours, whilst it is not an effective process within Portsmouth Harbour.

Kurtosis (the concentration or peakedness of the distribution) is a measure of the ratio between the sorting in the tails, to the sorting in the central portion of the distribution (McManus, 1988). If the central portion is better sorted than the tails, the frequency curve is said to be excessively peaked or leptokurtic (Lindholm, 1987). Sediment deposits consisting of mixed populations are typically platykurtic (Sly, 1978). Kurtosis values of the samples in the area are largely platy and very platykurtic (see Table 5.3 and 5.2). Figure 5.13 shows a scatterplot of kurtosis against mean grain size data for all the samples. Platykurtic conditions result from mixtures of sand with silt, and from silt with clay. Strongly leptokurtic conditions can be observed within the sand and clay sized samples. These samples are H4, H5, H6, H7 (Portsmouth Harbour), H12 (Langstone Harbour), R8, R9, R10 (The River Beaulieu), R17 (The River Test), 4, 8, (Southampton Water), 29 and 31 (the open (seaward) end).

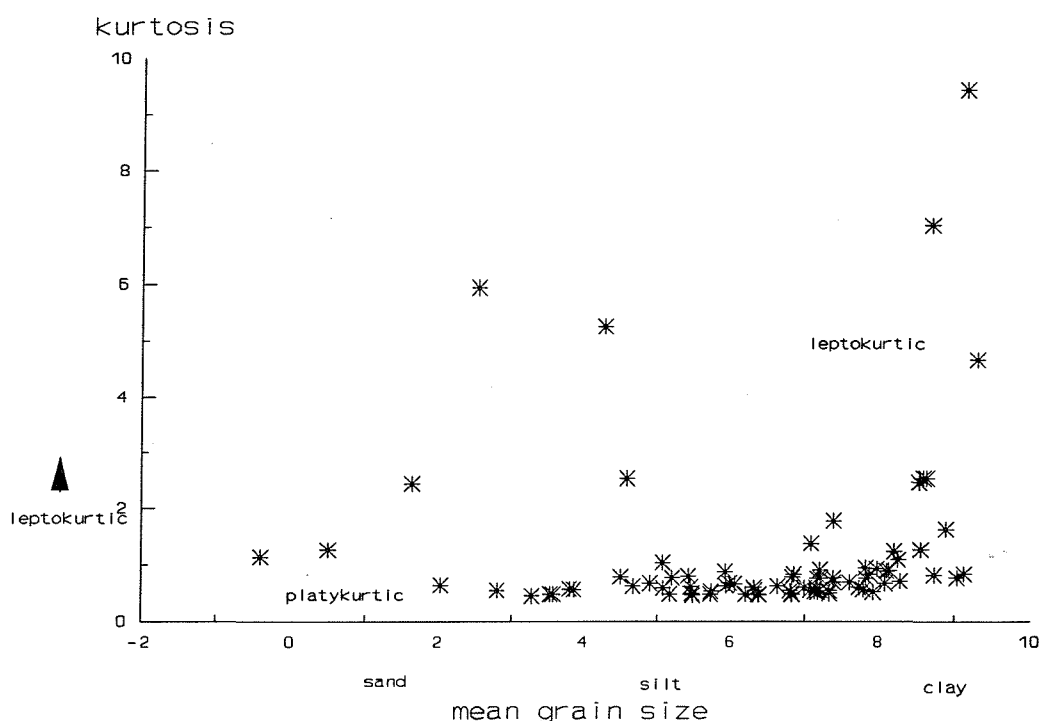


Figure 5.13 : *A plot of kurtosis against mean grain size, for all the surficial sediment samples.*

5.1.4. Scatterplots of Textural Parameters

Bivariate scatterplots of textural parameters have been used by many authors (Folk & Ward, 1957; Glaister & Nelson, 1974; Allen, 1971; Miola & Weiser, 1968) to understand the geological significance of the size parameters. Folk & Ward (*op.cit.*) have stated that a plot of skewness against kurtosis is a useful technique in interpreting the genesis of sediments. Mean grain size, plotted against sorting and skewness, provides information on the primary sedimentation conditions in the Solent region. Figure 5.14 shows a plot of sorting against mean grain size. The overall correlation between the two parameters indicates that sorting improves as the mean grain size becomes finer. Samples R8, R1, R21 (upstream of the Rivers Beaulieu, Keyhaven and Itchen, respectively) and H12 (from the entrance to Langstone Harbour) differ from this general trend. The trend suggests the mixing of a coarse population with a fine population, upwards on the diagram (Folk & Ward, *op.cit.*). Nordstrom (1977) has pointed out that tidal currents appear to represent an efficient transport process, but an inefficient sorting mechanism. Therefore, sediments in tidally-dominated areas are typically coarser grained, less well sorted and negatively skewed. Samples from Southampton Water and the East Solent are clustered into disparate groups, suggesting that they are influenced by different transport mechanisms. On Figure 5.15, the skewness is plotted against mean grain size. In general, skewness becomes negative as the mean size decreases. Samples are clustered into two main groups, displaying the same trend; as the mean grain size decreases, the skewness becomes more negative. Southampton Water samples lie to the lower right of the Figure, with the exceptions of Samples 7 and 10, whereas samples from the East Solent are distributed over a broader range. Sediments associated with tidally-dominated areas are characteristically less well sorted and negatively skewed (Duane, 1964; Allen, *op.cit.*). The clustering of the samples might be an indication of the variation of energy conditions within the various areas.

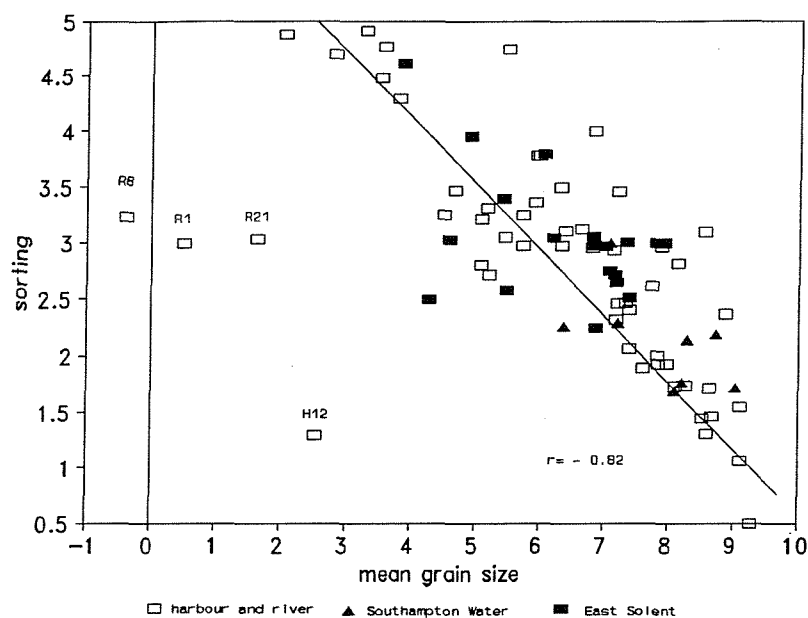


Figure 5.14 : A plot of sorting against mean grain size (r is presented on the basis of rejection of the outlying samples).

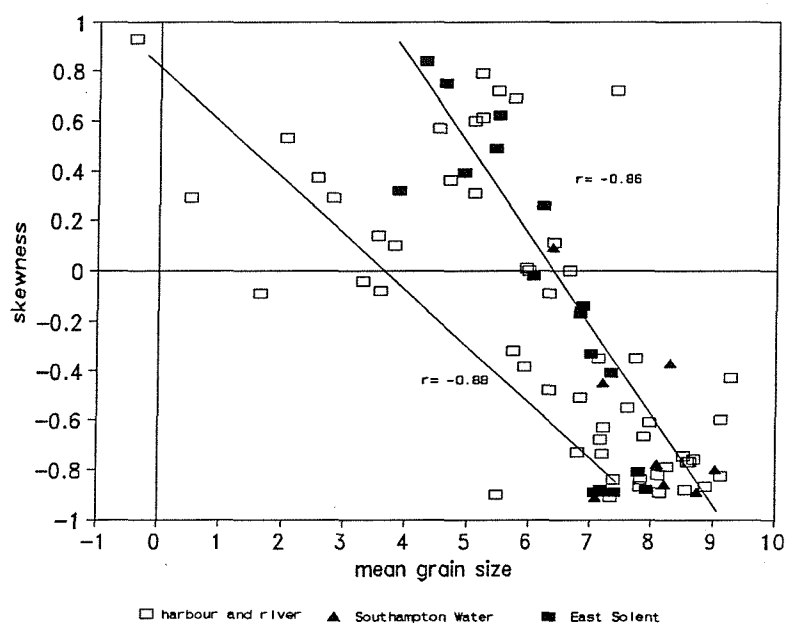


Figure 5.15 : A plot of skewness against mean grain size (r 's are presented as two separate trends).

5.1.5. Grain Size Distributions: Concluding Remarks

- (i) The general classification of grain size (Figure 5.2) indicates that two different sediment populations occur in the East Solent and Southampton Water. Two end members (clay and sand) occur in variable proportions in the East Solent, whereas silty clay dominates Southampton Water. The percentage of sand and silt in Southampton Water samples is variable, whilst the percentage of clay is almost constant.
- (ii) The distribution pattern of the different sediment types (Figure 5.3) suggests that sand-sized sediments might be transported from both, the West Solent and the open (seaward) end of the East Solent. The East Solent is floored with sand and clay in variable proportions, displaying different sedimentary features to the West Solent and offshore. The riverine sediment input to Southampton Water is of variable grain size. However, the bulk of the deposited sediment is silty clay within the channel. Sediment characteristics differentiate Portsmouth from Langstone and Chichester Harbours. Well developed tidal deltas within Langstone and Chichester Harbours reflect a sediment exchange through the inlet straits, whereas the Portsmouth Harbour sediments are fine-grained and do not appear to receive coarse input from the inlet mouth.
- (iii) Histograms of the grain size of sediments from Southampton Water indicate a dominant fine mode in the clay range. Most samples show a bimodal distribution, which is transformed into a trimodal distribution in the vicinity of Calshot Spit; this may be, therefore, a source for the sand-sized material. East Solent sediments may be classified into two groups; one is dominated by a coarser mode, whilst the other is dominated by a finer mode. However, a trimodal distribution can be observed in Samples 19 (Gilkicker Point), 20 (northern coast of the Isle of Wight), 23 and 28 (open end of the East Solent). This pattern may be an indication of the oscillatory transport direction at these locations. Sediment transport may occur in both directions at these locations; the one may be towards the east in the northern side of the East Solent (Lee-on-Solent) and the other could be from the open end to the inner part (Gilkicker Point) of the East Solent. Portsmouth Harbour samples have an

almost unimodal distribution of clay within the tidal inlet of the harbour, whereas Langstone and Chichester samples have trimodal and multimodal distributions.

(iv) Grain size textural parameters reflect the general transport pattern, to some extent: the mean grain size suggests a consistent coarsening, from Southampton Water towards the East Solent. There may be an anthropogenic input of sediment into the River Itchen. Likewise, the similarity in the grain size parameters between the River Test and the head of the Southampton Water may suggest the dominant influence of the River Test. The variations in the sediment trends along the main channel of Southampton Water might be attributed to a landward bottom movement occurring in the vicinity of the Calshot Spit. Although grain size trends in the East Solent are not clear, they may support (iii), above *i.e.* one transport path might be towards the east along the northern side of the East Solent (Lee-on-Solent), whilst the other might be from the open end to the inner part (Gilkicker Point) of the East Solent. An additional transport path from Cowes (Isle of Wight), towards the east (Spithead), may also be discerned.

(v) Scatterplots differentiate between transport-deposition processes occurring in the East Solent and Southampton Water. Southampton Water samples are finer, better sorted and negatively skewed, whereas the East Solent samples vary over a broader range, suggesting mixing of sediments from more than one source.

5.1.6. Trend Vector Analysis

In an attempt to determine the direction of net sediment transport, grain size parameters were applied to the trend vectors technique developed by Gao & Collins (1991, 1992). Although the sampling strategy in this study is not ideal for the application of this model, it provides supporting evidence to the arguments developed elsewhere in this thesis. The technique is a modification of the specific sediment trend analysis which was developed by McLaren & Bowles (1985). Trend vectors are filtered and transformed into transport vectors, representing the net transport paths. The details of the technique are presented in Gao & Collins (1991,

1992). The sediment trend vectors are illustrated in Figure 5.16. Arrows indicate the direction of net sediment transport and the length of the arrows indicates the relative magnitude of the movement, or dominance of the process. Net sediment transport occurs downstream in the rivers. Within Southampton Water sediment transport is downstream, until Sample 7. The arrows indicate a transport path upstream at Samples 7, 10 (Calshot Spit), and 3 (the western approach to Southampton Water). At the mouth of the estuary, the arrows indicate a transport direction to the east. All the trend vectors on the northern side of the East Solent point towards the inner part of the channel. The main transport direction along the Isle of Wight is SE. Trend analysis shows no significant movement of material at the open (seaward) end, towards the East Solent; this might be indicative of depositional processes (Gao, pers. comm.). The arrows within the harbours imply transport towards the bay-head.

The trend vectors technique is in agreement with the arguments developed above for the river and Southampton Water samples. However, interpretations for the East Solent are not in agreement. The reason for this difference may be attributable to the inappropriate sampling strategy used here. The trend vector technique requires a condensed grid sample pattern for sampling, in order to eliminate background noises. In contrast, the sampling pattern adopted in this study was based upon fine-grained (muddy) areas. Nonetheless, this approach has provided an alternative procedure to the interpretation of transport pathways, which could be developed further in the future.

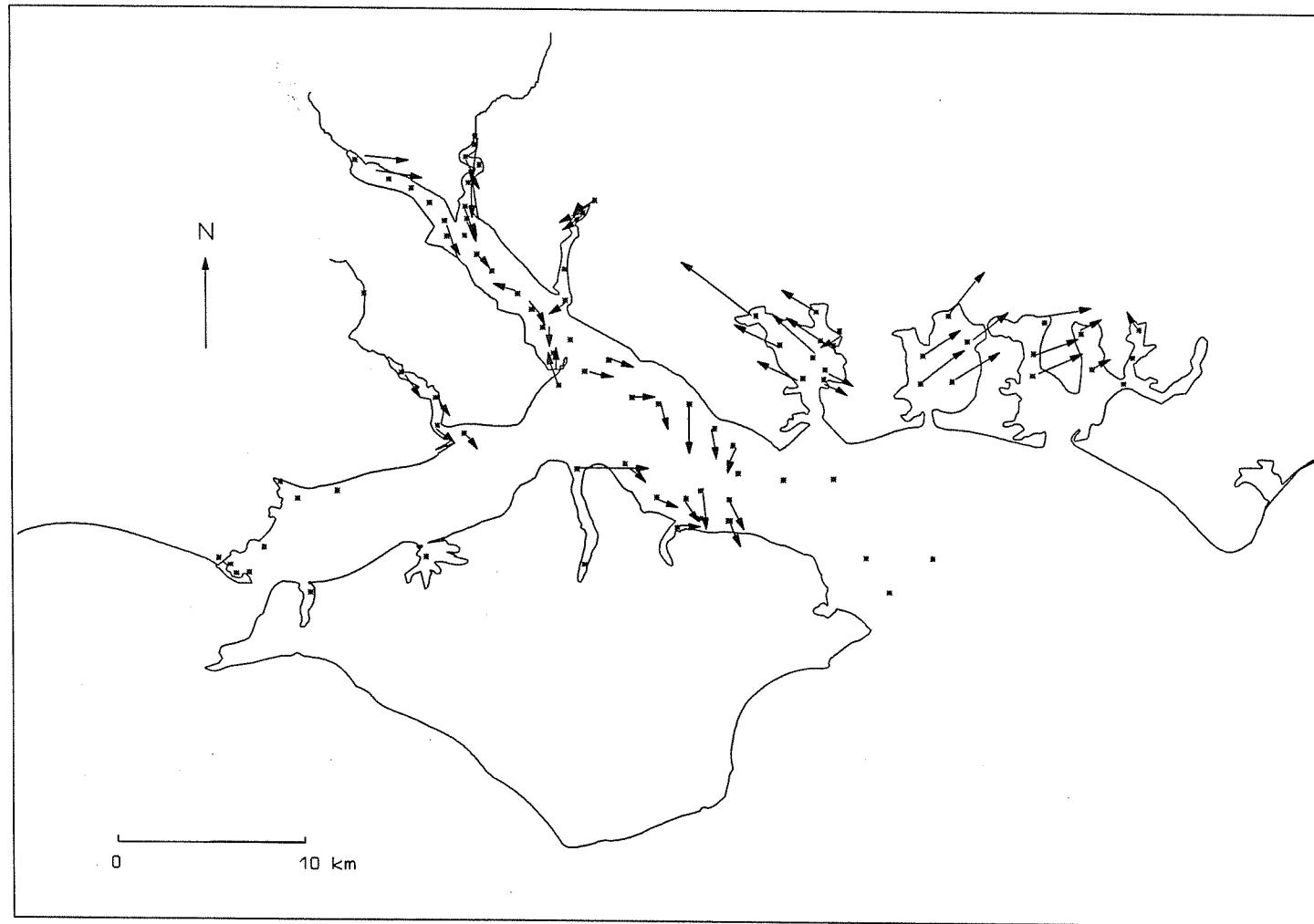


Figure 5.16 : *Sediment transport vectors as determined by the Gao approach (1991, 1992) (i.e. modified 'McLaren technique').*

5.2. The Distribution of Clay Minerals within Surface Sediments

The clay mineralogy of all the samples from the Solent region consists mainly of illite, smectite, and kaolinite, with trace amounts of chlorite. The values presented below were calculated on the basis of the assumption that the clay fraction consisted of these minerals alone (Table 5.4).

Table 5.4 : Proportional abundances and ratios of clay minerals in the surface sediments (continued on following pages).

Sample No	Smectite (%)	Illite (%)	K+C (%)	Peak Heights (cm)			Ratio (height)	
				smectite	illite	k+c	S/I	S/K
H1	39	41	20	1.3	1.7	1.9	0.8	0.7
H2	35	41	24	2.3	4.3	4.8	0.5	0.5
H3	32	42	26	1.8	3.6	4.3	0.5	0.4
H4	31	43	26	1.9	3.4	3.9	0.6	0.5
H5	34	43	23	2.1	3.9	4.6	0.5	0.5
H6	38	38	24	2.3	3.4	4.3	0.7	0.5
H7	37	41	22	2.5	3.9	4.7	0.6	0.5
H8	46	33	21	1.1	1.1	1.1	1	1
H9	45	37	18	2.6	2.5	2.5	1	1
H10	36	40	24	2.4	4.2	4.4	0.6	0.5
H11	38	39	23	2.3	3.1	3.7	0.7	0.6
H12	38	41	21	1.9	3.4	3.2	0.6	0.6
H13	45	36	19	4.2	4.5	4.7	0.9	0.9
H14	40	39	21	3	3.7	4.2	0.8	0.7
H15	41	38	21	2.6	3.6	4	0.7	0.7
H16	35	43	22	1.7	2.4	2.9	0.7	0.6
H17	40	39	21	2.3	3	3.1	0.8	0.7
H18	45	30	25	2.5	2.2	3.5	1.1	0.7
H19	51	33	16	3.6	3.8	5.5	0.9	0.7
H20	39	39	22	2.7	3.4	3.8	0.8	0.7
H21	42	37	21	2.5	2.9	3.4	0.9	0.7
H22	44	37	19	2.4	3.1	3.2	0.8	0.8
H23	42	37	21	2.6	3.1	3.5	0.8	0.7

Table 5.4 (continued) : Proportional abundances and ratios of clay minerals in the surface sediments.

Sample No	Smectite (%)	Illite (%)	K+C (%)	Peak height (cm)			Ratios	
				smectite	illite	k+c	S/I	S/K
R1	29	45	26	1.5	4	4.3	0.4	0.3
R2	28	45	27	2.1	4.7	5.9	0.4	0.4
R3	31	44	25	1.5	3.6	3.8	0.4	0.4
R4	31	46	23	1.9	4.2	4.6	0.5	0.4
R5	29	43	28	2	4	4.9	0.5	0.4
R6	33	39	28	2.8	5	6.2	0.6	0.5
R7	29	44	27	2.2	4.5	5.3	0.5	0.4
RB	61	29	10	4.7	2.6	2.9	1.8	1.6
R8	36	41	23	1.6	3.8	4.3	0.4	0.4
R9	35	42	23	2.2	4.3	5	0.5	0.4
R10	30	44	25	2.4	4.9	5.8	0.5	0.4
R11	33	42	25	2.4	4.5	5.3	0.5	0.5
RT	50	31	19	1.8	1.6	2.4	1.1	0.8
R12	43	37	20	2.4	3	3.2	0.8	0.8
R13	44	37	19	2.4	2.9	3.7	0.8	0.6
R14	38	40	22	1.9	2.6	3.1	0.7	0.6
R15	36	41	23	1.7	2.8	3.3	0.6	0.5
R16	34	41	25	1.7	2.8	3.4	0.6	0.5
R17	27	43	30	3.4	7	8.6	0.5	0.4
R18	32	42	26	1.4	2.9	3.3	0.5	0.4
RI	48	38	15	0.8	0.5	0.6	1.6	1.3
R19	57	30	13	NC	NC	NC	-	-
R20	57	27	16	1.3	1.1	1	1.2	1.3
R21	52	34	14	1.1	1.2	1.2	0.9	0.9
R22	43	37	20	1.9	2.4	2.6	0.8	0.7
R23	38	39	23	1.7	2.1	2.4	0.8	0.7
R24	43	38	19	2	2.4	3	0.8	0.7
R25	35	40	25	1.7	2.4	2.9	0.7	0.6
R26	55	32	13	3.2	3	2.9	1	1.1
R27	53	32	15	2.6	2.5	3.2	1	0.8
R28	44	36	20	2.7	3.4	4	0.8	0.7
R29	41	37	22	2.3	3.1	3.8	0.7	0.6
R30	34	43	23	2	3.5	4.2	0.6	0.5
R31	34	42	24	2.2	4.1	4.8	0.5	0.5
R32	36	41	23	2.5	4.4	5.1	0.6	0.5
R33	38	40	22	2	3.6	3.9	0.6	0.5
R34	39	41	20	2.1	3.6	3.9	0.6	0.5
R35	42	34	24	1.5	2.2	2.9	0.7	0.5

Table 5.4 (continued) : Proportional abundances and ratios of clay minerals in the surface sediments.

Sample No	Smectite (%)	Illite (%)	K+C (%)	Peak Heights (cm)			Ratio (height)	
				smectite	illite	k+c	S/I	S/K
1	28	45	27	1.7	3	3.7	0.6	0.5
2	32	42	26	2.6	4.9	5.8	0.5	0.4
3	40	39	21	2.6	3.6	4	0.7	0.7
4	40	38	22	1.7	2.2	2.6	0.8	0.7
5	33	41	26	1.5	2.8	3.3	0.5	0.5
6	34	41	25	2.2	3.8	4.4	0.6	0.5
7	34	42	24	1.9	3.1	3.6	0.6	0.5
8	38	40	22	2.3	3.5	4	0.7	0.6
9	38	40	22	1.9	3	3.1	0.6	0.6
10	31	43	26	2	3.6	4.4	0.6	0.5
11	33	42	25	1.6	2.8	3.3	0.6	0.5
12	35	41	24	2.6	3.7	4.3	0.7	0.6
13	29	44	27	1.7	2.8	3.3	0.6	0.5
14	36	40	24	2.3	3.3	3.9	0.7	0.6
15	34	41	25	1.8	3.2	3.8	0.6	0.5
16	28	43	29	1.6	3.3	4.2	0.5	0.4
17	28	44	28	2	3.5	4.2	0.6	0.5
18	42	37	21	NC	NC	NC	-	-
19	34	42	24	2	3.4	3.9	0.6	0.5
20	35	42	23	2.2	3.7	4.2	0.6	0.5
21	34	41	25	2.2	3.6	4.5	0.6	0.5
22	27	45	28	1.1	2.8	3.5	0.4	0.3
23	33	40	27	1.6	2.7	3.3	0.6	0.5
24	39	40	21	2.2	3.4	3.9	0.6	0.6
25	35	39	26	1.7	2.7	3.4	0.6	0.5
26	34	40	26	2	2.9	3.5	0.7	0.6
27	35	39	26	2.3	3.2	3.9	0.7	0.6
28	36	39	26	2.0	2.8	3.5	0.7	0.6
29	28	43	29	1.3	2.7	3.4	0.5	0.4
30	30	41	29	1.4	2.6	3.5	0.5	0.4
31	28	43	29	1.3	2.6	3.4	0.5	0.4

5.2.1. Proportional Abundance of Clay Minerals

The relative clay mineral abundances in all the samples are plotted on a ternary diagram (Figure 5.17.). A linear trend in the data is evident, forming a continuum which is dominated by changes in the relative proportions of smectite to kaolinite + chlorite and illite. The ratio of kaolinite + chlorite to illite is not constant, but increases with decreasing smectite content. The relatively low scatter about a line drawn through the points is consistent with mixing between two clay mineral sources (Karlin, 1980); one relatively high in smectite and the other relatively high in kaolinite + chlorite and illite.

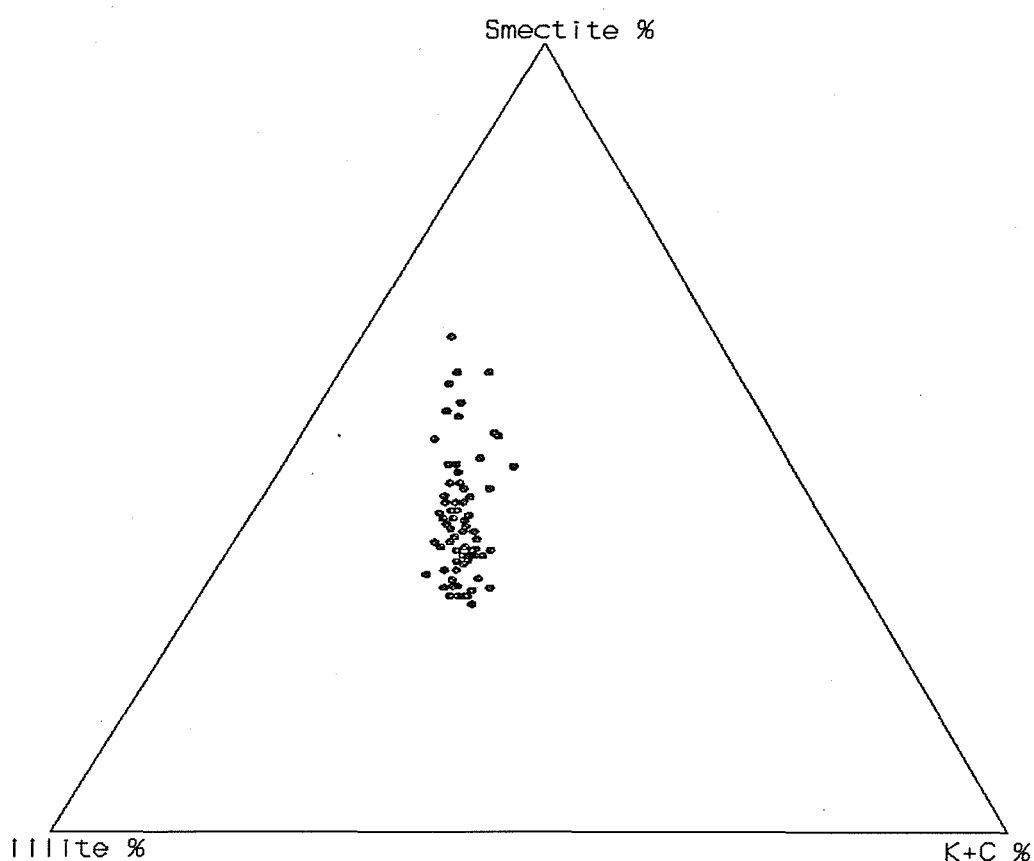


Figure 5.17 : Ternary diagram of clay minerals (*K+C % denotes the percentage of kaolinite and chlorite*).

5.2.2. Spatial Distribution of Clay Minerals

Illite: is the most common clay mineral found in the surface sediments of the area, with a mean proportion of around 40% (Figure 5.18 and Table 5.4); it is less abundant upstream in the Rivers Itchen (30%), Test (31%), Hamble (32%) and Beaulieu (29%). An increase occurs in all the rivers in the downstream direction. The percentage of illite fluctuates around 40% in Southampton Water (38-43%) and the East Solent (37-45%). The maximum value of 45% occurs in the middle of the East Solent and in the vicinity of the River Keyhaven. From the open (seaward) end (St Helen's Road) to the inner part of the East Solent, a decrease in illite concentration can be observed (from 43 to 39%). Illite concentrations are highly variable in the harbour regions, but on average appears to be higher in Portsmouth Harbour (40-43%) than in Langstone and Chichester Harbours (33-41%). In the West Solent, the percentage of illite varies within a narrow range of 42-45%.

Smectite: is rather less abundant than illite over the region, with a mean of 35% (Figure 5.19). In contrast to illite, it occurs most abundantly upstream in the Rivers Itchen (48%), Test (50%), Hamble (55%) and Beaulieu (61%), and is remarkably variable over the rest of the area; it varies within the range of 31 to 40% in Southampton Water, and 28 to 42% in the East Solent. The bay-head of the harbours contain higher proportions of smectite than those in the inlets. The Portsmouth samples contain 30 to 40% of smectite; this is less than the Langstone and Chichester samples (40-50%). In the West Solent, the percentage of smectite may increase towards the east (from 28 to 33%).

Kaolinite and chlorite: these percentages have been calculated jointly, due to their low concentration and to the problems induced by overlapping peaks (see Section 4.2.2.). Kaolinite + chlorite percentages, in general, remain between 20 and 29% (Figure 5.20); they are low upstream in the Rivers Itchen (15%), Test (19%), Hamble (13%) and Beaulieu (10%) and increase downstream. Southampton Water samples have percentages which range from 22 to 26%. In the East Solent, kaolinite + chlorite abundances are slightly higher than in Southampton Water,

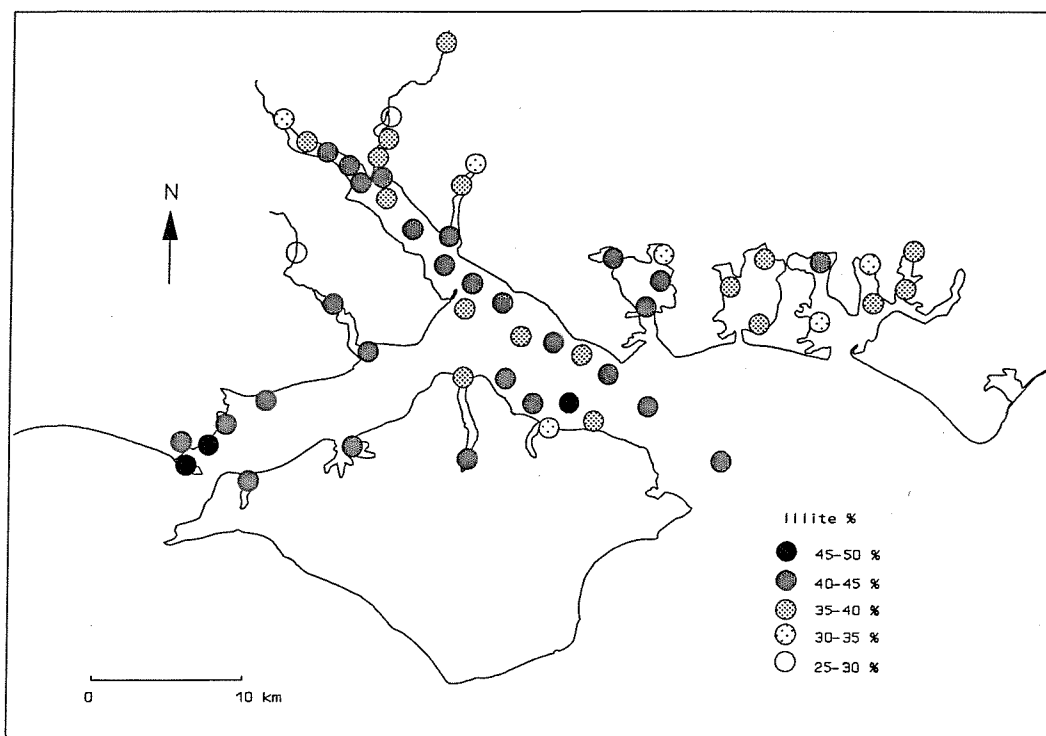
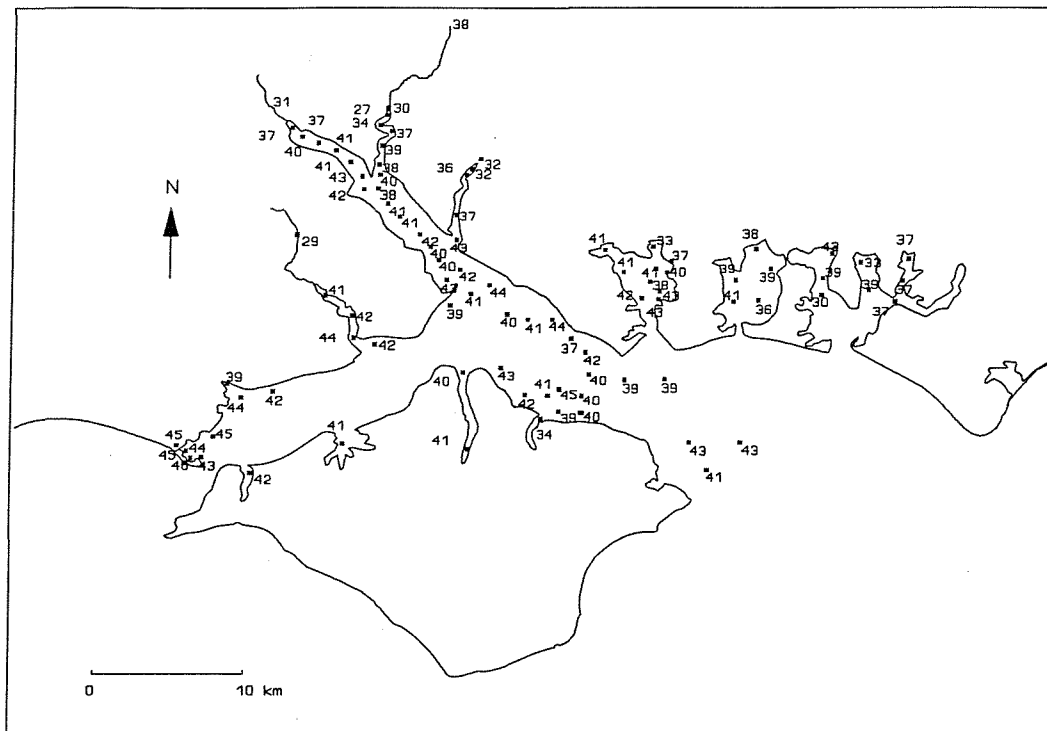


Figure 5.18 : The distribution of illite in the surface sediments of the Solent.

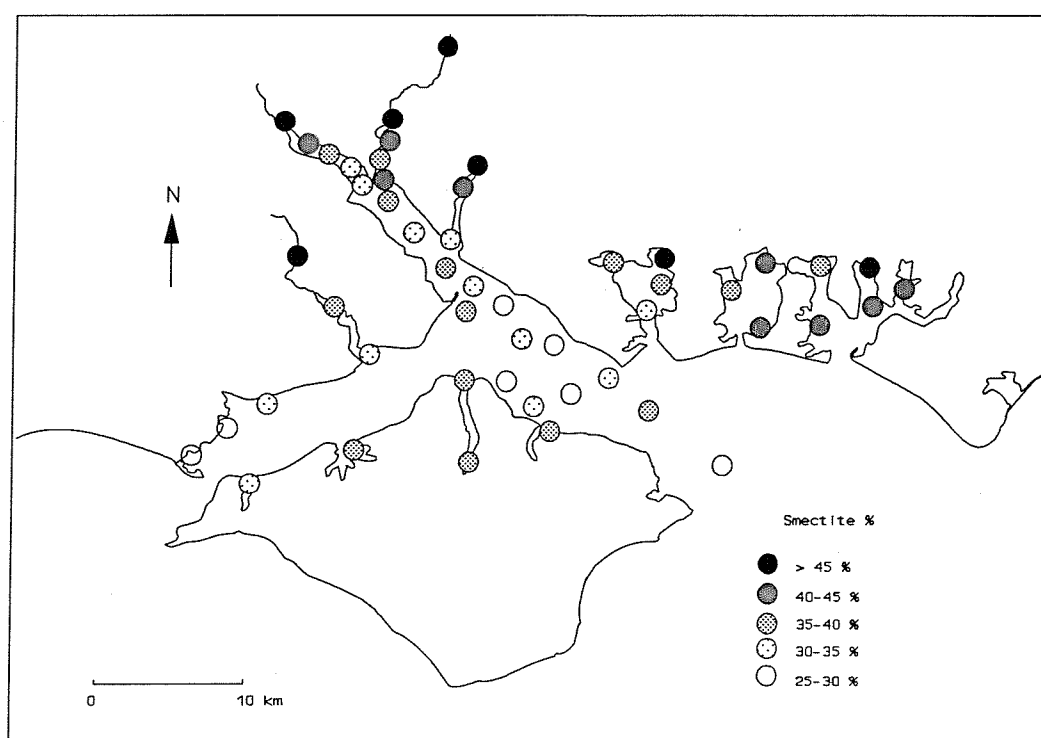
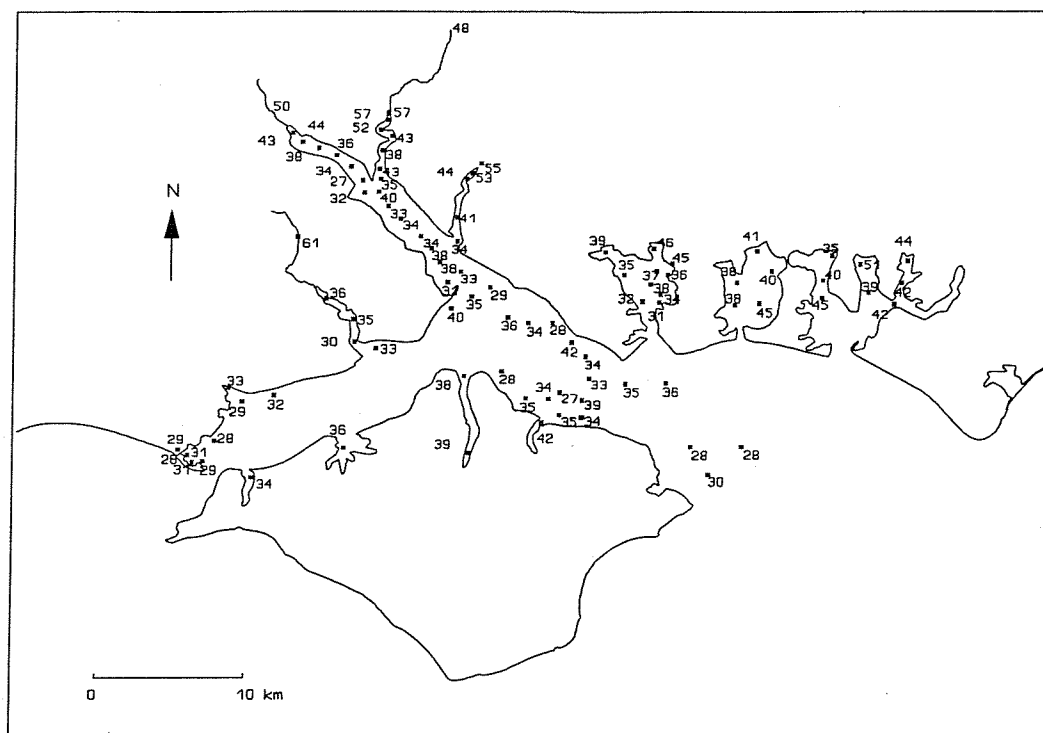


Figure 5.19 : The distribution of smectite in the surface sediments of the Solent.

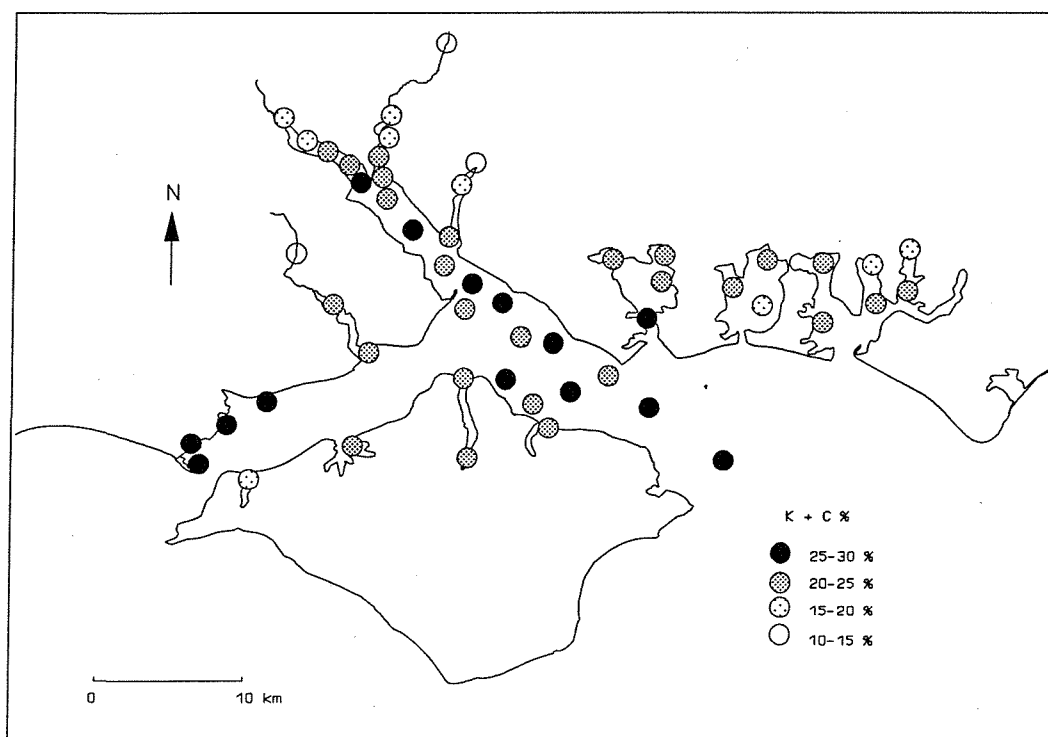
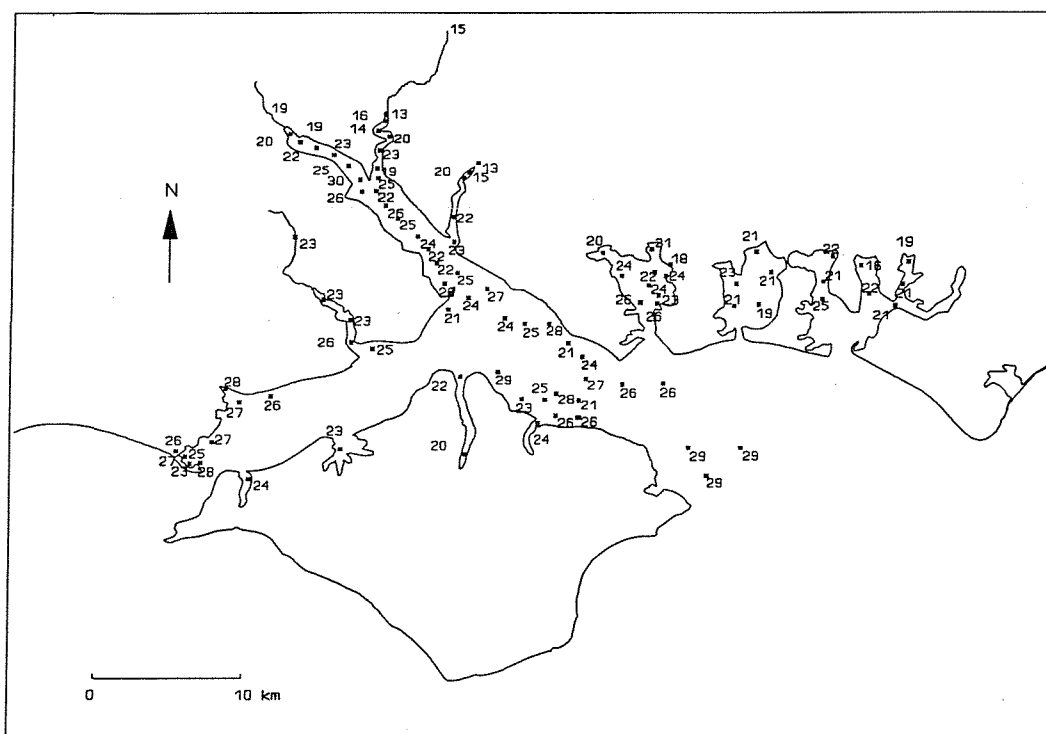


Figure 5.20 : The distribution of K+C in the surface sediments of the Solent.

lying between 24 to 29%. At the open end of the East Solent (St Helen's Road), these minerals remain at a constant level (29%) and are amongst the highest concentrations over the whole area. The Portsmouth Harbour samples contain 20 to 26% of kaolinite + chlorite, but the Langstone and Chichester samples have lower values (16 to 22%). In the West Solent, kaolinite + chlorite concentrations decrease (27 to 21%) from west to east.

5.2.3. Clay Mineral Ratios

Clay mineral ratios were calculated from their peak heights. The distribution of smectite/illite ratios (S/I) in the Solent region is shown in Figure 5.21. The ratio varies between 0.4 to 1.8, becoming progressively higher upstream in samples collected from the Rivers Itchen (1.6), Hamble (1.1) and Beaulieu (1.8). Southampton Water samples have a range which lies at between 0.5 to 0.7. The upper part of the main channel has values of 0.5, which increase to 0.7 at the mouth of the estuary. In the East Solent, the ratio fluctuates between 0.4 to 0.7, whereas in St Helen's Road (open end), constant values of 0.5 are found. The West Solent nearshore sediments have also almost constant values of 0.5 (0.4-0.5 in the Keyhaven samples). The Portsmouth Harbour sediments have values in the range of 0.5 to 1, whereas the Chichester samples have ratios of between 0.6 to 1.1.

The dispersal pattern of the smectite/(kaolinite+chlorite) $[S/(K+C)]$ ratios in the Solent region is similar to that of the S/I ratios. The ratio decreases downstream in the Rivers Test (0.8 to 0.4), Itchen (1.3 to 0.6), Hamble (1.1 to 0.5) and Beaulieu (1.6 to 0.5). The Southampton Water samples exhibit values of 0.5 and 0.6. The East Solent samples have variable values, which lie in the range of 0.3 to 0.6. The West Solent sediments have a rather constant ratio, which is almost 0.4. The Portsmouth Harbour samples are variable and range between 0.4 to 1.0. Finally, the Langstone and Chichester samples exhibit values of 0.6, 0.7 and 0.8.

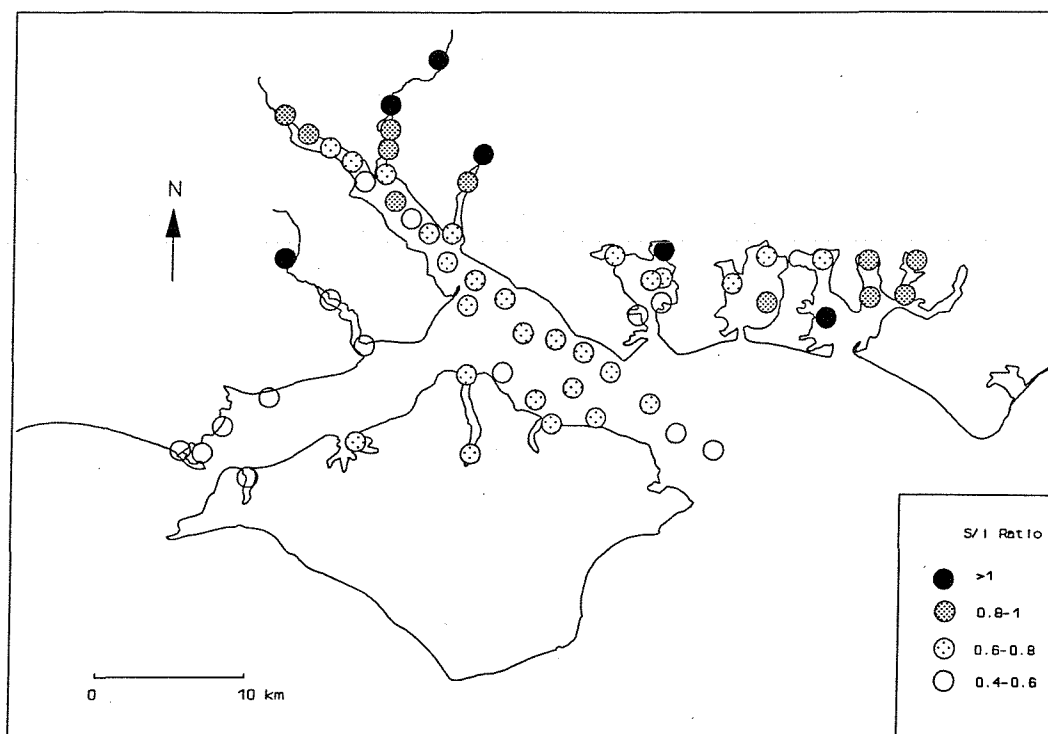


Figure 5.21 : *The distribution pattern of the S/I ratio in the surficial sediments of the Solent.*

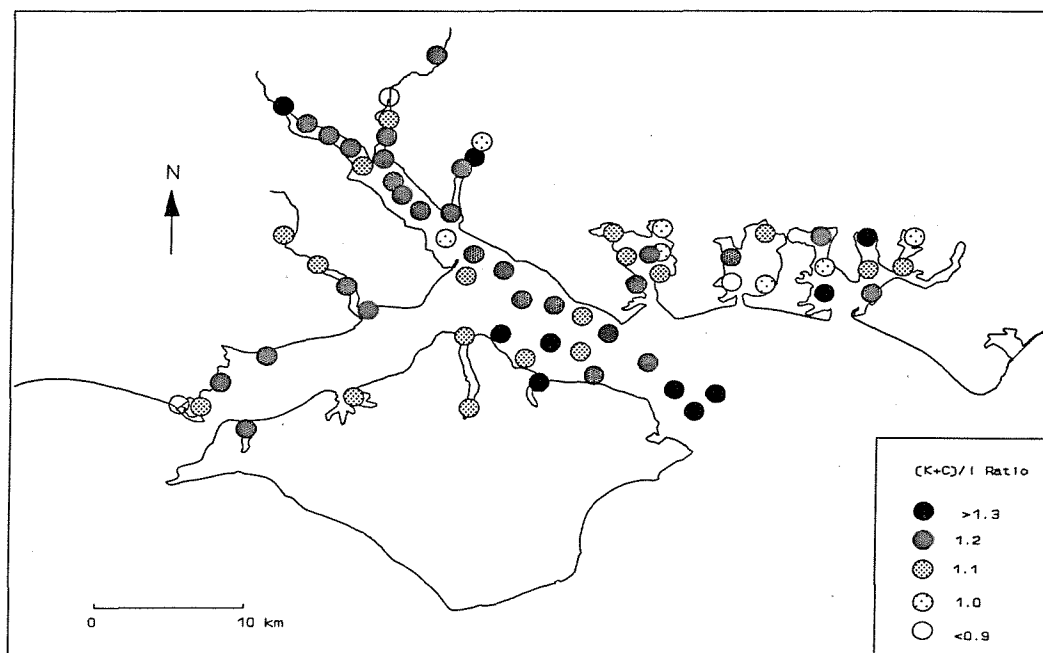


Figure 5.22 : *The distribution pattern of the (K+C)/I ratio in the surficial sediments of the Solent.*

The dispersal pattern of the (K+C)/I ratio is shown in Figure 5.22. Although the trends are not as obvious as those of the two previous ratios, the values appear on average to be lower but more variable in the harbours and upstream regions. The highest ratios (1.3) are found on the southern side of the East Solent and at St. Helen's Road.

5.2.4. Clay Mineral Distributions: Concluding Remarks

Dispersal patterns of the clay minerals are related strongly to the composition of the source material or provenance and reflect the transport pathways of the fine-grained sediments (Dyer, 1986; Chamley, 1989; Shaw, 1973; Weaver, 1989; Griffin *et al.*, 1968). The clay mineralogy of the surface sediments in the area should be a function, therefore, of the geological formations which surround the Solent Estuarine System and the transport pathways within the system. The geological formations (Chapter 3) within the Solent region contain montmorillonite (smectite), illite, and kaolinite and chlorite in varying proportions. Gilkes (1966) has divided the Tertiary sediments of the Hampshire Basin into two clay mineral provinces. The western province is characterized by kaolinite-illite (KI), from the West Country granites, whilst the highly montmorillonitic (SI) sediments of the eastern province (smectite-illite-subordinate kaolinite and trace chlorite) were derived partially from the dissolution of Chalk. There is a general trend of decreasing illite and kaolinite + chlorite, towards the east in the West Solent. This trend might be a result of proximity to the two provinces, namely KI in the west and SI in the east.

After considering the source effect on the availability and abundance of the clay minerals, it is necessary to examine the dispersal pattern, which will be dominated by the transportation processes. The spatial distribution of clay minerals is dominated by two distinctive features:

- (i) smectite is concentrated within the upper reaches of the Rivers Itchen, Test, Hamble and the upper parts of the harbours - it decreases downstreams

from these locations, whilst illite and K+C show an inverse trend;
and (ii) the ratio of K+C to illite increases with decreasing smectite content,
in a seaward direction.

Since smectite is present in higher percentages upstream in the rivers, it could be argued that there is a terrestrial source of smectite, whereas illite and K+C could be marine-derived. The ternary diagram (Figure 5.17) also supports the hypothesis that two sources supply sediment into the area; one is high in smectite, whilst the other is high in illite. The decrease in smectite with distance downstream may suggest a landward source, mainly from the Rivers Itchen, Test and Hamble. On the other hand, the illite and K+C contents show a contrasting tendency, increasing downstream. These distribution trends are consistent with mixing between two sources: fluvially-derived smectite-rich material, with a relatively low ratio of kaolinite + chlorite to illite; and material of marine origin poorer in smectite and with a higher ratio of kaolinite + chlorite to illite. The variations (or fluctuations) in concentration along Southampton Water and within the East Solent may be indicative of dilution effects and the reworking of sediments.

Figure 5.23 shows the variation of the three ratios along a transect from the upper reaches of the River Itchen, along Southampton Water, to the open (seaward) end of the East Solent. There is a distinct decrease in the S/I and S/(K+C) ratios, from the River Itchen to the entrance of Southampton Water (1.6 to 0.6 and 1.3 to 0.6 respectively). The (K+C)/I ratio shows a slight but significant, increase towards the East Solent. The effect of mixing between the two different sources (riverine and marine) can be detected on the basis of a decrease in the S/I and S/(K+C) ratios. Southampton Water is, therefore, the mixing zone. The concentration of illite and K+C increases within Southampton Water, relative to the rivers. The Portsmouth Harbour samples differ somewhat from those of Langstone and Chichester. Illite and K+C concentrations are slightly lower in Chichester and Langstone Harbours. This reduction may relate to the different sources and/or hydrodynamical activity within each of the harbours. The West Solent samples do not show significant differences from those of the East Solent. However, towards

the east, smectite increases from 28 to 40%, illite decreases from 45 to 39% and K+C decreases also from 27 to 21%.

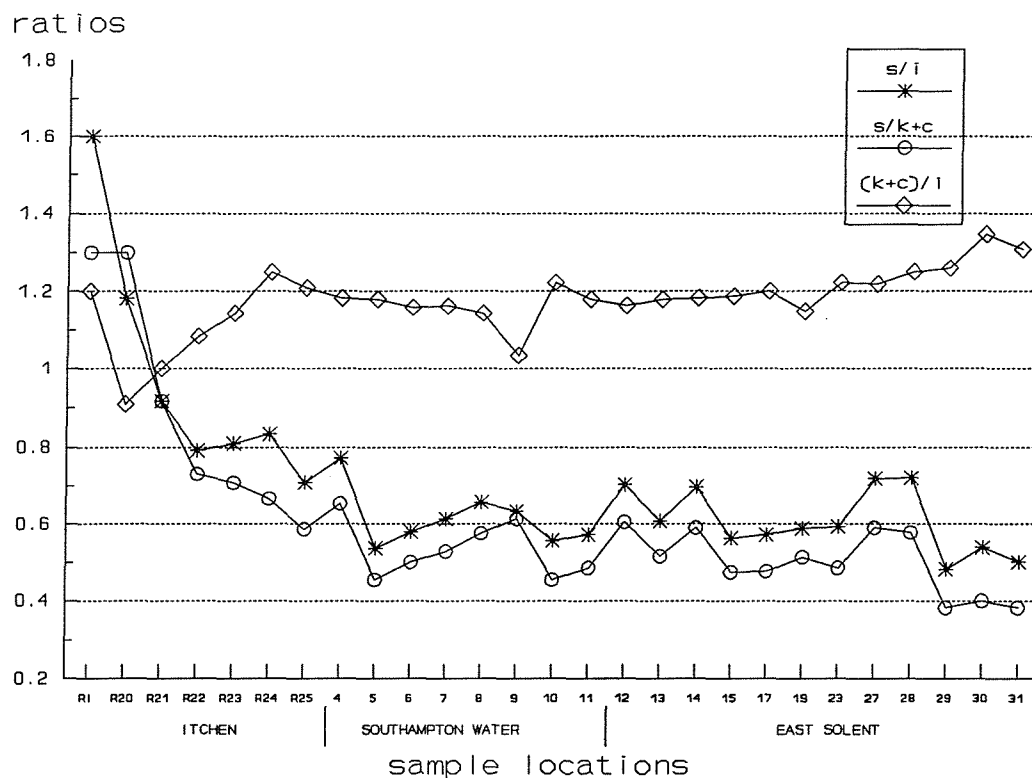


Figure 5.23 : Distribution pattern of clay mineral ratios from landward to seaward (for sample locations, see Figure 5.1).

There are other possible explanations for the present clay mineral distribution. Abrupt changes in the ratio of smectite to illite or K+C may be attributed to diagenetic alteration (Johns & Grim, 1958; Park *et al.*, 1986). Johns & Grim (*op.cit*) observed such a pattern in the Mississippi River Delta and concluded that illite and kaolinite are the product of early diagenesis of montmorillonite. However, diagenesis is believed to have only a minor effect on surface sediments (Edzwald & O'Melia, 1975).

Size segregation or differential flocculation mechanisms have been used to

explain the dispersal pattern of clay minerals within recent sediments (Gibbs, 1977; Whitehouse *et al.*, 1960). The laboratory experiments undertaken by Whitehouse *et al.*, (*op.cit*) have shown that illite and kaolinite flocculate at lower salinities than smectite. However, kinetic studies by Edzwald & O'Melia (1975) demonstrate that illite is more stable than kaolinite and smectite. Feuillet & Fleischer (1980) have pointed out that if either differential settling by particle size or flocculation of a clay mineral species were to occur, one clay mineral maximum should be located near the estuary head; this should be followed by a decrease caused by its reduction, in suspension. With a mixing mechanism, a continuous decrease or increase would be expected. In the present study (Figure 5.23) no such maximum can be seen to support differential flocculation in Southampton Water. The continuous decrease of smectite with distance is explained most readily by the gradual dilution of smectite-rich riverine material by another source, which is poorer in smectite.

Smectite is the finest of the clay minerals and can be removed selectively from areas of active movement and transported far away, whilst illite and kaolinite settle with increasing salinity. Flocculation caused by salt water intrusion could provide the mechanism for differential settling of the clay minerals (*i.e.* illite, kaolinite + chlorite are deposited when they meet the salt water, whilst smectite remains in suspension because of its small size). Nevertheless, this process does not explain the available conditions in the Solent region. Figure 5.24 presents a plot of smectite against mean grain size. No strong association can be identified from these data; this implies that the abundance of clay minerals is independent of grain size. If smectite has been carried selectively, a positive association between these variables should be evident.

There are other factors that must be taken into account when explaining clay mineral distributions by flocculation (Meade, 1972): (i) the concentration of suspended sediment should be high (grams per litre) - whereas suspended sediment concentrations ranging from 2 to 50 mg l⁻¹ at the surface and mid-depth have been reported in Southampton Water at high tide; and (ii) the tidal velocities in estuarine

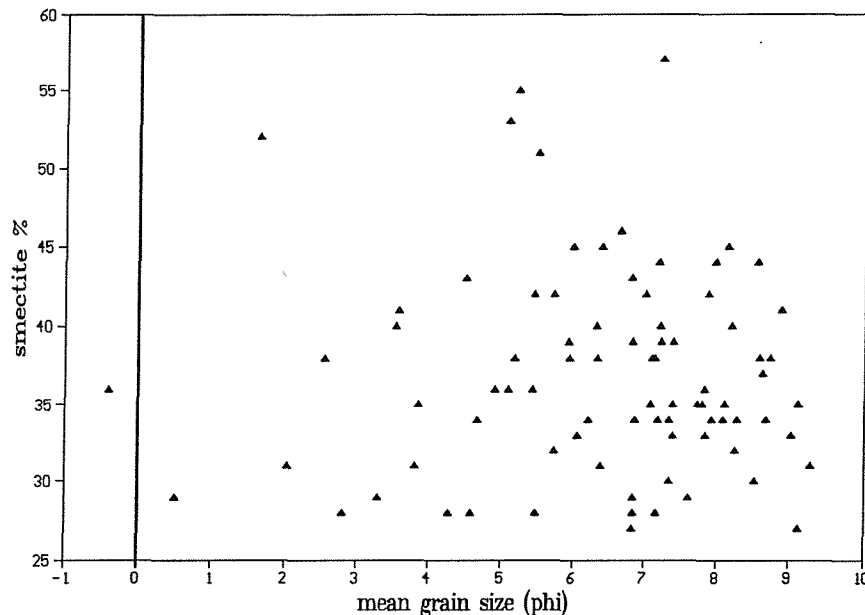


Figure 5.24 : *A plot of smectite percentage against mean grain size, for all the surficial sediment samples.*

waters are often great enough to prevent the deposition of fine sediments - in contrast, tidal velocities are up to 2 ms^{-1} and 1.3 ms^{-1} in the West and East Solent, respectively. Hence, the dispersal pattern of clay minerals over the area cannot be dominated by size segregation and differential settling.

The most important factors controlling the deposition of sediments in estuaries are the dynamic processes, influenced by river discharge, tide, and wind; these cause circulation and mixing in the estuarine waters (Meade, 1972). In moderately stratified estuaries, sedimentation is related to the net landward transport of bottom sediments by the predominantly landward flow of bottom waters (Meade, *op.cit.*). Sediments in well-mixed estuaries move in similar ways to those in moderately stratified estuaries. In highly stratified estuaries, sediments move under a wide range of river inflow conditions. The direction of the bottom flow can

be both landward and seaward, depending upon the flood stage of the river and the presence of a salt wedge. When the salt wedge retreats from the river mouth, the direction of bottom flow is from landward to seaward; this sequence is reversed when the salt wedge re-enters the estuary (Meade, 1972).

Southampton Water is a partially mixed estuary (Dyer, 1980). Highly stratified conditions are found only in the upper reaches of the estuaries (Webber, 1980). When the distribution pattern of clay minerals is considered as a response to dynamic activity within the system, illite-K+C rich sediment is likely to be represent a marine source, whilst the decreasing amount of smectite suggests a riverine source. The increasing amounts of illite and K+C and decreasing amount of smectite, from the main channel of Southampton Water to the East Solent, suggests an active dilution (*i.e.* mixing with another component) mechanism. In this particular case, mixing with the marine-derived component (Illite-K+C) may be caused by transport in response to landward-directed bottom currents, from the East Solent to Southampton Water. Depending upon the variations in the tidal phases and river run-off, bottom sediments may move both to landward and seaward (Meade, *op.cit.*). These changes in transport direction may cause fluctuations in the composition of the clay minerals along the channels.

The variations in the concentration of clay minerals in the West Solent might be a reflection of an eastward transportation pathway. The size distribution of suspended sediment in the Solent was found to be a bimodal mixture of very fine and medium silt, which was composed mainly of quartz, kaolinite, illite and calcite. It has been suggested that the surface sediments of the Solent must have originated principally in Christchurch Bay due to erosion of cliff and beach material; these are diluted by Southampton Water sediments at the confluence of the West and the East Solent (Srisaengthong, 1982). An increasing smectite content and decrease in the amount of illite and K+C in the West Solent could be attributed to a supplementary transport pathway, from the western extent of the system (Hurst Spit) towards the east.

CHAPTER 6

RESULTS : Geochemical Investigations

6.1. Trace Metal Distribution of Surficial Sediments

6.1.1. Total Metal Concentrations

The total heavy metal concentration of the samples is presented in two ways (Table B3, of Appendix B), as "total" and "sum", which are now defined. The "total" metal concentration is the concentration of metal within the unfractionated (whole) sample. The "sum" value is that derived from the metal concentration within the various size fractions of the sample, and can be described as:

$$M \sum = (M_{sand} \times w\% \text{ sand}) + (M_{silt} \times w\% \text{ silt}) + (M_{clay} \times w\% \text{ clay})$$

M_{sand} = metal conc. within sand fraction;

M_{silt} = metal conc. within silt fraction;

M_{clay} = metal conc. within clay fraction;

$w\%$ = weight percent of the size fraction

The agreement between the two values varies between the elements: Al, $r=0.82$; Co, $r=0.64$; Cu, $r=0.88$; Cr, $r=0.85$; Fe, $r=0.73$; Pb, $r=0.89$; Mn, $r=0.87$; Ni, $r=0.87$, and Zn $r=0.77$ (with $n=76$ and significance level= 0.00). In most cases, the sum concentrations are higher than the total metal concentrations; this may suggest contamination during size separation. Incomplete size separation

might also be a reason *i.e.* flocculation of very fine sized particles might have prevented the complete segregation of the silt and clay fractions (see Chapter 4). Hence, clay sized materials (containing a high level of trace metals) have been determined within the silt fraction. In general, the differences between the total and sum concentrations are large in samples collected from the harbours (namely Portsmouth H5 and H6; Langstone, H13; Chichester, H16, and the river samples, R17, R21, R4, R28). The samples with large differences between total and sum concentrations are those which are either very fine (90 % clay) or very coarse (90 % sand). Consequently, it may be considered that the size separation procedure used here was not completely efficient. Nevertheless, correlation between the two types of data lies mostly within the 95 % confidence limits.

The total metal concentration determinations are the best values to use when examining the extent of the metal levels distributions in the sediments (Loring & Rantala, 1992), since there are fewer analytical steps to execute when determining the value. Therefore, the total metal concentrations of surficial sediments will be examined initially (Table 6.1).

6.1.2. The Range in Total Metal Concentrations

Co concentrations range between 7 to 42 ppm in the Solent region. The minimum values are 7 ppm (R1 and 31), 8 ppm (11 and 29), and 9 ppm (H11 and 20), whereas the maximum values are 42 ppm (R28), 37 ppm (H22) and 34 ppm (H3). Maximum values found in the Hamble and Beaulieu Rivers, Portsmouth and Chichester Harbours, and in the main channel of Southampton Water.

Cr concentrations range from 12 to 137 ppm. The minimum Cr concentrations are 12 ppm (31), 14 ppm (29), 19 ppm (R1) and the maximum concentrations are 137 ppm (H3), 113 ppm (R17) and 106 ppm (6). Cr is most concentrated in the Portsmouth and Chichester Harbours, and the Test and Hamble Rivers.

Table 6.1 : Total metal concentrations within all the samples analysed - units are ppm (continued on following pages) (for sample locations, see Figure 5.1).

Sample No	Al	Co	Cu	Cr	Fe	Pb	Mn	Ni	Zn
KEYHAVEN RIVER									
R1	20,000	7	33	19	14,000	51	49	9	77
R2	47,000	20	20	50	38,000	300	170	33	95
R3	47,000	19	76	36	38,000	62	150	31	160
R4	41,000	19	150	40	86,000	330	250	41	370
R5	53,000	24	22	50	41,000	55	150	39	120
LYMINGTON RIVER									
R6	72,000	27	13	60	52,000	43	200	40	99
R7	65,000	25	5	57	53,000	26	290	46	76
BEAULIEU RIVER									
R9	76,000	32	17	63	56,000	42	220	56	110
R10	63,000	23	3	50	39,000	30	240	46	74
R11	62,000	21	15	86	38,000	52	140	49	120

Cu concentrations range from 3 to 160 ppm. The minimum values are 5 ppm (R7), 6 ppm (31 and R31) and 8 ppm (H13), whereas maximum values are 160 ppm (R22), 147 ppm (R4), 127 ppm (R21) and 103 ppm (H8). The samples from the Keyhaven and Itchen Rivers, and Portsmouth Harbour are associated with high concentrations. In general, the samples from the East Solent and the Beaulieu River have low concentrations.

Mn concentrations range from 49 to 543 ppm. The minimum values are 49 ppm (R1), 113 ppm (29), 124 ppm (H21) and the maximum values are 543 ppm (H3), 501 ppm (R17) and 476 ppm (6). Mn is most concentrated in Portsmouth Harbour and the River Test. Samples from the West Solent, Langstone and

Table 6.1 (continued): Total metal concentrations within all the samples analysed - units are ppm (for sample locations, see Figure 5.1).

Sample No	Al	Co	Cu	Cr	Fe	Pb	Mn	Ni	Zn
TEST RIVER									
R12	43,000	18	16	36	34,000	49	170	30	96
R13	32,000	18	48	45	35,000	74	180	36	190
R14	71,000	23	64	95	64,000	44	280	48	190
R17	91,000	31	17	110	40,000	34	500	30	110
ITCHEN RIVER									
R19	18,000	14	86	36	19,000	160	130	31	240
R21	34,000	26	130	55	39,000	220	390	51	330
R22	42,000	13	160	64	36,000	440	210	34	300
R23		12	95	43	36,000	180	220	29	280
R24	22,000	25	94	39	18,000	97	180	46	180
R25	78,000	24	66	77	60,000	120	350	45	210
HAMBLE RIVER									
R26	30,000	16	26	61	31,000	54	140	23	100
R27	43,000	21	47	60	38,000	72	160	28	180
R28	68,000	42	75	81	71,000	120	380	64	240
R29	72,000	22	61	90	62,000	62	290	41	190
R30	27,000	13	10	49	21,000	53	150	28	110
ISLE OF WIGHT									
R31	52,000	19	6	51	38,000	23	320	45	64
R32	40,000	13	36	37	29,000	29	280	33	68
R33	41,000	14	58	44	27,000	52	250	37	95
R34	63,000	21	56	77	50,000	99	290	52	180
R35	63,000	18	21	43	48,000	58	280	39	120

Table 6.1 (continued) : Total metal concentrations within all the samples analysed - units are ppm (for sample locations, see Figure 5.1).

Sample No	Al	Co	Cu	Cr	Fe	Pb	Mn	Ni	Zn
PORTSMOUTH HARBOUR									
H1	53,000	20	86	70	41,000	250	160	48	250
H2	75,000	26	34	57	54,000	77	260	53	130
H3	91,000	34	40	140	69,000	75	540	94	220
H4	83,000	31	58	64	57,000	84	300	60	160
H5	55,000	19	18	57	39,000	41	230	43	95
H6	74,000	23	29	64	41,000	60	240	50	120
H7	77,000	26	31	63	53,000	77	250	54	130
H8	48,000	14	100	49	25,000	140	220	40	180
H9	33,000	10	29	38	22,000	37	160	29	77
H10	64,000	23	26	64	49,000	56	270	48	120
LANGSTONE HARBOUR									
H11	49,000	9	21	41	28,000	62	140	17	150
H13	29,000	7	8	23	23,000	50	140	13	59
H15	42,000	17	74	62	32,000	69	160	30	170
CHICHESTER HARBOUR									
H16	43,000	15	27	51	31,000	60	150	35	93
H17	47,000	14	20	38	38,000	58	160	27	110
H18	54,000	17	25	61	43,000	32	180	32	130
H20	40,000	12	13	36	33,000	19	130	25	91
H21	49,000	11	19	30	30,000	63	120	21	93
H22	81,000	37	61	82	68,000	150	130	76	230
H23	42,000	21	20	52	44,000	45	180	27	77

Table 6.1 (continued) : Total metal concentrations within all the samples analysed - units are ppm (for sample locations, see Figure 5.1).

Sample No	Al	Co	Cu	Cr	Fe	Pb	Mn	Ni	Zn
THE WEST SOLENT									
1	48,000	21	10	44	46,000	31	190	31	64
2	60,000	28	7	57	37,000	35	180	41	78
3	63,000	31	10	49	53,000	41	370	50	91
THE EAST SOLENT									
12	51,000	23	30	74	35,000	51	260	52	100
13	42,000	12	15	39	35,000	72	230	24	90
14	35,000	12	7	22	34,000	36	180	17	76
15	48,000	22	17	54	47,000	64	260	31	96
16	44,000	18	16	60	36,000	51	250	39	100
17	40,000	16	18	57	43,000	43	260	36	94
18	62,000	17	22	52	44,000	87	250	34	130
19	32,000	20	15	53	43,000	51	220	30	120
20	31,000	9	15	25	29,000	69	180	18	83
21	49,000	21	21	75	19,000	52	220	49	92
22	38,000	18	13	45	42,000	43	220	26	65
23	48,000	22	16	54	51,000	50	250	33	87
25	61,000	29	21	59	61,000	59	290	43	100
26	42,000	13	14	30	34,000	52	190	27	93
28	52,000	15	16	28	35,000	55	180	30	110
29	9,000	8	9	14	29,000	7	110	13	32
30	37,000	12	14	35	35,000	64	200	23	82
31	16,000	7	6	12	28,000	10	130	10	48

Table 6.1 (continued) : Total metal concentrations within all the samples analysed - units are ppm (for sample locations, see Figure 5.1).

Sample No	Al	Co	Cu	Cr	Fe	Pb	Mn	Ni	Zn
SOUTHAMPTON WATER									
4	67,000	30	48	96	42,000	80	420	70	150
5	95,000	24	62	78	63,000	97	430	53	200
6	77,000	32	46	110	56,000	68	480	70	170
7	69,000	21	61	69	53,000	46	360	45	160
8	50,000	22	40	71	51,000	76	370	58	190
9	62,000	18	26	53	51,000	60	300	37	130
10	44,000	17	18	74	23,000	51	240	39	100
11	29,000	8	12	36	34,000	16	130	15	67

Chichester Harbours contain low concentrations of Mn.

Ni concentrations range between 9 to 94 ppm. The minimum concentrations are 9 ppm (R1), 10 ppm (31) and 13 ppm (H13 and 29). The maximum concentrations are 94 ppm (H3), 76 ppm (H22), 70 ppm (4 and 6) and 64 ppm (R28). Ni is most concentrated in Portsmouth Harbour, Chichester Harbour, the River Hamble and Southampton Water.

Pb concentrations lay within a range of 7 to 437 ppm. The minimum values are 7 ppm (29), 10 ppm (31) and 16 ppm (11), whilst the maximum values are 437 ppm (R22), 331 ppm (R4), 300 ppm (R2) and 249 ppm (H1). Pb concentrations are high in the Itchen and Keyhaven Rivers and Portsmouth Harbour.

Zn concentrations vary between 32 to 371 ppm. The minimum concentrations are 32 ppm (29), 48 ppm (31) and 59 ppm (H13), whilst the maximum concentrations are 371 ppm (R4), 326 ppm (R21) and 302 ppm (R22). Zn is high in Southampton Water, the Test, Itchen, Keyhaven and Hamble Rivers and all the

harbours.

Al concentrations vary between 9,000 to 95,000 ppm. The minimum values are 9,000 ppm (29), 16,000 ppm (31), 17,000 ppm (R19), whilst the maximum values are 95,000 ppm (5) and 91,000 ppm (R17 and H3). Al is high in the main channel of Southampton Water, Portsmouth and Chichester Harbours, and the River Test.

Fe concentrations range between 18,000 to 86,000 ppm. The minimum values are 14,000 ppm (R1), 18,000 ppm (R24) and 19,000 ppm (21 and R19), whereas the maximum values are 86,000 ppm (R4) 71,000 ppm (R28) and 69,000 ppm (H3). Fe is high in the Keyhaven and Hamble Rivers, the Portsmouth and Chichester Harbours, and the main channel of Southampton Water.

The total heavy metal concentrations in the Solent sediments are compared with reference averaged concentrations for the near shore muds (Chester, 1990) in Table 6.2. The minimum values of Co, Cu, Fe, Ni and Pb are comparable with those of the reference concentrations, but the maximum concentrations of Co, Cu, Pb, and Zn are higher. Maximum concentrations of Cr and Ni are similar to the reference values, and Mn is generally lower. High concentration of Co might be attributable to the low accuracy of the analysis (see Table 4.4).

Table 6.2 : Average metal concentrations of near shore muds (after Chester, 1990).

Trace Element	Near-Shore Mud	Range of Concentrations found in this study
Cr	100 ppm	12-140 ppm
Cu	48 ppm	3-160 ppm
Ni	55 ppm	9-94 ppm
Co	13 ppm	7-42 ppm
Pb	20 ppm	7-440 ppm
Zn	95 ppm	32-370 ppm
Mn	850 ppm	49-540 ppm
Fe	69,900 ppm	18,000-86,000 ppm

6.1.3. Spatial Distribution of Total Metals

The spatial distribution of total metals is illustrated in Figures 6.1 to .9. Some general features will be described, although the patterns obtained are somewhat noisy.

Co is most concentrated in the Hamble, Test and Beaulieu Rivers, the entrance of Portsmouth Harbour and the bay-head of Chichester Harbour. There is a decreasing trend along the Beaulieu River, whereas an increasing trend occurs in the Itchen and Test Rivers. The high concentrations can be observed also at the western approach to Southampton Water and in the main channel of Southampton Water. In general, concentrations of Co seem to increase from west to east across the West Solent and are almost constant in the East Solent (Figure 6.1).

Cr concentrations are higher in the Test and Hamble Rivers and the upstream area of the main channel of Southampton Water, compared to those of the East Solent. They increase downstream in the Test, Itchen and Hamble Rivers. There is a trend of decreasing Cr concentrations from the inner part to the open end of the East Solent. Cr concentrations are higher in Portsmouth Harbour and the bay-head of Chichester Harbour than in Langstone Harbour (Figure 6.2).

Cu is elevated significantly in the Itchen and Keyhaven Rivers, and the bay-head locations of the harbours. Although it is uniform in the East Solent, elevated concentrations are found close to Wootton Creek in the southern part and locally on the coast of Lee-on-Solent. It is very low in the few samples from the West Solent, with the exception of the Keyhaven River samples (Figure 6.3).

Mn concentrations increase downstream in the River Test, and in the main channel of the Southampton Water, and abruptly decrease to the mouth of the estuary. Samples from Portsmouth Harbour have higher Mn concentrations, compared to those of Langstone and Chichester Harbours. Mn decreases towards the West Solent and the open (seaward) end of the East Solent (Figure 6.4).

Ni is most concentrated in Portsmouth Harbour, the Hamble and Beaulieu Rivers, and in Southampton Water, and decreases from Southampton Water to the

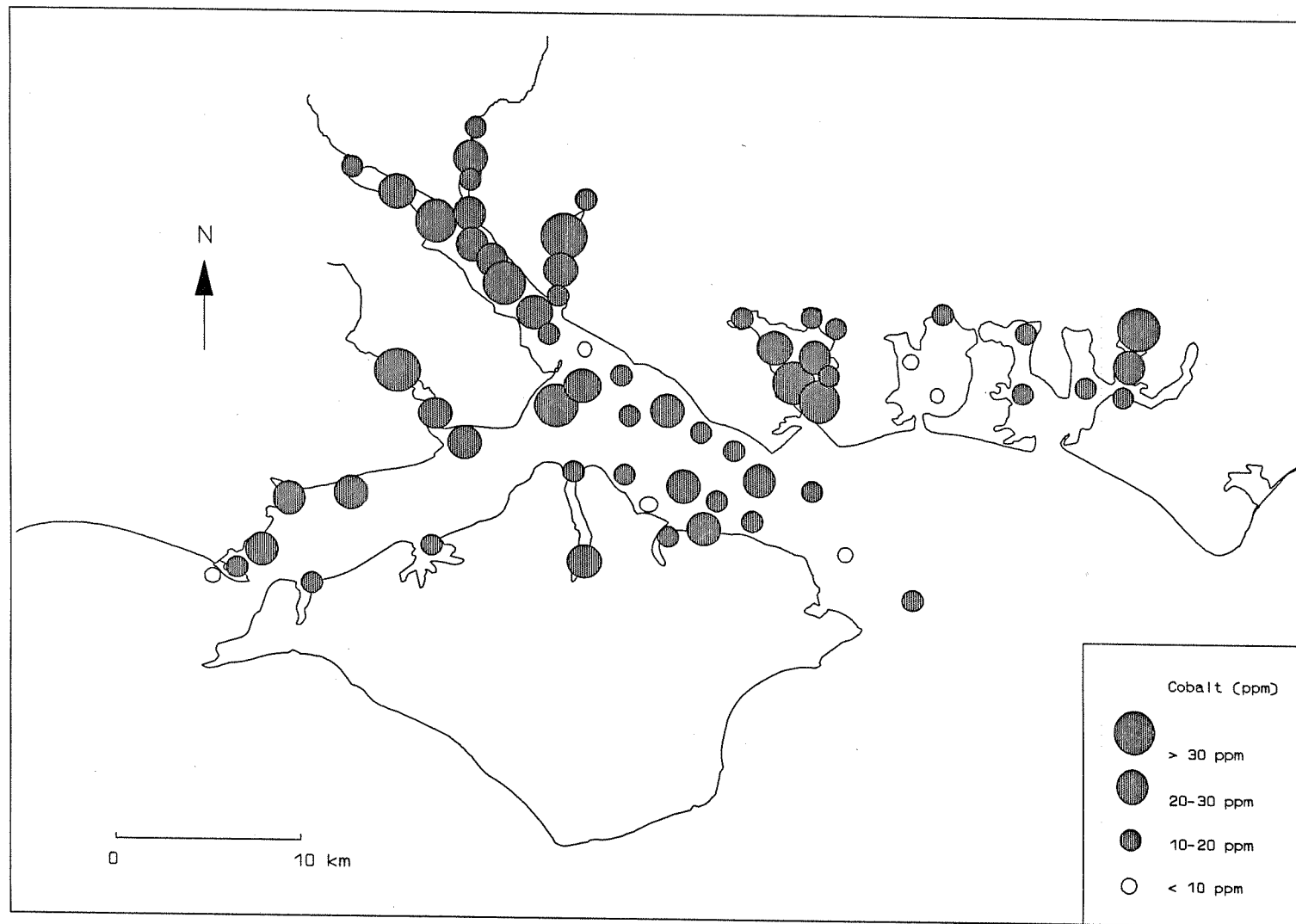


Figure 6.1 : *The distribution of total Co in the surficial sediments of the Solent Region.*

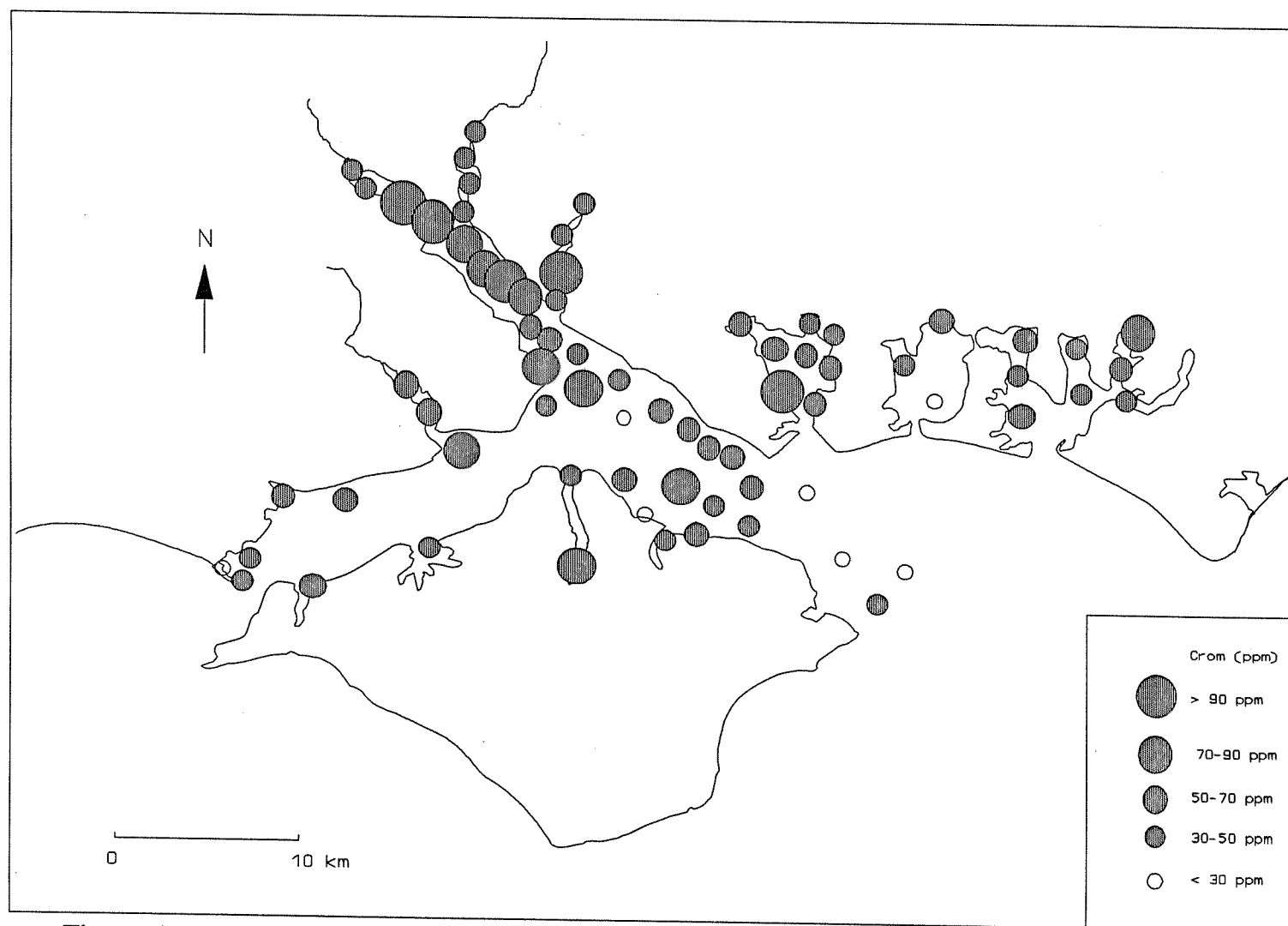


Figure 6.2 : *The distribution of total Cr in the surficial sediments of the Solent Region.*

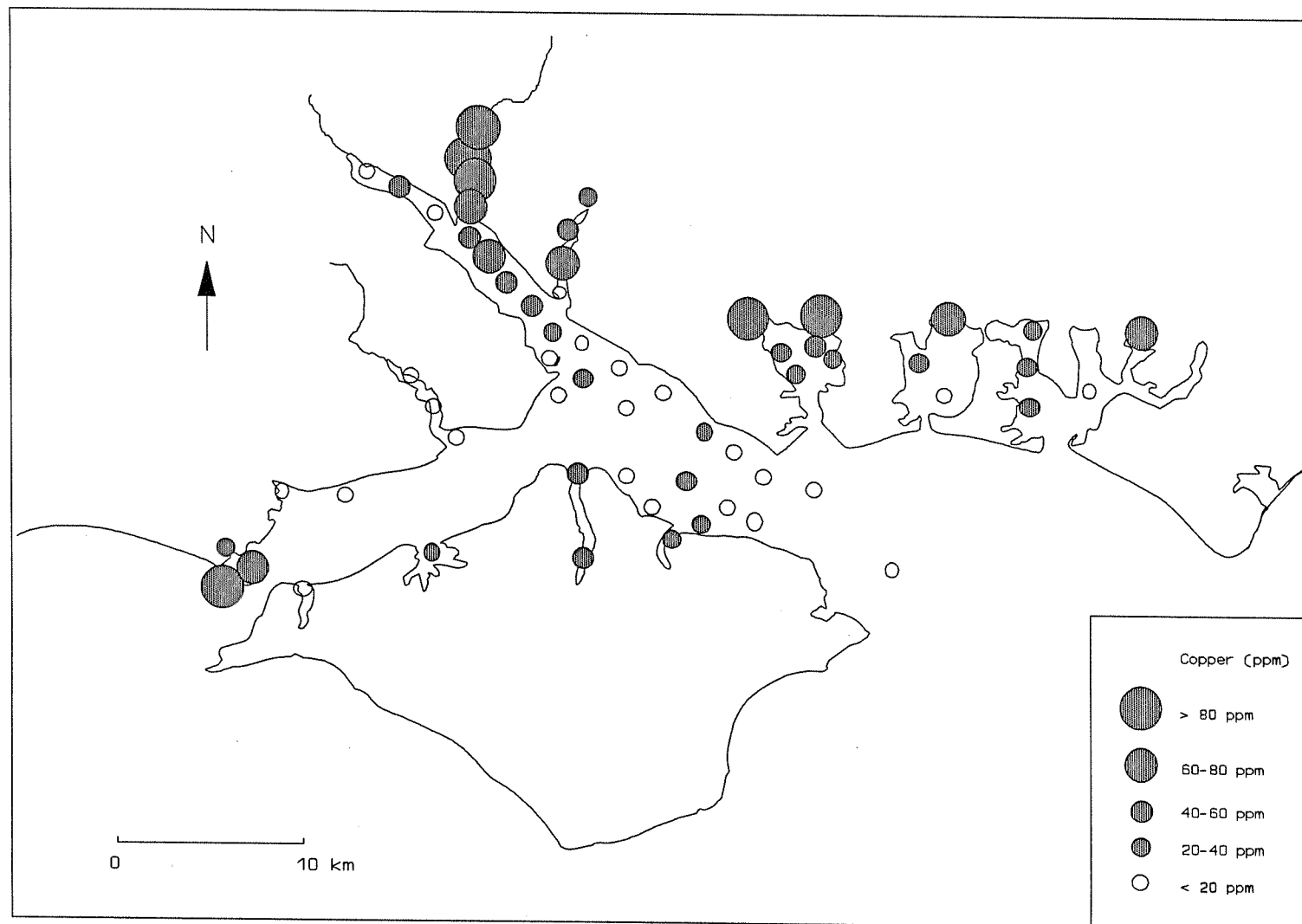


Figure 6.3 : *The distribution of total Cu in the surficial sediments of the Solent Region.*

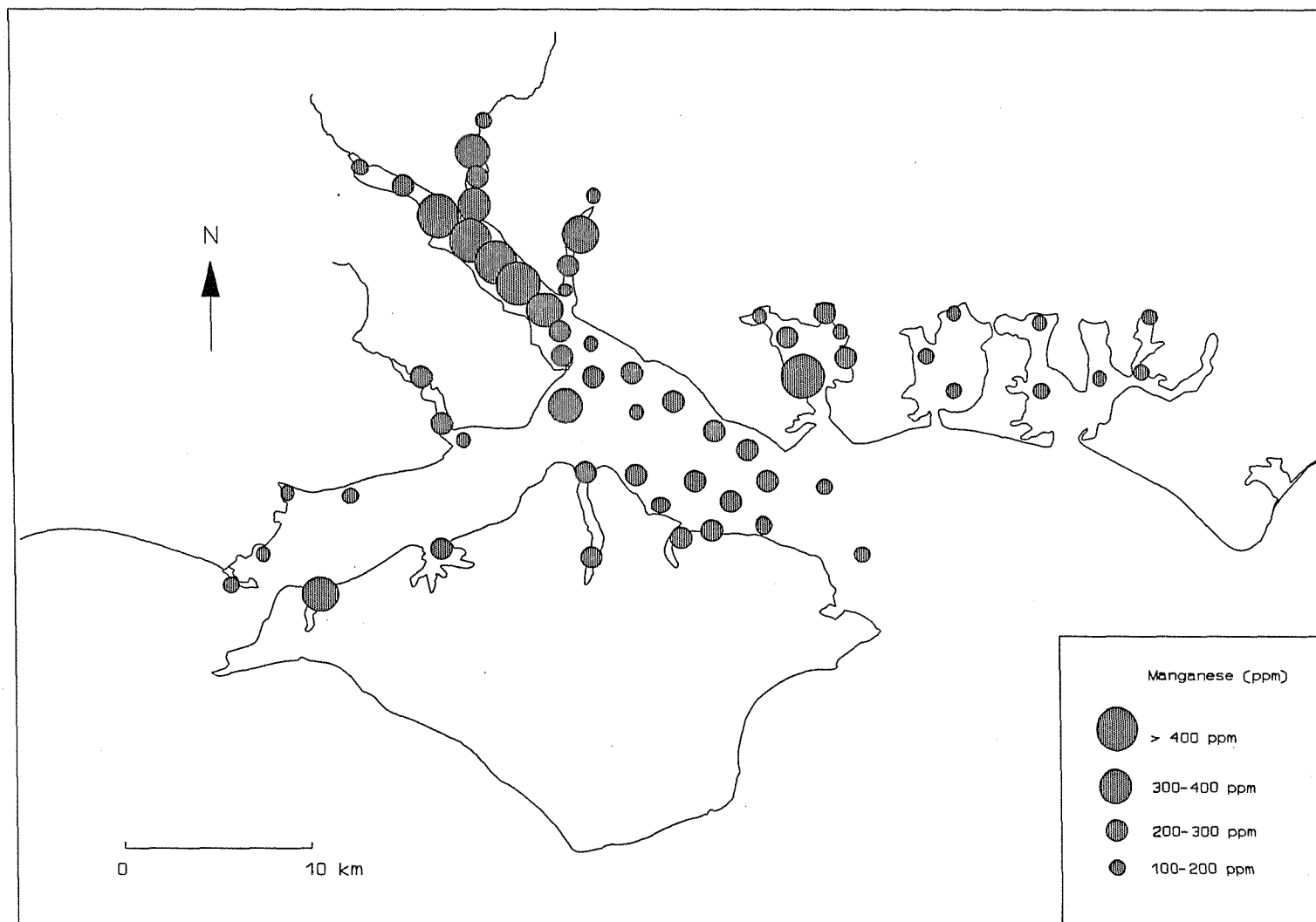


Figure 6.4 : *The distribution of total Mn in the surficial sediments of the Solent Region.*

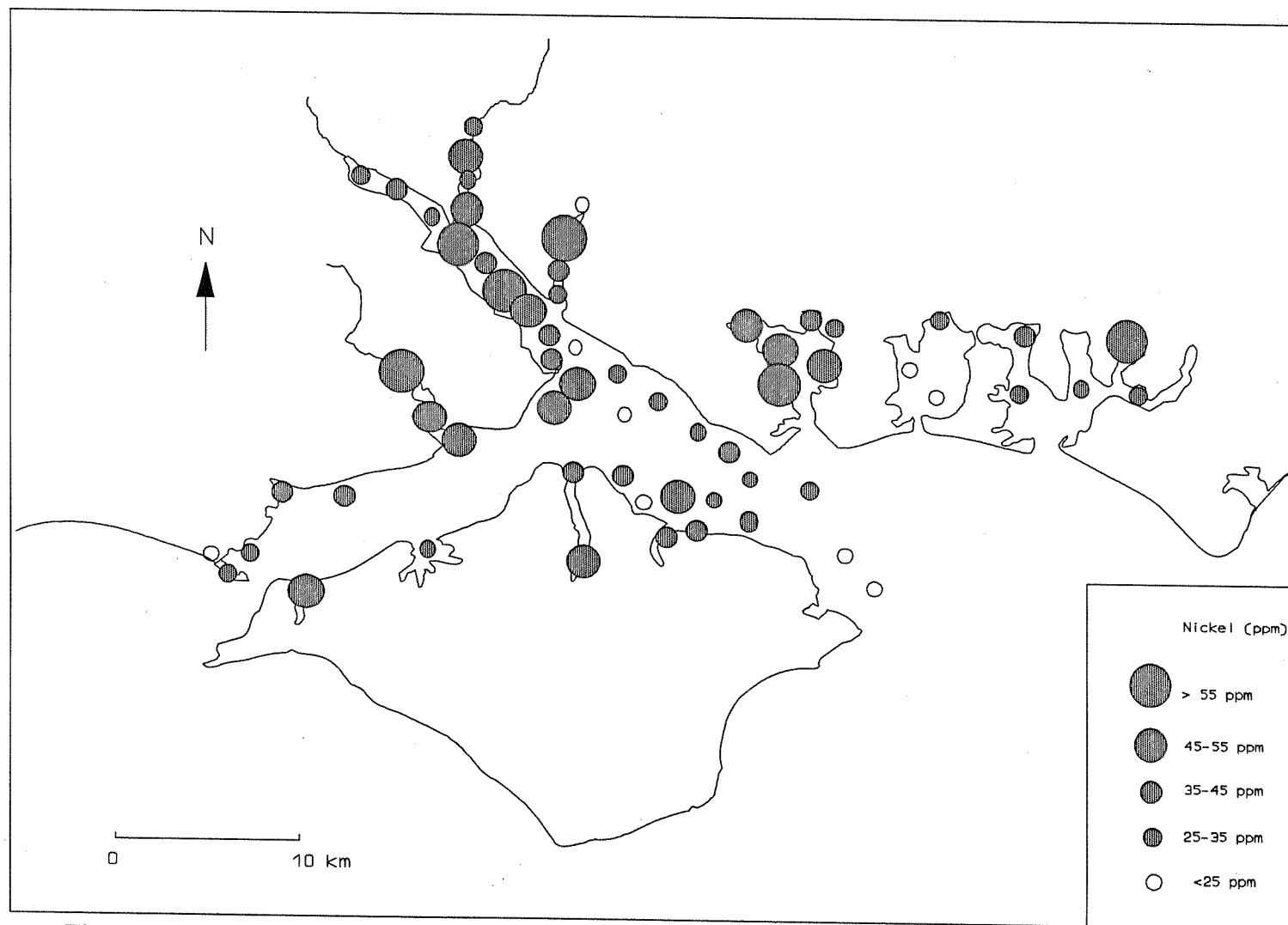


Figure 6.5 : *The distribution of total Ni in the surficial sediments of the Solent Region.*

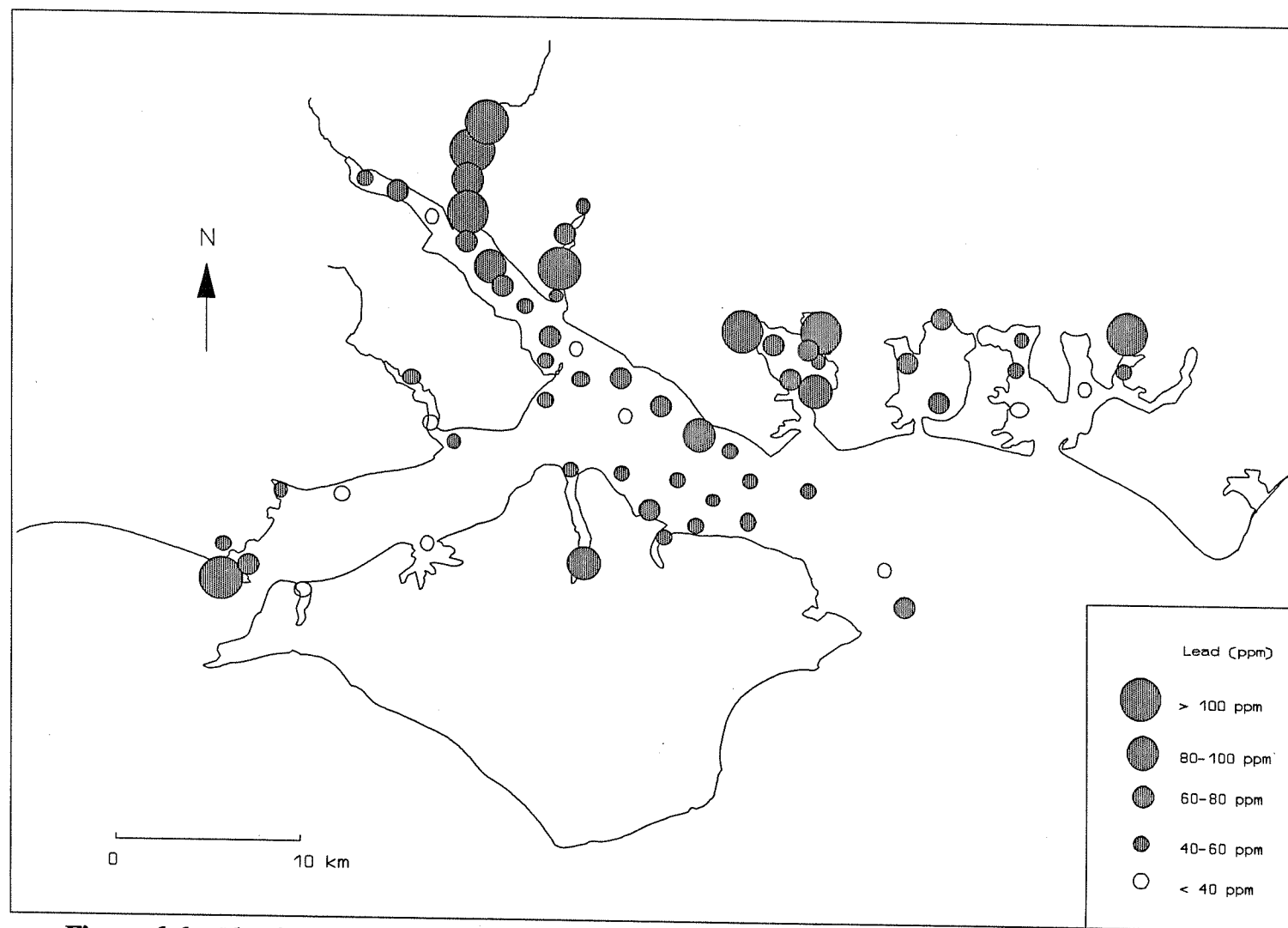


Figure 6.6 : *The distribution of total Pb in the surficial sediments of the Solent Region.*

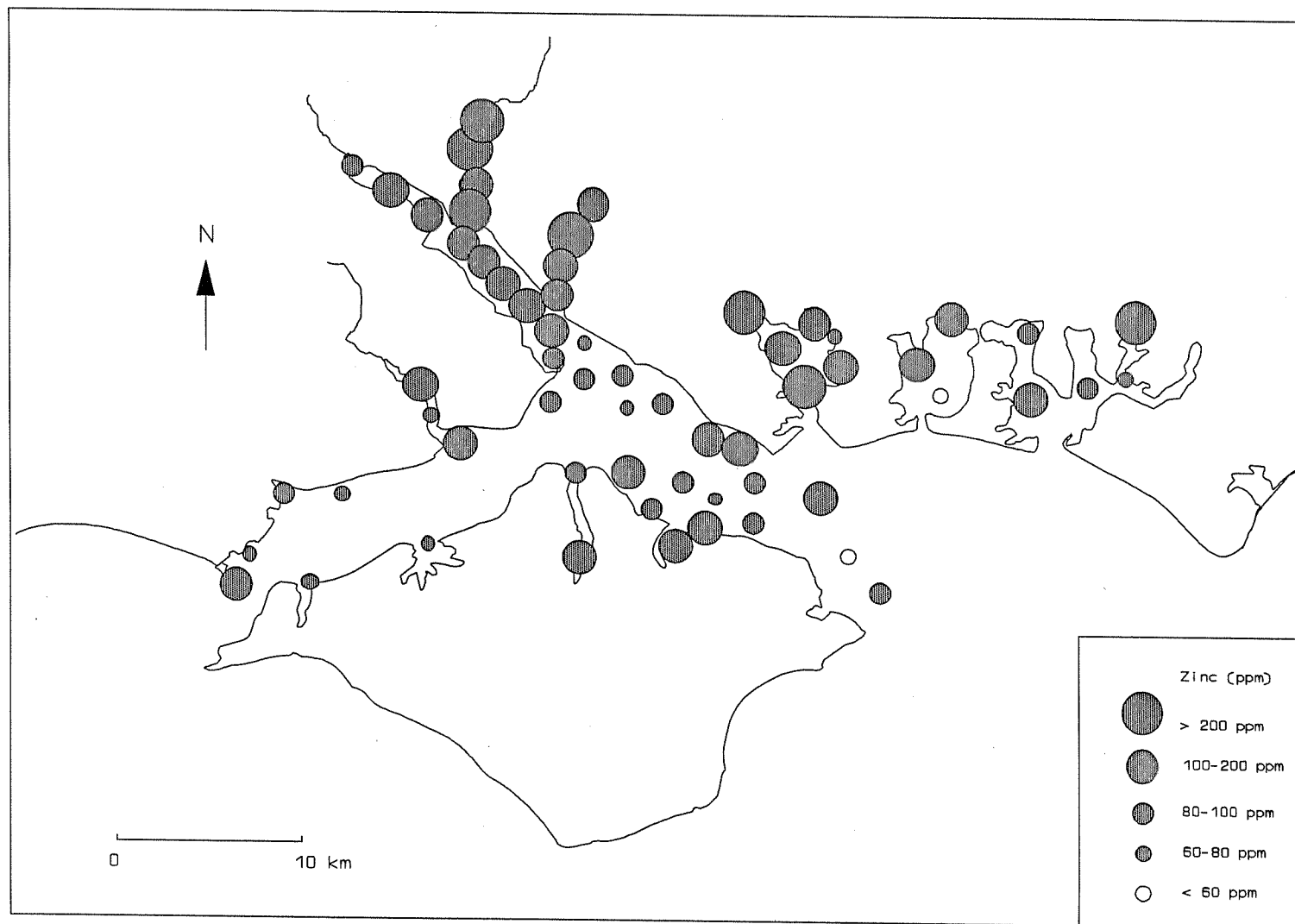


Figure 6.7 : *The distribution of total Zn in the surficial sediments of the Solent Region.*

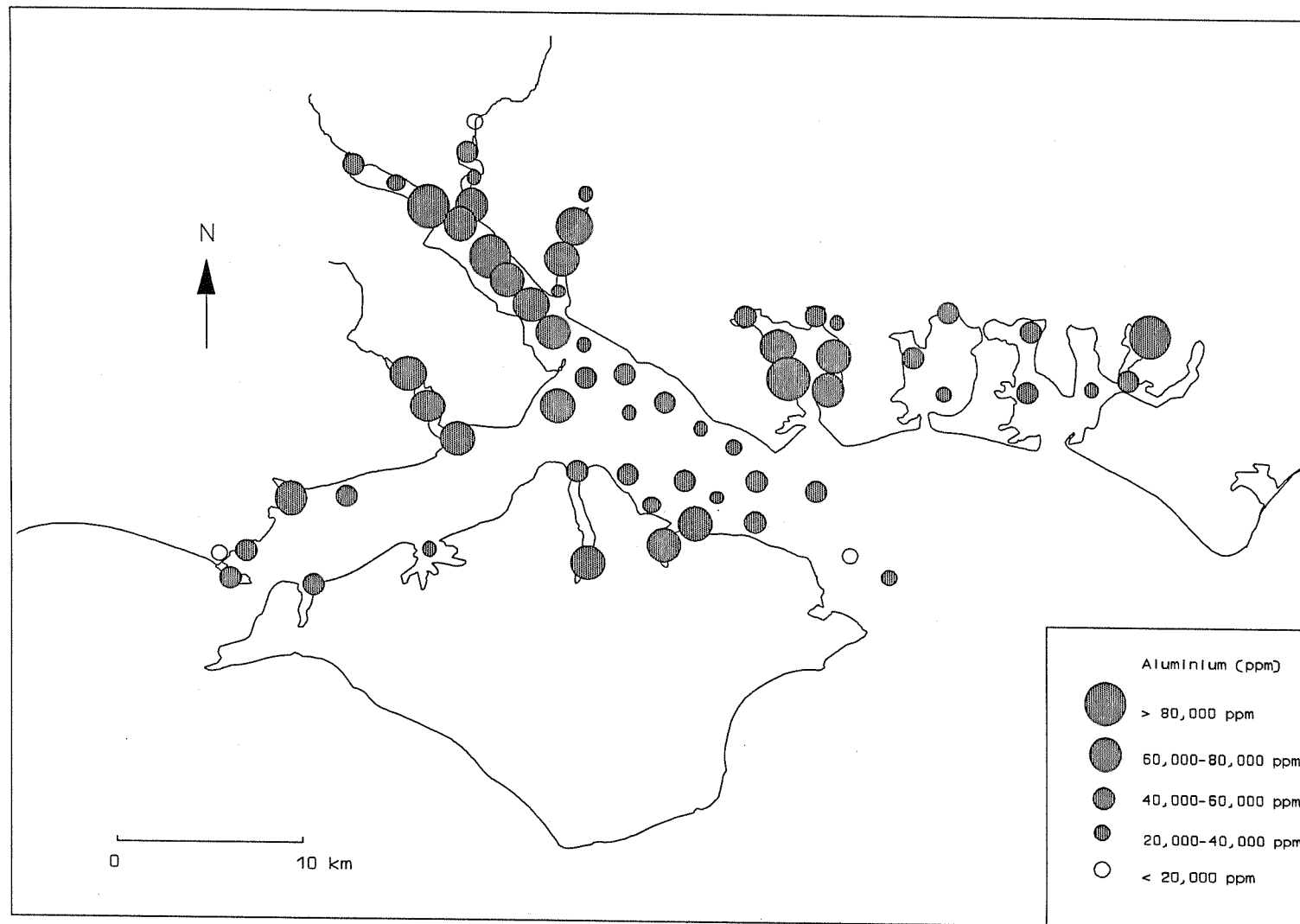


Figure 6.8 : *The distribution of total Al in the surficial sediments of the Solent Region.*

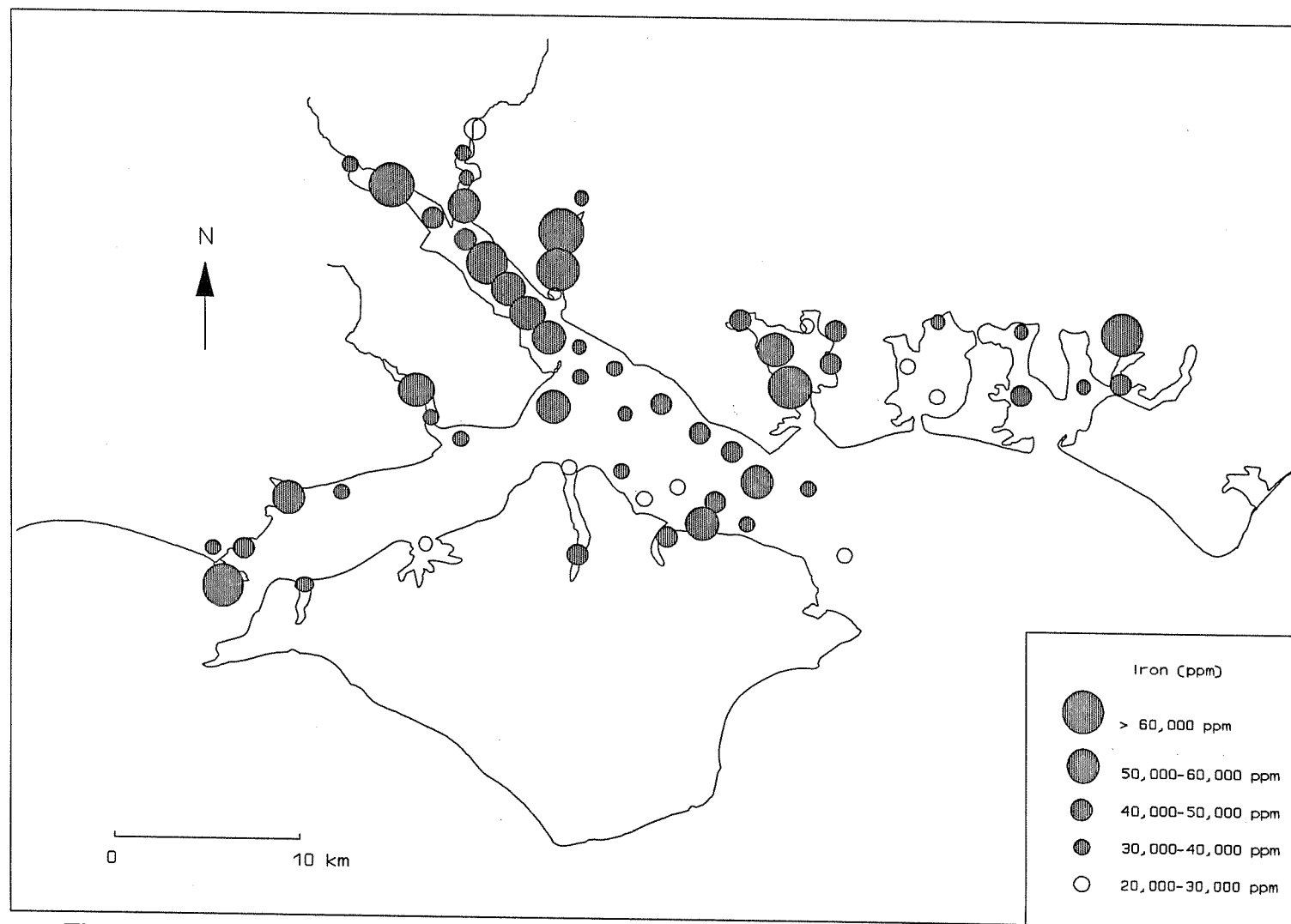


Figure 6.9 : *The distribution of total Fe in the surficial sediments of the Solent Region.*

East Solent. It is almost constant along the northern side of the East Solent, and is more concentrated on the southern side (Figure 6.5).

Pb is most concentrated in the Itchen, Hamble, Keyhaven and the Medina Rivers, and Portsmouth and the bay-head of Chichester Harbours. Pb concentrations are relatively constant in the East Solent, with the exception of local elevations along the coast of Lee-on-Solent (Figure 6.6).

Zn is concentrated in all the rivers and harbours of the area. There is an abrupt decrease at the confluence of Southampton Water and the East Solent. Local higher concentrations can be observed along the coast of Lee-on-Solent and close to Wootton Creek on the southern side of the East Solent (Figure 6.7).

Al concentrations are highest in Southampton Water, Portsmouth Harbour and the Test, Hamble and Beaulieu Rivers. The concentration of Al decreases at the confluence of Southampton Water, and is almost constant in the East Solent. Local higher concentrations can be observed in the vicinity of Wootton Creek (Figure 6.8).

Fe is most concentrated in Southampton Water and the Test, Hamble, Beaulieu and Keyhaven Rivers, and Portsmouth and Chichester Harbours. It decreases at the confluence of Southampton Water and the East Solent. However, a slight increasing trend can be seen along the coast of Lee-on-Solent and in the vicinity of the Wootton Creek (Figure 6.9).

6.1.4. Grain Size Dependency of Metal Concentrations

It is well known that metals are enriched in fine-grained (rather than coarse) sediments because the specific surface area of fine-grained sediments is higher (Ackermann *et.al*, 1983; Horowitz & Elrick, 1987; Förstner & Wittmann, 1979). Elements are present in markedly smaller concentrations in the sand fraction than in the silt and clay fraction and are usually not affected by the anthropogenic influences (Ackermann, 1980). The actual concentration of a trace metal in a sediment is often dependent, therefore, on the grain size of the sediment, with the

concentration increasing as grain size decreases. This increase represents primarily the changing pattern of mineral composition with grain size. Clay minerals, which have a high metal content, dominate the smaller grain sizes, whereas quartz and feldspar, which have low metal contents, dominate the sand fraction (Filipek & Owen, 1978). The total concentration of the metals has been plotted against the percentage of the clay size fraction, to examine the relationship between the metal and grain size (Figure 6.10).

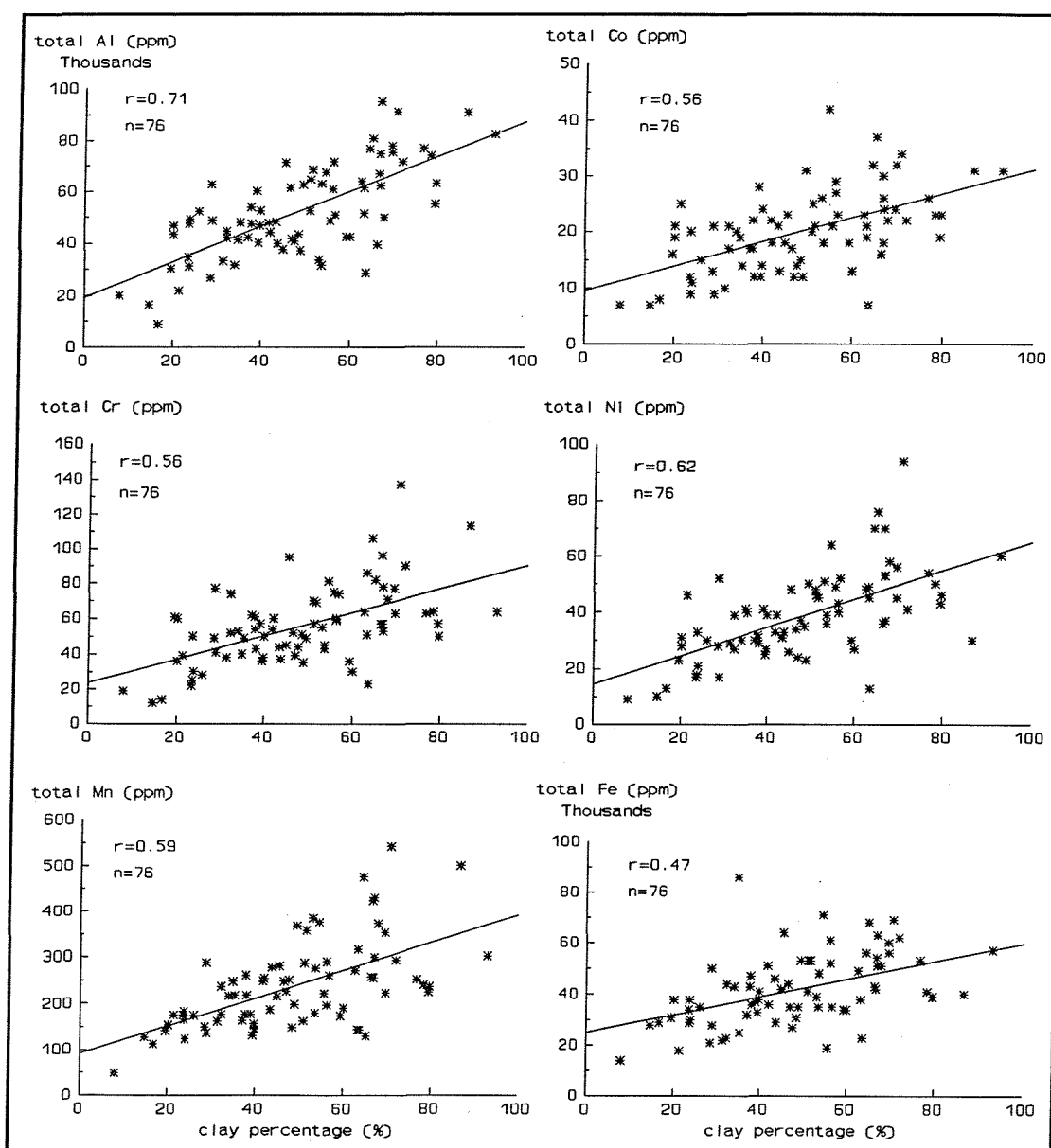


Figure 6.10 : *Correlations between total metal content and percentage of clay (continued on next page).*

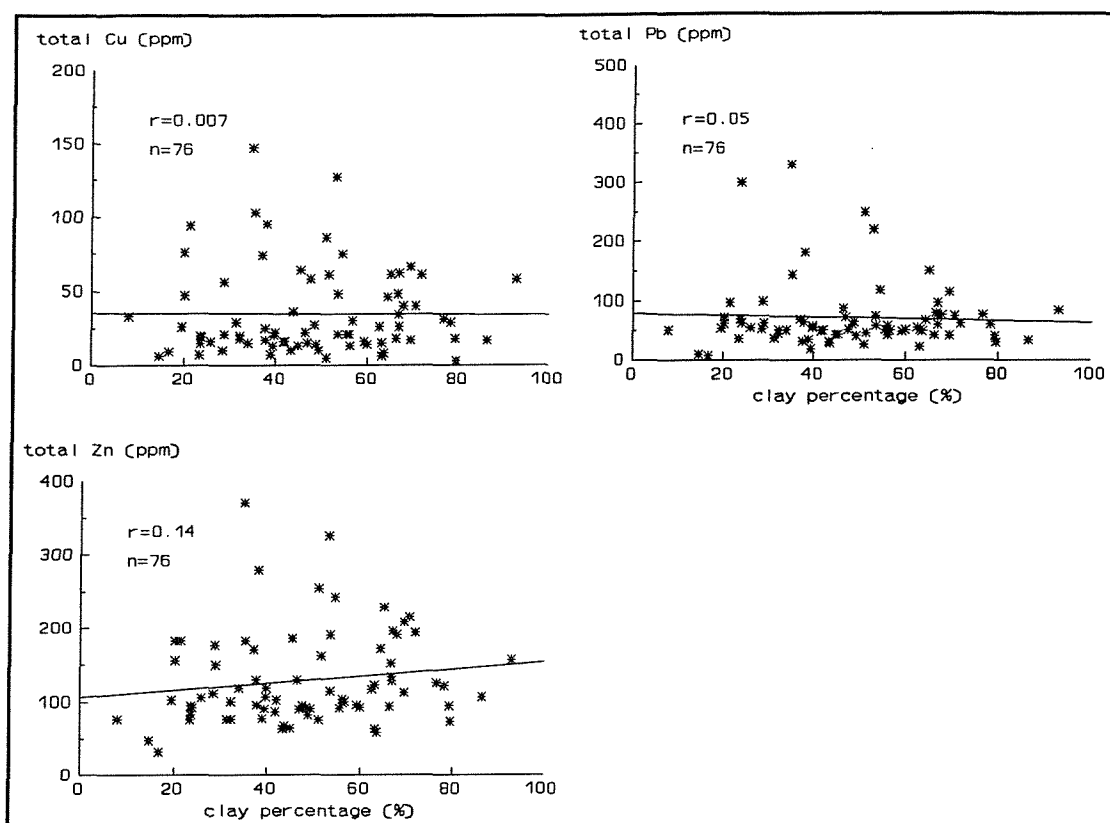


Figure 6.10 (continued): *Correlations between total metal content and percentage of clay.*

Al, Co, Ni, Mn, and Cr are well correlated with the percentage of clay; they increase as the percentage of clay increases, whereas Cu, Pb, and Zn are not well correlated with the percentage of clay. Fe displays an intermediate correlation. The metal correlation with decreasing grain size is considered generally to be part of the natural population (Loring & Rantala, 1992). Consequently, deterioration in this correlation might be indicative of an anomalous (anthropogenic) population.

6.1.5. Trace Metal Concentrations in the Different Size Fractions

The metal content of the various size fractions is given in Table B4 of Appendix B and Figure 6.11. The data may be useful for tracing the regional dispersal pattern of metals associated with a specific size fraction (Loring &

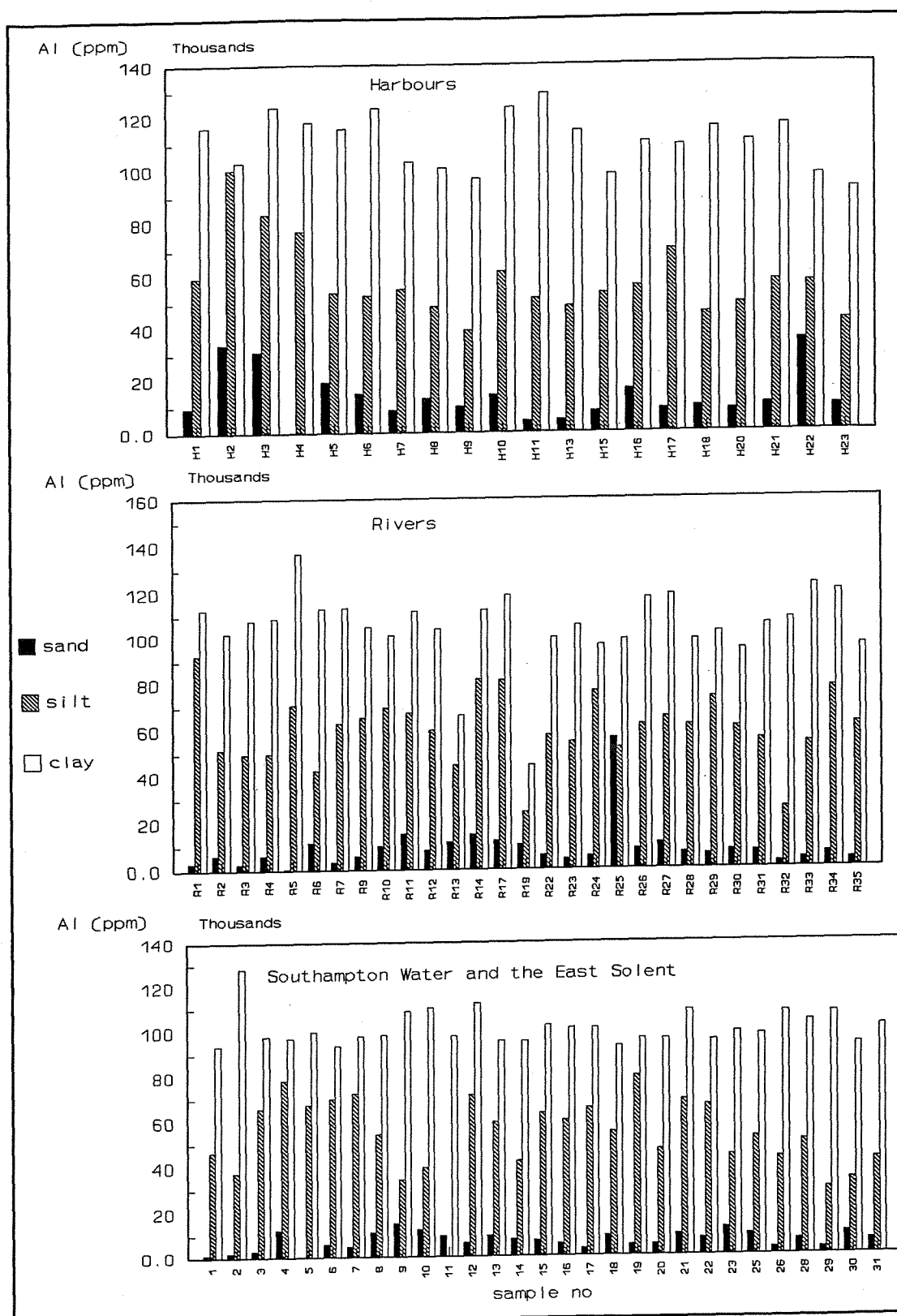


Figure 6.11 : Metal content of the sand, silt and clay fractions (continued on following pages).

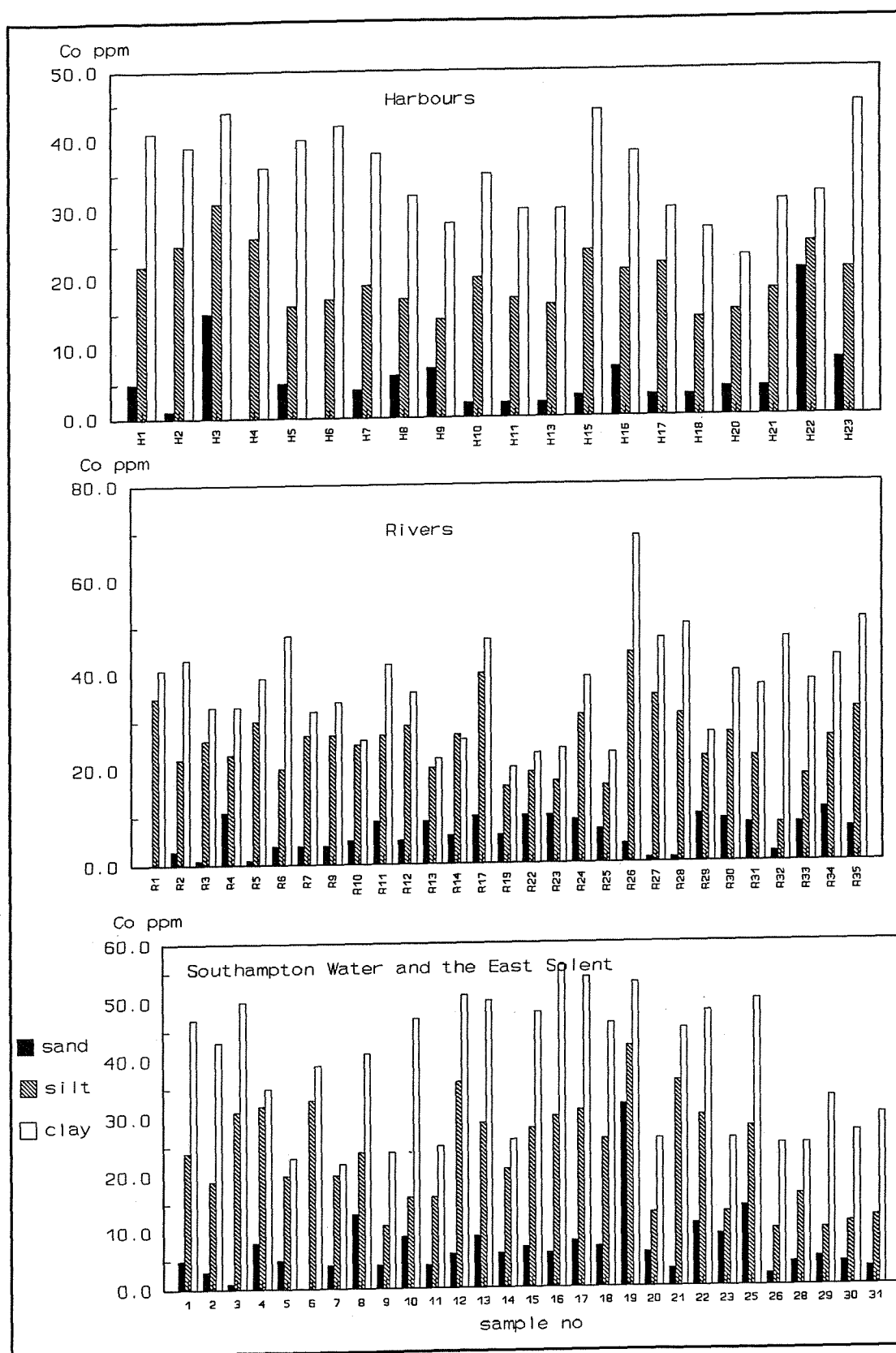


Figure 6.11 (continued): Metal content of the sand, silt and clay fractions.

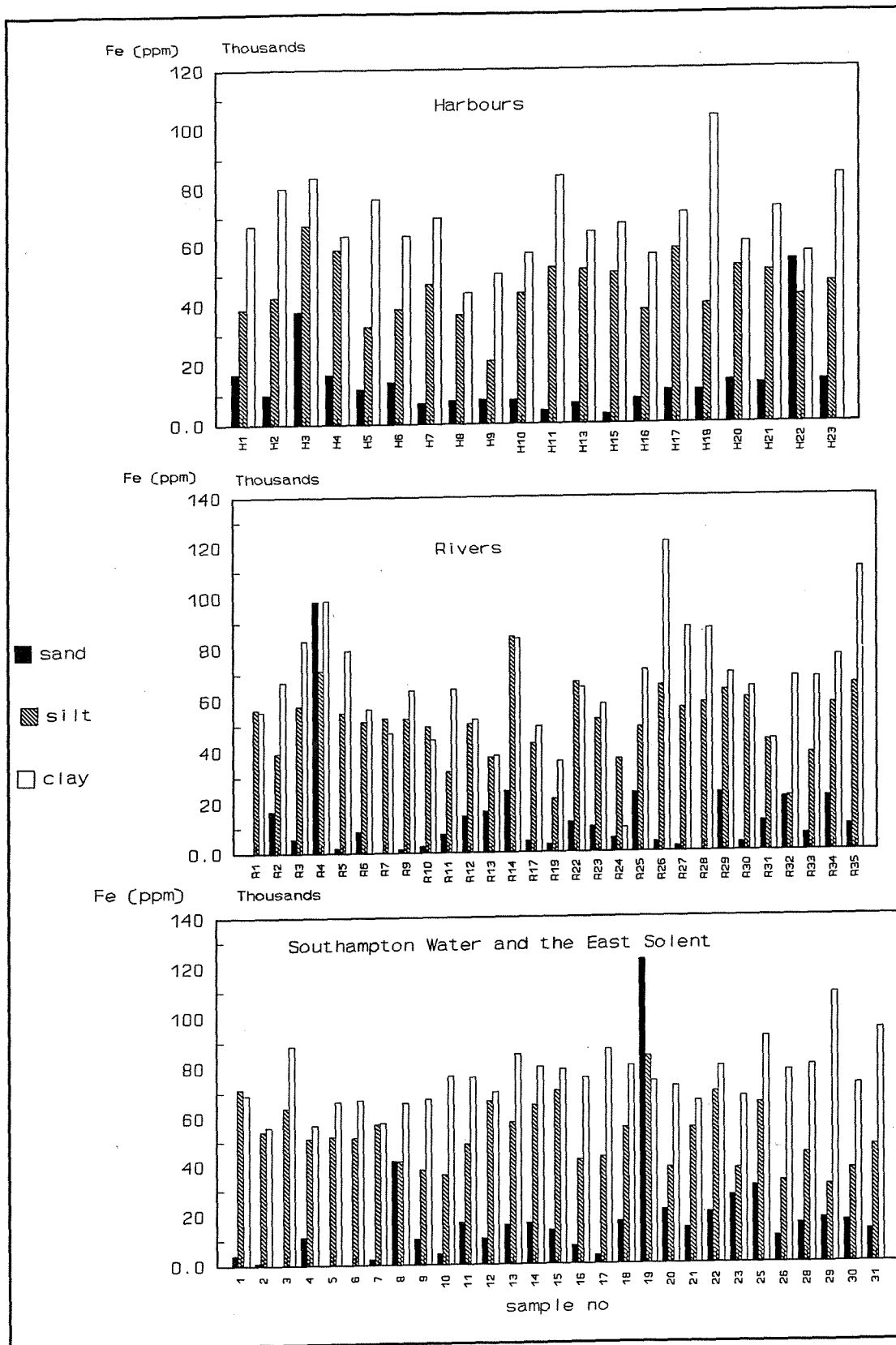


Figure 6.11 (continued): Metal content of the sand, silt and clay fractions.

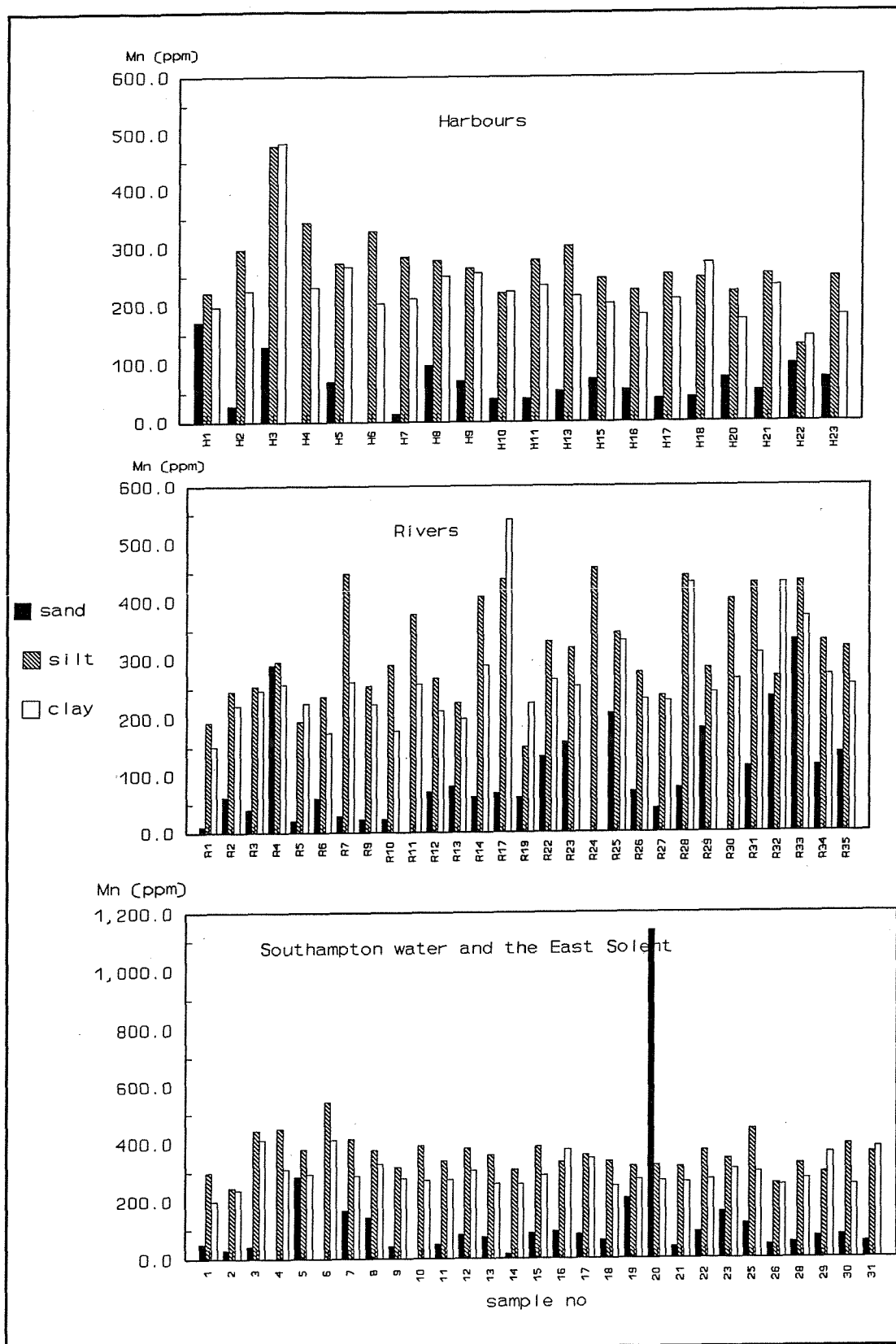


Figure 6.11 (continued): Metal content of the sand, silt and clay fractions.

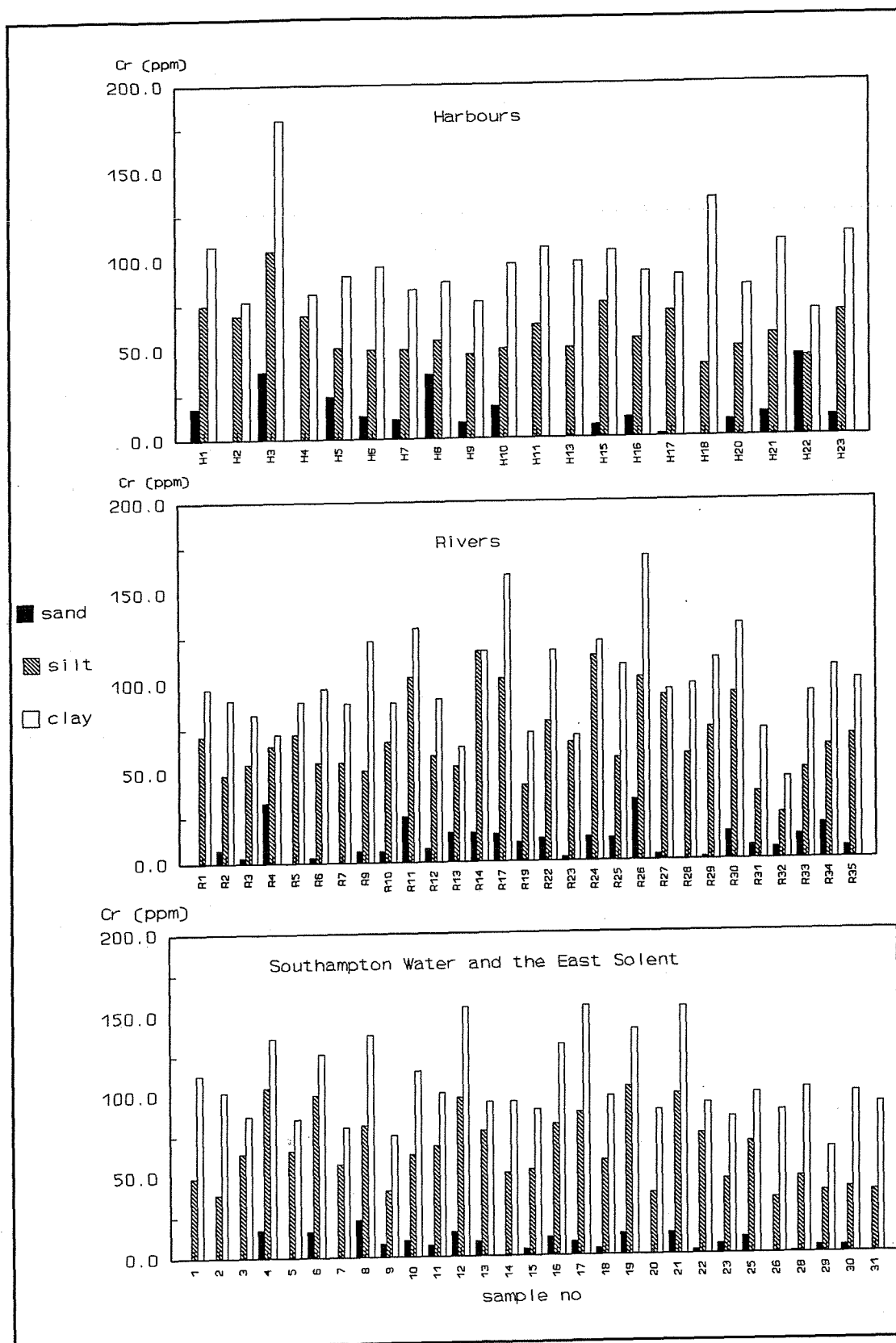


Figure 6.11 (continued): Metal content of the sand, silt and clay fractions.

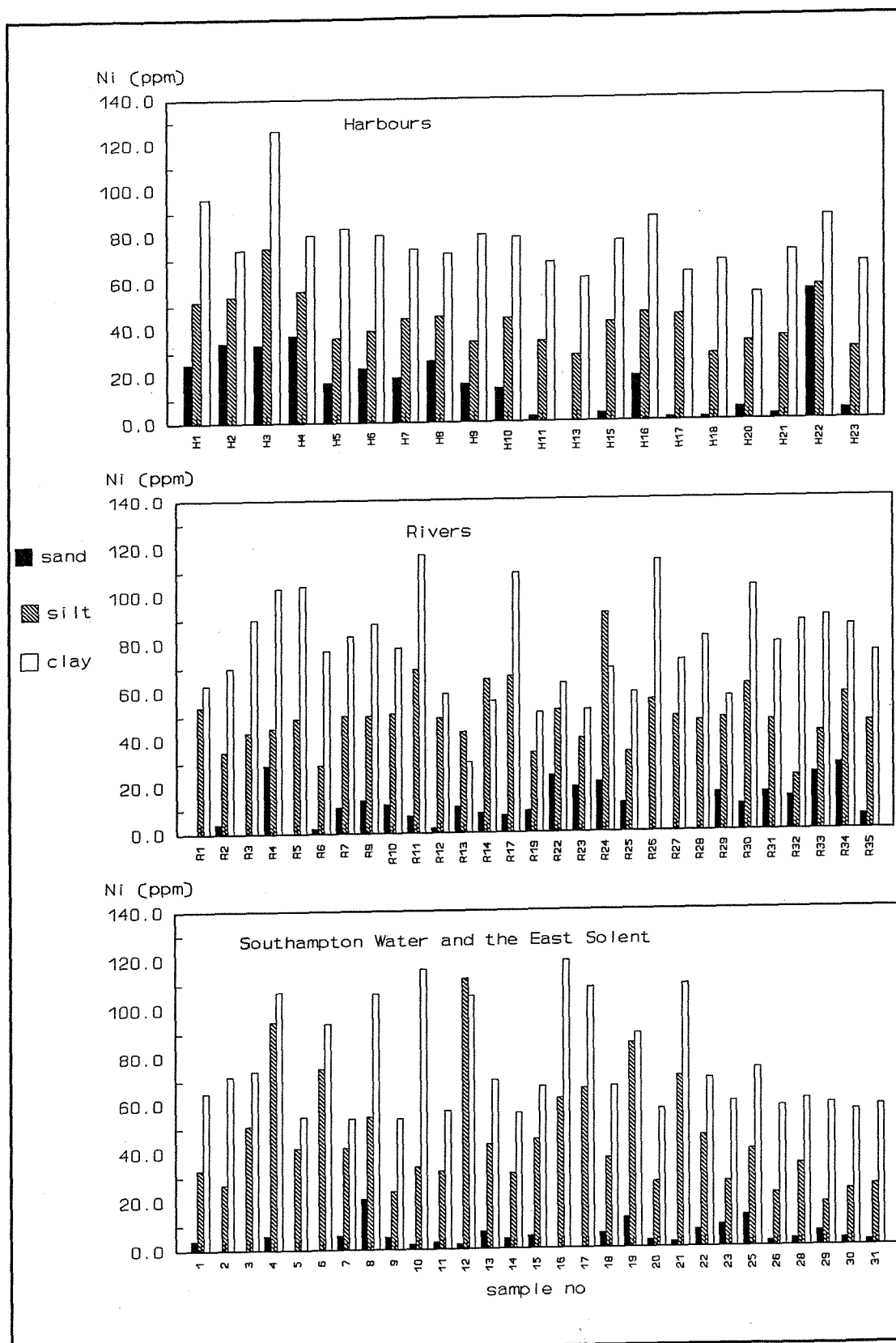


Figure 6.11 (continued): Metal content of the sand, silt and clay fractions.

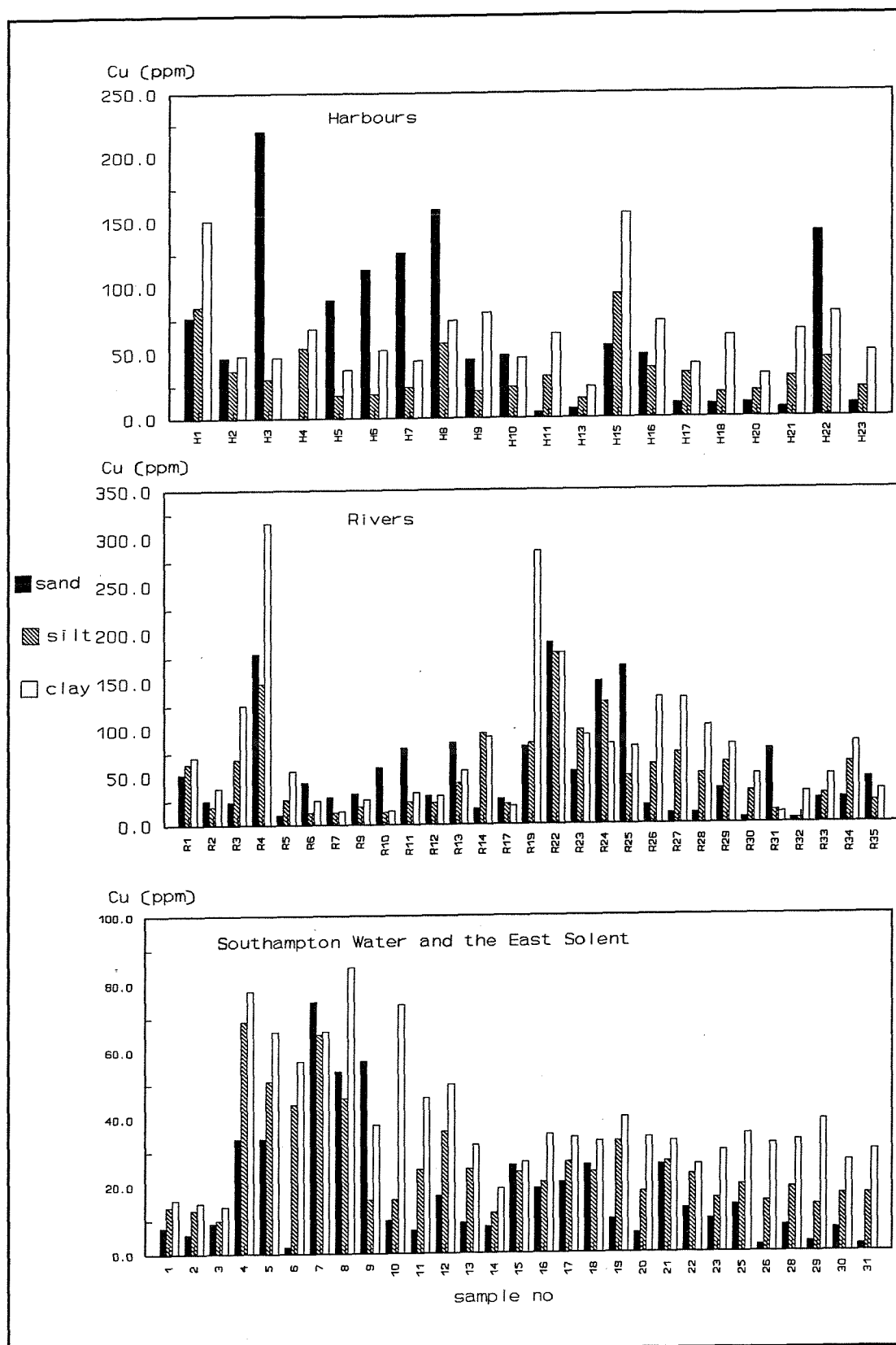


Figure 6.11 (continued): Metal content of the sand, silt and clay fractions.

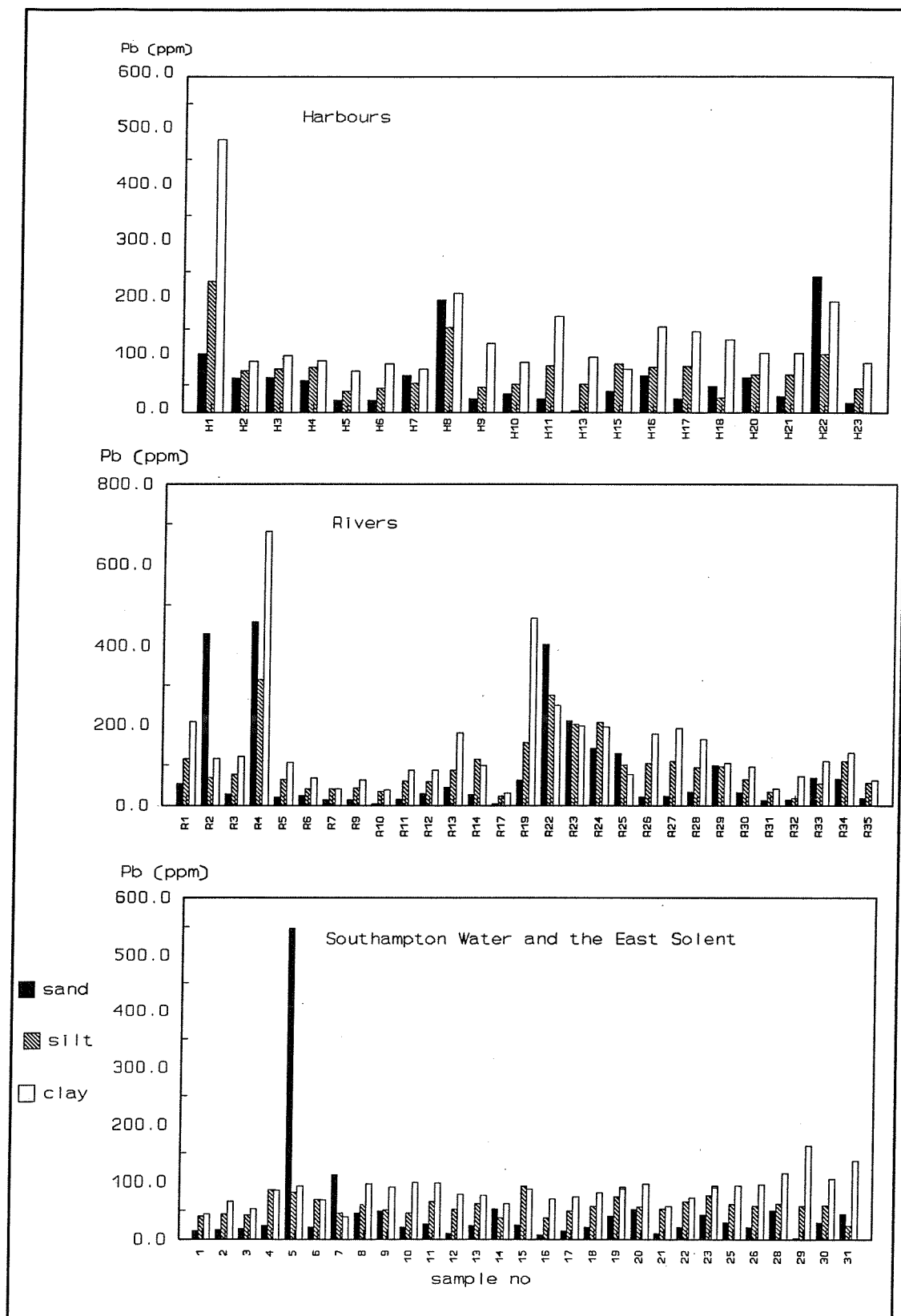


Figure 6.11 (continued): Metal content of the sand, silt and clay fractions.

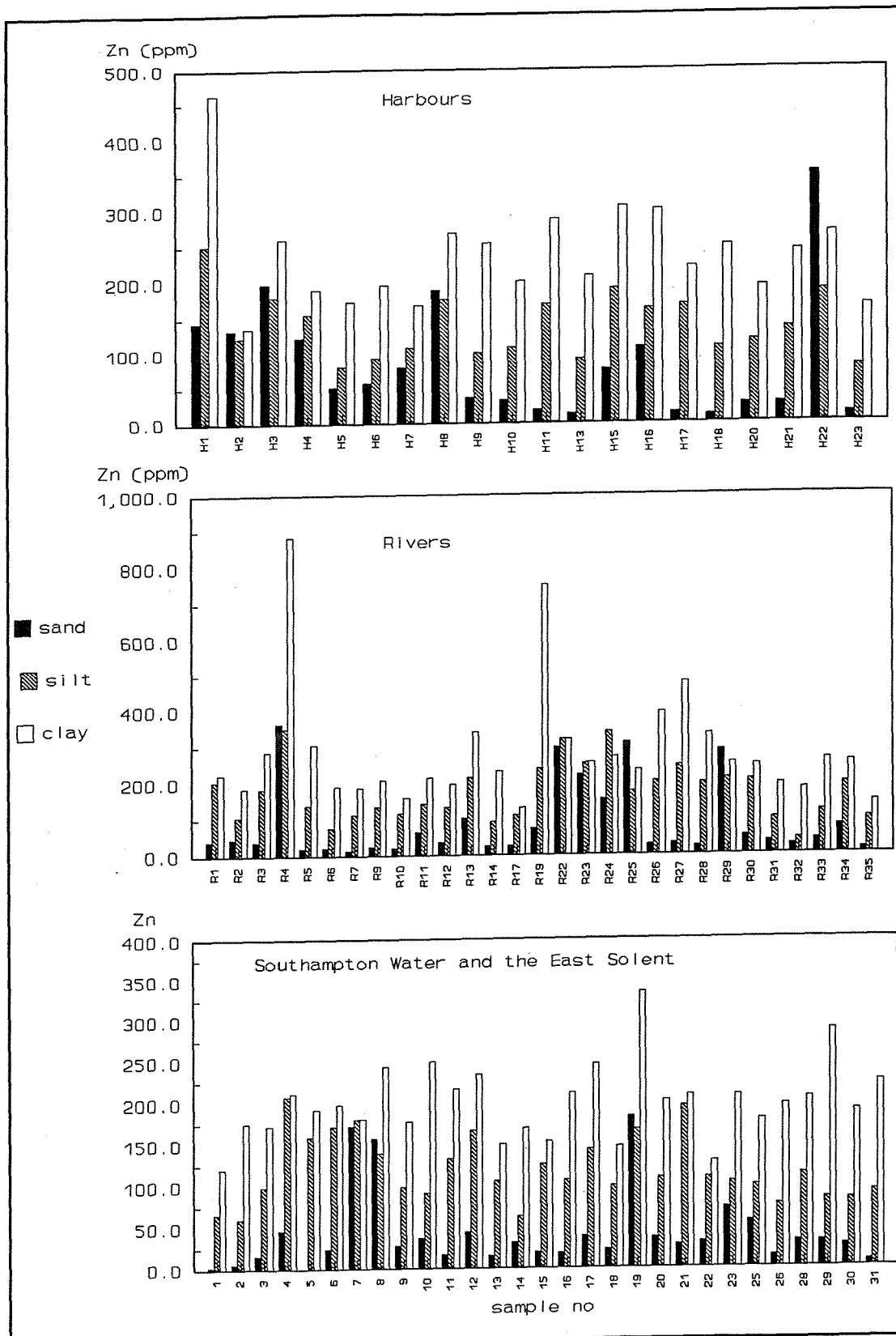


Figure 6.11 : Metal content in the sand, silt and clay fractions.

Rantala, 1992). The numbers presented in Table B4 and on Figure 6.11 are absolute total metal concentrations in the sand, silt and clay size fractions; they have not been normalized by the weight percent of the related size fractions in the total sediment.

In most cases, the metals are more concentrated within the silt and clay fractions. Al, Fe, Mn, Co, Cr, and Ni are concentrated mainly in the fine grain size (silt and clay) in all the samples. There are, however, some exceptions.

Cu concentrations are less grain size-dependent than the other metals. The samples from the harbours (H3, H5, H6, H7, H8, H9, H10, H16, H22), rivers (R4, R6, R7, R10, R11, R12, R13, R17, R22, R24, R25, R31), the main channel of Southampton Water (7, 8, 9) and the East Solent (15) have high concentration of Cu in the sand size fraction. Similarly, the Pb content of samples from the harbours (H8, H22), rivers (R2, R4, R22, R23, R25, R33) and the main channel of Southampton Water (5, 7) is higher in the sand fraction. Zn is mostly concentrated in the fine size fraction, with the exception of samples R4, R22, R23, R25, and R29 from the rivers and 7, 8, 19 from the main channel of Southampton Water and the East Solent, which have higher Zn concentrations in the sand fraction. Fe is most concentrated in the fine size fraction with the exceptions of Samples H22, R4 and 14. Mn tends to be concentrated within the silt fraction.

The deposition of coatings on inert materials is one of the major reasons for the relatively high metal contents of coarse-grained sediments (Förstner & Salomons, 1980). Mudroch & Duncan (1986) found decreasing metal concentrations with decreasing grain size for Fe, Cr, and Co and concluded that this relationship was an indication of an identical source of Fe, Cr and Co, most likely originated from a steel plant. Krumgalz (1989) determined a similar type of enrichment in the sand fraction of the contaminated sediments from Haifa Bay (Israel), explaining them in terms of the formation of large agglomerates during the drying procedures. Small sediment particles may be cemented both by dissolved organic matter and by sea salts, to form large agglomerates. It is possible that plant debris and cemented clay agglomerates might have given erroneous metal concentrations within the sand

size fraction of the samples in this study, possibly leading to the low precision of total digestion of the sand fraction (section 4.2.3). On the other hand, it is noticeable that certain metals (Cu, Pb, Zn, and Fe) are elevated in the same samples, mainly from the rivers and harbours. Therefore, it is also possible that anomalous concentrations of sand-sized detrital heavy minerals contain the metals. All the enrichments in the sand size are from the same locations; the River Keyhaven, the River Itchen, Portsmouth Harbour and in the vicinity of Esso refinery station in Southampton Water.

Since the trace metals are concentrated mainly in the fine-grain size fractions, particularly in the clay fraction, it is necessary to examine the general distribution pattern of trace metals within the clay size fraction. Besides, the transport pathway of sediment may be determined by following the metal concentration of the fine (silt-clay) size fraction, because they are most likely to be carried in suspension (Salomons & Förstner, 1984). The metal concentrations of the clay size are illustrated in Figures 6.12 to .17, and the patterns are summarised below.

Co is elevated in the East Solent. High concentrations occur on the northern and southern sides (Ryde and Wootton Creek) of the East Solent, and decrease towards the open end (Figure 6.12). The sample from upstream of the Hamble River has the highest concentration (69 ppm)

Cr displays a similar pattern to **Co**; higher concentrations occur in the East Solent, at the confluence of Southampton Water, within Portsmouth Harbour, upstream of the River Hamble and within the River Test (Figure 6.13). It is almost constant (100-150 ppm) in samples from the River Itchen and Southampton Water, decreasing locally.

Cu has a distinctive pattern. It varies between 50 to 100 ppm within Southampton Water, decreasing towards the confluence, and is remarkably lower in the East Solent (Figure 6.14). There appear to be two 'hot-spots'; one is upstream of the River Itchen and the other is in the River Keyhaven.

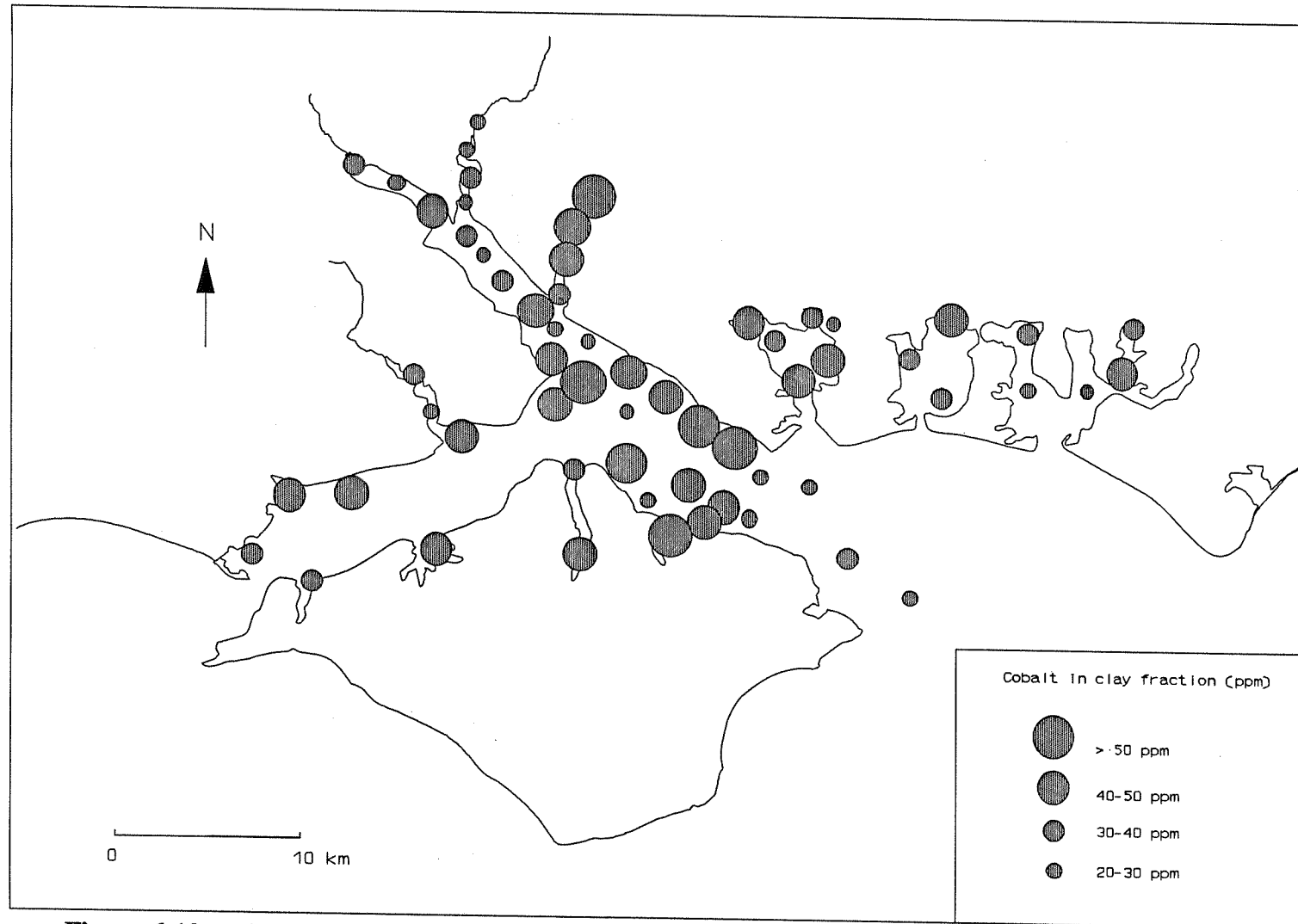


Figure 6.12 : *The distribution of Co in the clay fraction of surficial sediments throughout the area of study.*

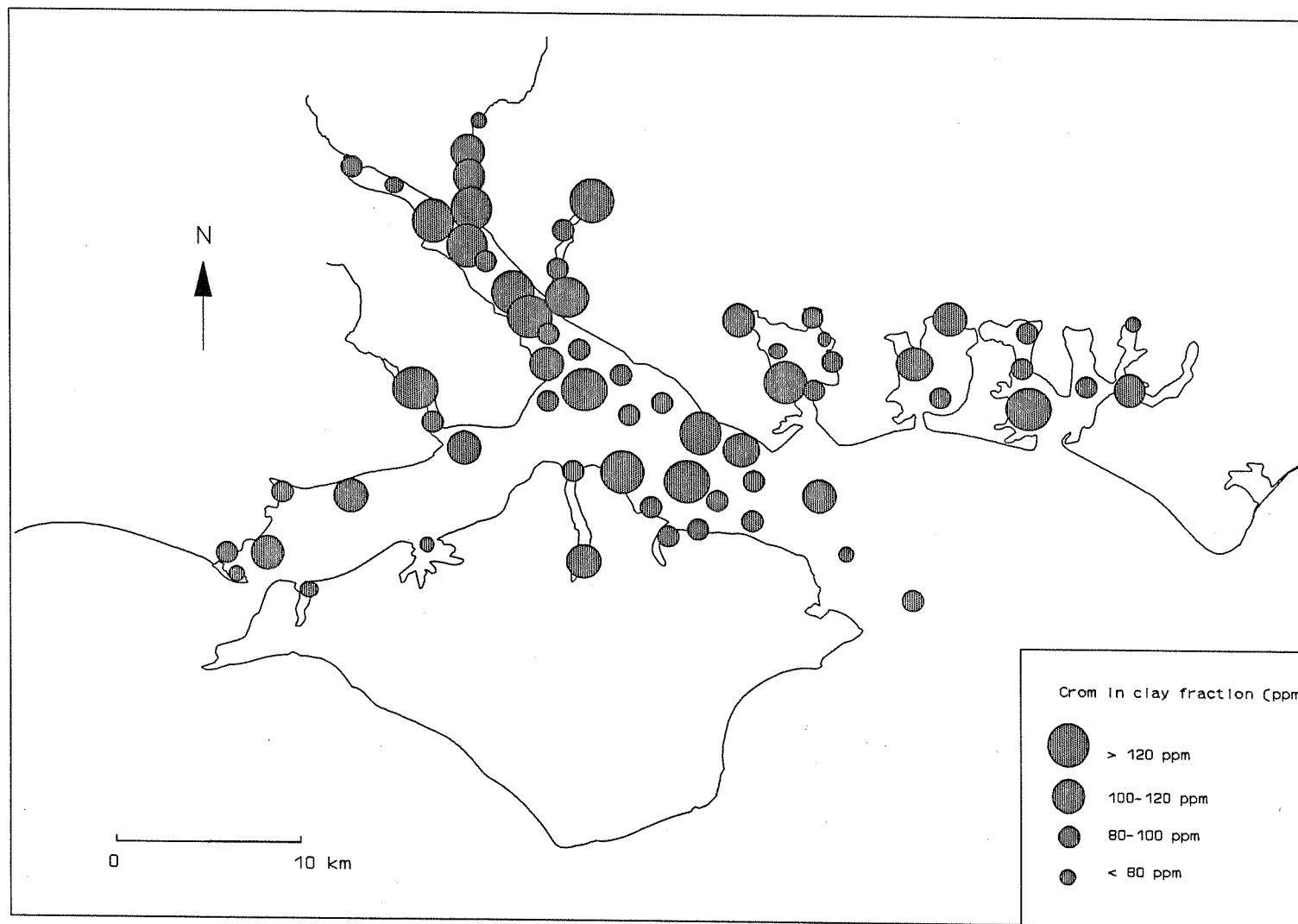


Figure 6.13 : *The distribution of Cr in the clay fraction of surficial sediments throughout the area of study.*

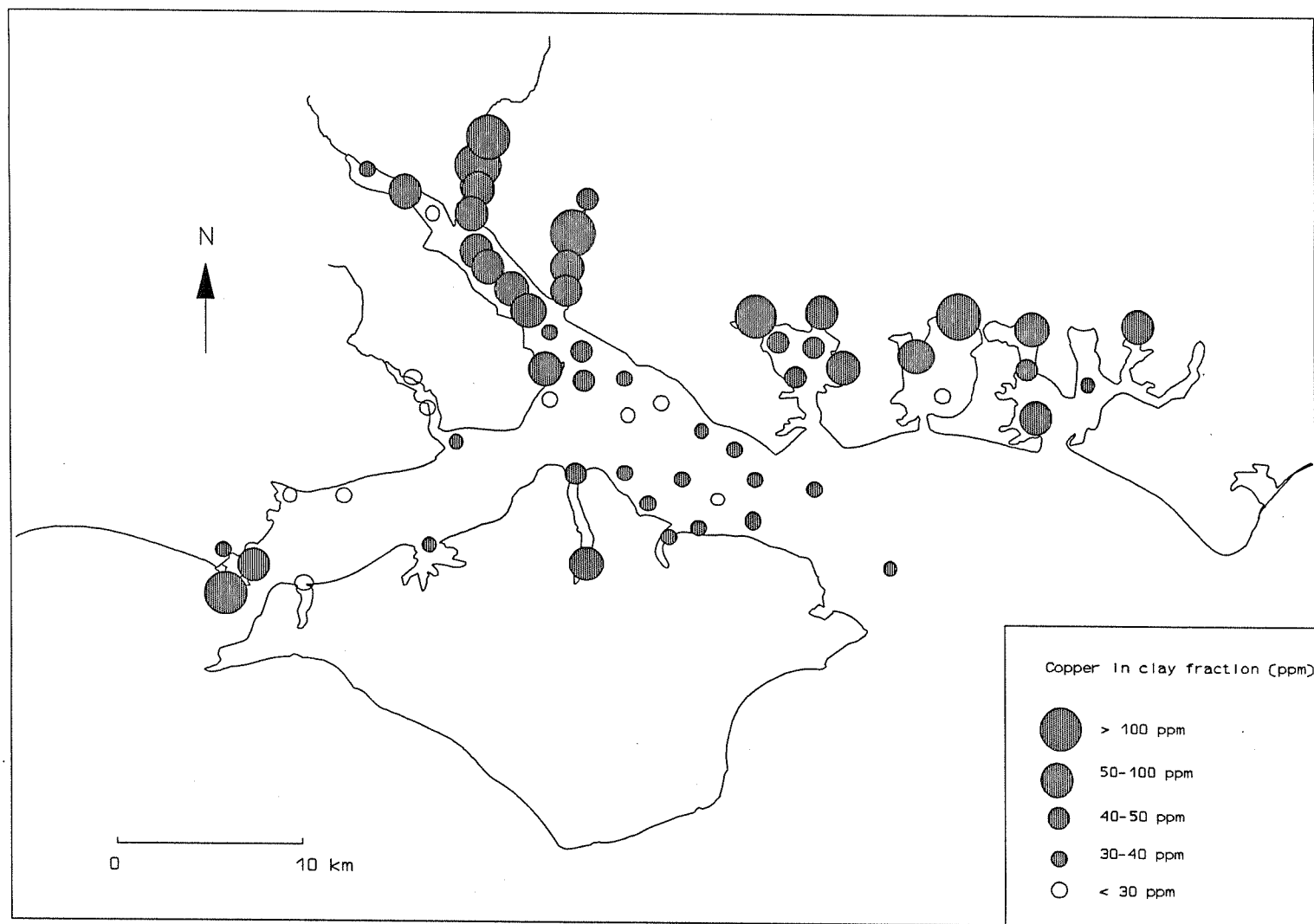


Figure 6.14 : *The distribution of Cu in the clay fraction of surficial sediments throughout the area of study.*

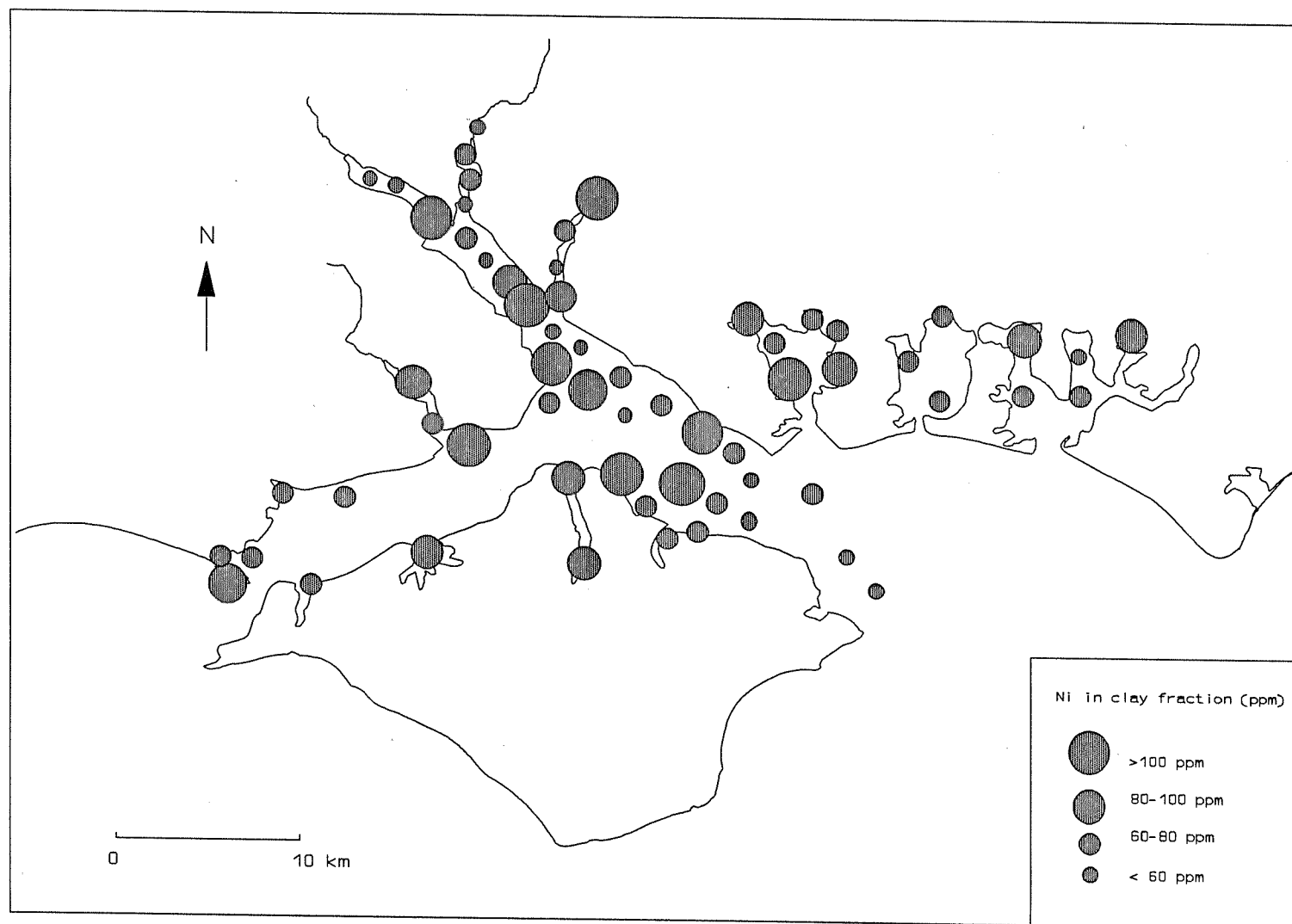


Figure 6.15 : *The distribution of Ni in the clay fraction of surficial sediments throughout the area of study.*

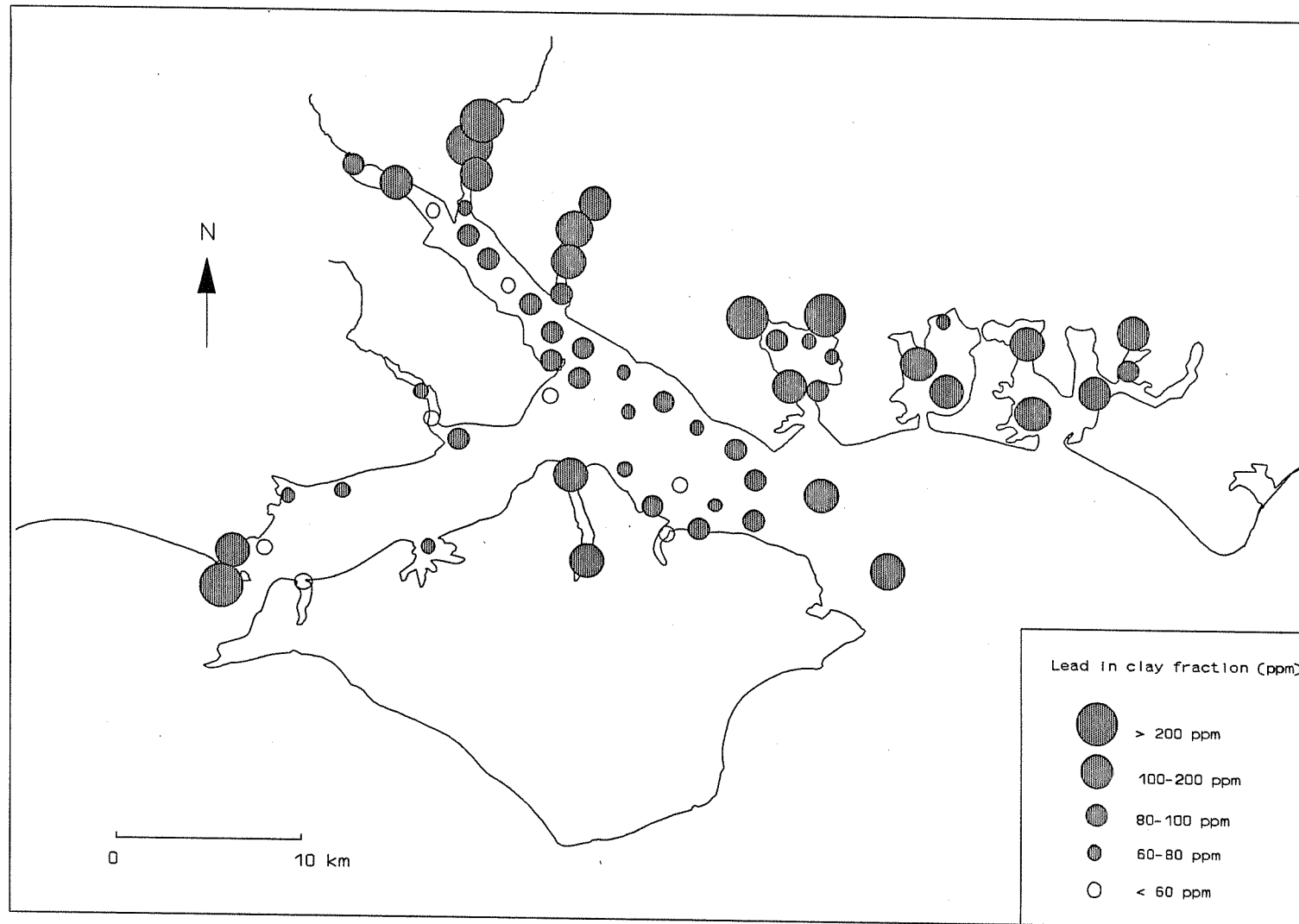


Figure 6.16 : *The distribution of Pb in the clay fraction in surficial sediments throughout the area of study.*

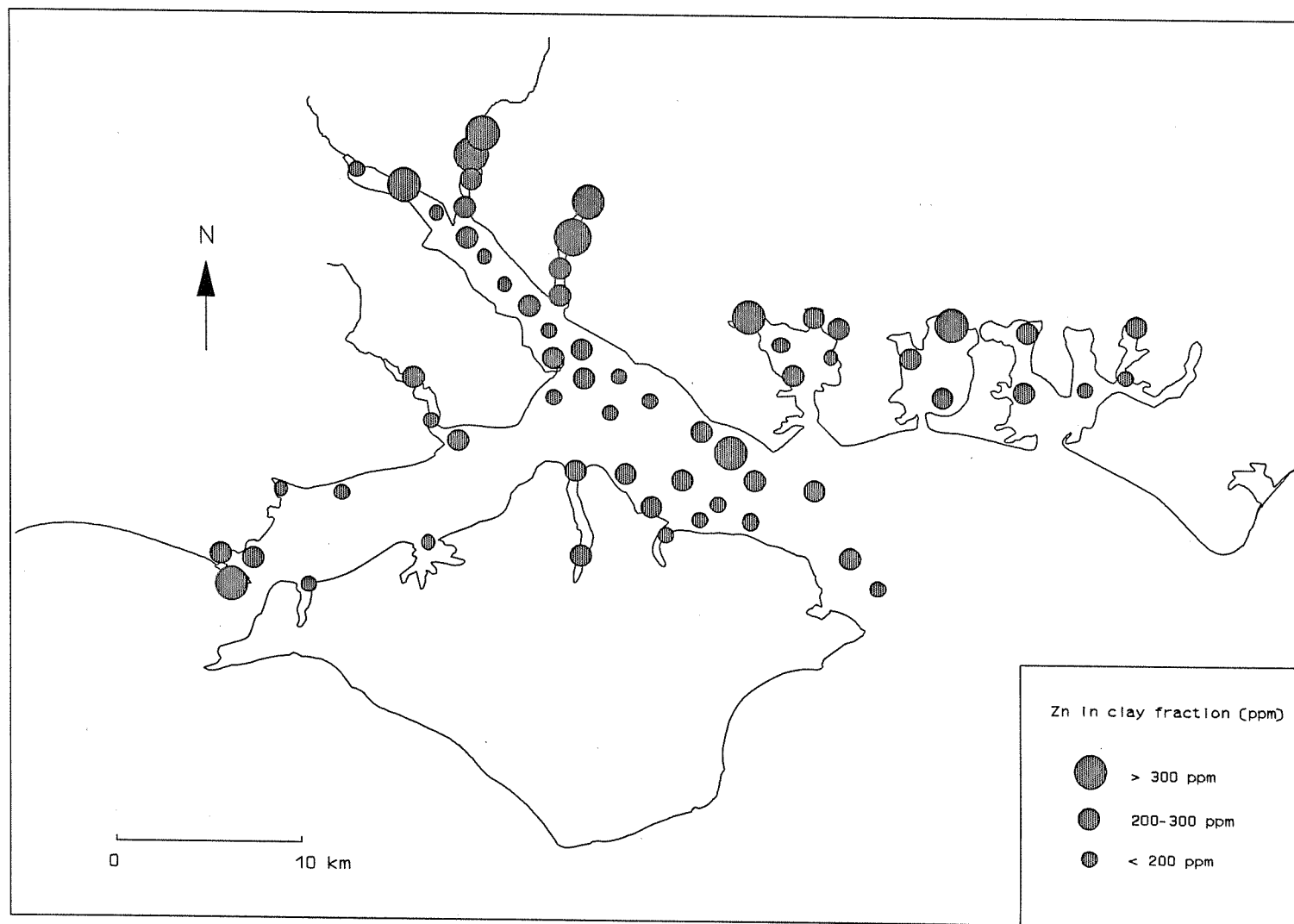


Figure 6.17 : *The distribution of Zn in the clay fraction of surficial sediments throughout the area of study.*

Ni is remarkably variable throughout the region (Figure 6.15). Elevated concentrations occur in Southampton Water, Portsmouth Harbour, the Rivers Keyhaven, Test and Hamble, and locally in Southampton Water. It tends to decrease towards the open (seaward) end in the East Solent.

Pb concentrations are high in the Rivers Itchen, Hamble and Keyhaven, and in Portsmouth Harbour (Figure 6.16). They are very low in the West Solent and the Lymington and Beaulieu Rivers. There is a consistent increase along the main channel of Southampton Water, which is dissimilar to the other metal distribution patterns, as are the elevated concentrations in the open end of the East Solent.

Zn displays a dispersal pattern which is similar to Pb, to some extent (Figure 6.17). It is high in the samples from the Keyhaven, Itchen, and Hamble Rivers, and Portsmouth Harbour; it is highly variable within the main channel of Southampton Water and the East Solent. Sediments from the northern side and the open end of the East Solent and in the vicinity of Calshot Spit contain high concentrations of Zn.

6.1.6. Normalization of Data

Normalization is necessary to compensate for the natural variability of trace metals in sediments and also to allow intercomparison of sediments from different locations (Loring, 1991; Luoma, 1990). In most cases, Al can be used as a reference element to normalize any grain size variability in sediments (Din, 1992). It is a major constituent of fine-grained aluminosilicates, with which the bulk of the trace metal are associated. Hence, normalization with respect to Al compensates for changes in the input rates of various diluents or variations in sedimentation rates (Loring, *op.cit.*; Loring & Rantala, 1992). If a given trace metal does not covary with Al, this may indicate that the metal is associated with an additional input to the crustal component of the clay minerals (Din, *op.cit.*). In Figure 6.10, a plot of total Al against grain size illustrates a positive correlation between Al and the percentage of clay ($r=0.71$). Therefore, Al can be used as a normalizing element in the present

study area. Scatterplots of metal concentrations against Al have been constructed depicting regression lines with 95 % prediction limits. Metal concentrations plotting above the 95% limit are considered to be due to (anthropogenic) contamination. Positive associations indicate that Al is an effective major chemical constituent with which to normalize for the grain size effect on most of the natural trace metal variability. Also, that anomalous metal/Al ratios above a certain range can be interpreted as an indication of metal contamination in this region (Loring, 1991).

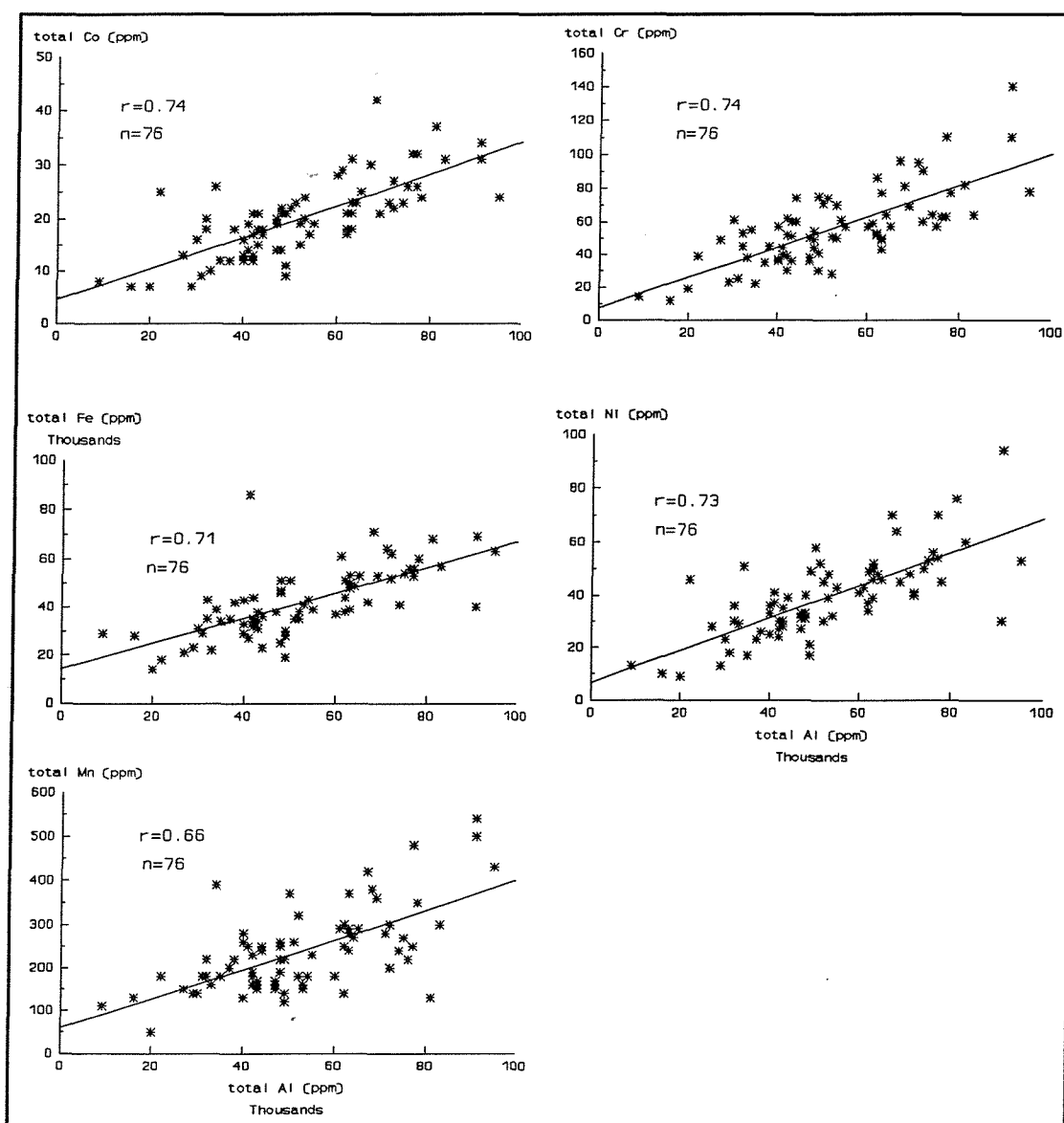


Figure 6.18 : Correlations between total trace metal and Al concentrations for the surficial sediments (continued on next page).

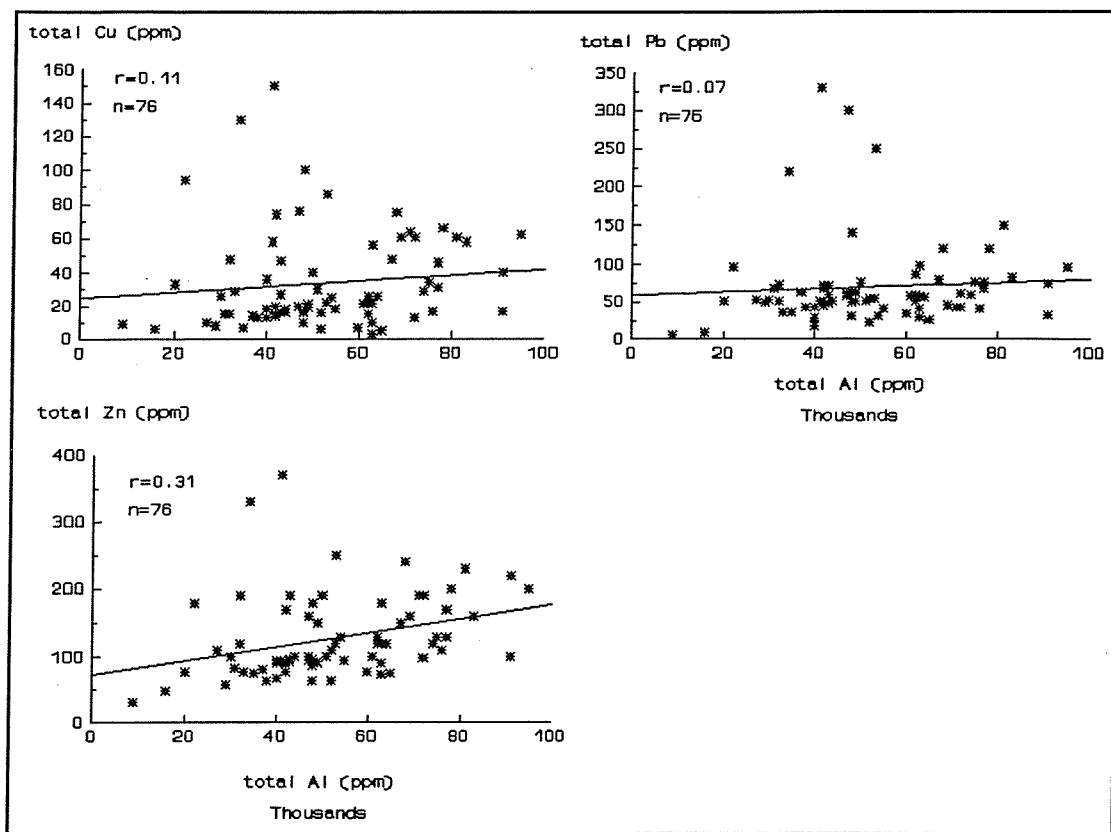


Figure 6.18 (continued): Correlations between trace metal and Al concentrations for the surficial sediments.

Total Al correlates with Co ($r=0.74$), Cr ($r=0.74$), Fe ($r=0.69$), Ni ($r=0.73$) and Mn ($r=0.65$), whereas Cu ($r=0.11$), Pb ($r=0.07$) and Zn ($r=0.31$) are associated with poor correlation coefficients (Figure 6.18). As Loring & Rantala (1992) have suggested, samples believed to be anomalous (*i.e.* samples which have high concentrations of Cu, Pb and Zn in the sand fraction, described in Sections 6.1.4 and 6.1.5) should be removed from the graph, and replotted (Figure 6.19). Correlation coefficients of Cu, Pb and Zn improve after rejection of anomalous samples; Cu $r=0.81$, Pb $r=0.77$ and Zn $r=0.80$. The samples rejected, shown on Figure 6.20, are from the Rivers Itchen, Test, Hamble and Keyhaven and the bay-head locations of Portsmouth, Langstone and Chichester Harbours. This pattern is in agreement with the distribution of the total metal concentrations in the

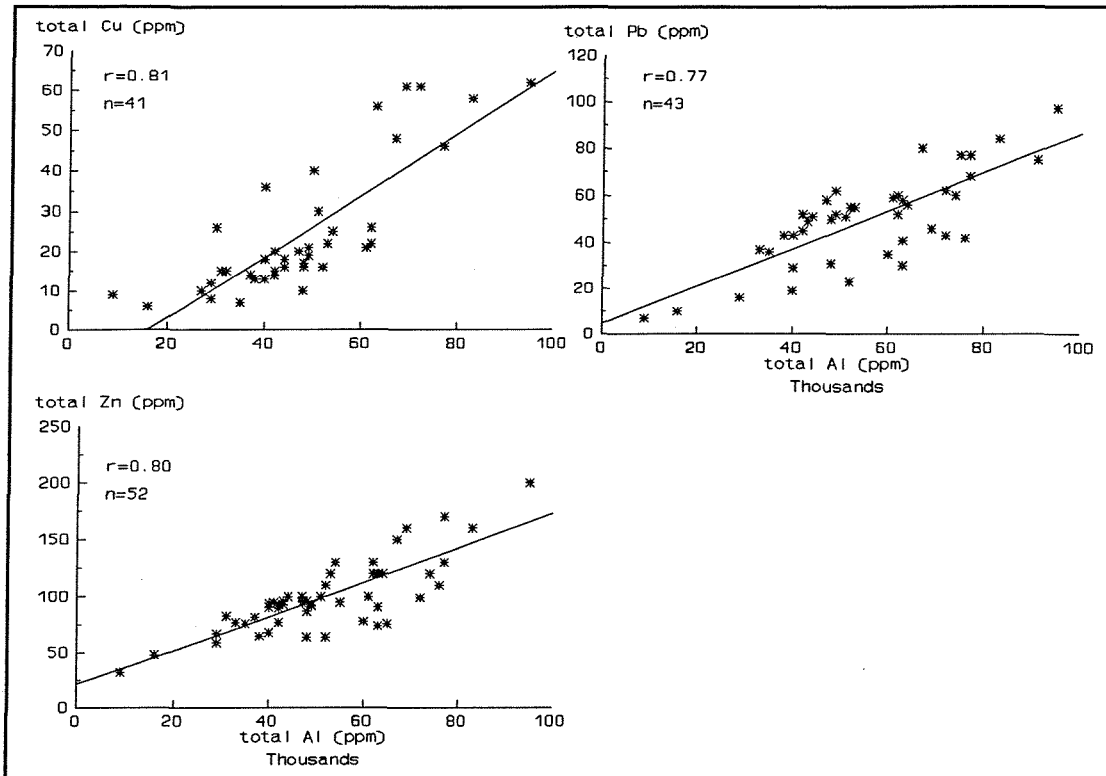


Figure 6.19 : Correlations between Cu, Pb, Zn and Al concentrations for the surficial sediments, after rejection of outlying samples (sig.level=0.00).

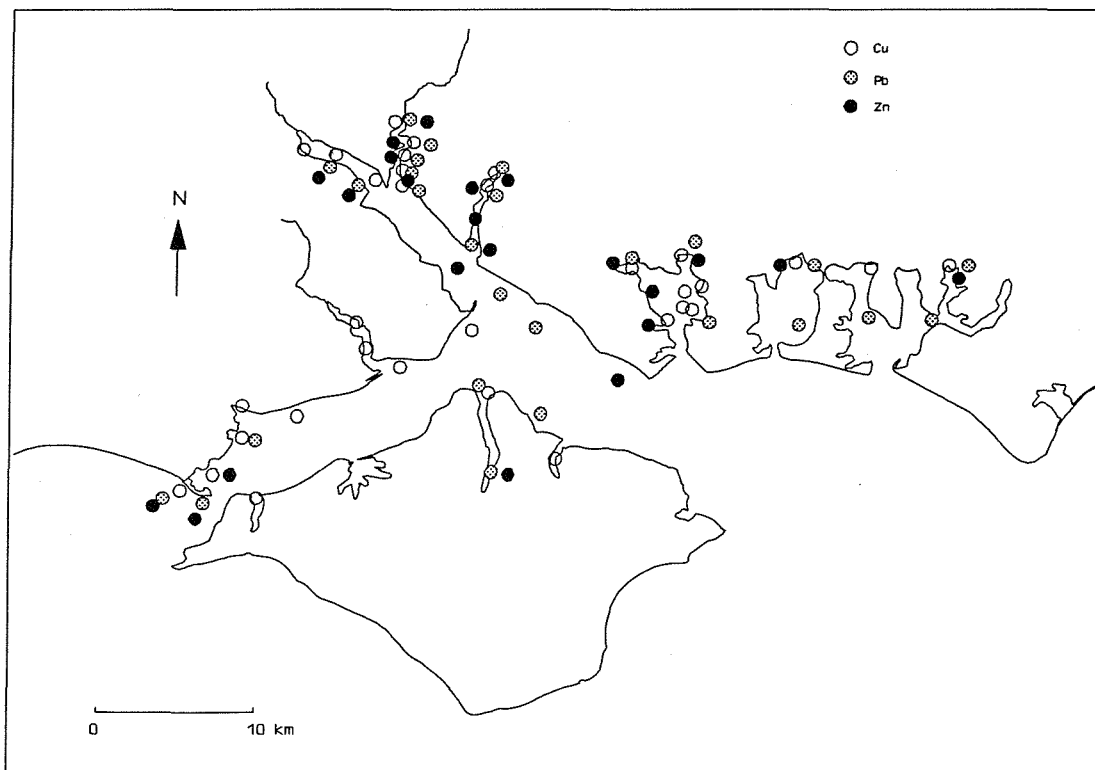


Figure 6.20 : The location of samples containing anomalous concentrations of Cu, Pb and Zn in the surficial sediments.

region (see Figures 6.3, .6 and .7). Consequently, these samples might be considered as representative of anthropogenic inputs to the system.

6.1.7. The Source and Transportation of Metals

Total metal concentrations and the metal concentrations in the three size fractions (sand, silt and clay) are plotted for a transect section, from the River Test along the main channel of Southampton Water to the open end of the East Solent (Figure 6.21). Three types of trend may be defined along this section, although most of the metal trends are noisy:

- (i) all the total metal concentrations decrease along the section;
- (ii) the metal concentrations in all three size fractions decreases consistently along the section, for Cu only;
- and (iii) the metal concentrations in the clay fraction increase along the section - this is true for Fe, Zn and Pb.

The remainder of the metals in the three size fractions show great variability. Al in the sand and silt fractions appears to decrease along the section, whereas Al in the clay fraction is almost constant. Mn displays a similar trend to Al. Co, Cr and Ni in the silt and clay fractions are elevated in the East Solent.

The mean grain size is plotted along the same section, in order to highlight the potential effect of grain size variations (Figure 6.22). The mean grain size increases along the section. Plots of total metal/total Al ratios along the transect are shown in Figure 6.23, in order to eliminate the grain size variations.

In general, the normalized ratios are variable (with abrupt peaks); however, some consistent trends can be noticed. Most of total metal/Al ratios decrease from the rivers to the mouth of Southampton Water and increase in the East Solent (total Cu/Al, total Co/Al, total Pb/Al, and total Zn/Al). Total Mn/Al and total Fe/Al ratios increase slightly from Southampton Water to the East Solent; they are very high at the open (seaward) end. Total Cr/Al and total Ni/Al ratios show great variability, being low at the confluence of Southampton Water and the East Solent,

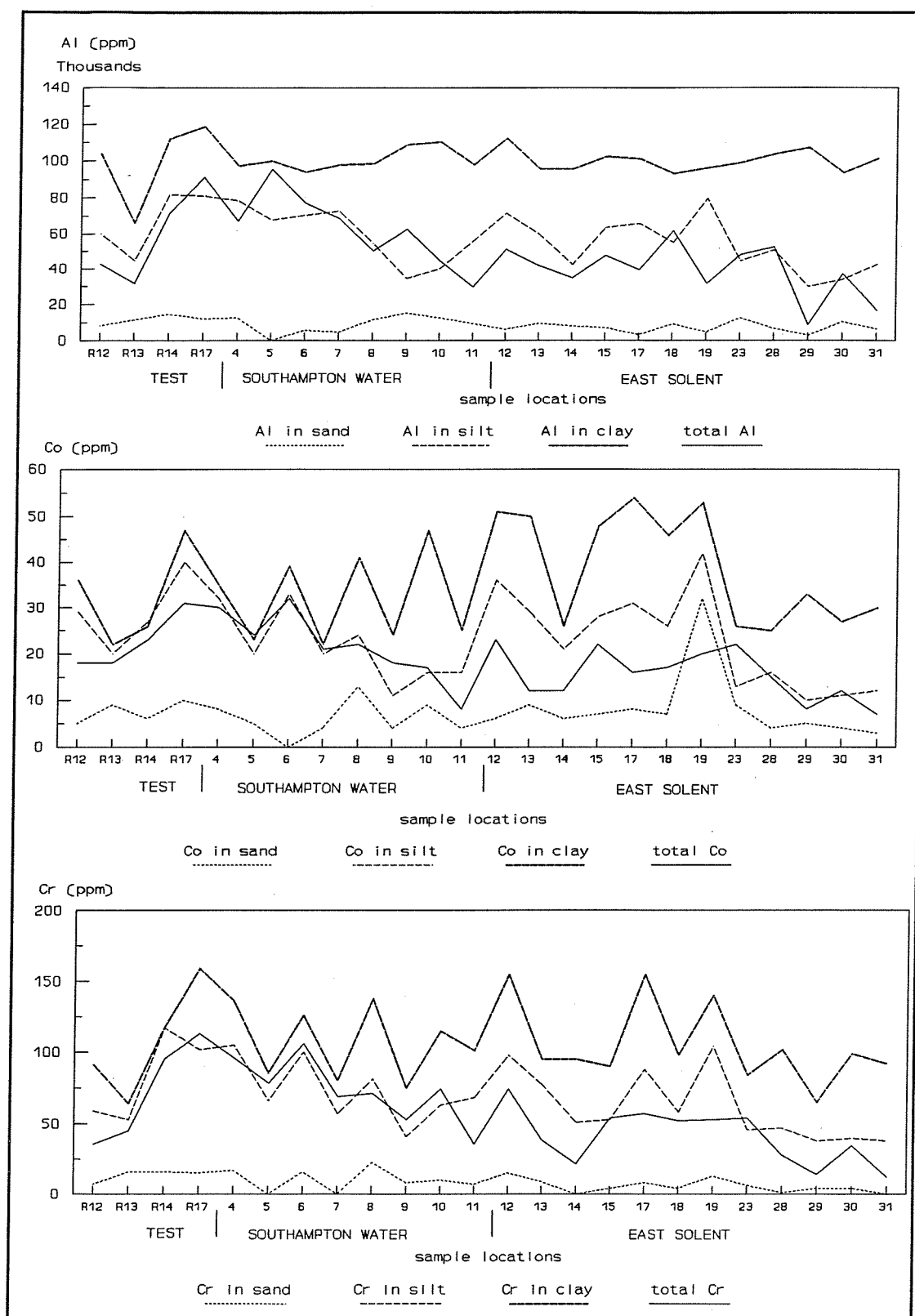


Figure 6.21 : Metal concentrations in the various size fractions of the surficial sediments, along a transect from the River Test to seaward.

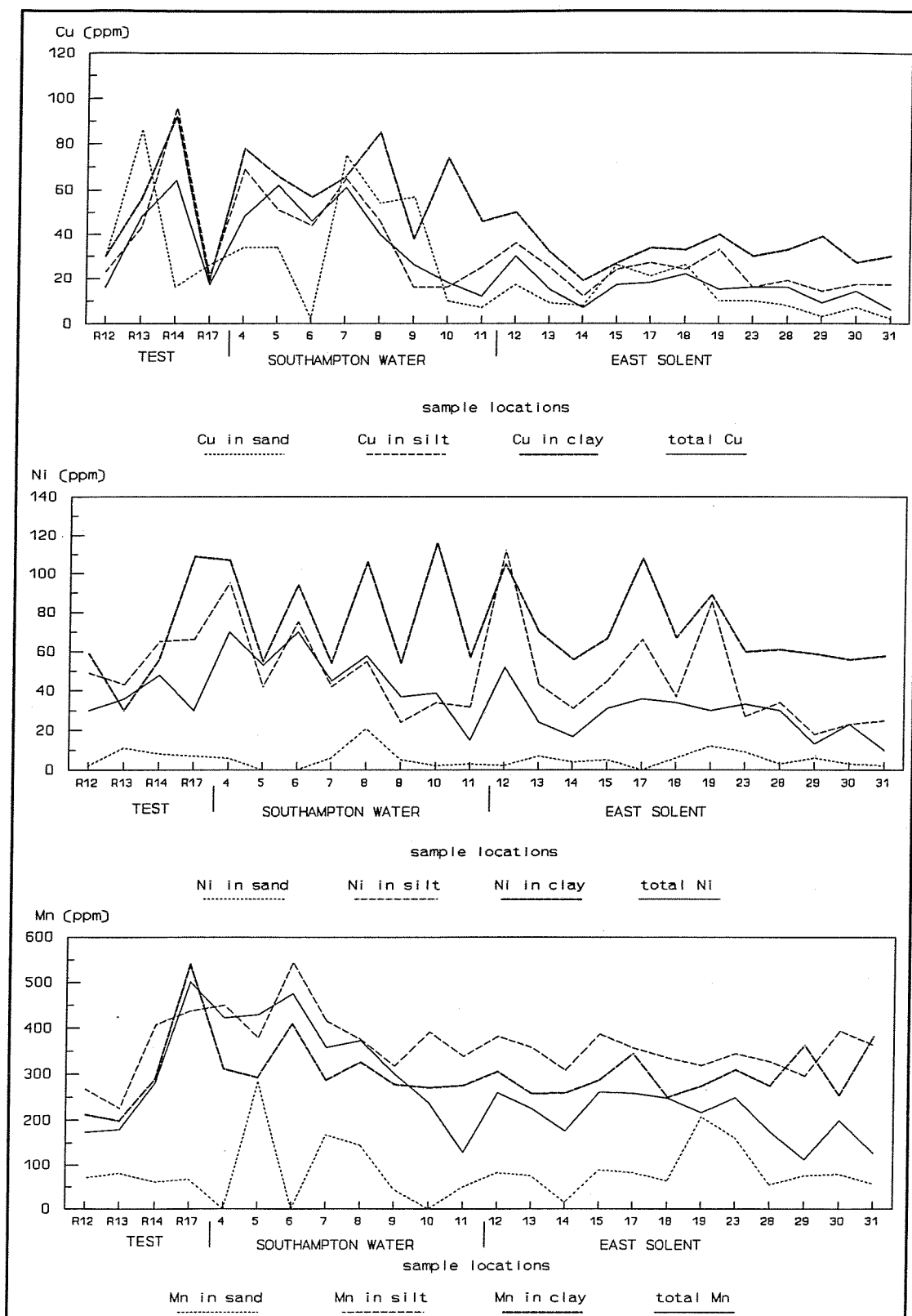


Figure 6.21 (continued): Metal concentrations in the various size fractions of the surficial sediments, along a transect from the River Test to seaward.

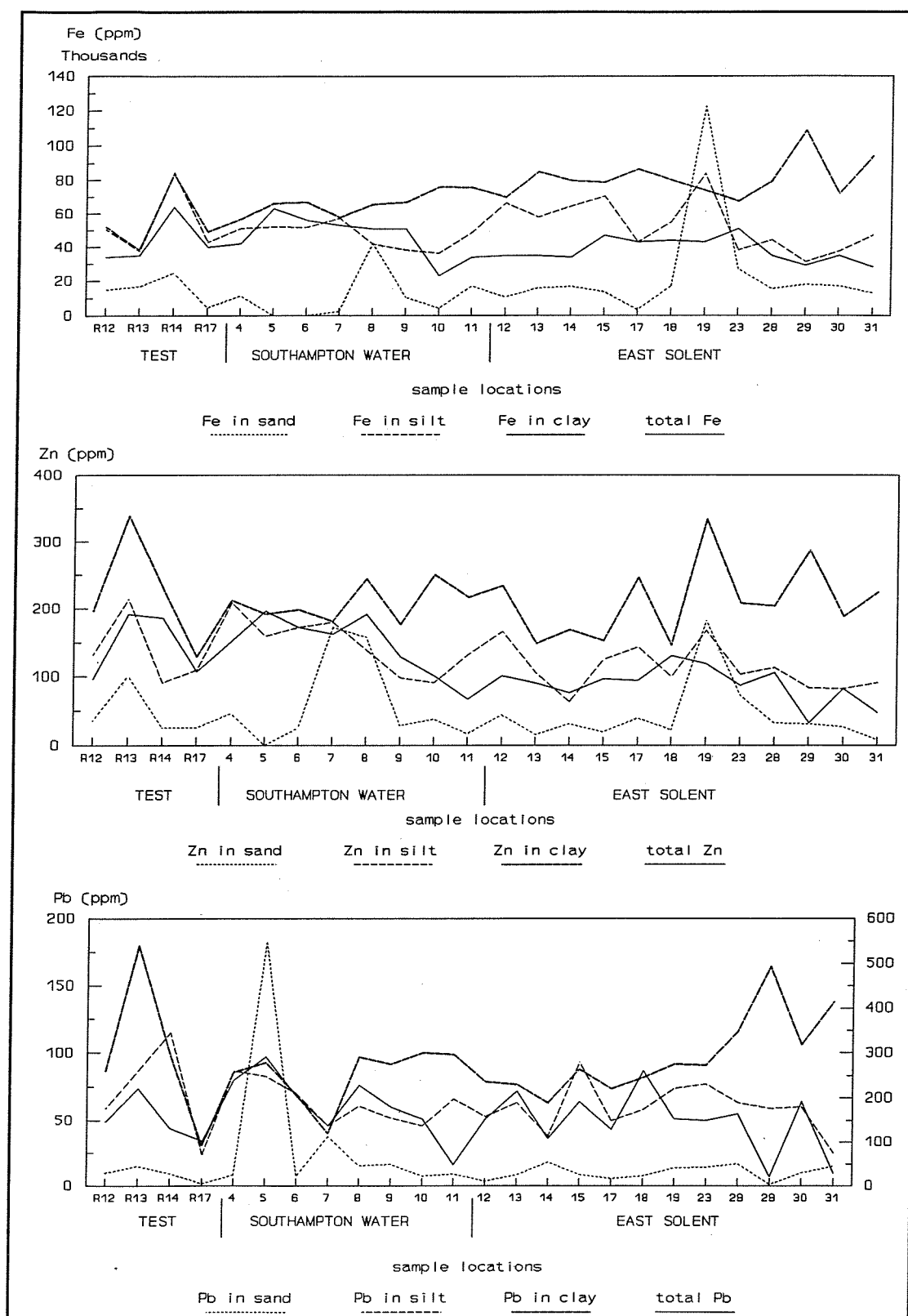


Figure 6.21 (continued): Metal concentrations in the various size fractions of the surficial sediments, along a transect from the River Test to seaward.

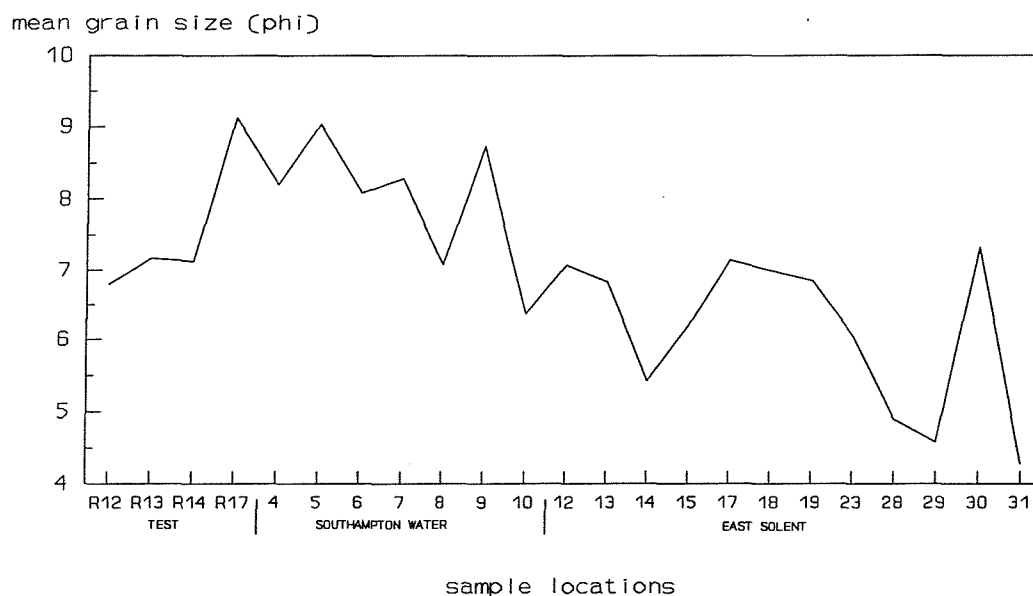


Figure 6.22 : *Variations in the mean grain size of the surficial sediments, along the same transect as in Figure 6.21.*

and fluctuating towards the open end. These normalized patterns are similar to the distribution of trace metal concentrations in the clay fraction (Figure 6.21). The distribution pattern of the mean grain size suggests a relative coarsening along the section towards the East Solent. Everaats & Fischer (1992) have found similar distribution patterns of elevated metal concentrations in the decreasing proportion of the fine-grained fraction in the surface sediments from the Southern Bight of the North Sea. These investigators explained this pattern in terms of the sedimentation of suspended particulate matter with elevated levels of trace metals. Elevated ratios along the section towards to the East Solent may be attributed also to variations in trace metal sources. The Rivers Test, Itchen and Hamble appear to be the main source of the Cr, Cu, Pb and Zn supply to Southampton Water. The northern side of the East Solent and the open end of the East Solent also seem to be receiving metals from another source. Since the elevated metal concentrations are associated with the clay size fraction in these area, it is likely that sedimentation of suspended particulate matter with elevated levels of trace metals is responsible for the elevated

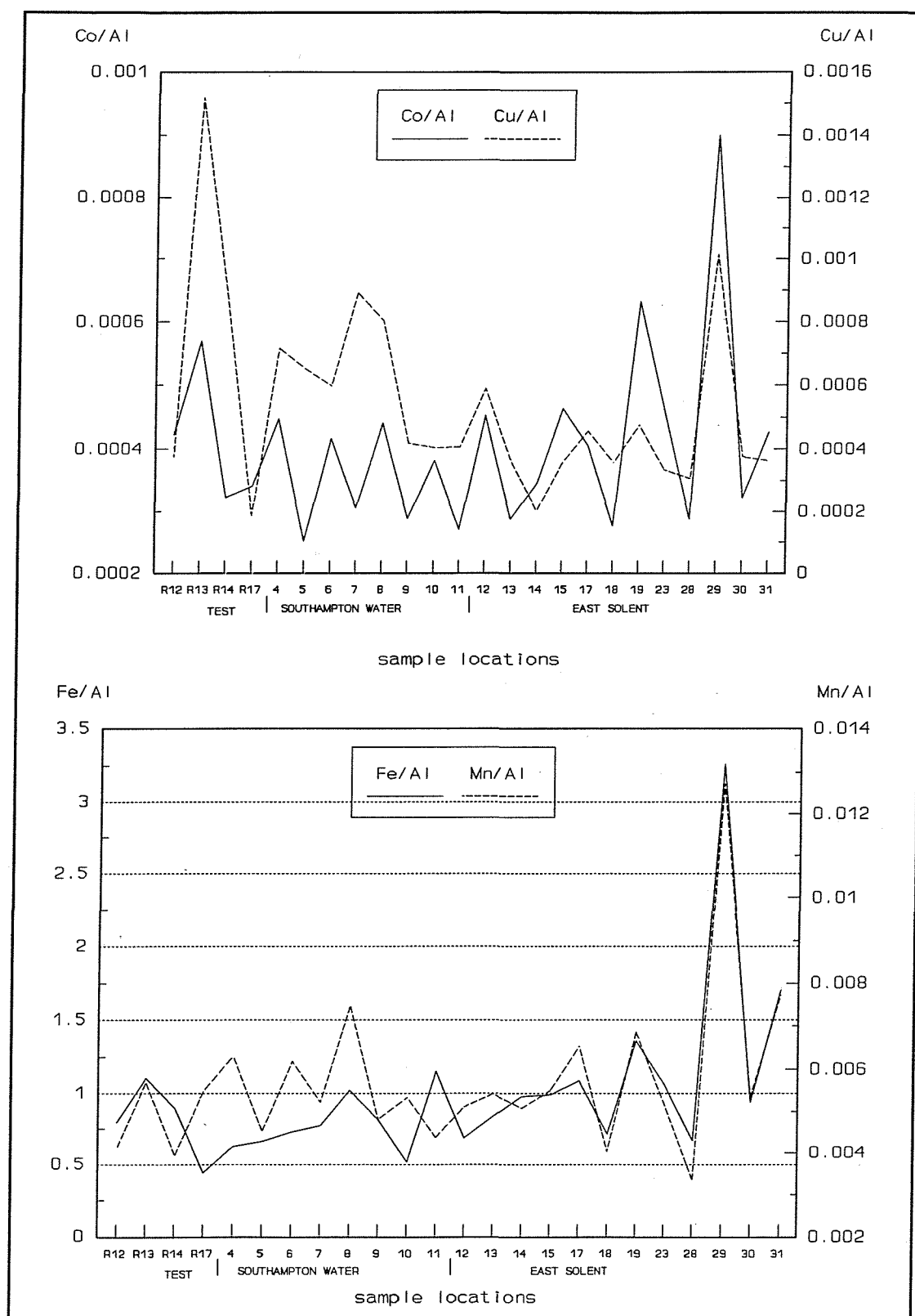


Figure 6.23 : Metal/Al ratios in the surficial sediments, along the same transect as in Figure 6.21 (continued on next page).

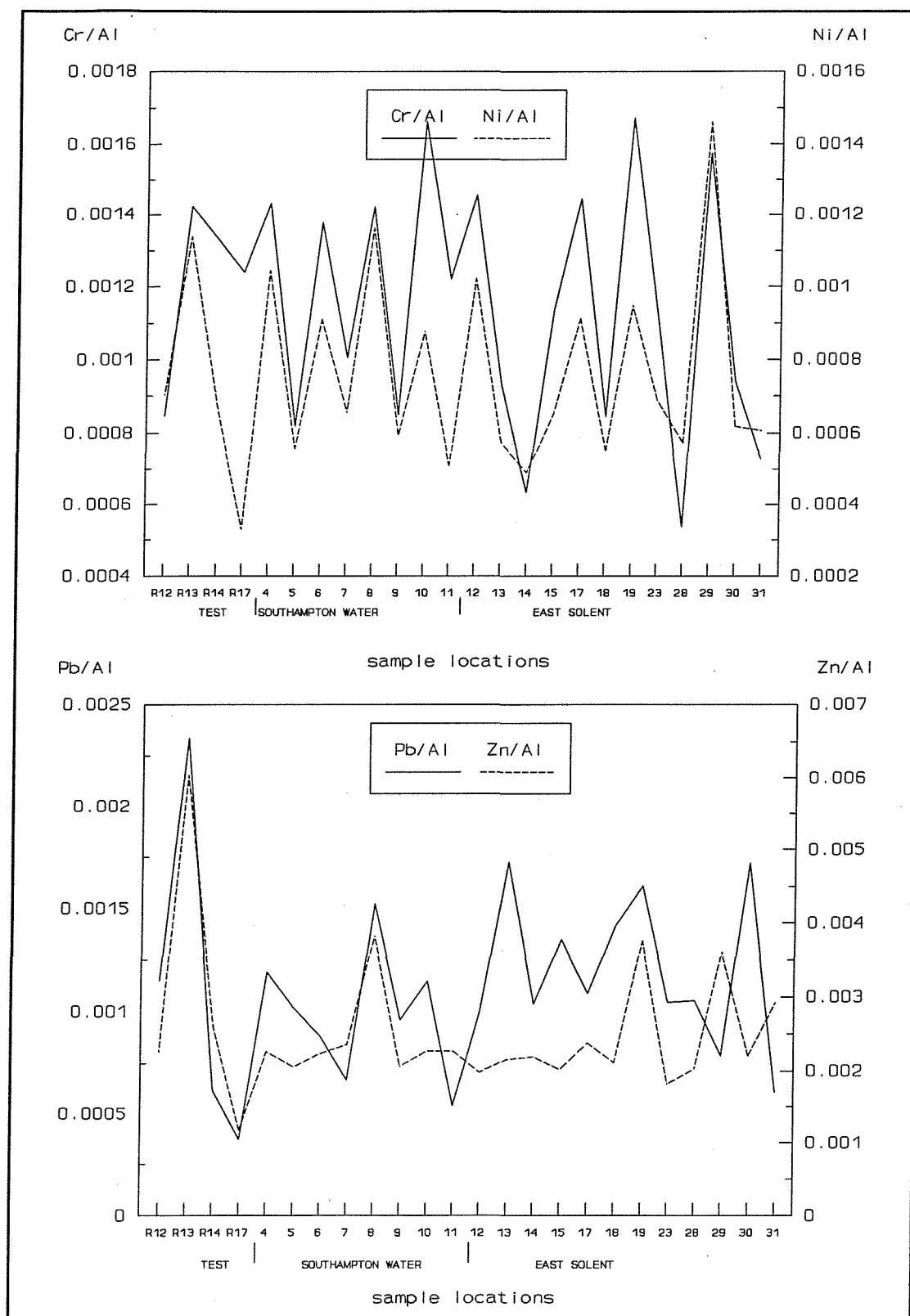


Figure 6.23 (continued): Metal/Al ratios in the surficial sediments, along the same transect as in Figure 6.21.

ratios of the East Solent sediments.

6.2. Metal Fractionation in Geochemical Phases

Samples from two cores were used for the sequential (selective) extraction of trace metals. The locations of the cores are shown in Figure 6.24; X1 is in the upper reaches of Southampton Water and X5 is from the mouth of the estuary. This strategy was adopted to detect any alteration in the spatial distribution of the phase association of metals within the estuarine sediments. The results of the selective extraction procedure are shown in Table B5, of Appendix B and Figures 6.25 to .26.

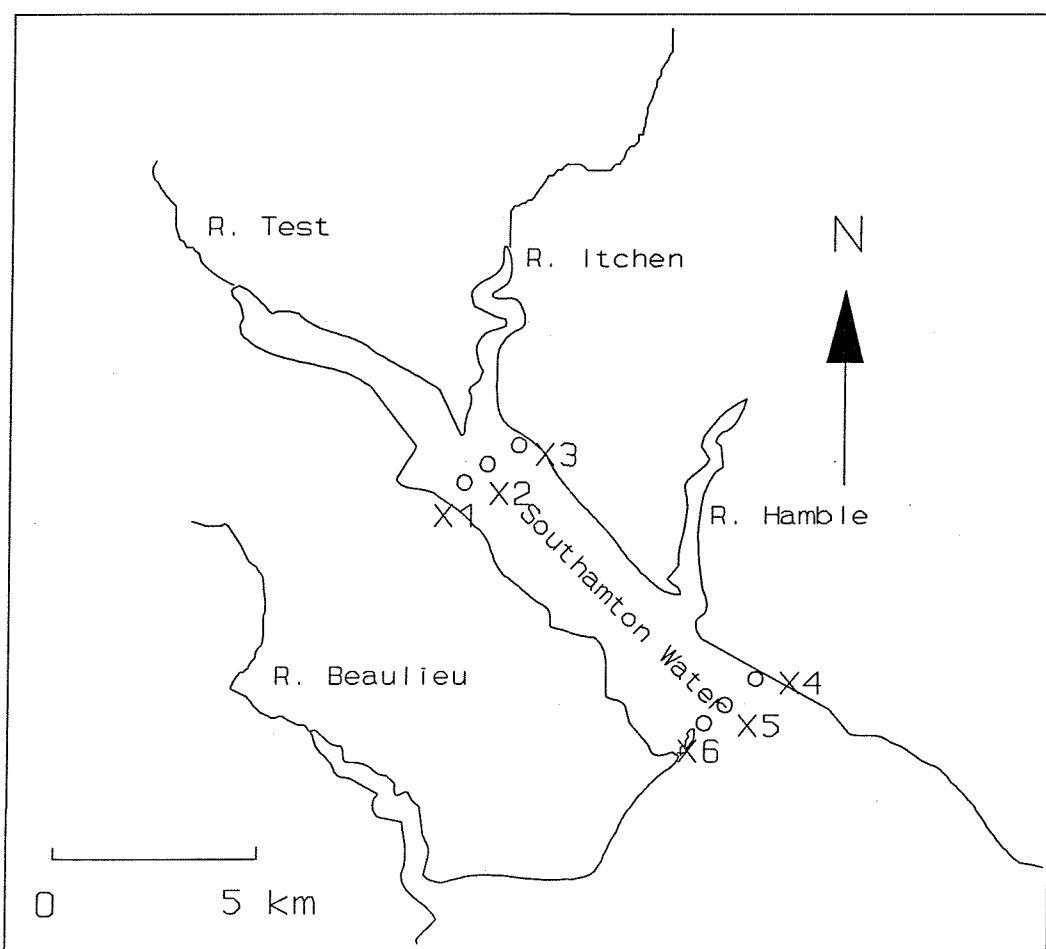


Figure 6.24 : Core samples locations in Southampton Water.

Three geochemical phases have been *operationally defined* as "reducible" (including exchangeable, carbonates and Fe-Mn oxides), "oxidizable" (organic), and "residual" (mineral crystal structure). At the same time, it should be noted that the distribution of trace metals in any chemically-extracted fraction is defined more by the method of extraction than fundamental properties of the natural environment itself (Brannon *et.al*, 1977).

Core X1 was 15 cm in length, and a colour change was observed along the core; the first 3 cm were greenish grey, whereas the remainder was dark grey-black. Core X5 was 10 cm in length and was greenish grey throughout. The first 4 cm consisted of sandy clay, with the proportion of clay increasing visibly along the core. The cores were sectioned and analyzed at 1 cm intervals. The geochemical fractionation of metals in the uppermost estuary (Core X1) will be described first.

The major partitioning of Co, Cr, Cu, Mn, Ni, Fe, Pb, and Zn is within the reducible phase 3 (Figure 6.25). Organic phase partitioning is detected in small proportions for Cr, Cu, Ni, Pb, Zn and Fe, but not for Co. In most cases, the organic contribution of metals is smaller than the residual contribution. The primary partitioning of Al is into the residual phase. However, there is an appreciable amount of Al in the reducible phase (a very small concentration can be detected in the organic fraction). The residual Fe is relatively low, in comparison with other near shore sediments (see table 6.2).

Phase associations for most metals are similar at the mouth of the estuary (Core X5) (Figure 6.26). There are, however, some differences. All the metal concentrations in the three phases are smaller than at the head of the estuary (X1). Co, Cu, Fe, Mn, Ni, Pb, and Zn again show a major partitioning into the reducible phase. Cr displays remarkably variable partitioning, with respect to depth within the core. Co can be detected in the organic phase, whereas organic Cr is not detected.

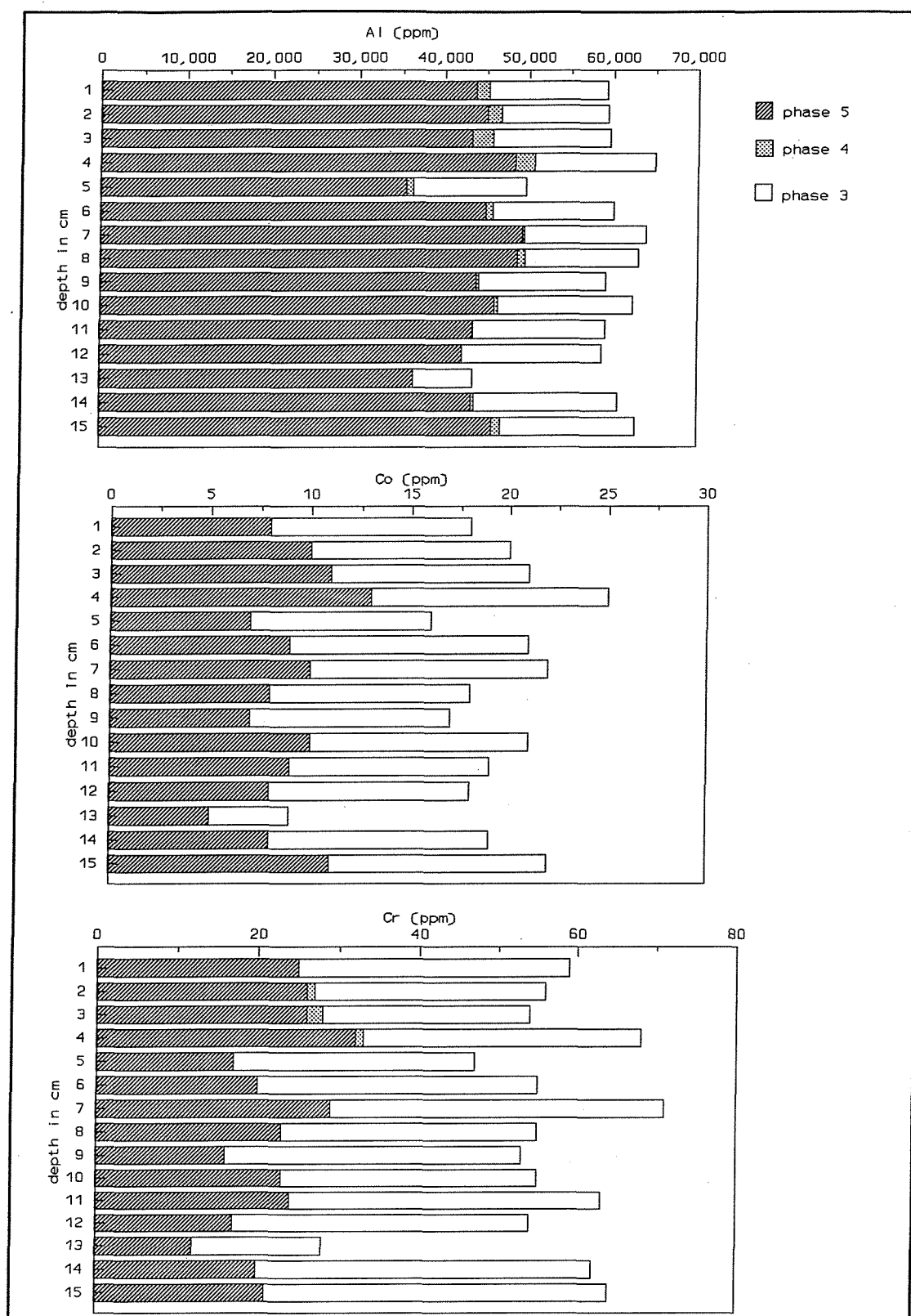


Figure 6.25 : The phase association of metal concentrations in Core X1 (phase 3=reducible, phase 4= organic, phase 5=residual).

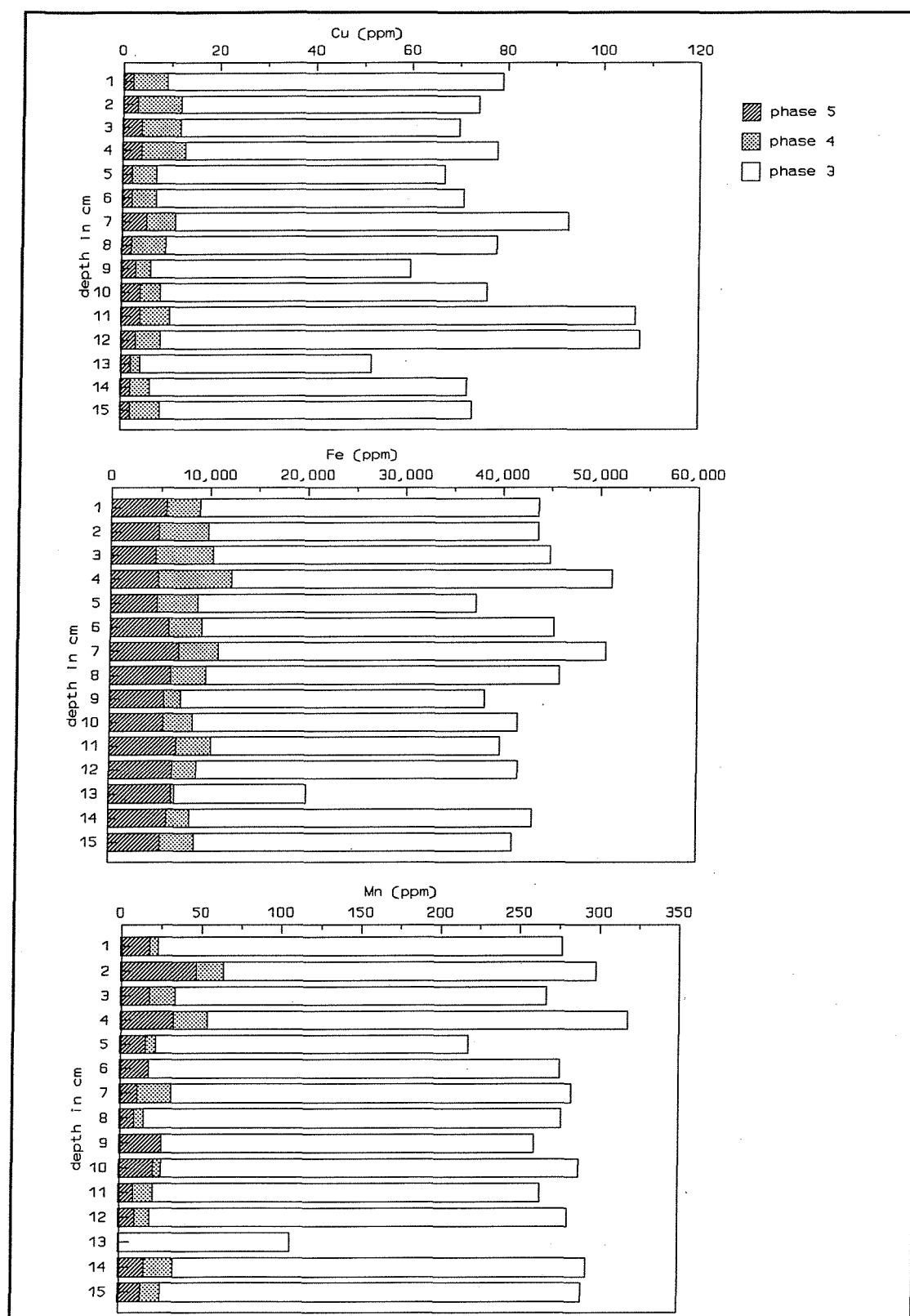


Figure 6.25 (continued): The phase association of metal concentrations in Core XI (phase 3=reducible, phase 4=organic, phase 5=residual).

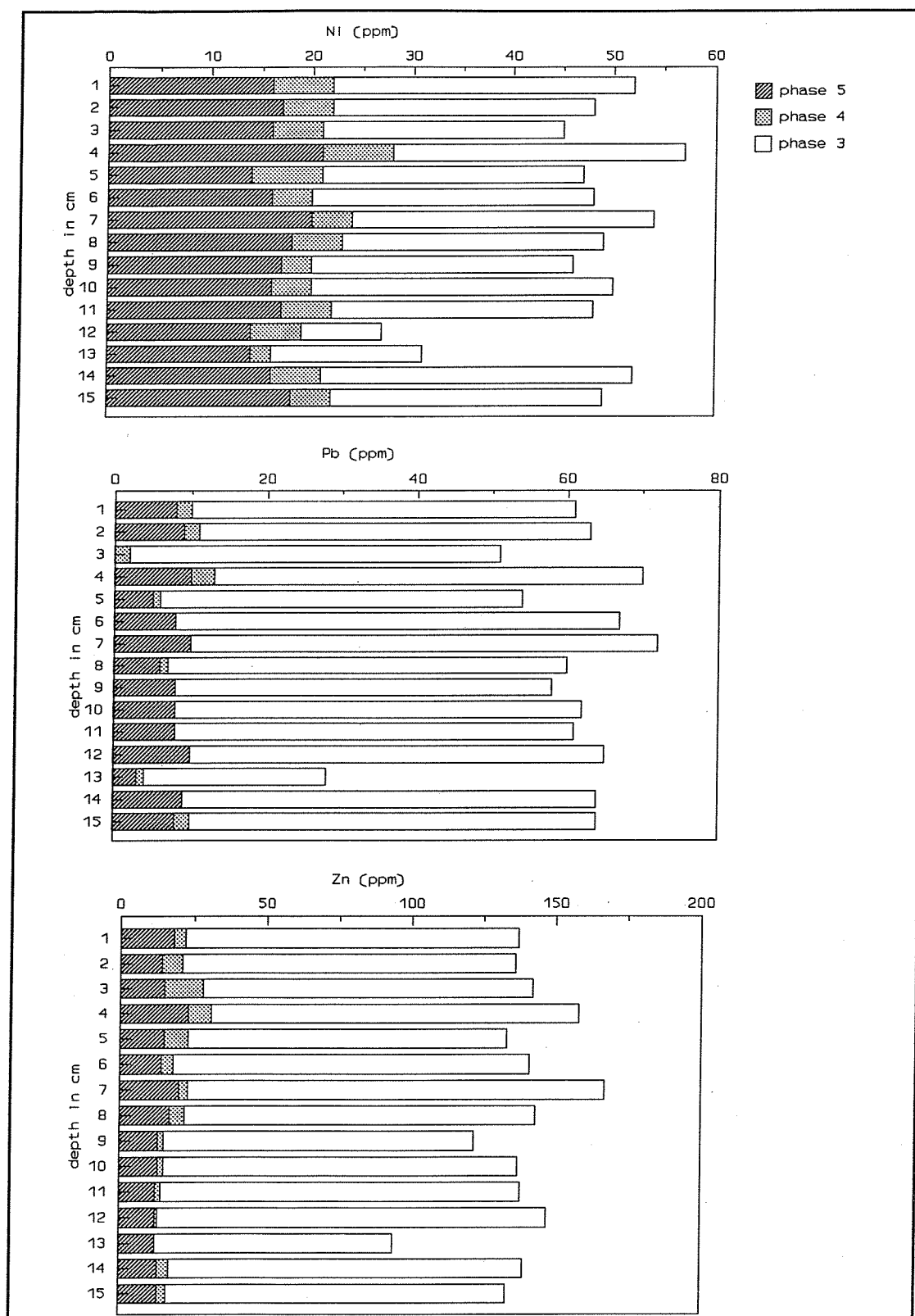


Figure 6.25 (continued) : *The phase association of metal concentrations in Core XI (phase 3=reducible, phase 4=organic, phase 5=residual).*

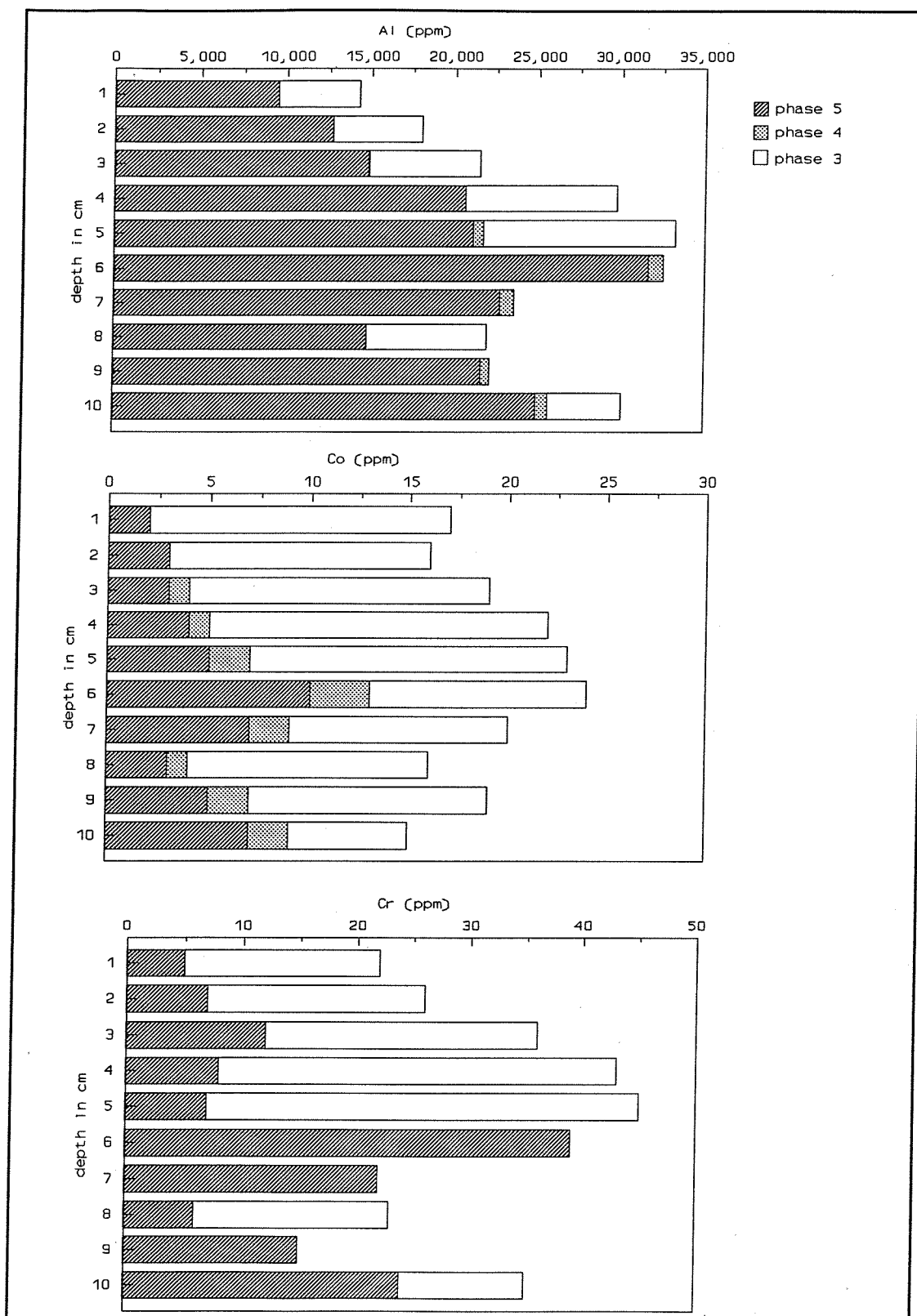


Figure 6.26 : The phase association of metal concentrations in Core X5 (phase 3=reducible, phase 4=organic, phase 5=residual).

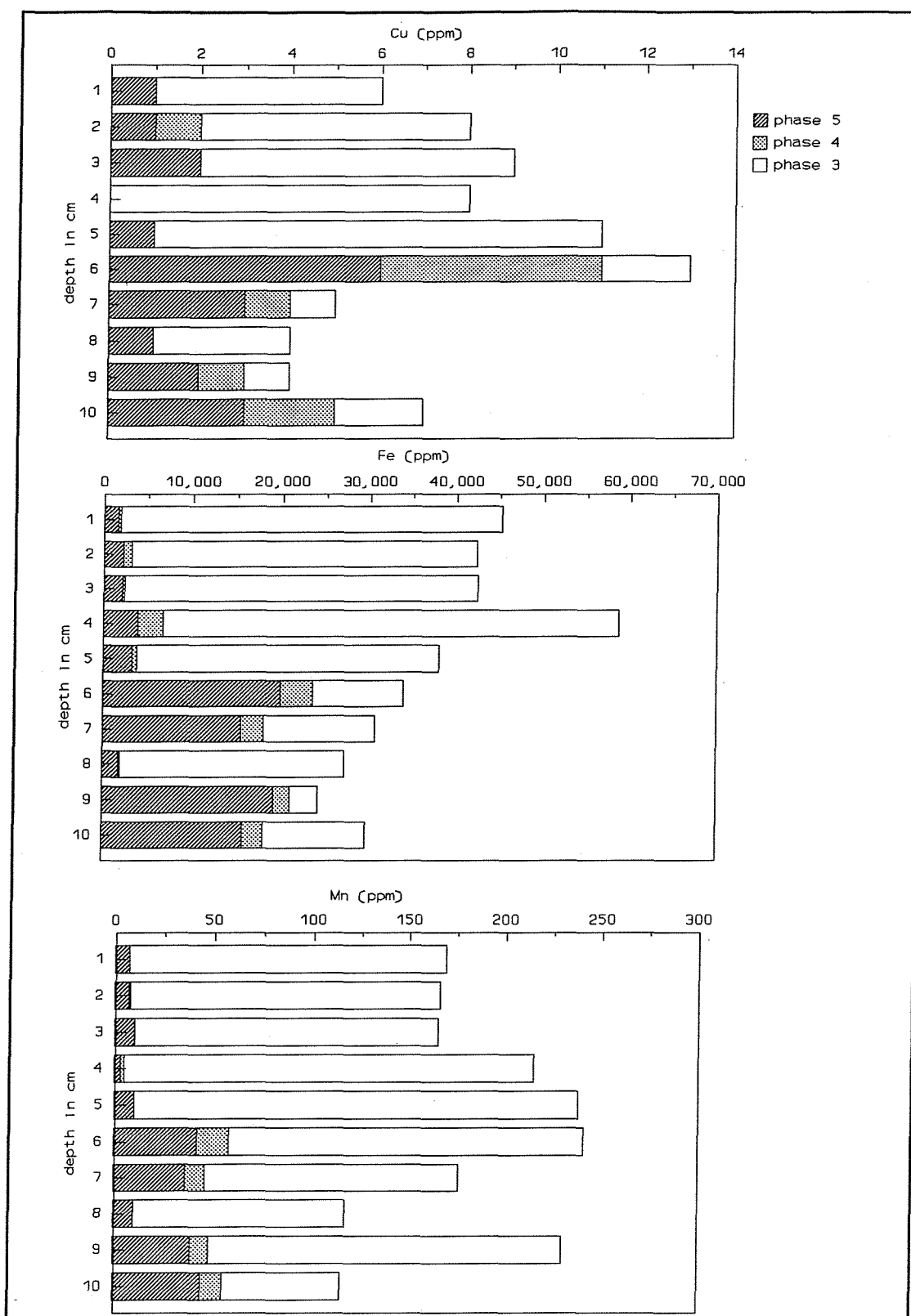


Figure 6.26 (continued) : The phase association of metal concentrations in Core X5 (phase 3=reducible, phase 4=organic, phase 5=residual).

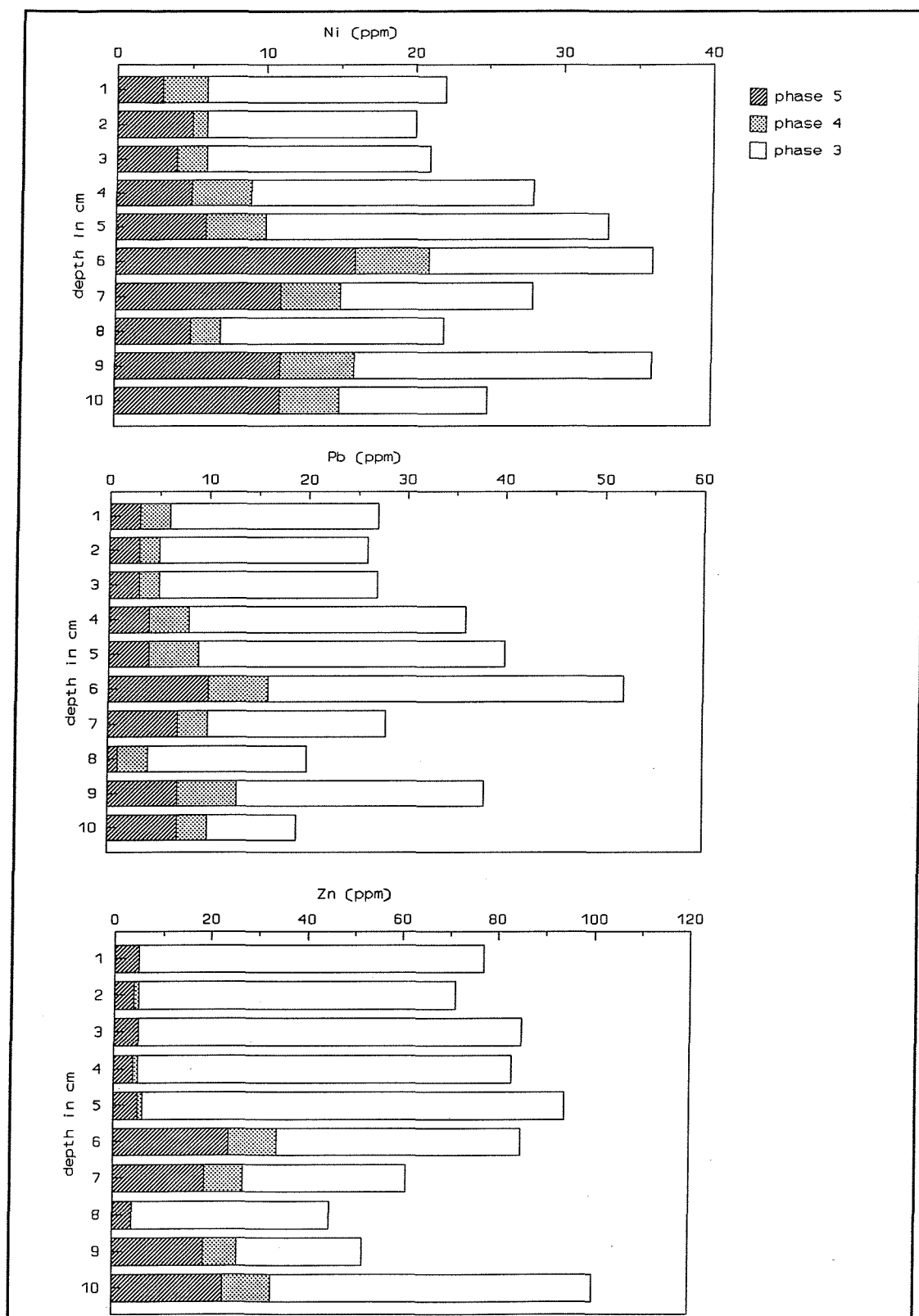


Figure 6.26 (continued) : The phase association of metal concentrations in Core X5 (phase 3=reducible, phase 4=organic, phase 5=residual).

6.2.1. Vertical Distribution of Metals

All the metals show a wide range of concentrations within the reducible phase along core X1 (Figure 6.27). In general, a decrease in reducible metal concentrations is observed at 12 cm. There is no significant change in sediment texture at this depth; the main colour change is at 4 cm. A decrease in the concentration of most of the metals can be observed below 4 cm; however, this is not definite in every case. Residual Fe, Mn, Ni, Cu, Pb and Zn do not show large variations and display a relatively constant pattern, whereas residual Co and Cr have a wide range of concentrations and show a similar pattern to the reducible phase.

Core X5 differs slightly from X1 (Figure 6.28). Metal concentrations down the core are remarkably variable. For most metals, the residual phase becomes more important than the reducible, below 5 cm. Residual Co increases at the expense of reducible Co. Ni shows the same pattern as Co. Reducible Cr almost disappears and the residual phase dominates. Reducible Cu increases from 1 to 4 cm, with an abrupt decrease being observed at 5 cm. Fe displays the same pattern as Cu. Residual Mn, Pb and Zn show similar patterns to the other metals, but the variations are less pronounced. Residual Al increases from 1 to 5 cm, decreasing below this depth. Such a dramatic change in the residual metal concentrations, over a short distance, can be explained by strong physical mixing processes.

6.2.2. Organic Carbon Content association With Trace Metals

Organic matter plays an important role in the chemical behaviour of trace metals and their deposition and transportation in estuaries, since it is able to bind or chelate trace metals and take part in diagenetic processes after deposition (Salomons & Förstner, 1984). Metals associated with organic matter can comprise a large fraction of the total concentration (Bewers & Yeats, 1981).

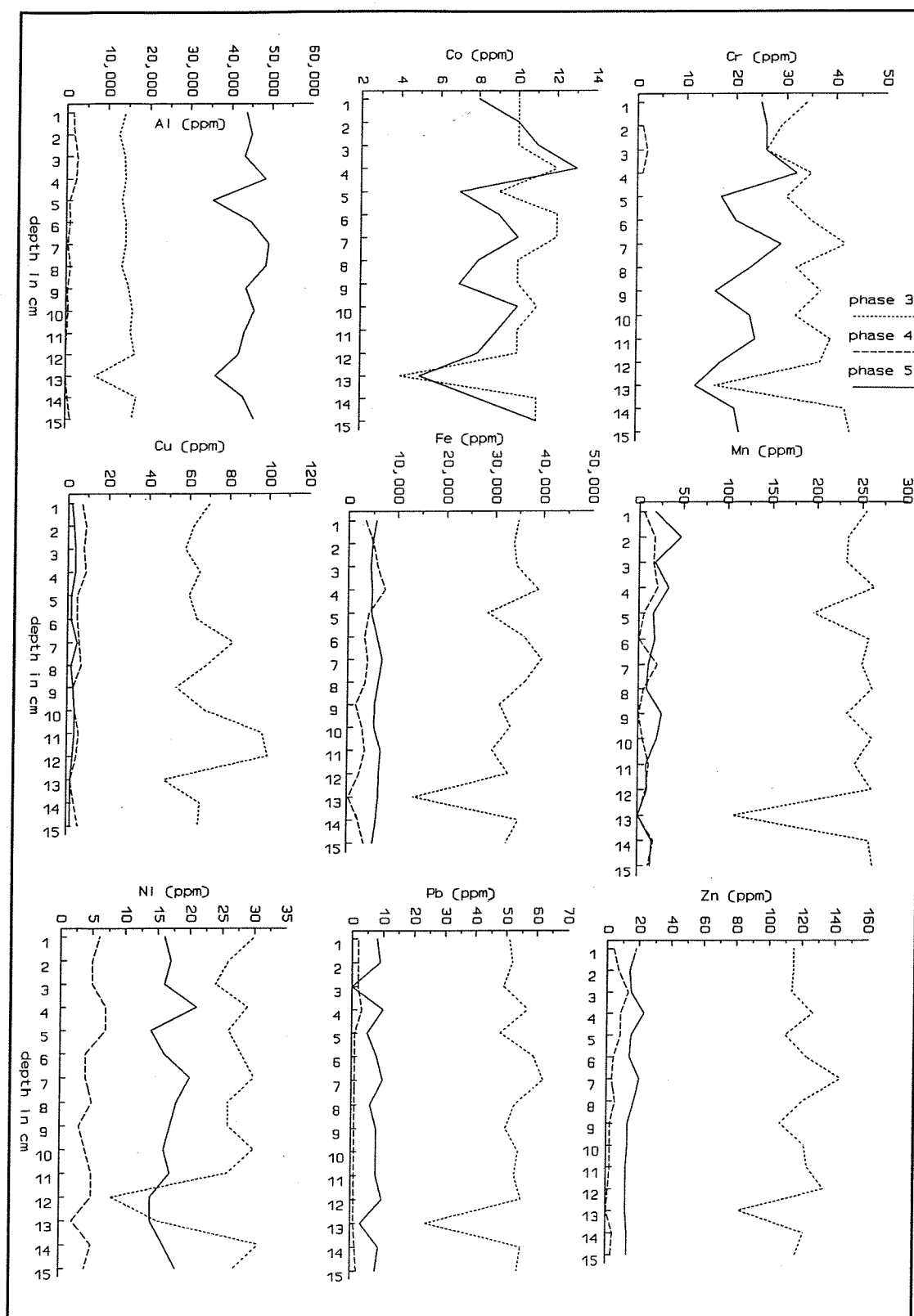


Figure 6.27 : Vertical variations of metal concentrations in the three extraction phases in core X1.

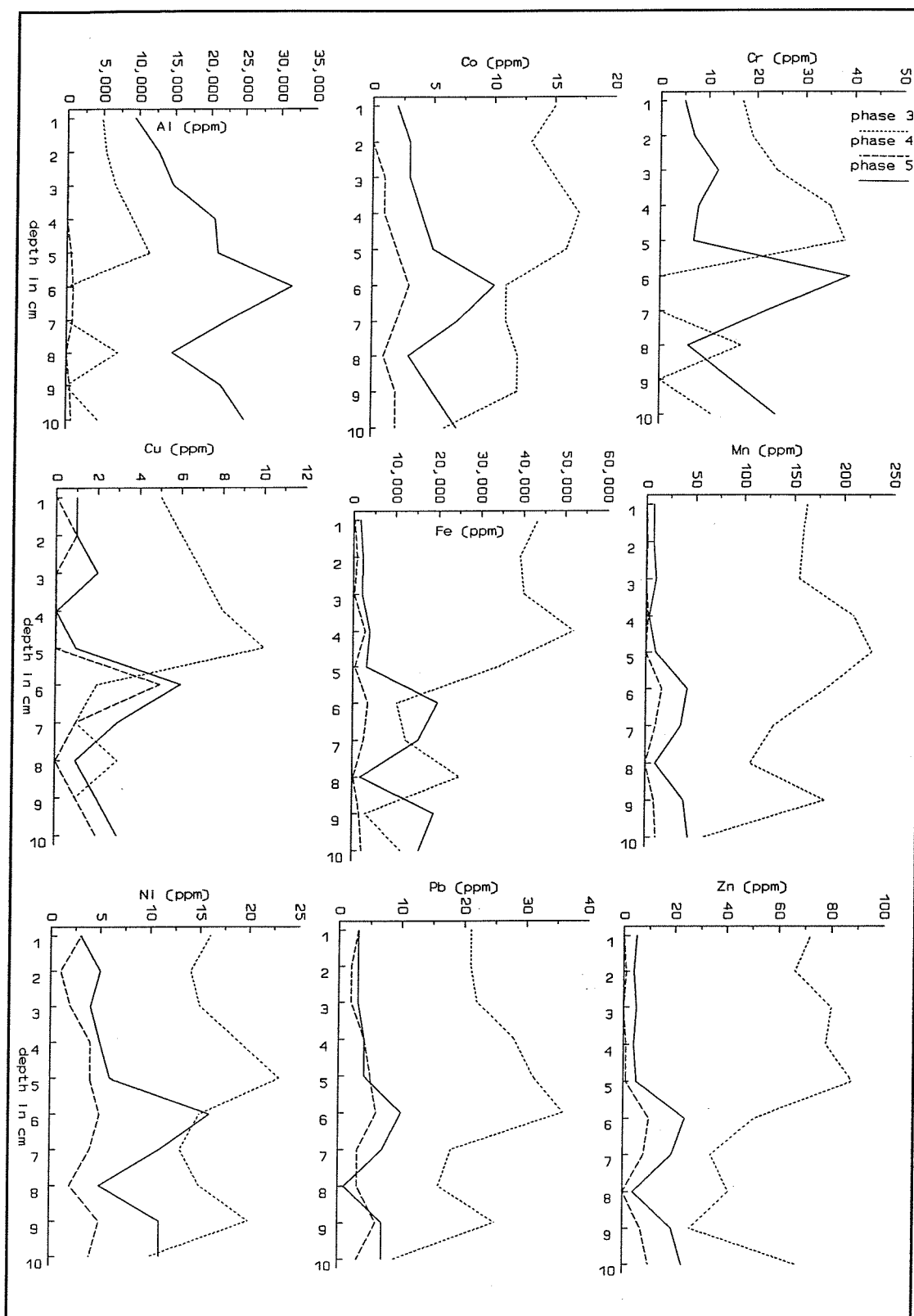


Figure 6.28 : Vertical variations of metal concentrations in the three extraction phases in core X5.

It has been observed also that organic matter could be an important sink for dissolved metals during estuarine mixing (Boldrin *et al.*, 1989; El Ghobary & Latouche, 1986; Martin *et al.*, 1987; Sholkovitz, 1976).

The organic carbon content of the surface samples is presented in Table 6.3. and the spatial variation of these values is shown on Figure 6.29. The organic carbon content varies between 0 to 5 % in the harbours, 0 to 8 % in the rivers and 0.5 to 4 % in the West Solent, Southampton Water and the East Solent. High values are found in the Rivers Test (8 %) and Itchen (6 %) and the bay-head locations of the Portsmouth, Langstone and Chichester Harbours. Sediments from the upper reaches of Southampton Water have higher values (> 2 %) which decrease downstream (0.66 %). In the East Solent, they are constant at approximately 1 % with the exception of sample 23 (4.16 %). Portsmouth Harbour samples also show similar values (~ 1 %). The tidal inlets of Langstone Harbour have values of lower than 1 %. The organic carbon content of the Beaulieu river sediments decreases gradually downstream.

Most of the total metal concentrations do not show a strong correlation with the organic carbon content. Pb, $r=0.53$; Cu, $r=0.57$; and Zn $r=0.56$ (with $n=80$ and significance levels $=0.00$) exhibit the strongest associations with organic carbon. This comparison is in agreement with the sequential extraction results, although the organic phase is not the primary phase for these metals. The results are in agreement with Armannsson *et.al* (1985), who stated that the metal content of sediments throughout the Southampton Water estuary were not correlated with the organic carbon content.

Table 6.3 : The organic carbon content of surficial samples in the Solent Region (continued on following pages).

Sample No	Organic C (%)	Carbonate C (%)
1	1.4	1.0
2	1.5	0.4
3	1.7	0.6
4	2.8	1.0
5	2.3	1.0
6	2.8	0.1
7	2.3	1.4
8	1.7	0.6
9	1.9	1.4
10	0.9	1.1
11	0.7	1.0
12	0	2.2
13	1.0	1.0
14	0.5	1.5
15	1.3	0.9
16	1.0	1.5
17	1.4	0.9
18	1.2	1.0
19	0.4	0.8
20	0.8	0.9
21	1.0	0.4
22	1.1	0.8
23	4.2	N/A
24	1.3	1.0
25	1.2	1.3
26	0.8	0.9
27	0.7	0.2
28	1.1	1.0
30	0.8	0.9
31	0.3	0.7

Inorganic (carbonate) values are also included for comparative purposes.

Table 6.3 (continued) : The organic carbon content of surficial samples in the Solent Region.

Sample No	Organic C (%)	Carbonate C (%)
RIVERS		
R4	4.1	4.6
R6	1.1	0.4
R7	1.4	2.3
R8	2.0	0.7
R9	2.8	2.1
R10	1.6	0.5
R11	1.3	0.7
R12	2.8	0.9
R13	8.3	3.9
R14	8.1	1.5
R17	1.3	0.2
R19	0	9.3
R20	2.7	0.9
R22	6.9	0.3
R23	3.1	2.8
R24	4.1	1.2
R27	1.2	0.1
R28	2.7	0.4
R29	2.5	2.3
R30	1.3	2.0
R31	1.0	1.6
R32	0.6	1.0
R33	2.0	1.7
R34	3.4	2.8
R35	1.8	0.9

Table 6.3 (continued) : The organic carbon content of surficial samples in the Solent Region.

Sample No	Organic C (%)	Carbonate C (%)
HARBOURS		
H1	4.4	0.7
H2	2.6	0.4
H3	1.7	0.9
H4	3.2	0.6
H5	1.8	0.7
H6	1.9	0.7
H7	1.8	0.9
H8	2.6	2.0
H9	0.9	1.1
H10	1.7	0.7
H11	0.6	0.9
H12	0	0.3
H13	0.8	1.4
H14	1.5	1.3
H15	2.4	0.4
H16	2.1	0.4
H17	1.3	0.7
H18	1.2	0.5
H19	0.8	0.9
H20	1.1	0.3
H21	1.0	0.6
H23	0.9	0.5

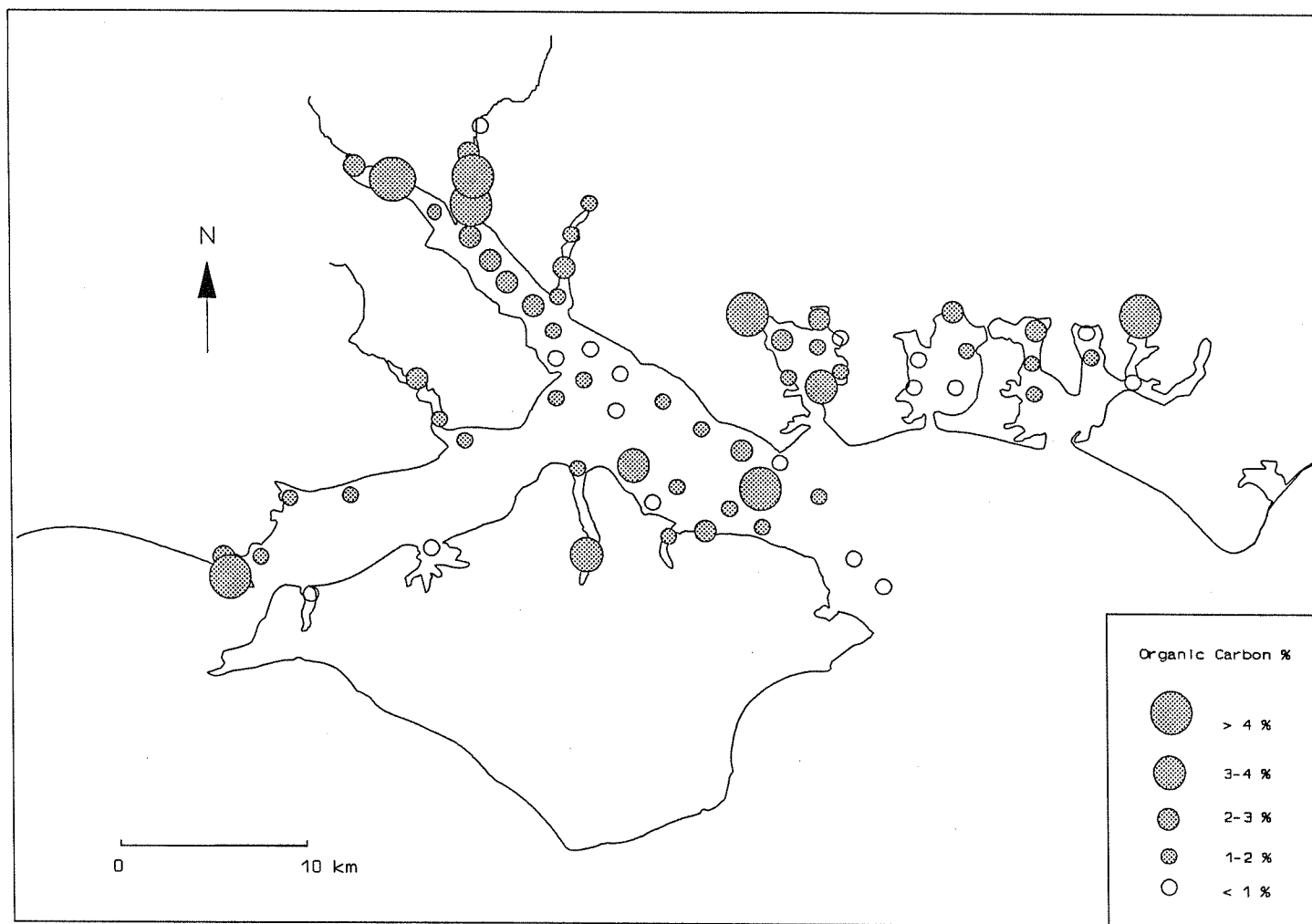


Figure 6.29 : *The distribution of organic carbon in surficial samples in the Solent Region.*

6.2.3. Fe and Metals Relationships

Fe is an important element in aquatic geochemical processes, since its various oxide and hydroxide forms act as scavengers for trace metals (Chester, 1990). In natural geochemical sediment populations, Fe correlations with other metals show positive trends since the concentration of Fe changes with changing mineralogy (crustal element), sediment particle size (which usually changes mineralogy), or the other naturally-occurring phenomena (transformation into another form under reducing conditions) (Rule, 1986). Sediment samples which belong to the same geochemical population should fall along the same regression line. Selective extraction revealed that the greatest proportion of Fe lies in the reducible phase (Figures 6.25 and 6.26). Such a response indicates that the majority of sediment Fe may exist as free Fe oxides (Brannon et al, 1977). Fe oxides and sulfides play an important role in the scavenging of trace metals from the estuarine system. Total trace metal relationships with total Fe show a positive correlation (Figure 6.30). The metals in all the samples, particularly Al ($r=0.71$), Co ($r=0.69$), Cr ($r=0.64$), Ni ($r=0.62$), and Mn ($r=0.57$), exhibit positive correlation with total Fe. Cu ($r=0.22$), Pb ($r=0.19$), and Zn ($r=0.42$) are more scatter. In Figure 6.31, correlations between these metal with Fe seems to be reinforced (Cu $r=0.70$, Pb $r=0.69$ and Zn $r=0.74$), after rejection of the same anomalous samples described in section 6.1.6. The correlation between trace metals and Fe might be an indication of co-precipitation with Fe oxides or sulfides. This argument is supported by sequential extraction results *i.e.* most of the trace metals are found in reducible phase. Outliers (rejected) samples might indicate that there are more point sources for these metals.

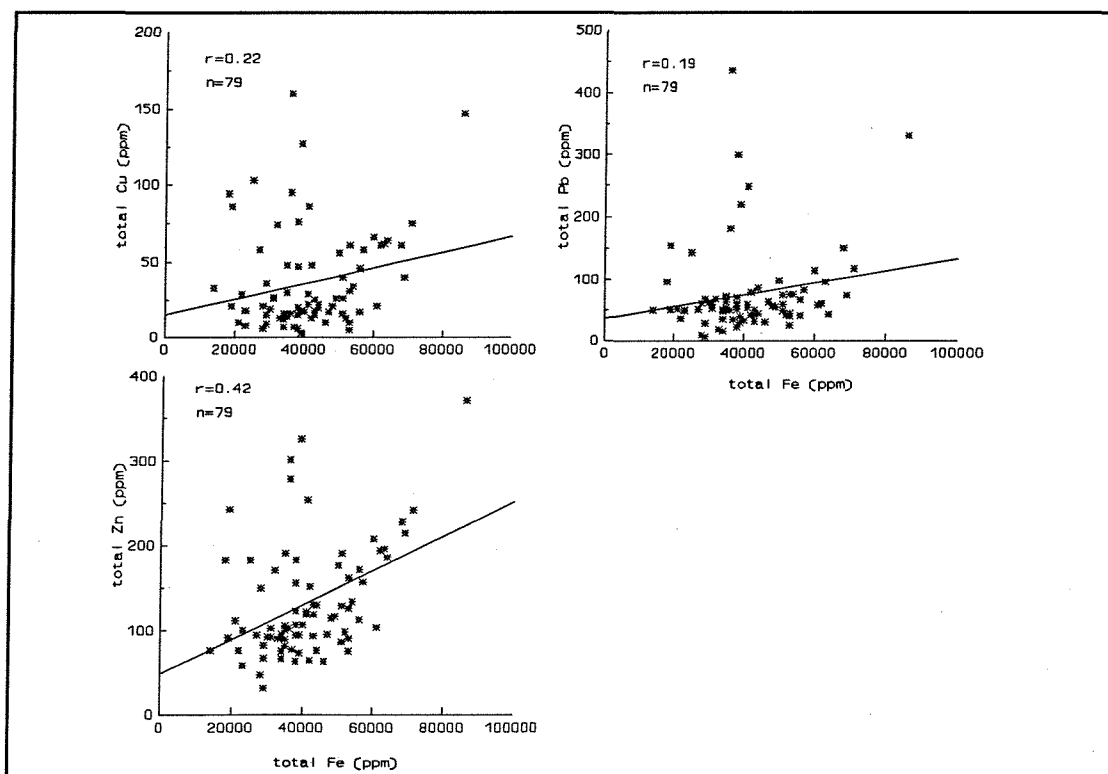
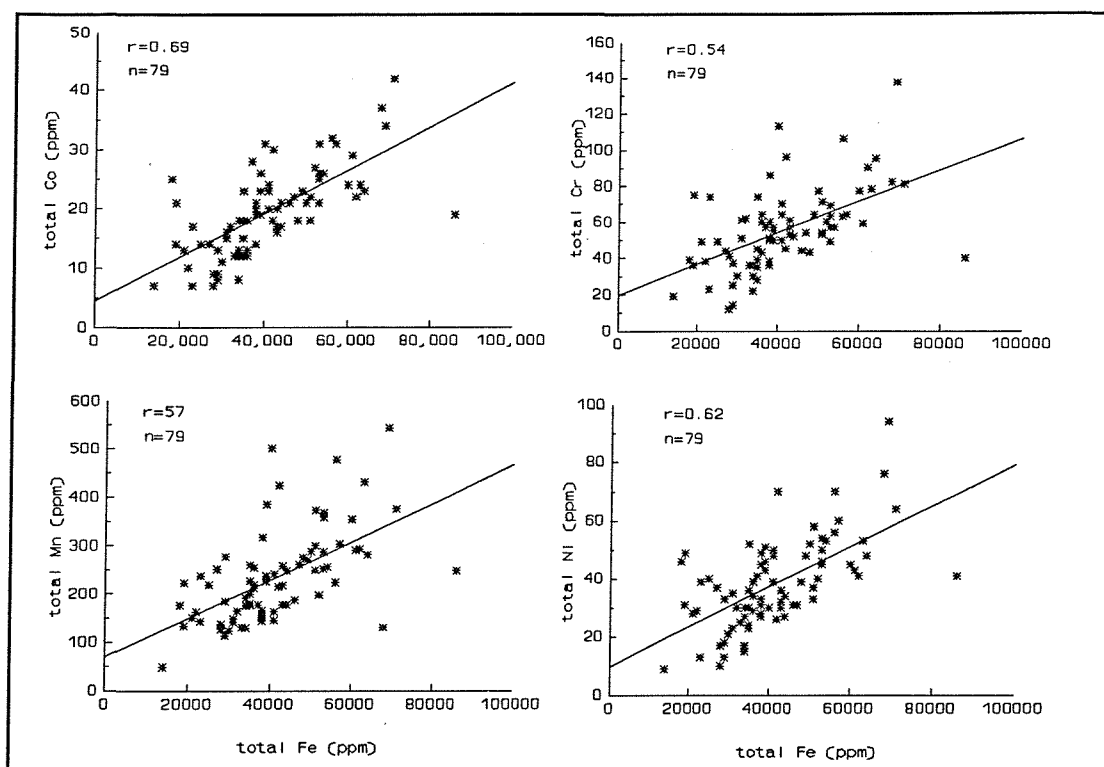


Figure 6.30 : *Correlations between trace metals and Fe, in the surficial sediments of the Solent.*

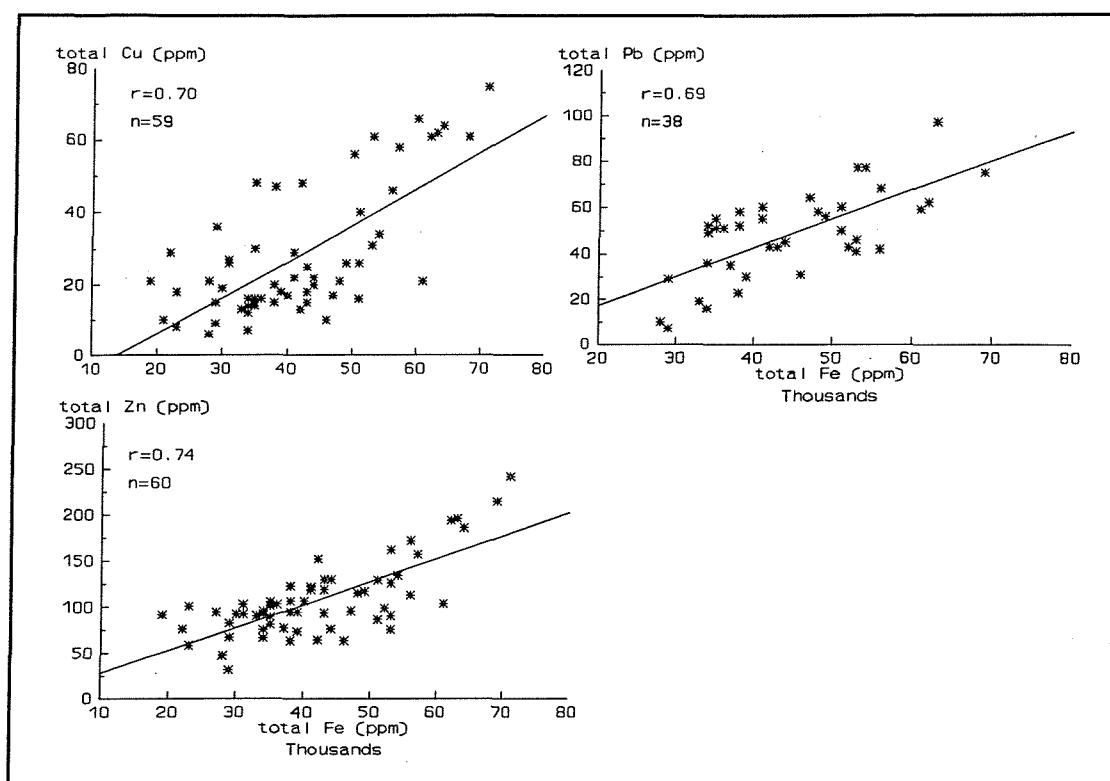


Figure 6.31 : *Correlations between Cu, Pb, Zn and Fe after rejection of outlier samples (sig.level=0.00).*

6.2.4. Trace Metal Distributions: Concluding Remarks

Total metal concentrations in the Solent region are, in general, comparable with the average concentrations of near shore muds, with the exceptions of Co, Cu, Pb and Zn. The spatial distribution of total metals suggest that the main source areas are riverine *i.e.* the Test (Co, Cr, Mn), the Itchen (Cu, Pb, Zn), the Hamble (Co, Cr, Ni, Pb, Zn), and the Keyhaven Rivers (Cu, Pb, Zn), the Portsmouth (Co, Cr, Cu, Mn, Ni, Pb, Zn), the Langstone (Cu, Zn), and Chichester Harbours (Cu, Ni, Pb, Zn), and Southampton Water (Cr, Mn, Ni). All the trace metals, with the exceptions of Pb and Zn, are elevated in the main channel of Southampton Water and decrease generally in the East Solent. Pb and Zn have high concentrations along the coastline of Lee-on-Solent. High concentrations of Zn are found also in the vicinity of Cowes and Wootton Creek, and at the open (seaward)

end of the Solent. Portsmouth Harbour appears to have higher metal concentrations, compared to those of Langstone and Chichester Harbours. The major elements, Al, Mn and Fe, have similar trends to the trace metals, increasing in Southampton Water and decreasing in the East Solent. The distribution of Al is a function of the abundance of the clay minerals. Southampton Water and Portsmouth Harbour sediments consist of mainly fine-grained (clay sized) material, which is in agreement with this assertion.

The grain size dependency of metals is variable in the Solent Region. The percentage of clay correlates with most of the metals, although the relationship is not strong enough to be the dominant mechanism. Therefore, there must be other factors controlling the enrichment of metals (association with Fe-Mn oxides or sulfides and/or anthropogenic inputs). Cu, Pb and Zn behave independently of grain size, particularly in samples from the rivers and harbours. These metals are more concentrated than in the average equivalent sediments (near shore muds) and do not show a significant correlation with Al. Hence, they are indicator of anthropogenic accumulation. The correlation between these metals and organic carbon might possibly be related to association with sulphides under reducing conditions in the estuarine environment.

The spatial distribution pattern of the absolute metal concentrations in the clay size fraction indicates that the River Itchen is the main source of Cr, Cu, Pb, and Zn to Southampton Water. Co and Ni appear, on average, to be higher in the East Solent and within the tidal flats of the West Solent. Phillips (1980) has reported that the Itchen River receives pollution from two sewage treatment works, one at the mouth of the estuary and the other upstream at Portswood SDW (see Figure 3.15). Armannsson *et.al.* (1985) concluded that elevated inputs of Cu have occurred in the region of the Esso oil refinery, due to the discharge of effluents.

In order to monitor sediment transport pathways associated with trace metal concentrations, trends (total metal, absolute metal in three size fractions and normalized metal concentrations) were determined in a seaward direction (Section 6.1.7). In most cases, the decrease of metal concentrations in this direction has

been attributed to the mixing of polluted riverine and unpolluted marine sediments in the estuaries. Trace metals are transported along the rivers towards the estuarine and marine environment, mainly by material in suspension. In response to tidal currents and other hydrodynamic features in the estuary, marine suspended matter is transported into the estuary and will mix with riverine suspended matter (Salomons & Eysink, 1981; Irion & Zöllmer, 1987, 1990; Paalman & Van Der Weijden, 1992; Salomons & Mook, 1987; Boldrin *et.al.*, 1989; Duinker & Nolting, 1976, 1978). The mixing ratio of fluvial and marine sediments may be calculated from carbon isotopes (Salomons & Eysink, 1981; Salomons & Mook, *op.cit.*) and %Ca (Nolting *et.al.* 1989). The isotopic composition of carbonates and %Ca indicate a high proportion of marine-derived material, where low metal concentrations are observed. Irregular variations in metal concentrations have been explained by changes in the mixing ratio of marine and fluvial-derived sediments along the estuary (Salomons & Mook, *op.cit.*). In the Solent Estuarine System, the significant decrease in total metal concentrations along Southampton Water suggests a similar physical mixing processes between polluted riverine sediments with less polluted marine sediments (from, perhaps, the West and East Solent), as in the other studies above. However this trend is not consistent with normalized data, with the exception of Cu which shows a definite mixing pattern. Normalization of the total metal concentrations with Al has revealed a similar pattern to those of the absolute metal concentrations in the clay size fraction: two 'hot spots' appear, one in the river, another one in the open end of the East Solent. Dilution effects can be detected on the basis of the decrease in total Co/Al, total Cu/Al, total Pb/Al and total Zn/Al ratios from the River Test to the mouth of Southampton Water. The proportion of clay-sized material in the East Solent is very low (samples 29, 30, 31; 17%, 15%, 49% respectively), as illustrated in Figure 5.3. This observation means that, despite a very small weight percentage of fine fraction, there is greater contamination of this fraction. Such contamination might be attributable to local inputs or may be due to metals transported associated with suspended matter into the East Solent, from other areas. Although Wootton Creek and the coastline of Lee-on-Solent seem to be

the local sources, there is no possible sources (*i.e.* presence of industrial effluent discharges) located for anthropogenic metal inputs.

In the present study, carbonate carbon values are used as the same manner as in other studies described above, assuming carbonate carbon as a tracer for marine sources. However, this may not be completely suitable for the study area, since the surrounding geological formations are mostly Chalk (Chapter 3). Figure 6.32 shows the same data (total metal/Al) along the same transect, with carbonate carbon added. Carbonate carbon display an irregular pattern as in metal ratios. Carbonate carbon decreases where the metals increase (especially for, Co/Al, Fe/Al, Ni/Al and Mn/Al). This relationship may imply a changing ratio between marine and riverine sources, which are variable throughout the system. However, Cu/Al, Pb/Al and Zn/Al ratios are not significantly inverse. Correlation between carbonate carbon and metal ratios can be observed within the riverine samples along the transect, suggesting that there might also be a riverine source for carbonate.

The sequential extraction of metals from the core samples shows that the metals are mainly associated with mobile (reducible) phase. In most estuarine environments, it is believed that metals (especially, Cu, Pb and Zn) are transported to the bottom with Fe-Mn oxyhydroxides. The oxides and hydroxides are later transformed to sulphides under anoxic conditions (Kersten & Förstner, 1987; Kitano *et al.*, 1980). It is likely that Fe-metal correlations for all the samples also suggest that the metals might be co-precipitated with sulfides. The geochemical investigation of core samples indicates that sediments are influenced by different process upstream, than at the mouth of the estuary. Core X5 (at the mouth of the estuary) displays lower and remarkably variable metal concentrations with depth compare to Core X1 (at the head of the estuary). This pattern might be an indication of the physical mixing of sediments entering by landward-directed bottom currents, with those transported from the main channel of Southampton Water.

Since estuaries are physically and chemically dynamic systems, both physical and chemical aspects must be considered when studying the sediment-associated geochemical transport of trace metals (Kersten & Förstner, 1986). The

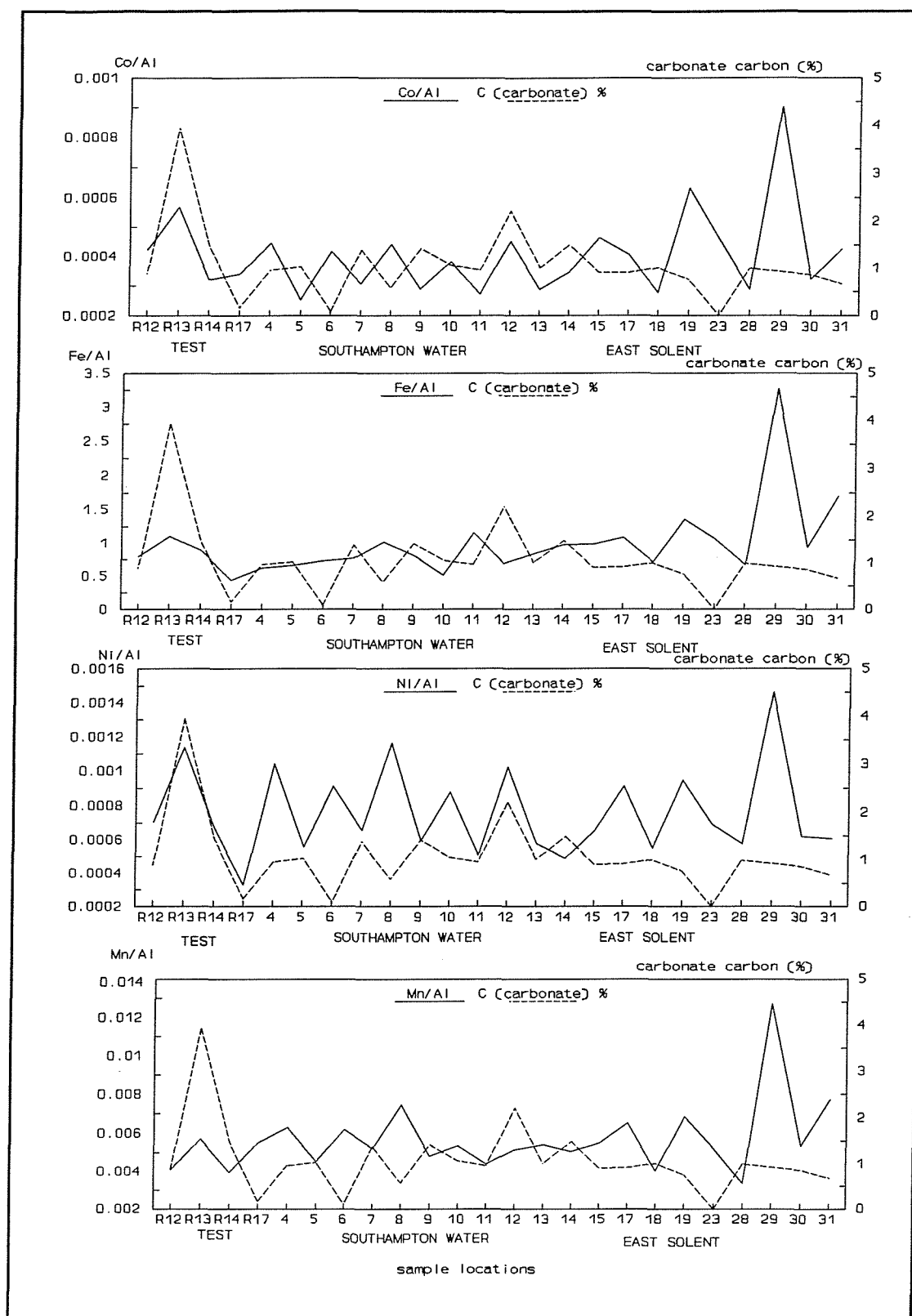


Figure 6.32 : Changes in Metal/Al ratios and carbonate carbon in the surficial sediments, from the River Test to seaward (continued on next page).

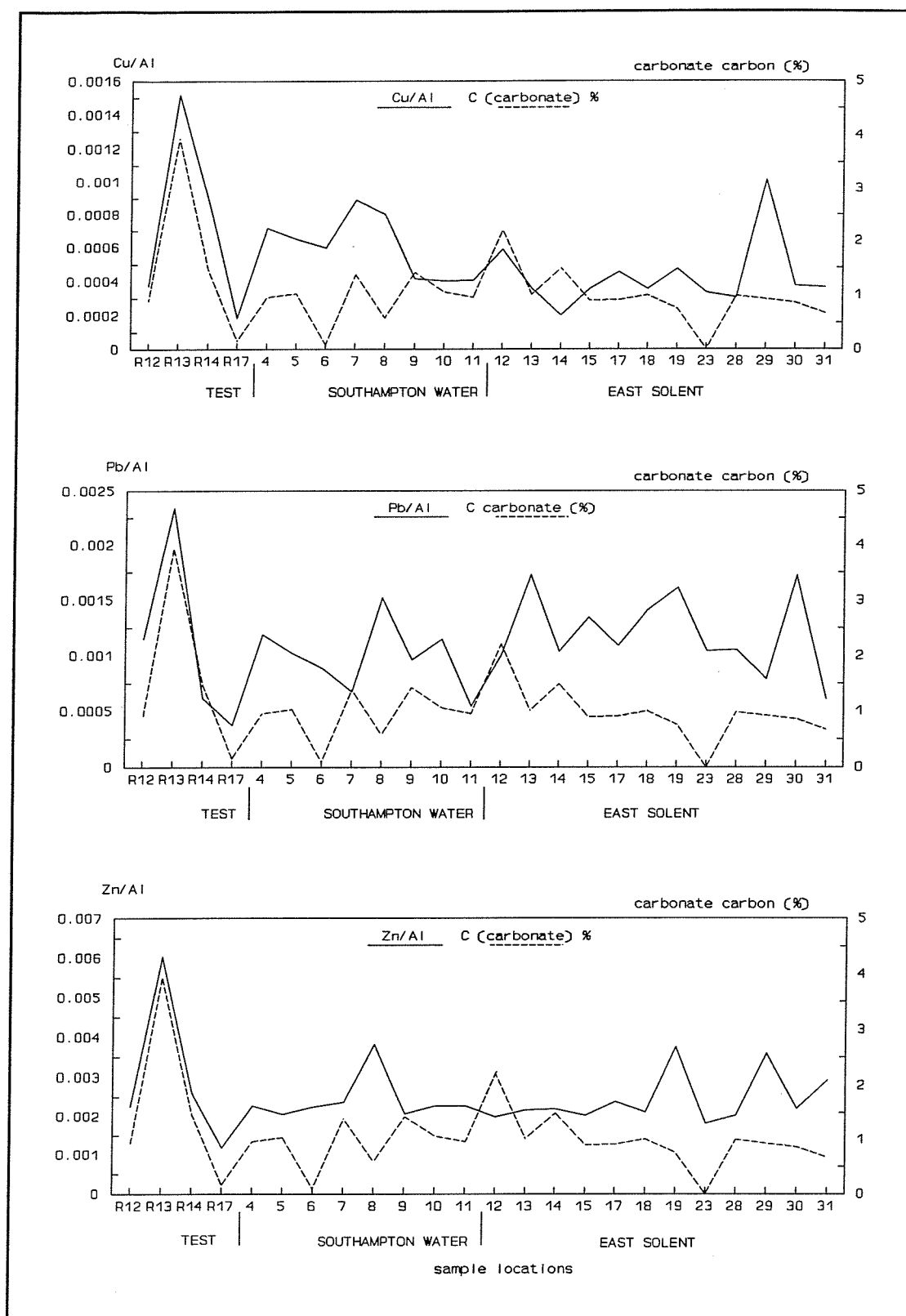


Figure 6.32 (continued) : Changes in Metal/Al ratios and carbonate carbon in the surficial sediments, from the River Test to seaward.

resultant patterns presented in this particular study might be a response to chemical processes, however, such as mobilization and diagenesis. Removal and/or addition processes may occur, changing the concentrations of certain elements after deposition, especially those which are susceptible to redox changes (Fe, Mn) (Salomons & Mook, 1987). Elevated total Fe/Al and total Mn/Al ratios might be attributed to remobilization during/after deposition. Nevertheless, this argument does not explain thoroughly the decrease in the total metal concentrations along the main channel of Southampton Water. Duinker & Nolting (1976) have stated that the increase in concentration for at least a number of metals should be detected from freshwater to seawater, if mobilization is occurring. No such observation can be seen in the data available from the River Test to Southampton. There is also no significant change in the relative proportion of mobile (reducible) phase of metals, at the mouth and upstream of the estuary. Hence, it is possible that the mobilization occurring in this study area is related partly to reducing conditions, but is not an efficient mechanism to explain the spatial distribution pattern of metals.

CHAPTER 7

DISCUSSION AND CONCLUSIONS

The results of the examination of the grain size distribution, clay mineralogy and trace metal content of the fine-grained surficial sediment of the Solent Estuarine System have been presented in Chapter 5 and 6. In this Chapter, associations between these various parameters, with respect to the sediment sources and transport pathways, will be considered further.

7.1. Recent Sedimentation

Recent sedimentological characteristics of the area should be considered as a response to the geological, hydrological and bathymetric conditions of the sedimentary environment, as well as a response to transportation and depositional processes (Dyer, 1986).

Grain size analysis of samples has been used to define the recent sedimentological characteristics of the area. Sand is abundant in the West Solent, in the East Solent, and the surrounding offshore areas of the Solent, where gravel is also abundant. The clay (fine-grained) component occurs mainly in the tidal flats, inlets and the harbours. The percentages of sand and silt in the surficial sediments of Southampton Water are variable, whilst the percentage of clay remains almost constant. The bulk of the sediment contained within the main channel is silty clay. This bimodality is altered to a trimodal distribution in the vicinity of Calshot Spit, suggesting that Calshot Spit might be an additional source for sand-sized material. The East Solent is floored by a mixture of sand and clay, in variable proportions. Trimodal distributions can be observed in Samples 19 (Gilkicker Point), 20 (northern coast of the Isle of Wight), 23 and 28 (the open (seaward) end of the East Solent). This pattern might indicate the influence of more than one source of sand.

Mobile gravel beaches occur between Lee-on-Solent and Langstone Harbour and, along the northern coastline of the Isle of Wight (SHELL, 1985).

Wave activity appears to influence the distribution of the coarse-grained materials. The West Solent is floored mainly by coarse material (Dyer, 1980,) displaying a different composition to that of the East Solent. Such a variation might be controlled by the tidal features of the region. The tidal currents in the West Solent are much stronger than those in the East Solent (2 ms^{-1} and 1.3 ms^{-1} surface currents on springs, respectively). The amount of water entering and leaving the West Solent is higher than that in the East Solent (Webber, 1980). Therefore, it is possible that the deposition of fine-grained sediments in the West Solent is prevented by the strong tidal currents.

The harbour inlets are composed of sediments of variable grain size. Portsmouth Harbour differs than the other two harbours, in containing mostly unimodal clay sized sediment; it does not appear to receive coarse-grained sediment input from its mouth. In contrast, Langstone and Chichester Harbours seem to be receiving coarser sediments from offshore. The wave regime might be the reason for the different size of material deposited in the harbours (Figure 3.6). Significant maximum wave heights of around 2 m have been observed in the offshore area, decreasing in a westerly direction from Selsey Bill to Gilkicker Point (SHELL, 1986; Gao & Collins, 1991). Hence, wave activity provides a mechanism for sediment exchange between the offshore waters and the inlets to Langstone and Chichester Harbours, but not with Portsmouth Harbour. Well-developed tidal deltas within Langstone and Chichester Harbours are indicative of sediment exchange through the inlet straits. The inlet strait of Portsmouth Harbour is relatively narrow and long, compared to those of Langstone and Chichester Harbours. This characteristic might be another reason preventing the exchange of coarse sediment into Portsmouth Harbour.

Deposition of fine-grained sediments within any tidal environment is dependent upon tidal velocities. Fine-grained sediment deposits prevail, for example, where the currents are reduced (Postma, 1967). Integrating sediment

characteristics with the hydrography of the system, three regions may be defined within the present area of investigation; these are described below.

(i) The West Solent. Gravel and sand dominate the channel deposits. Tidal currents are high enough to prevent fine-grained sediment deposition. Fine-grained sediments entering from Hurst Spit may be deposited in tidal flats along the coast, where tidal currents are reduced.

(ii) The East Solent. Tidal currents are lower in comparison to the West Solent. Sand and clay sized sediments, in variable proportions, floor the area. The influence of wave activity is represented by the coastal form (*i.e.* boulder (large gravel) beaches) between Gilkicker Point and Portsmouth Harbour.

(iii) Southampton Water. Riverine sediment inputs to Southampton Water are variable in composition. However, the bulk of the sediment consists of silty clays within the channel. This distribution is partly a result of reduced tidal velocities and the absence of wave activity.

7.2. Sources and Transportation of Sediment

In Chapter 2, a number of case studies of the clay mineralogy of fine-grained sediments used in the determination of transport pathways were presented. The dispersal pattern of clay minerals is related strongly to the source material (provenance) and reflects the transport pathways of fine-grained sediments (Weaver, 1989, Chamley, 1989). The present investigation identifies two prevailing sources throughout the system. The distribution patterns and the ratios of the clay minerals are consistent with the mixing of material from these sources. A smectite-rich riverine source mixes with a smectite-poor marine sediment, throughout Southampton Water and the East Solent. The marine-derived sediments may be entering from both of the seaward ends of the system.

The distribution pattern of the trace metal concentrations suggests also two sources for the trace metals. The sources are the rivers discharging into Southampton Water and the open (seaward) end of the Solent System. The pattern suggests

also the physical mixing of the source materials, although there are irregularities in the pattern itself. Irregular variations in metal concentrations have been explained elsewhere by changes in the mixing ratio of the marine and fluvially-derived sediments along the Sheldt Estuary (Salomons & Mook, 1987). The mixing ratio of fluvial and marine sediments here, as calculated from the isotopic composition of carbonates, indicated high proportion of marine-derived material where low metal concentrations are observed. The variable pattern in the metals could be caused by either variations in the local mixing ratio or localised (additional) inputs. It is possible that the mixing ratio of the two fine-grained sediment sources changes throughout the Solent System, as a result of the tidal predominant characteristics. Webber (1980) has suggested that ebb currents are faster than the corresponding flood currents and, therefore, provide a mechanism for the flushing of fine-grained size sediments in a seaward direction. If this was the prevailing case, no fine-grained sediment would be deposited in Southampton Water and in the East Solent. However, if this mechanism is opposed successively by the flood currents transporting sediment in a landward direction, then the fast ebb current and slow flood currents would be expected to change the mixing ratio of the two sources. Variable patterns of carbonate carbon reflect of this changing mixing ratio. Likewise, recent sedimentation patterns are indicative of the changing energy conditions in the system.

The transportation patterns suggested by this study are in general agreement with previous assertions. Dyer (1980) defined transport pathways in the Solent Estuarine System (Figure 3.14) to be in an eastward direction in the West Solent, and from southeast to west in the East Solent. This investigator emphasized that the muds in the inlets and harbours are mainly marine-derived. Houghton (1986) found reworked Cretaceous and recent coccoliths in sediments from Southampton Water and the tributary estuaries, concluding that they are transported into Southampton Water in suspension by marine currents and on flood tides. The number of reworked coccoliths in the West Solent are lower than in the East Solent and Southampton Water. Sediments in the West Solent are thought to originate from the

lower Barton Beds, which are exposed in different cliff sections in Christchurch Bay. The distribution of reworked and recent coccoliths in the surface sediments suggests strongly a transport pathway from the East Solent into Southampton Water. Srisaengthong (1982) suggested that marine sediments, originating principally in Christchurch Bay due to erosion of cliff and beach material, are diluted by Southampton Water sediments in the confluence of the West and the East Solent.

In summary, fine-grained sediment originates from both fluvial and marine sources within the Solent Estuarine System. Southampton Water, the West and East Solent are the regions where the marine and riverine sediments meet and mix. The effects of the mixing of different sources can be detected on the basis of the grain size characteristics, the clay mineralogy and the trace metal variations at the confluence of the Rivers Itchen, Test and Southampton Water. Figure 7.1 illustrates a conceptual transport model on the basis of grain size distributions and clay mineralogy of the fine-grained sediments within the Solent Estuarine System.

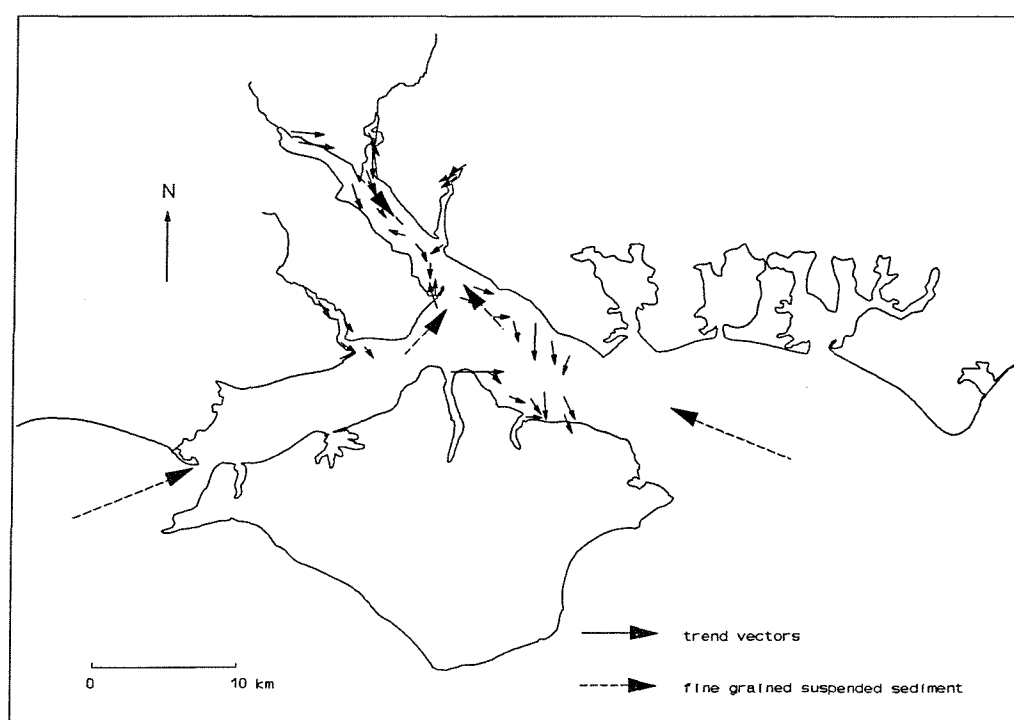


Figure 7.1 : *A conceptual model for fine-grained sediment transportation in the Solent.*

7.3. Geochemical Factors and Anthropogenic Inputs

Geochemical phase associations of trace metals indicate that the major partitioning of metals is in the reducible phase (*i.e.* labile). Positive correlations with Fe and metals suggests that the metals might be co-precipitated with Fe oxides or sulphides. In most studies reviewed in Chapter 2, it is believed that the estuarine environment supports precipitation of metals with sulfide under reducing conditions. The metals Cu, Pb and Zn show significant differences when compared with the others investigated. They tend to correlate less well with grain size and are particularly strongly associated with the reducible fraction in the selective leaching scheme. The coherence of this group of metals may partly reflected their strong tendency to form insoluble sulphides, but anthropogenic enrichment is a further factor which must be taken into account.

The surface enrichment of Cu, Pb and Zn due to anthropogenic inputs is recognized and illustrated in Figure 6.20. The location of these anomalous concentrations can be compared with Figure 3.15. The Rivers Test, Itchen and Hamble receive sewage discharges. A number of outfalls, a refinery and a chemical industrial complex are shown along the main channel of Southampton Water. The possible sources of excess amount of metals within Portsmouth Harbour might be sewage effluent from Fareham Creek and also Naval Dockyard activities. The samples from Keyhaven (Hurst Spit) contain very high metal concentrations, particularly in the coarse size fraction. This pattern might be related to the availability of heavy minerals.

7.4. Future Studies

The research undertaken here aimed to elucidate the contribution of geochemistry to the understanding of sediment transport pathways in an estuarine system. Sediments from the estuarine environment are subjected to a variety of

physical, chemical and biological processes. Therefore, data collected from such systems should be integrated in an interdisciplinary manner and considered collectively. From this point of view, a number of suggestions for further studies are outlined below.

(i) Analysis of seasonally collected suspended matter. The amount, composition and trace metal content of suspended sediments should be determined. This approach may assist in obtaining complete information on the prevailing mixing process. Further, the mixing ratio should be examined, using a conservative tracer such as isotopic composition. Establishment of the mixing ratio should assist in developing a better understanding of chemical and physical processes within the estuary.

(ii) Age determination combined with trace metal distribution of the bottom sediments should be undertaken to distinguish natural fluxes from those which are anthropogenic in origin. Such an investigation may establish the background level of trace metals and contribute information to understanding chemical processes following deposition of the sediments.

REFERENCES

- ACKERMANN, F. (1980). A procedure for correcting the grain size effect in heavy metal analyses of estuarine and coastal sediments. *Environ. Technol. Lett.* **1**, 518-528.
- ACKERMANN, F., BERGMANN, H. & SCHLEICHERT, U. (1983). Monitoring of heavy metals in coastal and estuarine sediments-A question of grain-size: <20 micron vs. <60 micron. *Environ. Technol. Lett.* **4**, 317-328.
- ALLEN, G.P. (1971). Relationship between grain size parameter distribution and current patterns in the Gironde Estuary (France). *J. Sedim. Petrol.* **41**, 74-88.
- AOKI, S., OINUMA, K., SUDO, T. (1974). The distribution of clay minerals in the recent sediments of the Japan Sea. *Deep Sea Res.*, **21**, 299-310.
- ARMANNSSON, H., BURTON, J.D., JONES, G.B. & KNAP, A.H. (1985). Trace metals and hydrocarbons in sediments from the Southampton Water Region, with particular reference to the influence of oil refinery effluent. *Mar. Environ. Res.*, **15**, 31-44.
- ASHRAF, M. (1982). Mixing of the Test and Itchen tributaries into Southampton Water. Msc. Thesis. Department of Oceanography, University of Southampton.
- ASTON, S.R. & CHESTER, R. (1976). Estuarine sedimentary processes. In: *Estuarine Chemistry* (ed. J.D. BURTON, & P.S. LISS), pp. 37-52. Academic Press, London.
- AVOINE, J. (1986). Sediment exchanges between the Seine estuary and its adjacent shelf. *J. Geol. Society, London*, **144**, 135-148.
- BAGNOLD, R.A. & BARNDORFF-NIELSEN, O. (1980). The pattern of natural size distributions. *Sedimentology*, **27**, 199-207.
- BALISTRERI, L.S. & MURRAY, J.W. (1984). Marine scavenging: Trace metal

- adsorption by interfacial sediment from MANOP Site H. *Geochim. Cosmochim. Acta*. **48**, 921-929.
- BARNDORFF-NIELSEN, O., DALSGAARD, K., HALGREEN, C., KUHLMAN, H., MØLLER, J., SCHOU, G. (1982). Variation in particle size distribution over a small dune. *Sedimentology*, **29**, 53-65.
- BARTON, M.E. (1979). Engineering geological aspects of dock and harbour engineering in Southampton Water. *Q. Jl. Engng. Geol.* **12**, 243-255.
- BCR Information (1988). The certification of the contents (mass fractions) of As, Cd, Cr, Cu, Hg, Ni, Pb, Sc, Se and Zn in three sediments. Estuarine sediment CRM 277, Lake sediment CRM 280, river sediment CRM 320. (ed. B. GRIEPINK & H. MUNTAN). Commission of the European Communities, Brussels, Luxembourg.
- BEWERS, J.M. & YEATS, P.A. (1981). Behaviour of trace metals during estuarine mixing. In: *River inputs to Ocean Systems* (ed. J.M. MARTIN, J.D. BURTON, & D. EISMA), pp. 103-115. Paris: UNEP/UNESCO.
- BISCAYE, P.E. (1965). Mineralogy and sedimentation of recent deep-sea clay in the Atlantic Ocean and adjacent seas and oceans. *Geol. Soc. Bull.*, **76**, 803-832.
- BGS, British Geological Survey (1988). Marine aggregate survey: A study undertaken by the BGS on behalf of the Crown Estate. Phase 2, South Coast, Scale 1:250,000. Map 1, Bathymetry.
- BOLDRIN, A., JURACK, M., MENEGAZZO VITTURI, L., RABITTI, S. & RAMPAZZO, G. (1989). Geochemical considerations on trace element distributions in suspended matter and sediments at the river-sea interface, Adige River Mouth, northern Adriatic Sea. *Appl. Geochem.* **4**, 409-421.
- BORDOVSKY, O.K. (1965). Sources of organic matter in marine basins. *Mar. Geol.*, **3**, 5-31.
- BRANNON, J.M., ROSE, J.R., ENGLER, R.M., SMITH, I. (1977). The distribution of heavy metals in sediment fractions from Mobile Bay, Alabama. In: *Chemistry of Marine Sediments* (ed. T.F. YEN), pp. 125-

- 150, Ann Arbor Sci. Publ., Michigan
- BRINDLEY, G.W. & BROWN, G. (1980). *Crystal Structures of Clay Minerals and their X-Ray Identification*. Mineralogical Society Monograph; no.5., Mineralogical Society, London.
- BROWN, G. & BRINDLEY, G.W., (1980). X-Ray diffraction procedures for clay mineral identification. In: *Crystal Structures of Clay Minerals and their X-Ray Identification* Mineralogical Society Monograph; no. 5, (ed. G.W. BRINDLEY & G. BROWN), pp. 305-361. Mineralogical Society, London.
- BRULAND, K.W., BERTINE, K., KOIDE, M. & GOLDBERG, E.D. (1974). History of metal pollution in Southern California coastal zone. *Environ. sci. Technol.* **8**, 425-432.
- BRÜGMAN, L. (1988). Some peculiarities of the trace metal distribution in Baltic Waters and sediments. *Mar. Chem.* **23**, 425-440.
- BULLER, A.T. & McMANUS, J. (1979). Sediment sampling and analysis. In: *Estuarine Hydrography and Sedimentation* (ed. K.R. DYER), pp. 87-130. Cambridge University Press.
- BURTON, J.D. (1976). Basic properties and processes in estuarine chemistry. In: *Estuarine Chemistry* (ed. J.D. BURTON & P.S. LISS), pp. 1-36. Academic Press, London.
- BURTON, J.D. & LISS, P.S. (1976). *Estuarine Chemistry*. Academic Press, London.
- CARLO ERBA (1988). *Instruction Manual*.
- CARR, J.F., de TURVILLE, C.M., JARMAN, R.T. & SPENCER, J.F. (1980). Water temperatures in the Solent Estuarine System. pp. 36-43., NERC Publications Series C, no. 22.
- CAUWET, G. (1987). Influence of sedimentological features on the distribution of trace metals in marine sediments. *Mar. Chem.*, **22**, 221-234.
- CHAMLEY, H. (1989). *Clay Sedimentology*. Berlin: Springer-Verlag, 623 pp.
- CHESTER, R. (1975). Trace elements in sediments from the Lower Severn Estuary and Bristol Channel. *Mar. Pollut. Bull.* **6**, 92-96.

- CHESTER, R. (1990). *Marine Geochemistry*. Unwin Hyman Ltd.
- CHRISTIANSEN, C., BLAESILD, P., DALSGAARD, K. (1984). Re-interpreting 'segmented' grain size curves. *Geol. Mag.*, **121**, 47-51.
- CLAYTON, T. (1991). Computer Program for calculating clay mineral abundances from digitized diffraction patterns. Department of Geology, University of Southampton. Unpublished.
- COUGHLAN, J. (1979). Aspects of reclamation in Southampton Water. In: *Estuarine and coastal land reclamation and water storage* (ed. B. KNIGHTS & A.J. PHILLIPS), pp. 99-125, Estuarine and Brackish-water Sciences Association, England.
- CRAIB, J.S. (1965). A sampler for taking short undisturbed marine cores. *J. Cons. perm. Int. Explor. mer.* **30**, (1), 34-39.
- CURRAY, J.R. (1961). Tracing sediment masses by grain size modes. In: *21st. Int. Geol. Congr. Part 23*, **6**, (ed. K. HANSEN), pp. 119-130. Copenhag.
- DE GROOT, A.J. & ALLERSMA, E. (1975). Field observations on the transport of heavy metals in sediments. In: *Heavy Metals in the Aquatic Environment*, A supplement to Progress in Water Technology, (ed. P.A. KRENKEL). Int. Conf. Supplement Progress in Water Technol., pp. 85-97.
- DE GROOT, A.J., SALOMONS, W. & ALLERSMA, E. (1976). Processes affecting heavy metals in estuarine sediments. In: *Estuarine Chemistry* (ed. J.D. BURTON & P.S. LISS), pp. 131-153. Academic Press, London.
- DIN, Z.B. (1992). Use of aluminium to normalize heavy-metal data from estuarine and coastal sediments of Straits of Melaka. *Mar. Pollut. Bull.* **24**, 484-491.
- DREVER, J.I. (1973). The preparation of oriented clay mineral specimens for X-ray diffraction analysis by a filter-membrane peel technique. *Am. Mineral.*, **58**, 553-554.
- DUANE, D.B. (1964). Significance of skewness in recent sediments, Western Pamlico Sound, North Carolina. *J. sedim. Petrol.* **34**, 864-874.
- DUINKER, J.C. & NOLTING, R.F. (1976). Distribution model for particulate

- trace metals in the Rhine Estuary, southern Bight and Dutch Wadden Sea. *Neth. J. Sea Res.*, **10**, 71-102.
- DUINKER, J.C. & NOLTING, R.F. (1978). Mixing, removal and mobilization of trace metals in the Rhine estuary. *Neth. J. Sea Res.*, **12**, 205-223.
- DURHAM, R.W. & JOSHI, S.R. (1984). Lead-210 dating of sediments from some Northern Ontario Lakes. In: *Quaternary Dating Methods*, Series of Developments in palaeontology and stratigraphy, No. 7, (ed. W.C. MAHANEY), pp. 75-85. Elsevier, Oxford.
- DYER, K.R. (1969). Some aspects of coastal and estuarine sedimentation. Unpublished Ph.D. Thesis, Department of Oceanography, University of Southampton, 102 pp + Figures.
- DYER, K.R. (1970). Linear erosional furrows in Southampton Water. *Nature*, **225**, 56-58.
- DYER, K.R. (1971). The distribution and movement of sediment in the Solent, Southern England. *Mar. Geol.* **11**, 175-187.
- DYER, K.R. (1975). The buried channels of the 'Solent River', southern England. *Proc. Geol. Ass.* **86**, 239-245.
- DYER, K.R. & KING, H.L. (1975). The residual water flow through the Solent, South England. *Geophys. J.R. astr. Soc.* **42**, 97-106.
- DYER, K.R. (1979). Estuaries and estuarine sedimentation. In: *Estuarine Hydrography and Sedimentation* (ed. K.R. DYER), pp. 1-18. Cambridge University Press.
- DYER, K.R. (1980). Sedimentation and sediment transport. NERC, Publication Series C, no. 22, pp. 20-24
- DYER, K.R. (1986). *Coastal and Estuarine Sediment Dynamics*. John Wiley & Sons, Chichester. 342 p.
- EDZWALD, J.K., O'MELIA, C.R. (1975). Clay distributions in recent estuarine sediments. *Clay. Clay M.*, **23**, 29-44.
- ELDERFIELD, H. & HEPWORTH, A. (1975). Diagenesis, metals and pollution in estuaries. *Mar. Pollut. Bull.* **6**, 85-87.

- EL GHOBARY, H. & LATOUCHE, C. (1986). A comparative study of the partitioning of certain metals in sediments from four near-shore environment of the Aquitaine coast (SW France). In: *Sediments and Water Interactions*, Proceedings of the Third International Symposium on Interactions between sediments and water, (ed. P.G. SLY), pp. 105-124. Springer Verlag, New York.
- ENGLER, R.M., BRANNON, J.M., ROSE, J. (1977). A practical selective extraction procedure for sediment characterization. In: *Chemistry of Marine Sediments* (ed. T.F. YEN), pp. 163-171, Ann Arbor Sci. Publ., Michigan.
- ESLINGER, E. & PEVEAR, D. (1988). *Clay minerals for Petroleum Geologists and Engineers*. Soc. of Economic Palaeontologists and Mineralogists, U.S.A. Short Course No.22.
- EVERAARTS, J.M. & FISCHER, C.V. (1992). The distribution of heavy metals (Cu, Zn, Cd, Pb) in the fine fraction of surface sediments of the North Sea. *Neth. J. Sea Res.*, **29**, 323-331.
- FAIRCHILD, I., HENDRY, G., QUEST, M. & TUCKER, M.E. (1988). Chemical analysis of sedimentary rocks. In: *Techniques in Sedimentology* (ed. M.E. TUCKER), pp. 274-354. Blackwell, Oxford.
- FERNEX, F.E., SPAN, D., FLATAU, G.N., RENARD, D. (1986). Behaviour of some metals in surfacial sediments of the Northwest Mediterranean Continental Shelf. In: *Sediments and Water Interactions*, Proceedings of the third international symposium on interactions between sediments and water, (ed. P.G. SLY), pp. 353-369. Springer Verlag, New York.
- FEUILLET, J.P. & FLEISCHER, P. (1980). Estuarine circulation: controlling factor of clay mineral distribution in James River estuary, Virginia. *J. sedim. Petrol.*, **50**, 267-279.
- FILIPEK, H.L. & OWEN, R.M. (1978). Geochemical associations and grain size partitioning of heavy metals in lacustrine sediments. *Chem. Geol.* **26**, 105-117.
- FLETCHER, W.K. (1981). Analytical methods in geochemical prospecting. In:

- Handbook of exploration geochemistry*, Vol.1, (ed. G.J.S. GOVETT), pp. 109-138, Elsevier, Amsterdam.
- FOLGER, D.W. (1972). Texture and organic carbon content of bottom sediments in some estuaries of the United States. In: *Environmental Framework of Coastal Plain Estuaries*, Geological Society of America Memoir 133, (ed. B.W. NELSON), pp. 391-408.
- FOLK, R.L. & WARD, W.C. (1957). Brazos River bar: a study in the significance of grain size parameters. *J. sedim. Petrol.*, **27**, 3-26.
- FOLK, R.L. (1966). A review of grain size parameters. *Sedimentology*, **6**, 73-93.
- FÖRSTNER, U. & WITTMANN, G. (1979). *Metal Pollution in the Aquatic Environment*. Springer, Berlin.
- FÖRSTNER, U. & SALOMONS, W. (1980). Trace metal analysis on polluted sediments, Part 1: Assessment of sources and intensities. *Environ. Technol. Lett.*, **1**, 494-505.
- FÖRSTNER, U. & PATCHINEELAM, S.R. (1980). Chemical associations of heavy metals in polluted sediments from the Lower Rhine River. In: *Particulates in Water*, Adv. Chem. Ser. Amer. Chem. Soc., **189**, (ed. M.C. KAVAUNAGH & L.O. LECKIE), pp. 177-193.
- FÖRSTNER, U., AHLF, W., CALMANO, W., KERSTEN, M., SALOMONS, W. (1986). Mobility of heavy metals in dredged harbour sediments. In: *Sediments and Water Interactions*, Proceedings of the third international symposium on interactions between sediments and water, (ed. P.G. SLY), pp. 371-380. Springer Verlag, New York.
- FÖRSTNER, U. (1989). *Lecture notes in earth sciences*, 21. *Contaminated sediments*. 157 pp. Springer, Verlag.
- FRIEDMAN, G. (1961). Distinction between dune, beach and river sands from their textural characteristics. *J. sedim. Petrol.* **31**, 514-529.
- FREIDMAN, G.M. (1979). Address of the retiring President of the International Association of Sedimentologist: Differences in size distributions of populations of particles among sands of various origins. *Sedimentology*, **26**,

3-32.

- GALEHOUSE, J.S. (1971). Sedimentation analysis. In: *Procedures in Sedimentary Petrology* (ed. R.E. CARVER), pp. 69-94. Wiley, New York.
- GAO, S. & COLLINS, M.B. (1991). Potential impact of sea level changes, toward AD 2050, on the coastline from Hengistbury Head to Pagham (Southern England). A report prepared for the GeoData Unit, University of Southampton.
- GAO, S. & COLLINS, M.B. (1991). A critique of the "McLaren Method" for defining sediment transport paths: Discussion. *J. sedim. Petrol.* **61**, 143-146.
- GAO, S. & COLLINS, M.B. (1992). Net sediment transport patterns inferred from grain-size trends, based upon definition of 'transport vectors'. *Sedim. Geol.* **80**, 47-60.
- GIBBS, R.J. (1965). Error due to segregation in quantitative clay mineral X-ray diffraction mounting techniques. *Am. Mineral.*, **50**, 741-751.
- GIBBS, R.J. (1973). Mechanisms of trace metal transport in rivers. *Sci.*, **180**, 71-73.
- GIBBS, R.J. (1977). Clay mineral segregation on the marine environment. *J. sedim. Petrol.* **47**, 237-243.
- GILKES, R.J. (1968). Clay mineral provinces in the Tertiary sediments of the Hampshire Basin. *Clay Minerals*, **7**, 351-361.
- GILKES, R.J. (1978). On the clay mineralogy of upper Eocene and Oligocene sediments in the Hampshire Basin. *Proc. Geol. Ass.*, **89**, 43-56.
- GLAISTER, R.P. & NELSON, H.W. (1974). Grain-size distribution an aid in facies identification. *Bull. Can. Petroleum Geology* **22**, 203-240.
- GRIFFIN, J.J., WINDOW, H., GOLDBERG, E.D. (1965). The distribution of clay minerals in the World Ocean. *Deep Sea Res.*, **15**, 433-459.
- HARDY, R.G. & TUCKER, M.E. (1988). X-ray powder diffraction of sediments. In: *Techniques in Sedimentology* (ed. M.E. TUCKER), pp. 191-229. Blackwell, Oxford.

- HARLOW, D.A. (1979). The littoral budget between Selsey Bill and Gilkicker Point, and its relevance to coast protection works on Hayling Island. *Q. Jl. Engng. Geol.* **12**, 257-265.
- HARLOW, D.A. (1982). Sediment processes, Selsey Bill to Portsmouth. Unpublished Ph.D. Thesis, Department of Civil Engineering, University of Southampton.
- HATHAWAY, J.C. (1972). Regional clay mineral facies in estuaries and continental margin of the United States East Coast. In: *Environmental Framework of Coastal Plain Estuaries*, Geological Society of America Memoir **133**, (ed. B.W. NELSON), pp. 293-316.
- HEATH, G.R. & PISIAS, N.G. (1979). A method for the quantitative estimation of clay minerals in North Pacific deep-sea sediments. *Clay. Clay M.*, **27**, 175-184.
- HENDRIX, W.P. & ORR, C. (1972). Automatic sedimentation size analysis instrument. In: *Particle Size Analysis*, Soc. Analyt. Chem., (ed. M.J. GROVES & J.L. WYATT-SARGENT), pp. 133-146. London.
- HODSON, F. & WEST, I.M. (1972). Holocene deposits of Fawley, Hampshire, and the development of Southampton Water. *Proc. Geol. Ass. London*, **83**, 421-442.
- HOROWITZ, A. & ELRICK, K.A. (1987). The relation of stream sediment surface area, grain size and composition to trace element chemistry. *Applied Geochemistry*, **2**, 437-451.
- HOUGHTON, S.D. (1986). Coccolith assemblages in recent marine and estuarine sediments from the continental shelf of northwest Europe. Unpublished Ph.D. Thesis, Department of Geology, University of Southampton.
- HUBERT, J.F. (1964). Textural evidence for deposition of many western north Atlantic deep sea sands by ocean-bottom currents rather than turbidity currents. *J. Geol. Soc.*, **72**, 757-785.
- HUNTER, K.A. & LISS, P.S. (1982). Organic matter and the surface charge of suspended particles in estuarine waters. *Limnol. Oceanogr.* **27**, 322-335.

- INGRAM, R.L. (1971). Sieve analysis. In: *Procedures in Sedimentary Petrology* (ed. R.E. CARVER), pp. 49-67. Wiley, New York.
- IRIARTE, A. (1991). Picophytoplankton: ecological and physiological studies in cultural and natural coastal and estuarine waters. Unpublished Ph.D. Thesis, Department of Oceanography, University of Southampton.
- IRION, G. & ZÖLMER, V. (1990). Pathways of fine-grained clastic sediments - Examples from the Amazon, the Weser Estuary, and the North Sea. In: *Sediments and Environmental Geochemistry* (ed. D. HELING, P. ROTHE, U. FÖRSTNER & P. STOFFERS), pp. 351-367. Springer-Verlag, Berlin.
- JOHNS, W.D. & GRIM, R.E. (1958). Clay mineral composition of recent sediments from the Mississippi River Delta. *J. sedim. Petrol.* **28**, 186-199.
- JONES, A.S.G. (1971). A textural study of marine sediments in a portion of Cardigan Bay (Wales). *J. sedim. Petrol.* **41**, 505-516.
- JONES, K.P.N., McCABE, I.N. & PATEL, P.D. (1988). A computer-interfaced sedigraph for modal size analysis of fine-grained sediment. *Sedimentology*, **35**, 163-172.
- KARLIN, R. (1980). Sediment sources and clay mineral distributions off the Oregon Coast. *J. sedim. Petrol.* **50**, 543-560.
- KEMP, A.L.W., THOMAS, R.L., DELL, C.I., JAQUET, J.-M. (1976). Cultural impact on the geochemistry of sediments in Lake Erie. *J. Fish. Res. Board Can.*, **33**, 440-462.
- KERSTEN, M. & FÖRSTNER, U. (1986). Chemical fractionation of heavy metals in anoxic estuarine and coastal sediment. *Wat. Sci. Tech.*, **18**, 121-130.
- KERSTEN, M. & FÖRSTNER, U. (1987). Effects of sample pretreatment on the reliability of solid speciation data of heavy metals-Implications for the study. *Mar. Chem.* **22**, 299-312.
- KITANO, Y., SAKATA, M., MATSUMOTO, E. (1980). Partitioning of heavy metals into mineral and organic fractions in a sediment core from Tokyo Bay. *Geochim. Cosmochim. Acta.* **44**, 1279-1285.

- KOLLA, V., NADLER, L., BONATTI, E. (1980). Clay mineral distributions in surface sediments of the Philippine Sea. *Oceanol. Acta.*, **3**, 245-250.
- KRAUSKOPF, K.B. (1967). *Introduction to Geochemistry*. International Series in the Earth and Planetary Sciences. McGraw-Hill.
- KRUMGALZ, B.S. (1989). Unusual grain size effect on trace metals and organic matter in contaminated sediments. *Mar. Pollut. Bull.* **20**, 608-611.
- LEEDER, M.R. (1982). *Sedimentology, Process and Product*. Unwin Hyman, 343 pp.
- LEONI, L., SARTARI, F., SAIITA, M., DAMIANI, V., FERRETTI, O., and VIEL, M. (1991). Mineralogy, chemistry and grain size composition of recent sediments in the Northern Tyrrhenian Sea: Contribution to the study of sediment transport and distribution. *Environ. Geol. Water Sci.* **17**, 23-46.
- LI, Y., BURKHARDT, L., TERAOKA, H. (1984). Desorption and coagulation of trace elements during estuarine mixing. *Geochim. Cosmochim. Acta.* **48**, 1879-1884.
- LINDHOLM, R.C. (1987). *A practical approach to sedimentology*. Allen & Unwin Inc. 276 p.
- LONSDALE, B.J. (1969). A sedimentary study of the Eastern Solent. Msc. Thesis, Department of Oceanography, University of Southampton.
- LORING, D.H. (1991). Normalization of heavy-metal data from estuarine and coastal sediments. *ICES J. mar. Sci.*, **48**, 101-115.
- LORING, D.H. & RANTALA, R.T.T. (1990). Techniques in marine environmental sciences. Sediments and suspended particulate matter: Total and partial methods of digestion. *ICEOS*. No. **9**
- LORING, D.H. & RANTALA, R.T.T. (1992). Manual for the geochemical analyses of marine sediments and suspended particulate matter. *Earth-Science Reviews*, **32**, 235-283.
- LUOMA, S.N. (1990). Processes affecting metal concentrations in estuarine and coastal marine sediments. In: *Heavy metals in the marine environment* (ed.

- R.W. FURNESS & P.S. RAINBOW), pp. 51-66, CRC Press, Inc.
- MARTIN, J.W., NIREL, P. & THOMAS, A.J. (1987). Sequential extraction techniques: Promises and problems. *Mar. Chem.* **22**, 313-341.
- McLAREN, P. (1981). An interpretation of trends in grain size measures. *J. sedim. Petrol.* **51**, 611-624.
- McLAREN, P. & BOWLES, D. (1985). The effects of sediment transport on grain-size distribution. *J. sedim. Petrol.* **55**, 457-470.
- McLAREN, P. & LITTLE, D.I. (1987). The effects of sediment transport on contaminant dispersal: An example from Milford Haven. *Mar. Pollut. Bull.* **18**, 586-594.
- McMANUS, J., BULLER, A.T. & GREEN, C.D. (1980). Sediments of the Tay Estuary VI, sediments of the lower and outer reaches. *Proc. R. Soc. Edinb. B.*, **78**, 133-154.
- McMANUS, J. (1988). Grain size determination and interpretation. In: *Techniques in Sedimentology* (ed. M.E. TUCKER), pp. 63-85. Blackwell, Oxford.
- McMANUS, D.A. (1991). Suggestions for authors whose manuscripts include quantitative clay mineral analysis by X-ray diffraction. *Mar. Geol.*, **98**, 1-5.
- MEADE, R.H. (1972). Transport and deposition of sediments in estuaries. In: *Environmental Framework of Coastal Plain Estuaries*, Geological Society of America Memoir 133, (ed. B.W. NELSON), pp. 91-120.
- MELVILLE, R.V. & FRESHNEY, E.C. (1982). *The Hampshire Basin and adjoining areas*. Her Majesty's Stationary Office, London, 146 pp.
- MICROMERITICS (1989). *Instruction manual of SediGraph 5100*.
- MIOLA, R.J. & WEISER, D. (1968). Textural parameters an evaluation. *J. sedim. Petrol.* **38**, 45-53.
- MUDROCH, A. & DUNCAN, G.A. (1986). Distribution of metals in different size fractions of sediment from the Niagara River. *J. Great Lakes Res.*, **12**, 117-126.
- NEIHEISEL, J. & WEAVER, C.E. (1967). Transport and deposition of clay

- minerals southeastern United States. *J. sedim. Petrol.* **37**, 1084-116.
- NICHOLLS, R.J. (1987). Evolution of the Upper reaches of the Solent River and the formation of Poole and Christchurch Bays. In: *Wessex and the Isle of Wight: Field Guide*, Quaternary Research Association, (ed. K.E. BARBER), pp. 99-114. Cambridge.
- NISSENBAUM, A. & SWAINE, D.J. (1976). Organic matter metal interactions in recent sediments: the role of humic substances. *Geochim. Cosmochim. Acta.* **40**, 809-816.
- NOLTING, R.F., SUNDBY, B. & DUINKER, J.C. (1989). Minor and major elements in suspended matter in the Rhine and Meuse Rivers and estuary. *Neth. J. Sea Res.*, **23**, 255-261.
- NORDSTROM, K.F. (1977). The use of grain size statistics to distinguish between high and moderate-energy beach environments. *J. sedim. Petrol.* **47**, 1287-1294.
- OLIVIER, J.P., HICKIN, G.K. & ORR, C. (1970). Rapid, automatic particle size analysis in the subsieve range. *Powder Tech.* **4**, 257-263.
- PAALMAN, M.A.A. & VAN DER WEIJDEN, C.H. (1992). Trace metals in suspended matter from the Rhine/Meuse estuary. *Neth. J. Sea Res.*, **29**, 311-321.
- PARK, Y.A., KIM, S.C., CHOI, J.H. (1986). The distribution and transportation of fine-grained sediments on the inner continental shelf off the Keum River Estuary, Korea. *Cont. Shelf Res.*, **5**, 499-519.
- PASSEGA, R. (1964). Grain size representation by CM patterns as a geological tool. *J. sedim. Petrol.* **34**, 830-847.
- PEVEAR, D.R. (1972). Source of recent nearshore marine clays, southeastern United States. In: *Environmental Framework of Coastal Plain Estuaries*, Geological Society of America Memoir **133**, (ed. B.W. NELSON), pp. 317-335.
- PHILLIPS, A.J. (1980). Distribution of chemical species. NERC, Publication Series C, no. 22.

- PIERCE, J.W. & SIEGEL, F.R. (1969). Quantification in clay mineral studies of sediments and sedimentary rocks. *J. sedim. Petrol.* **39**, 187-193.
- PINET, P.R. & MORGAN, W.P. (1979). Implications of clay-provenance studies in two Georgia Estuaries. *J. sedim. Petrol.* **49**, 575-580.
- POWELL, R.P. (1977). Linear erosion furrows in Southampton Water: an introductory study. Msc. Thesis, Department of Oceanography, University of Southampton.
- POSTMA, H. (1967). Sediment transport and sedimentation in the estuarine environment. In: *Estuaries*, American Association for the Advancement of Science, no: **83**, (ed. G.H. LAUFF), pp. 158-179. Washington D.C.
- PYE UNICAM. (1979). Sp 9 Series AAS Users Manual, Cambridge, England.
- RAO, V.P. (1991). Clay mineral distribution in the continental shelf sediments from Krishna to Ganges river mouth, east coast of India. *Indian J. Mar. Sci.*, **20**, 7-12.
- ROMANS, C.G. (1979). A study of the Lower Test estuary and its evolution since 1966. Msc. Thesis, Department of Oceanography, University of Southampton.
- ROSENTAL, R., EAGLE, G.A., ORREN, M.J. (1986). Trace metal distribution in different chemical fractions of nearshore marine sediments. *Estuarine Coastal Shelf Sci.*, **22**, 303-324.
- RULE, J.H. (1986). Assessment of trace elements geochemistry of Hampton Roads Harbor and Lower Chesapeake Bay Are sediments. *Environ. Geol. Water Sci.*, **8**, 209-219.
- SALOMONS, W. & MOOK, W.G. (1977). Trace metal concentrations in estuarine sediments: mobilization, mixing or precipitation. *Neth. J. Sea Res.*, **11**, 119-129.
- SALOMONS, W. & MOOK, W.G. (1987). Natural tracers for sediment transport studies. *Cont. Shelf Res.* **7**, 1333-1343.
- SALOMONS, W. & EYSINK, W.D. (1981). Pathways of mud and particulate trace metals from rivers to the southern North Sea. In: *Holocene marine*

- sedimentation in the North Sea Basin*, Spec. Publs. Int. Ass. Sediment **5**, (ed. S.D. NIO, R.T.E. SCHUTTENHELM & Tj.C.E. VAN WEERING), pp. 429-450. Blackwell, Oxford.
- SALOMONS, W. & FÖRSTNER, U. (1980). Trace metal analysis on polluted sediments. Part II: Evaluation of environmental impact. *Environ. Technol. Lett.* **1**, 506-517.
- SALOMONS, W. & FÖRSTNER, U. (1984). *Metals in the Hydrocycle*. Springer Verlag.
- SCAFE, D.W. & KUNZE, G.W., (1971). A clay mineral investigation of six cores from the gulf of Mexico. *Mar. Geol.*, **10**, 69-85.
- SCHUBEL, J.R & HIRSCHBERG, D.J. (1981). Accumulation of fine-grained sediments in estuaries. In: *River inputs to Ocean Systems* (ed. J.M. MARTIN, J.D. BURTON & D. EISMA), pp. 77-85. Paris: UNEP/UNESCO.
- SCHUBEL, J.R. & KENNEDY, V.S. (1984). The estuary as a filter: An introduction. In: *The estuary as a filter*, The Estuarine research Federation, (ed. V.S. KENNEDY). Academic Press, Orlando, Florida.
- SEALEY, C. (1987). A study of the distribution of Al in the Itchen River and Southampton Water, Hampshire. Msc. Thesis, Department of Oceanography, University of Southampton.
- SENGUPTA, S. (1979). Grain size distribution of suspended load in relation to bed materials and flow velocity. *Sedimentology* **26**, 63-82.
- SHAW, H.F. (1978). The clay mineralogy of the recent surface sediments from the Cilicia Basin, Northeastern Mediterranean. *Mar. Geol.*, **26**, M51-M58.
- SHAW, H.F. (1973). Clay mineralogy of Quaternary sediments in the Wash Embayment, Eastern England. *Mar. Geol.*, **14**, 29-45.
- SHAW, T.J., GIESKES, J.M. & JAHNKE, R.A. (1990). Early diagenesis in differing depositional environments: The response of transition metals in pore water. *Geochim. Cosmochim. Acta.* **54**, 1233-1246.
- SHELL, U.K. Exp. & Prod. (1980, 1985, 1986). The Solent Estuarine System:

- Geomorphological aspects of the coastline. Environmental Report 20/85.
- SHOLKOVITZ, E.R. (1976). Flocculation of dissolved organic and inorganic matter during the mixing of river water and sea water. *Geochim. Cosmochim. Acta.* **40**, 831-845.
- SINGER, J.K., ANDERSON, J.B., LEDBETTER, M.T., McCAVE, I.N., JONES, K.P.N. & WRIGHT, R. (1988) An assessment of analytical techniques for the analysis of fine-grained sediments. *J. sedim. Petrol.* **58**, 534-543.
- SINEX, S.A. & HELZ, G.R. (1981). Regional geochemistry of trace elements in Chesapeake Bay sediments. *Environ. Geol.*, **3**, 315-323.
- SKEI, J. & PAUS, P.E. (1979). Surface metal enrichment and partitioning of metals in a dated sediment core from a Norwegian fjord. *Geochim. Cosmochim. Acta.* **43**, 239-246.
- SLY, P.G. (1978). Sedimentary Processes in Lakes. In: *Lakes-chemistry, geology, physics* (ed. A. LERMAN), pp. 65-89. Springer, Newyork.
- SMITH, J.N. & WALTON, A. (1980). Sediment accumulation rates and geochronologies measured in the Saguenay Fjord using the Pb-210 dating method. *Geochim. Cosmochim. Acta.* **44**, 225-240.
- SOULSBY, P.G., LOWTHION, D., HOUSTON, M. (1978). Observations on the effects of sewage discharged into a tidal harbour. *Mar. Pollut. Bull.* **9**, 242-245.
- SRISAENGTHONG, D. (1982). Suspended sediment dynamics and distribution in the Solent using Landsat MSS Data. Unpublished Ph.D. Thesis, Department of Oceanography, University of Southampton, 153pp + Figures.
- STEIN, R. (1985). Rapid grain-size analyses of clay and silt fraction by SediGraph 5000D: Comparison with Coulter counter and atterberg methods. *J. sedim. Petrol.* **55**, 590-593.
- STOKKE, P.R. & CARSON, B. (1973). Variation in clay mineral X-ray diffraction results with the quantity of sample mounted. *J. sedim. Petrol.*

- 43, 957-964.
- SUMMERS, J.K. (1983). Side-scan sonar survey of part of the eastern approach to the East Solent. Msc. Thesis. Department of Oceanography, University of Southampton.
- SVAROVSKY, L. & ALLEN, T. (1972). Performance of a new X-ray sedimentometer. In: *Particle Size Analysis*, Soc. Analyt. Chem., (ed. M.J. GROVES & J.L. WYATT-SARGENT), pp. 147-157. London.
- TESSIER, A., CAMPBELL, P.G.C., BISSON, M. (1979). Sequential extraction procedure for the speciation of particulate trace metals. *Analyt. Chem.*, **51**, 844-850.
- TUBBS, C.R. (1980). Processes and impacts in the Solent. pp. 1-6. NERC, Publication Series C, no. 22.
- VARION TECTHRON (19). AA-5 Analytical Methods for flame spectroscopy.
- VERARDO, D.J., FROELICH, P.I. & McINTYRE, A. (1990). Determination of organic carbon and nitrogen in marine sediments using the Carlo Erba NA-1500 Analyzer. *Deep Sea Res.* **37**, 157-165.
- VIETS, J.G. & O'LEARY, R.M. (1992). The role of atomic absorption spectrometry in geochemical exploration. *J. Geochem. Explor.*, **44**, 107-138.
- VISHER, G.S. (1969). Grain size distributions and depositional processes. *J. sedim. Petrol.* **39**, 1074-1106.
- VITTURI, L.M. & RABITTI, S. (1980). Automatic particle-size analysis of sediment fine fraction by SediGraph 5000D. *Geol. Appl. Idrogeol.* **XV**, 101-108.
- WEAVER, C.E. (1959). The clay petrology of sediments. *Clay. Clay M.*, **2**, 154-164.
- WEAVER, C.E. (1989). *Clays, muds and shales*. Series of Development in sedimentology, No. **44**. Amsterdam, Elsevier.
- WEBBER, N.B. (1979). An investigation of the dredging in Chichester Harbour approach channel and the possible effects on the Hayling Island coastline.

- A report prepared for Chichester Harbour Conservancy. Department of Civil Engineering, University of Southampton.
- WEBBER, N.B. (1980). Hydrography and water circulation in the Solent. pp. 25-35 NERC, Publication Series C, no. 22.
- WELCH, N.H., ALLEN, P.B. & GALINDO, D.J. (1979). Particle size analysis by pipette and SediGraph. *J. Environ. Quality*, **8**, 543-546.
- WEST, I.M. (1980). Geology of the Solent Estuarine System. pp. 6-18., NERC, Publication Series C, no. 22.
- WESTWOOD, I.J. (1982). Mixing and dispersion in Southampton Water. Unpublished Ph.D. Thesis. Department of Civil Engineering, University of Southampton, V1: 500 pp, V2: 458 pp and V3: 433 pp.
- WHITCOMBE, L.J. (1991). Shingle dynamics of the Hayling Island Area, including an assessment of onshore-offshore movement. MPhil. Upgrading Report, Department of Oceanography, University of Southampton.
- WHITEHOUSE, U.G., JEFFREY, L.M., DEBRECHT, J.D. (1960). Differential settling tendencies of clay minerals in saline waters. *Clay. Clay M.*, **7**, 1-79.
- WHITFIELD, M., TURNER, D.R. & DICKSON, A.G. (1981). Speciation of dissolved constituents in estuaries. In: *River inputs to Ocean Systems* (ed. J.M. MARTIN, J.D. BURTON & D. EISMA), pp. 132-139. Paris: UNEP/UNESCO.
- WILKINSON, J.J. (1991). Volatile production during contact metamorphism: the role of organic matter in pelites. *J. Geol. Soc. London.*, **148**, 731-736.
- WOOLEY, P.R.G. (1973). An investigation into Southampton Water and the Test estuary, with particular reference to their pollution status. Report No. CE/10/73, Department of Civil Engineering, University of Southampton.
- WRIGHT, P.L. (1974). The chemistry and mineralogy of the clay fraction of sediments from the southern Barents Sea. *Chem. Geol.*, **13**, 197-216.

APPENDICES

APPENDIX A : Analytical Techniques

A1. CORE SAMPLING

The Craib Corer

The Craib Corer is designed to collect a core, some 5-7 cm in diameter and 10-15 cm in length, with the surface layer undisturbed (Craib, 1965) (Plate 1). The system used here was made available to the Department by the Department of Geology, University of Wales at Cardiff.

The Sampler

The sampler consists of a tapered vertical frame attached to a horizontal circular frame, a hydraulic damper and a coring tube (Figure A1 to A3). A short tubular housing which carries the perspex coring tube has at its upper end a circular platform, to which lead weights can be added as required. A hinged sealing cover closes the upper end of the tubular housing. The coring tube is 15 cm in length beyond the lower end of the housing; it is held in position by a pair of springs. A Neoprene O-ring between the collar and the lower end of the housing ensures a watertight seal, when compressed by the springs. A rubber ball which rotates freely on its central spindle closes the lower end of the coring tube; this retains the sample without erosion of the lower end of the core (Craib, *op.cit*).

Operation of the Corer

The instrument operation is based upon a slow approach and penetration, using a hydraulic damper to control the rate of downward thrust of the coring tube; this enters the sediment on the basis of its weight alone. The piston of

the hydraulic damper is at the top of its stroke, when the sampler is ready to be lowered. The lower end of the perspex coring tube is 15 cm above the base frame and the closing ball is held against the outside of the coring tube. The hinged sealing cover is held open, in order to fill the hydraulic damper with water before taking the first of a series of samples.

The circular base-frame rests on the bottom, when the sampler is lowered to the sea-bed. The weighted corer sinks at a slow speed predetermined by the rate at which water escapes from the hydraulic damper, with the wire slack. The coring tube takes 15 seconds to descend the 15 cm to the surface of the substratum. The sealing cover and vertical bar are released by two cords attached to the frame, after the coring tube has penetrated 5 cm. The sealing cover is light enough to allow water to escape as the sample rises within the coring tube. The closing ball rests on the surface of the substratum while the coring tube completes its penetration, which takes at most 30 seconds. When the end of the coring tube leaves the surface of the substratum, the closing ball is forced down by the weight of the vertical bar. The ball is then drawn quickly into the mouth of the coring tube by the tension of two elastic cords of 6 mm square rubber, which snap the hinged yoke from a vertical to a horizontal position. The downward travel of the vertical bar is stopped, so that the hinge pin of the yoke is level with the bottom of the coring tube. The upward pull of the strong elastic cords holds the ball in the mouth of the tube (Craib, 1965).



Plate 1 : The Craib Corer, shown on the deck of the research vessel.

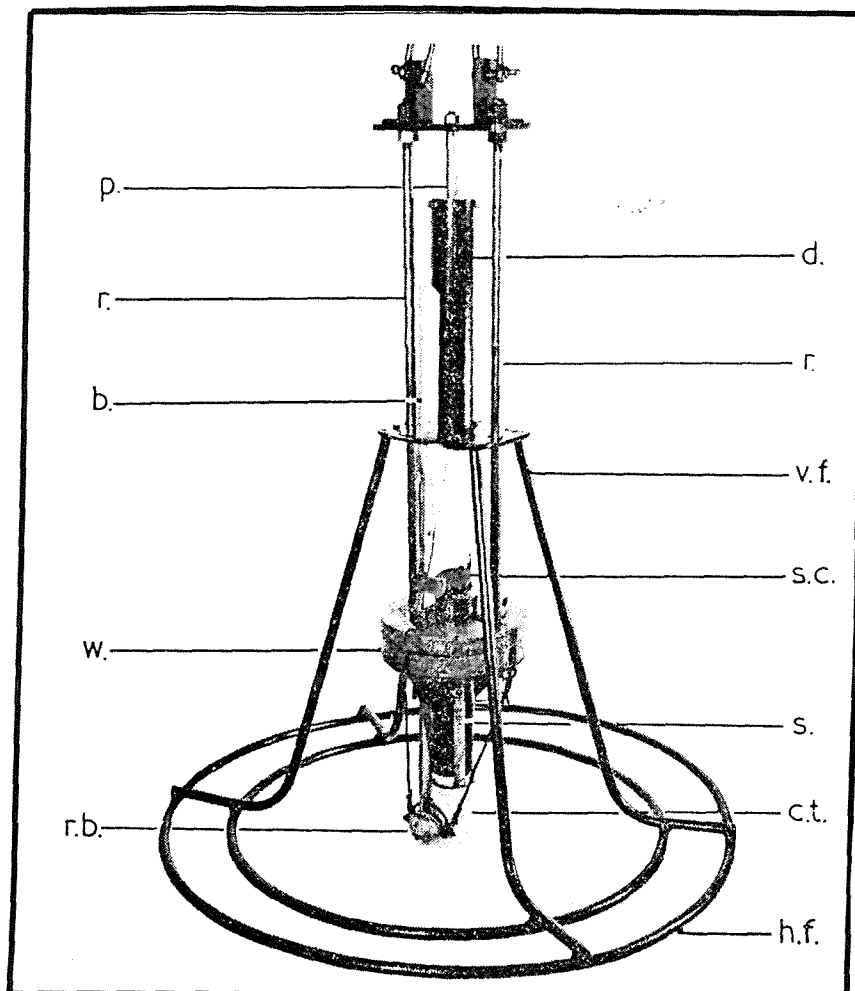


Figure A1 : Details of the Sampler. Key: p.piston rod; d, hydraulic damper; r, two vertical rods; b, heavy vertical bar; vf, vertical frame; sc, hinged sealing cover; w, lead weights; s, springs; ct, coring tube; rb, rubber ball; and hf, horizontal frame. (from Craib, 1965).

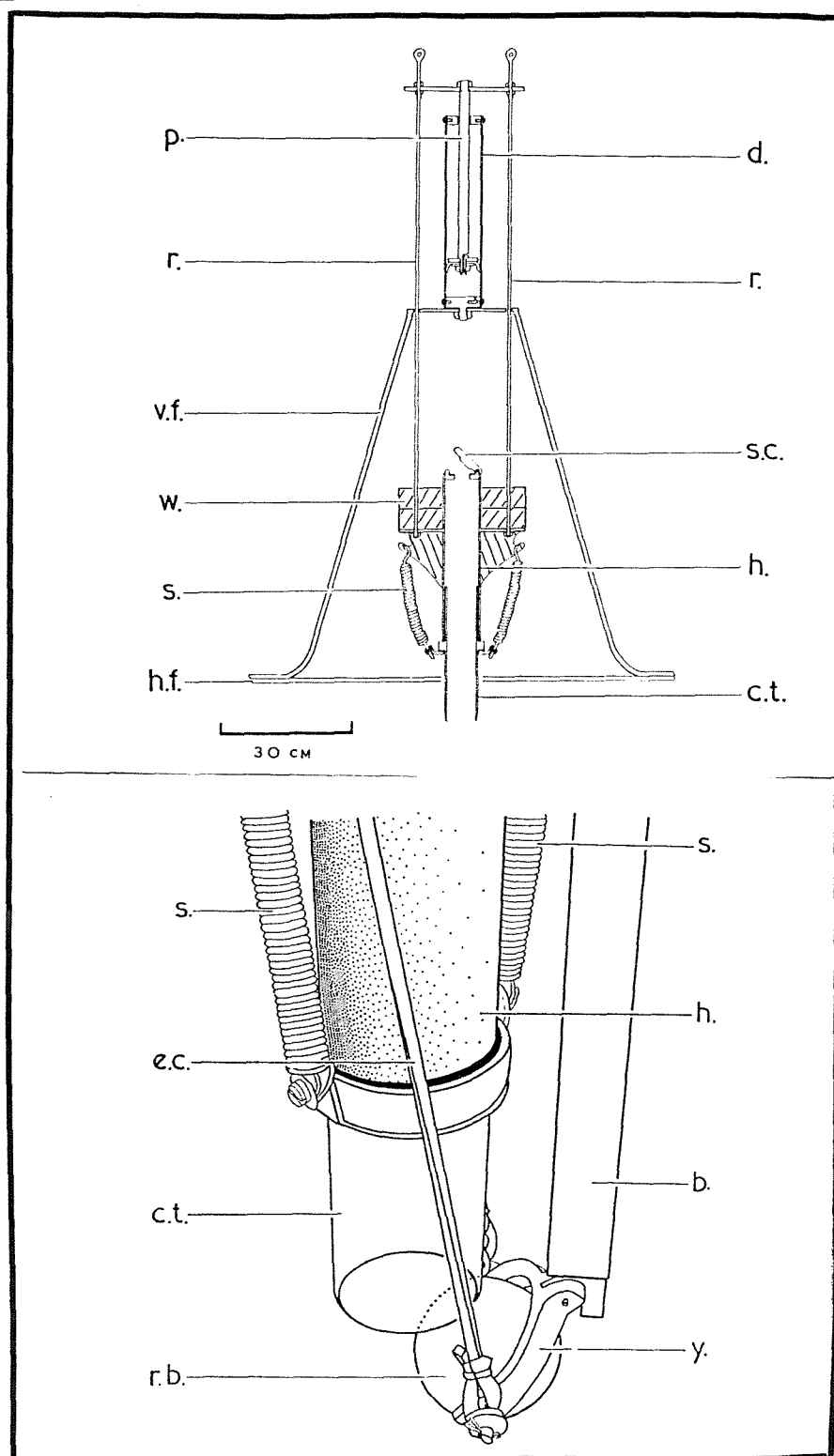


Figure A2 : *Vertical section of the sampler (upper) and the ball closing mechanism (lower).* Key: h, tubular housing; ec, square rubber; and y, yoke (from Craib, 1965).

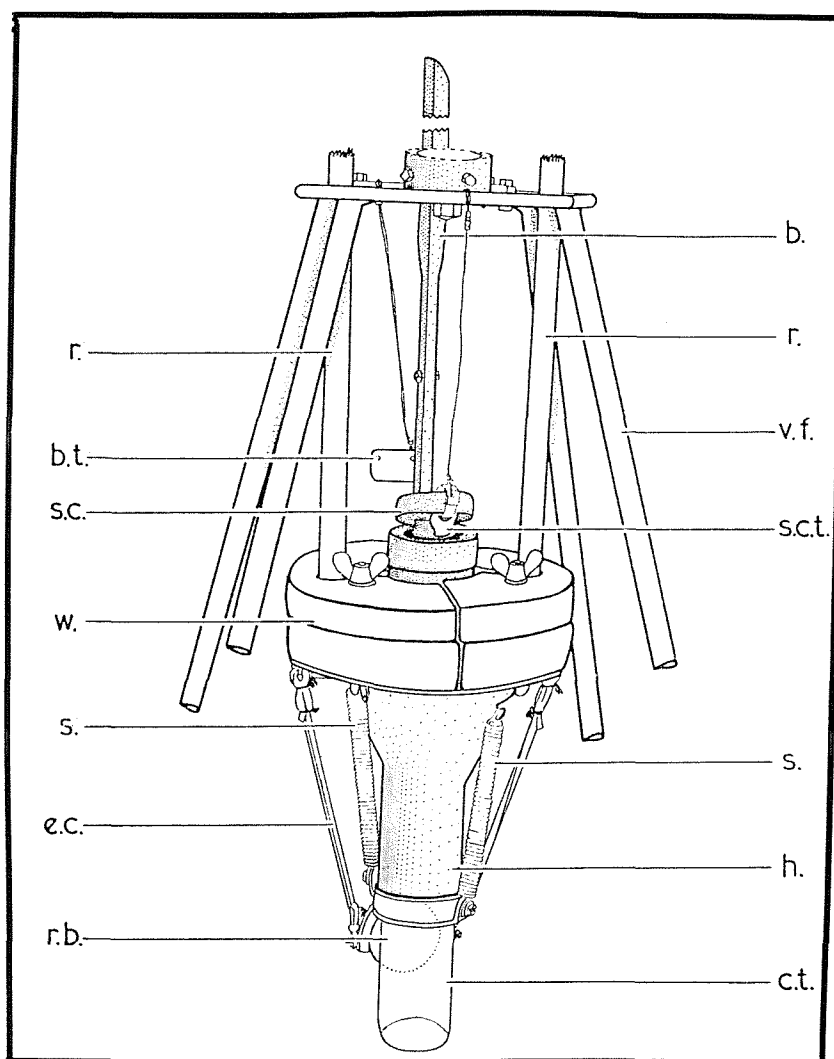


Figure A3 : *The coring tube and housing assembly.* Key: bt, vertical bar trip; sct, sealing cover trip (from Craib, 1965).



Plate 2 : The sampler being brought up on deck (upper) and the core tube showing a sample collected (some 10 cm in length), with overlying waters (lower).

A2. FINE-GRAINED SEDIMENT SIZE ANALYSIS

SediGraph

The Sedigraph 5100 Particle Size Analysis System determines the concentration of particles remaining at decreasing sedimentation depths, as a function of time by means of X-ray absorption. It calculates the distribution of particle diameters and provides several types of output on the distribution. The accuracy and consistency of the results depend upon: (1) the proper operation of the instrument; and (2) proper dispersion of the material being analyzed. In order to determine particle diameters accurately, the density and viscosity of the liquid used must be known, as well as the density of the particles. The range of particle sizes analyzed by this instrument is a function of the initial particle diameter. For example, if the initial diameter is 75 μm , the end of the program diameter is 0.25 μm . The program may be terminated, however, at a point earlier in the analysis. To measure particles from 63 to 1 μm takes approximately 30 min per sample. The sample concentration used is <2 VOL % (Singer *et al.*, 1988). The appropriate settling rates for various particle sizes are computed before commencing the analysis, using Stokes' Law. A vertical distance and an elapsed time are selected for each settling rate, such that a particle falling at a certain rate will cover a certain distance in a selected time. Relative particle concentration is then measured at the selected distance and time (Micromeritics Ins. Corp., 1989).

Initially, a homogeneous suspension sample is established in the mixing chamber. A magnetic stirrer located under the mixing chamber retains the particles suspended, by rapidly circulating the mixture. The circulation is then stopped and the relative concentration of particles is measured, at selected vertical distances from the top of the container and at elapsed times after the circulation has stopped. An X-ray beam is provided from a source inside the analyzer. A detection unit is placed directly across from the X-ray source. The analysis cell is placed in the path of the X-ray beam. Particles inside the cell cross the path of the beam, and absorb

X-rays. The amount of absorption at the point in the cell where the beam is located is determined as a percentage of the X-ray absorption, with the highest particle concentration for that sample. Based upon particle settling rates, this percentage is related to the maximum particle size above that point in the cell (Micromeritics Ins. Corp., 1989).

To minimize the time required for analysis, the sample cell is lowered continuously relative to the X-ray beam; thus, effective sedimentation depth decreases with time. This cell movement is synchronized with the X axis of the recorder, to indicate the equivalent spherical diameter corresponding to time and depth (Stein, 1985). The particle size associated with each concentration measurement is the size of the largest particle present, at the height and time of the measurement. All particles larger than that size have higher settling rates, having settled to a lower point in the container. Smaller particles are still present at the same concentrations, just above and below the specified point. Thus, the concentration measured at the specified point is the concentration of particles smaller than or equal to that particular grain size (Micromeritics Ins. Corp., *op.cit.*). The rates of particle settling due to gravity are calculated and the X-ray absorption (concentration) of particles at different heights and points in time are determined. The results of these determinations are provided, finally, as graph and tabular output.

In this study, several samples were analyzed in different size intervals in order to determine the rapid and efficient operational conditions for the SediGraph. Sample solutions were run with size ranges from 63 to 2 μm and 63 to 0.18 μm . The output results were compared by means of cumulative curves and grain size parameters. There were no significant differences in the results, but run times at the shorter size interval takes less time (6 min of 34 min). Comparisons of the two sets of data can be made from Figure A4 to A7 and Table A1. In Figures A4 and A5, tabular outputs of one of the sample which was run within the size range between 63 and 2 μm and 63 to 0.18 μm respectively, are illustrated.

Particle Size Analysis Solent		PAGE 1
SediGraph 5100 V2.01		
SAMPLE DIRECTORY/NUMBER: DIREC3 /125	UNIT NUMBER: 1	
SAMPLE ID: 8	START 15:16:19 08/23/90	
SUBMITTER: Southampton University	REPRT 15:22:41 08/23/90	
OPERATOR: Oya Algan	TOT RUN TIME 0:06:05	
SAMPLE TYPE: clay/silt OYA	SAM DENS: 2.6500 g/cc	
LIQUID TYPE: Water	LIQ DENS: 0.9942 g/cc	
ANALYSIS TEMP: 34.6 deg C	LIQ VISC: 0.7280 cp	
RUN TYPE: High Res		
STARTING DIAMETER: 63.00 μ m	REYNOLDS NUMBER: 0.42	
ENDING DIAMETER: 1.95 μ m	FULL SCALE MASS %: 100	
MASS DISTRIBUTION		
MEDIAN DIAMETER: NOT AVAILABLE	MODAL DIAMETER: 1.38 μ m	
DIAMETER (μ m)	CUMULATIVE MASS FINER (%)	MASS IN INTERVAL (%)
63.00	99.6	0.4
31.20	98.6	1.0
15.60	94.3	4.3
7.80	89.3	5.0
3.90	82.3	7.1
1.95	74.0	8.2

Figure A4: Tabular output of a sample run within size range of 63 to 2 μ m.

Particle Size Analysis Solent		PAGE 1
SediGraph 5100 V2.01		
SAMPLE DIRECTORY/NUMBER: DIREC3 /69	UNIT NUMBER: 1	
SAMPLE ID: 8	START 14:35:07 05/29/90	
SUBMITTER: Southampton University	REPRT 15:09:26 05/29/90	
OPERATOR: Oya Algan	TOT RUN TIME 0:34:04	
SAMPLE TYPE: clay/silt OYA	SAM DENS: 2.6500 g/cc	
LIQUID TYPE: Water	LIQ DENS: 0.9942 g/cc	
ANALYSIS TEMP: 34.6 deg C	LIQ VISC: 0.7286 cp	
RUN TYPE: High Speed		
STARTING DIAMETER: 63.00 μ m	REYNOLDS NUMBER: 0.42	
ENDING DIAMETER: 0.18 μ m	FULL SCALE MASS %: 100	
MASS DISTRIBUTION		
MEDIAN DIAMETER: 0.34 μ m	MODAL DIAMETER: 0.18 μ m	
DIAMETER (μ m)	CUMULATIVE MASS FINER (%)	MASS IN INTERVAL (%)
63.00	97.2	2.8
31.20	95.4	1.8
15.60	91.9	3.5
7.80	86.3	5.6
3.90	79.7	6.6
1.95	71.6	8.1
0.98	64.4	7.2
0.49	55.9	8.5
0.25	44.3	11.7
0.18	37.4	6.8

Figure A5 : Tabular output of the same sample as Figure A4, but run within a size range of 63 to 0.18 μ m.

The cumulative mass finer (%) than a particular size (*i.e.* $> 1.95\mu\text{m}$ ($\sim 2\mu\text{m}$)) is very similar (74% and 71.6%, respectively) in the two outputs. The mass (%) in interval is also almost the same (8.2 and 8.1 for $1.95\mu\text{m}$). The graphic outputs of the two runs illustrated in Figure A6.

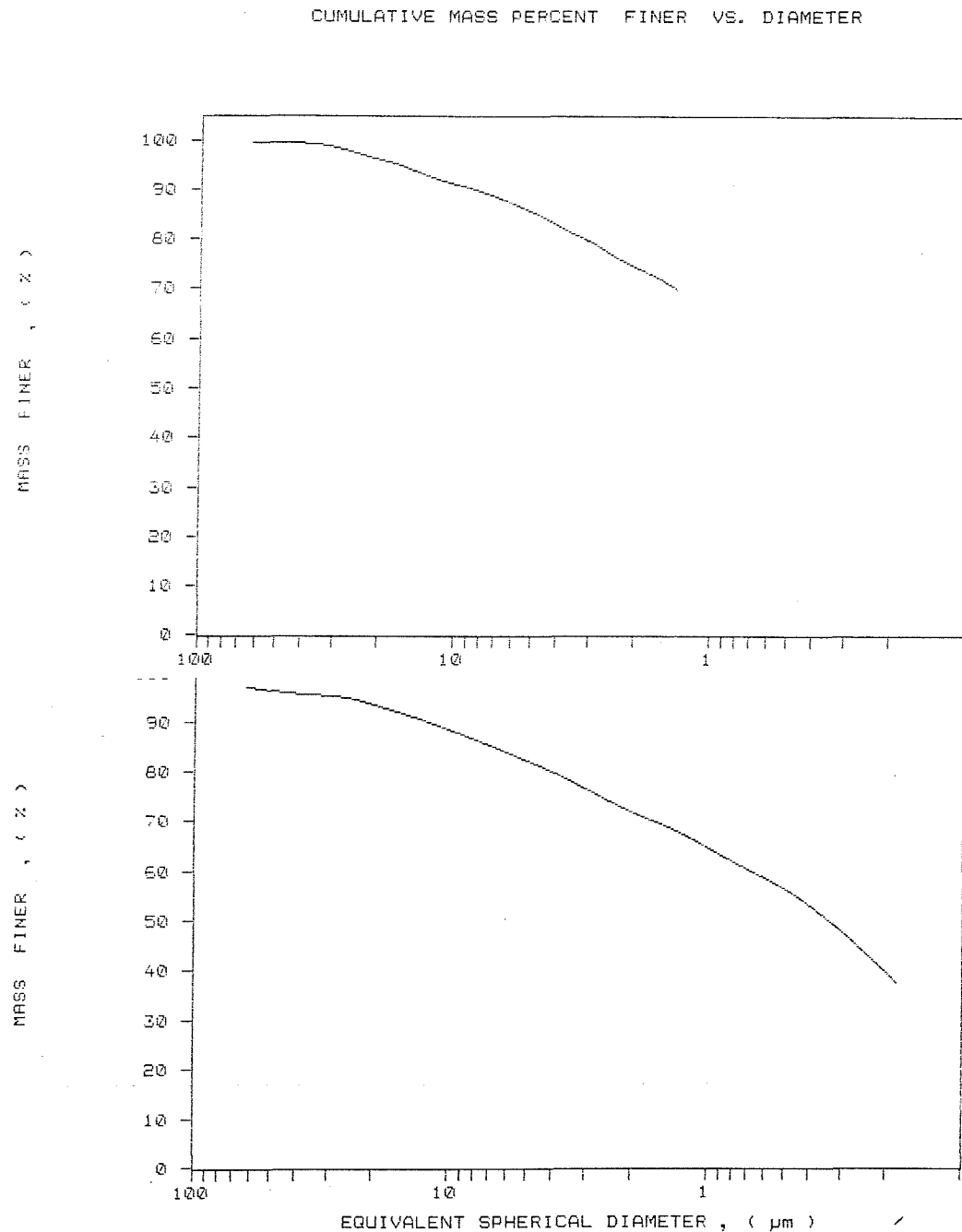


Figure A6 : Graphic outputs of the same sample of Figure A4 (upper) and Figure A5 (lower).

Cumulative frequency curves of the two run are illustrated in Figure A7. The curve termination at 10ϕ ($2\mu\text{m}$) shows the result of first (short) run. Statistical parameters were calculated from this plot of the two run and are compared in Table A1. The correlation coefficients between the parameters derived from the 2 analysis are: mean $r=0.99$; sorting $r=0.92$; skewness $r=0.98$; and kurtosis $r=0.99$. The descriptives of the parameters are, in most cases, the same.

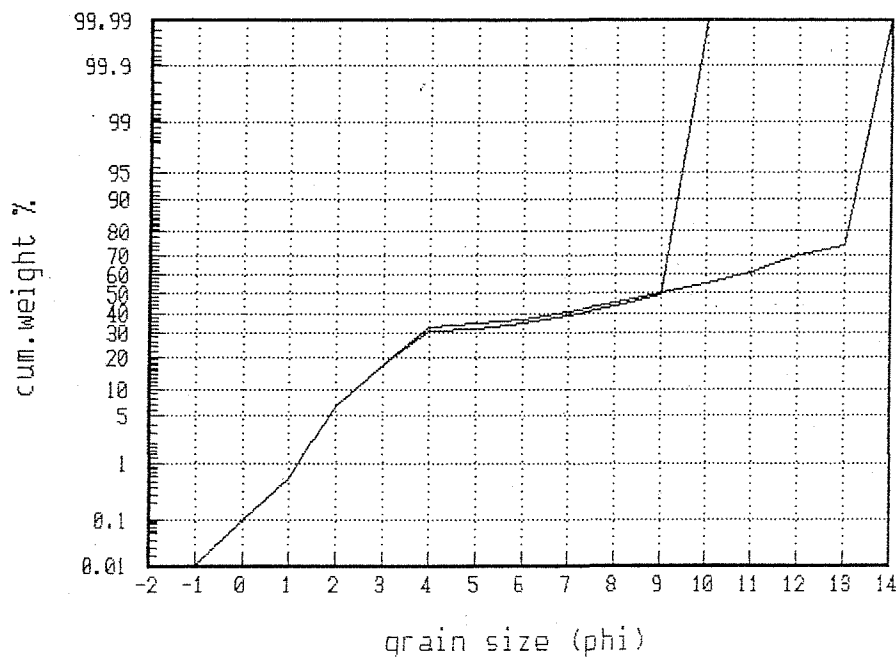


Figure A7 : *Cumulative frequency curves of the same sample.*

Table A1 : Comparison of statistical parameters of the samples analysed in the SediGraph over different size intervals.

Sample No	Mean	Sorting		Skewness		Kurtosis	
R1	0.70	3.0	vp	0.49	vp	1.55	vlepto
R1.1	0.50	2.99	vp	0.29	p	1.27	lepto
R2	3.17	5.54	ep	0.41	vp	0.72	platy
R2.1	2.80	4.69	ep	0.29	p	0.55	vplat
R3	3.17	6.34	ep	0.64	vp	0.87	platy
R3.1	2.03	4.87	ep	0.53	vp	0.64	vplat
R11	9.10	3.91	vp	-0.39	vn	0.71	platy
R11.1	7.38	2.40	vp	-0.84	vn	0.69	platy
R24	4.84	4.07	ep	0.66	vp	0.90	meso
R24.1	4.50	3.25	vp	0.57	vp	0.79	platy
4	9.45	2.99	vp	-0.41	vn	0.96	meso
4.1	8.20	1.76	p	-0.86	vn	1.24	lepto
8	8.50	4.50	ep	-0.38	vn	0.98	meso
8.1	7.08	2.99	vp	-0.91	vn	1.38	lepto
12	8.32	4.27	ep	-0.17	n	0.49	vplat
12.1	7.07	2.74	vp	-0.89	vn	0.55	vplat
17	8.72	4.24	ep	-0.38	vn	0.54	vplat
17.1	7.15	2.71	vp	-0.89	vn	0.60	vplat
21	8.50	4.17	ep	-0.25	vn	0.50	vplat
21.1	7.17	2.64	vp	-0.88	vn	0.52	vplat
H12	2.52	1.65	p	0.47	vp	7.19	exlep
H12.1	2.53	1.29	p	0.37	vp	5.94	exlep
H14	4.53	5.79	ep	0.34	vp	0.57	vplat
H14.1	3.53	4.47	ep	0.14	p	0.48	vplat
H19	6.17	7.54	ep	-0.63	vn	0.45	vplat
H19.1	5.48	4.74	ep	-0.90	vn	0.46	vplat

Sample no.1 denotes the short running of the sample. In Sorting Column: vp=very poor; ep=extremely poor; p=poor. In Skewness Column, vp=very positive; p=positively; vn=very negative; n=nearly symmetrical. In Kurtosis Column, lepto=leptokurtic; platy=platykurtic; vplat=very platykurtic; meso=mesokurtic; exlep=extremely leptokurtic.

A3. DETERMINATION OF CLAY MINERALS

X-Ray Diffraction

The basic principle of X-ray diffraction analysis is the "reflection" of X-rays by atomic planes in crystals, through an angle which is related quantitatively to the distance of separation of the atomic planes. X-rays are electromagnetic radiation of the same nature as light, with a much shorter wave length (Eslinger & Pevear, 1988).

X-rays are produced by the bombardment of a metal anode (the target) by high energy electrons, from a heated filament in a Roentgen X-ray tube (Hardy & Tucker, 1988). Radiation of a single wavelength is achieved by the use of a β filter or, alternatively, by using a crystal monochromater. The β filter consists of a thin metal foil, which is positioned in the X-ray beam after the beryllium window of the X-ray tube (Hardy & Tucker, *op.cit*).

Diffraction is performed by a goniometer. In the goniometer, X-rays are collimated to produce a subparallel beam. The divergent beam is focused at the sample, which is rotated at a regular speed (in degrees per minute). Mineral planes in the sample oriented at the appropriate angle diffract X-rays according to Bragg's Law:

$$n\lambda = 2d\sin\theta, \text{ where}$$

$$n = \text{integer}$$

$$\lambda = \text{wavelength of the X-rays}$$

$$d = \text{lattice spacing in \AA, and}$$

$$\theta = \text{angle of diffraction}$$

The direction of the primary X-ray beam remains constant, as the sample rotates around an axis normal to the primary beam (Lindholm, 1987). The goniometer arm and the attached detector tube rotate at twice the rate of the sample; thus, as the sample rotates through an angle of θ , the detector tube rotates through 2θ . The diffracted beam passes through a receiving slit and collimator. A scatter slit

is introduced also, to reduce any scattered X-rays from entering the detector tube. The signal produced by the X-ray photons on the detector is first amplified, then passed on to the electronic recording equipment (Hardy & Tucker, 1988). Output from the diffractometer may be in digital form, or as a strip chart recording the intensities with respect to 2θ . Microcomputers may be used also, permitting completely automated instrument operation and data processing (Hardy & Tucker, *op.cit.*). An example of the output of an XRD Phillips PW 1130 (used in this study) is presented as Figure A8.

Identification of Clay Minerals by XRD

Each clay mineral group has a particular type of layer structure and possesses a distinctive set of lattice spacings (Eslinger & Pevear, 1988; Lindholm, 1987). These lattice planes diffract at different angles, according to the Bragg equation. Hence, X-ray diffraction produces a unique series of reflections (peaks) on the diffractogram. This unique character is based upon the position of each reflection (as measured by 2θ) and the intensity of each reflection. The basal reflections allow identification of the minerals present in a clay sample.

Sample Preparation Techniques

The clay fraction ($<2\ \mu\text{m}$) is extracted and disaggregated, with a dispersing agent and/or by ultrasonic vibration. It is recommended that carbonates and organic matter are removed chemically (Hardy & Tucker, *op.cit.*). There are two types of sample orientation used commonly in X-ray diffraction (Lindholm, *op.cit.*): (i) oriented samples (where clay minerals lie with their basal planes parallel to the sample holder); and (ii) unoriented samples, where the lattice planes should be as randomly oriented as possible. There are many mounting techniques for preparing oriented samples such as pipetting onto a glass slide, centrifugation onto a ceramic tile, suction onto a ceramic tile and smearing onto a glass slide (Gibbs, 1965). Gibbs (*op.cit.*), Drever (1973) and Stokke & Carson (1973) have demonstrated that smearing onto a glass slide, suction onto a ceramic tile and powder press techniques

fulfilled the requirements of precision and accuracy of the analysis. The other techniques, based upon sedimentation of the material onto a glass slide or a ceramic tile, either by natural settling or by centrifuging, can cause size separation of the clay particles (Mc Manus, 1991).

Identification of the major clay minerals is performed by X-raying samples with four different treatments (Lindholm, 1987): (i) after air drying; (ii) after immersion in ethylene glycol vapour at 55°C; (iii) after heating to 375°C for 4 hours or 12 hours; and (iv) after heating to 550°C overnight. This method is followed in order to differentiate clay minerals which have similar lattice structures. The four principle clay mineral groups have the following basal spacings: kaolinite 7 Å; illite 10 Å; smectite 12-15 Å; chlorite 14 Å; and mixed layer minerals at intermediate or higher values (see Table A2) (Hardy & Tucker, 1988; Brown & Brindley, 1980). Identification of the minerals can be achieved by reference to the International Index or Comprehensive Table of Consecutive Lattice Spacings for the common clay minerals (Hardy & Tucker, *op.cit*). In this study, where the clay content was well known, only the glycolated traces were run in order to save time.

Table A2 : Basal Spacings of Clay Minerals (after Brown & Brindley, 1980).

Mineral	Air-dried	Glycolated	300-350°C	500-600°C
Illite	10 Å	10 Å	10 Å	10 Å
Smectite	15 Å	17 Å	10 Å	10 Å
Kaolinite	7 Å	7 Å	7 Å	-
Chlorite	14 Å	14 Å	14 Å	14 Å

Semi-Quantitative Estimation

The relative clay mineral content of a mixture can be determined by comparing the intensities of the strong reflections. The most common quantitative estimation of clay mineral abundance is to assume that the sum of the weighted peak areas of the clay minerals represents 100 % of the $<2\ \mu\text{m}$ material (Mc Manus, 1991). However, a number of factors complicate the quantification of the clay mineral content (Lindholm, 1987). The X-ray response for a particular clay mineral is dependent strongly upon, amongst other things, grain size, crystallinity, structure and chemical composition. For example, a sample containing equal amounts of illite, montmorillonite, and kaolinite will produce a diffractogram in which the kaolinite reflection is one and half times to twice as intense as the illite reflection, whereas the montmorillonite reflection is three to four times as intense as the illite peak. Additionally, sample pretreatment and treatment may also affect the relative peak intensity (Lindholm, *op.cit*). Pierce & Siegel (1969) determined five different calculation methods in semi-quantitative clay mineral studies, finding no uniformity among the results. The method which is most commonly used, proposed by Biscaye (1965), is to normalize the peak areas as follows: peak area of montmorillonite; 4 times the peak area of illite; and twice the peak area of kaolinite. Heath & Pisias (1979) used an internal standard which was 10 % talc, to estimate semi-quantitatively the clay mineralogy. This particular study showed little correlation between the clay percentages obtained with the internal standard and the percentages derived from Biscaye's method.

The estimation method utilised in present investigation is a modification of the Biscaye (1965) method: smectite, illite and kaolinite were divided by factors of 2.5, 1, and 2, respectively (Clayton, 1992). Modification was made to the factors used because of the different slits used in the present XRD (*i.e.* Phillips PW 1130) and those used by Biscaye.

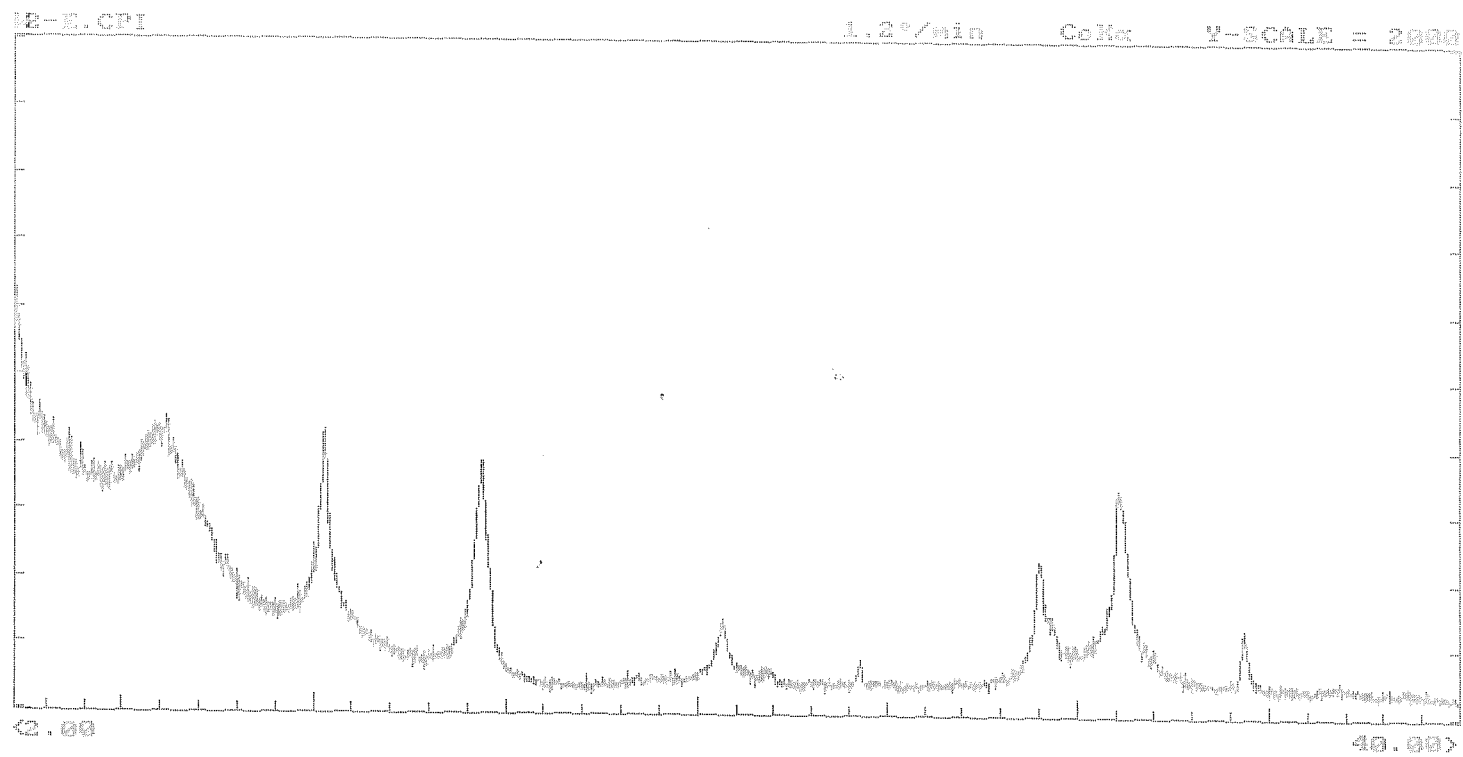


Figure A8 : *Representative XRD output of a Solent sediment sample (< 2 μ m).*

A4. DETERMINATION OF ELEMENTS

Atomic Absorption

AAS is used for the elemental analysis of rocks, sediments, minerals and water. The basic principle of AAS is the absorption of radiant energy by ground state atoms. When a substance containing small amounts of metallic elements is dispersed as an atomic vapour, it possesses the property of absorbing particular radiations. These radiations are identical in wavelength to those which the substance can emit (Fairchild *et al.*, 1988). AAS instrumentation requires a light source, a flame, an atomizer and a photomultiplier to measure the transmitted radiation. A monochromator inserted between the flame and the detection device isolates any interfering light. Radiation is produced by hollow cathode lamps. A graphite furnace can be used to examine elements at very low concentrations. The flame is fuelled by a mixture of two gases, usually a combination of acetylene, air, nitrous oxide, oxygen and hydrogen (Fairchild *et al.*, 1988). Air-acetylene is used for the majority of elements, since interferences are reduced and the signal/noise ratio is improved. The maximum temperature of the air-acetylene flame is 2600 K (Pye Unicam, 1979). Nitrous oxide-acetylene permits a large number of refractory oxide-forming elements to be determined, such as Ca and Al.

There are various interferences, namely spectral, matrix, chemical, ionization and background. The effects of interferences are observed as an enhancement or depression of the analysed signal (Viets & O'Leary, 1992). Spectral interferences are caused by overlapping absorption or emission spectra and can be resolved by choosing alternate wavelengths. Matrix interference may arise, if the sample and calibration standard matrix differ in composition. This interference can be corrected by preparing calibration standards matching the sample composition or by using the method of standard additions (Fletcher, 1981; Viets & O'Leary, *op.cit.*). Chemical interference may be caused by incomplete dissociation of refractory compounds during the atomization step, or by interferents reacting to form preventing the

formation of neutral ground state atoms (Varion Techtron). This problem can be solved by using a hotter flame to decompose the thermally stable form, or by adding an excess amount of an element which will form a thermally-stable compound with the interferent. Ionization has been found to be the most prevalent interference in determination of alkali and alkali earth elements. This can be overcome by including more readily ionized elements, such as K or Cs, in all solutions, (Pye Unicam, 1979; Viets & O'Leary, *op.cit*). Background interference is a type of spectral interference that occurs when molecular species absorb light over a broad spectral range. It arises also when small light-scattering particles pass through the sample cell, giving an apparent atomic absorption signal. An operational mode, background correction, is found commonly on most AAS; this can be used to eliminate the latter problem (Viets & O'Leary, *op.cit*).

Sample Preparation and Analysis

Samples are presented to the AAS machine in solution. The instrument is calibrated by standards of known concentrations (Table A3). Multi-element standards in 1 M HCl were used, in order to match the sample solution. This is necessary to avoid matrix interferences. Table A4 shows the effect of different matrixes on the measured Al concentrations; the most accurate value for the Al content of the reference solution is obtained with the standard which contains a similar composition to that of the sample (Al + Metals).

1 M HCl (diluted with Millique Water) is used as a blank, in which metals are usually negligible. Standard solution absorbances are measured and a calibration line is constructed. This relationship should be a straight line, but at higher concentrations it may be curvilinear. Sample solution concentrations can be calculated, by converting absorbance to concentration from the formula of the calibration line. The ability of an AAS to produce consistent and precise results is governed by its calibration (Pye Unicam, 1979). The operating conditions and detection limit of each element for the Pye Unicam are shown in Table A5.

Table A3 : Standard Solutions used in the investigation.

ELEMENT	Concentration ($\mu\text{g/ml}$)	Amount necessary for 100 ml flask (ml)
Al	200	20
	400	40
	600	60
	800	80
Co	0.5	0.05
	1	0.1
	2	0.2
Cr	2	0.2
	4	0.4
	8	0.8
Cu	0.5	0.05
	1	0.1
	2	0.2
Fe	20	2.0
	30	3.0
	40	4.0
K	200	20
	400	40
	600	60
	800	80
Mn	5	0.5
	10	1.0
	20	2.0
Ni	1	0.1
	2	0.2
	4	0.4
Pb	1	0.1
	2	0.2
	4	0.4
Zn	0.4	0.04
	1.0	0.1
	1.6	0.16

Standard solutions were prepared by using metal solutions at $1000 \mu\text{g ml}^{-1}$. Al was prepared by dissolving 1.758 g of AlKSO_4 into 100 ml of deionized water. K was prepared by dissolving 1.907 g of dried KCl in 1 litre of deionized water.

Table A4 : Accuracy and Precision of the Various Standard Solutions.

Al Standard Solution	Detected Concentration
Al + Metals	5.9 % \pm 3‰
Al + Cs	6.2 % \pm 3‰
Al alone	6.8 % \pm 4‰
Reference Material CRM 277	4.7 %

Al alone and Al + Cs are prepared by dissolving pure Al wire and dissolving AlKSO_4 into CsCl solution, respectively; these are diluted with 1 M HCl in appropriate concentrations.

Sample solutions are diluted, 1/60 times for Fe and 1/4 times for Al, with 1 M HCl to corresponding detection intervals.

Table A5 : Operating Conditions for the Determination of Various Elements by AAS.

ELEMENT	Al	Co	Cr	Cu	Fe	Mn	Ni	Pb	Zn
Optimum working range ($\mu\text{g/ml}$)	200-800	3-12	2-8	2-8	25-100	15-60	3-12	5-20	0.4-1.6
Sensitivity ($\mu\text{g/ml}$)	3.9	0.066	0.055	0.040	0.55	0.30	0.066	0.11	0.009
Wavelength (nm)	237.3	240.4	357.9	324.7	372.0	403.4	232.0	217.0	213.9
Spectral Band Pass (nm)	0.5	0.2	0.2	0.2	0.2	0.2	0.2	0.2	0.2
Burner Height (mm)	5-8	8-12	8-12	8-12	8-12	8-12	8-12	8-12	8-12
Lamp Current (mA)	10	15	10	5	15	12	15	6	5
Fuel	nitrous-oxide	acetylene	acetylene	acetylene	acetylene	acetylene	acetylene	acetylene	acetylene
Support	acetylene	air	air	air	air	air	air	air	air
Flame Stoichiometry	reducing	oxidizing	reducing	oxidizing	oxidizing	oxidizing	oxidizing	oxidizing	oxidizing

A5. ANALYSIS OF ORGANIC CARBON

A CARLO ERBA E.A. 1108 elemental analyzer (CHNO) was used to determine the total carbon, organic carbon and CaCO_3 content of the sediment samples. The principle of the method is based upon the complete and instantaneous oxidation of the sample by "flash combustion", which converts all the organic and inorganic substances into combustion products.

Performing the Analysis

The analyzer was calibrated with three standards, acetanilide ($\text{C}_8\text{H}_9\text{NO}$), and three blank tin capsules. Acetanilide contains 71.09 % C, 6.71 % H, 10.36 % N, and 11.84 % O. After calibration, a known amount of acetanilide was run as an unknown sample, in order to confirm the calibration and to check for drift. A known amount of dried and homogenized sample (~ 2 mg) was placed into a tin capsule, folded into a small spherical shape and then placed into the autosampler tray (Verardo *et al.*, 1990). Up to 50 samples can be run in a single batch. Acetanilide was analysed after every tenth sample, in order to constrain machine drift and allow estimation of relative and absolute errors. The sample held in the tin capsule is dropped inside the furnace, then purged with a continuous flow of helium. The helium flow is enriched temporarily with pure oxygen, hence, the sample and the container melt and the tin promotes a violent reaction (flush combustion) in a temporary enriched atmosphere of oxygen. Quantitative combustion is achieved then by passing the mixture of gasses over a catalyst layer. The resulting combustion gases pass through a reduction furnace and are directed then to a chromatographic column. The individual components are separated and evaluated as N_2 , CO_2 , water and SO_2 by means of a thermal conductivity detector; this gives an output signal proportional to the concentration of the individual components of the mixture (CARLO ERBA Ins. E.A., 1988). Examples of output spectra for a

standard and an untreated and an acid-treated sample are shown in Figures A9 to A11.

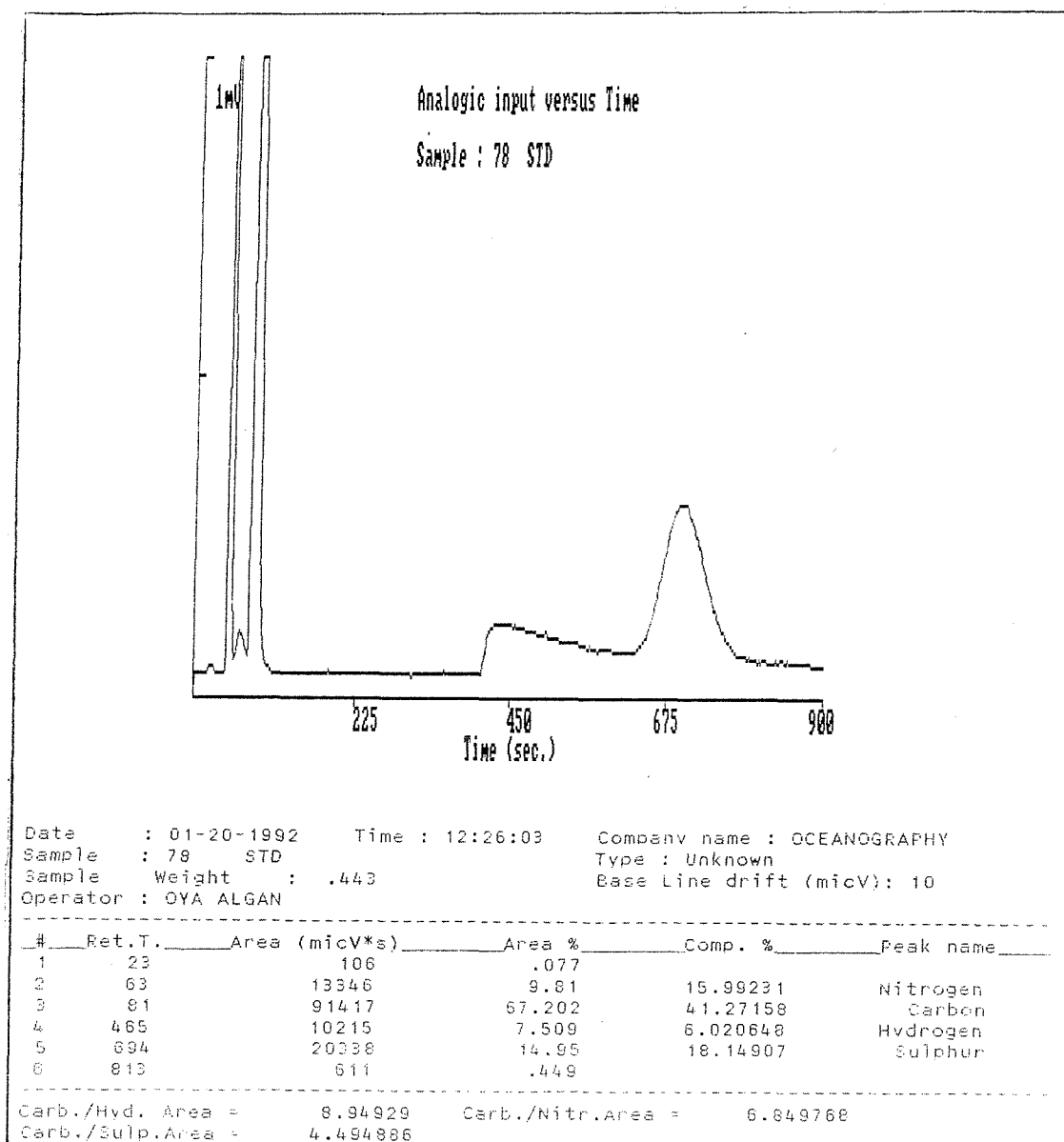


Figure A9 : Example of the Output from the Carlo Erba E.H. 1108 of a Standard, acetanilide.

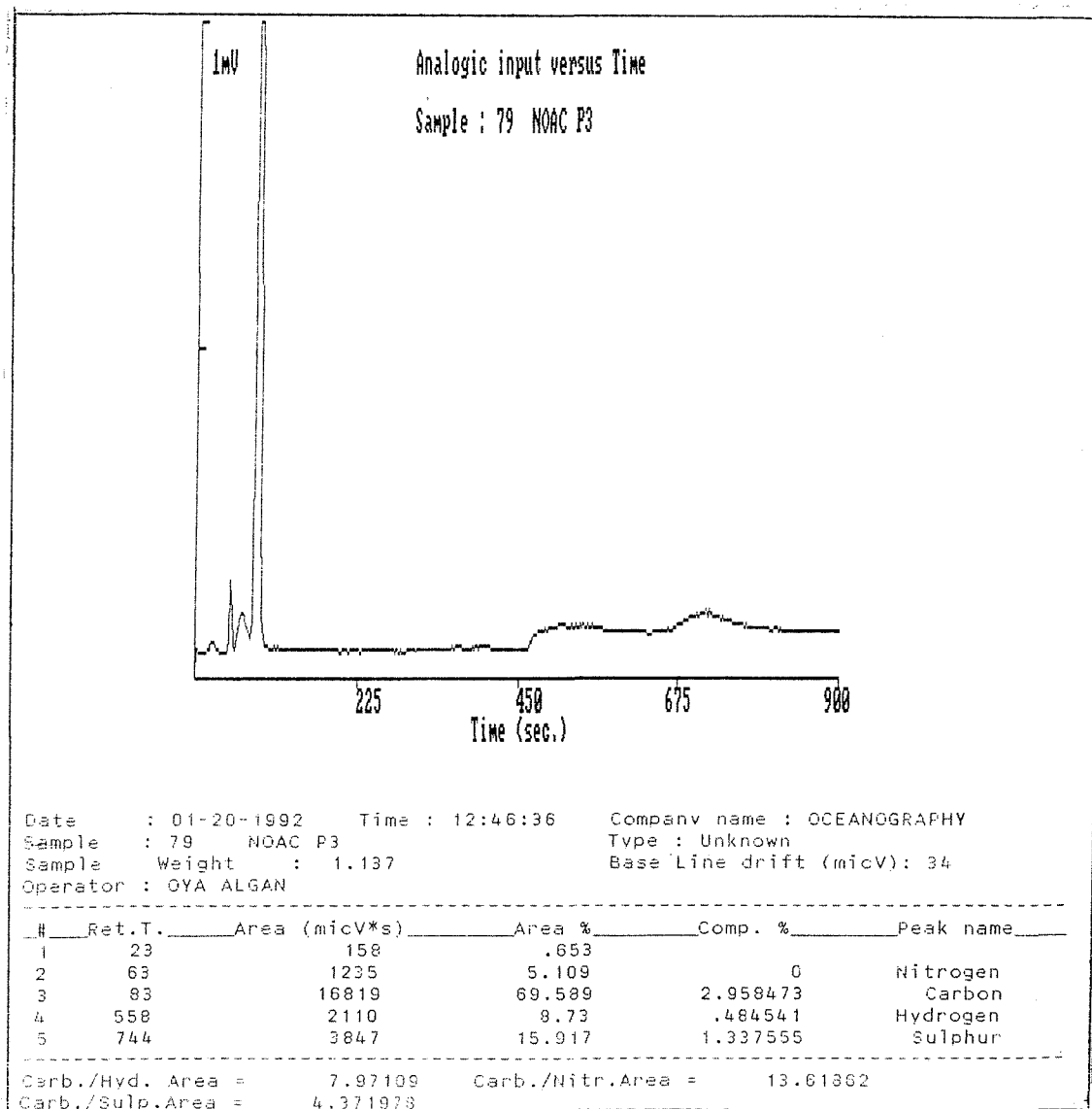


Figure A10 : Example of the Output from the Carlo Erba E.H. 1108 of an Unacidified Sample.

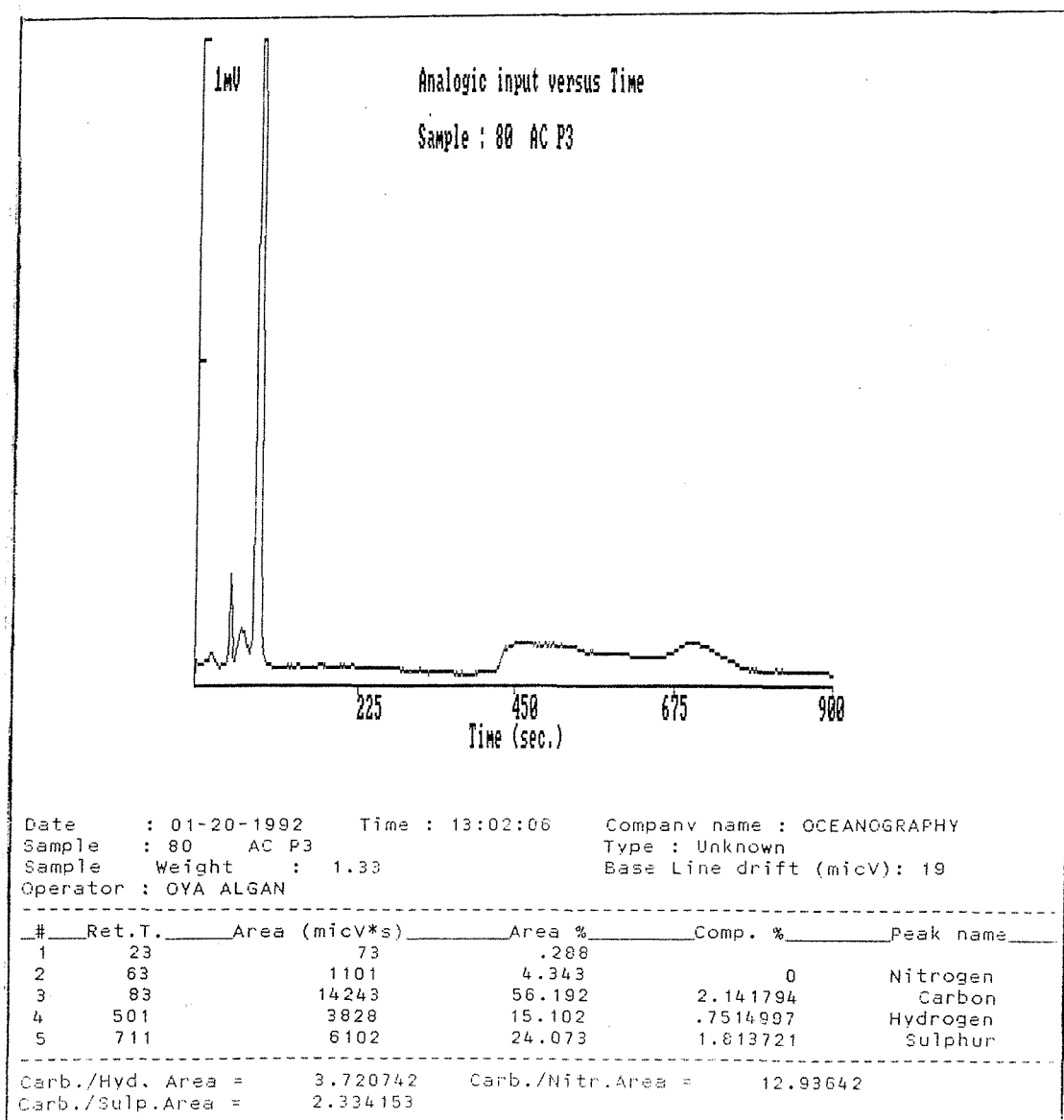


Figure A11 : Example of the Output of the Carlo Erba E.H. 1108 of the Acidified Sample (i.e. the same sample as in Figure A10).

APPENDIX B : Tables and Diagrams

B1. REFERENCE TABLES

Table B1 : Size classification of Sediment Grains (after Leeder, 1982).

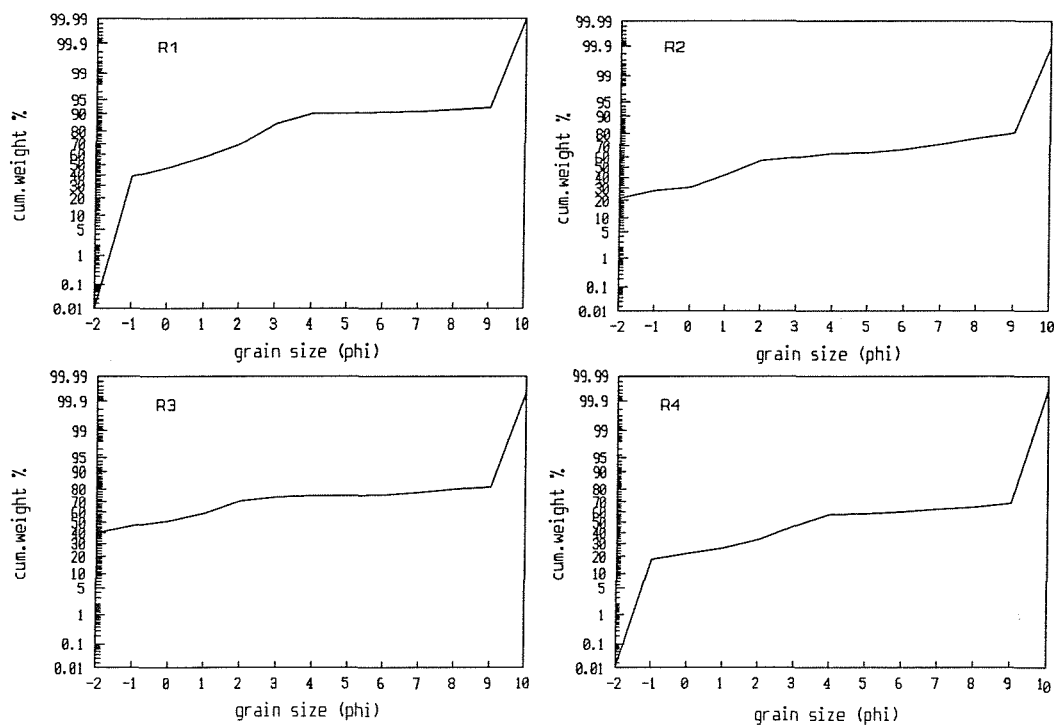
Wentworth Size Class		Milimeter (mm)	phi (ϕ)
GRAVEL		4	-2
	granule	2.83	-1.5
SAND	very coarse sand	2	-1
		1.41	-0.5
		1	0
	coarse sand	0.71	0.5
		0.5	1
	medium sand	0.35	1.5
		0.25	2
		0.177	2.5
	fine sand	0.125	3
		0.088	3.5
SILT	coarse silt	0.0625	4
		0.044	4.5
		0.031	5
	medium silt	0.0156	6
		0.0078	7
	very fine silt	0.0039	8
CLAY	clay	0.002	9
		0.00098	10

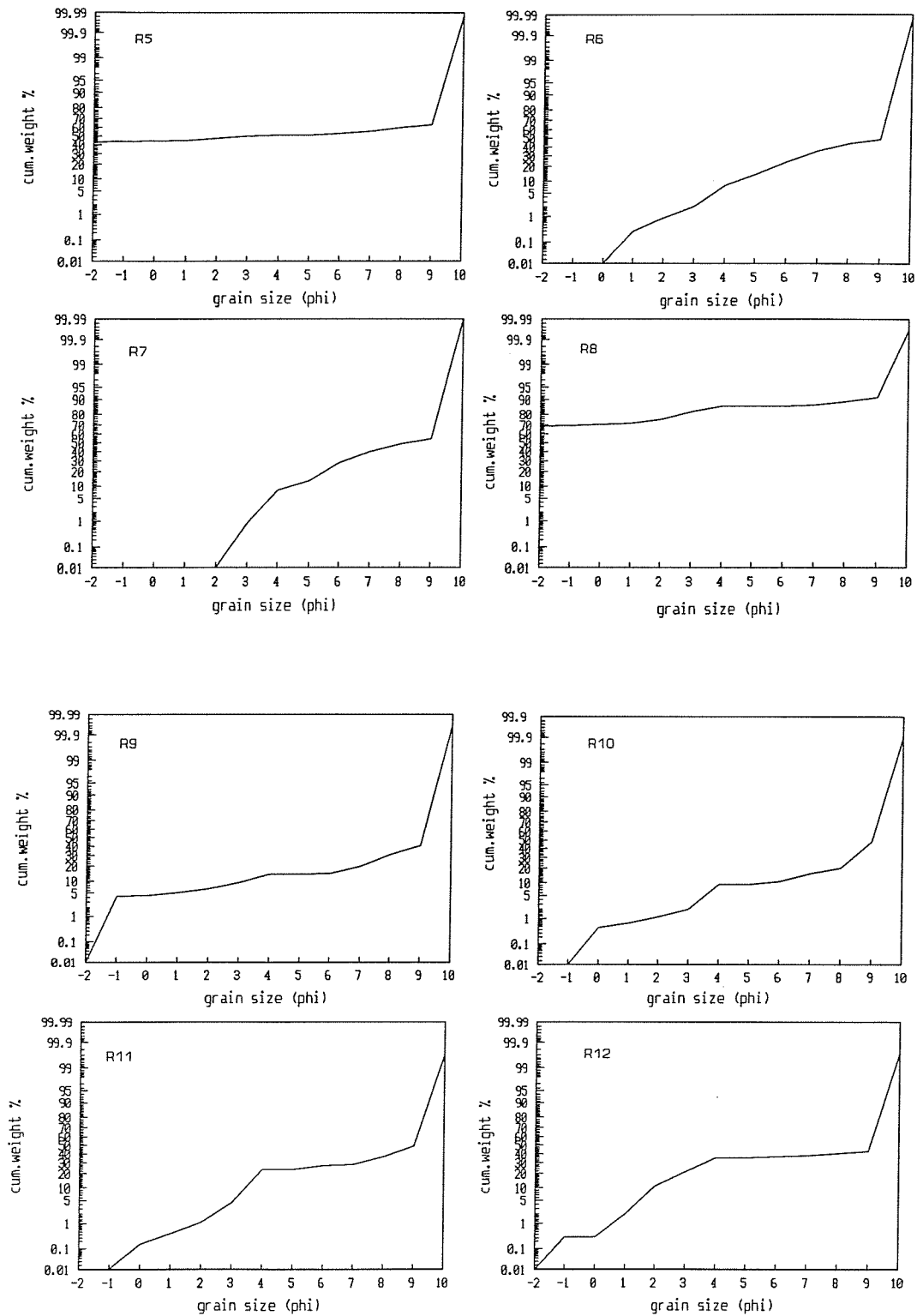
Table B2 : Settling Times used in the Clay Minerals and Grain Size Separation for Trace Metal Analysis (after Galehouse, 1971).

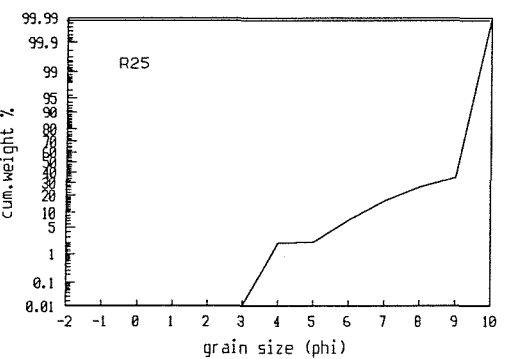
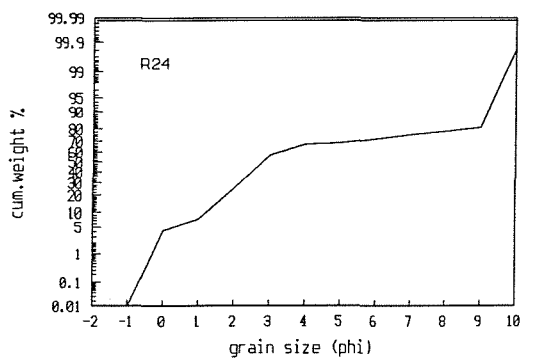
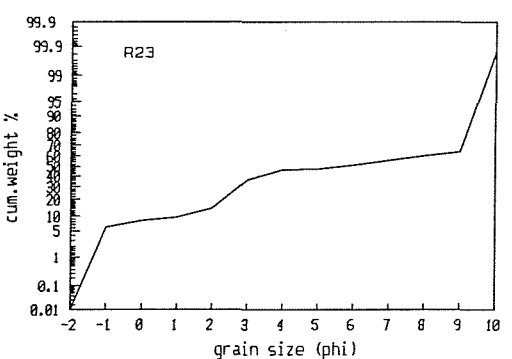
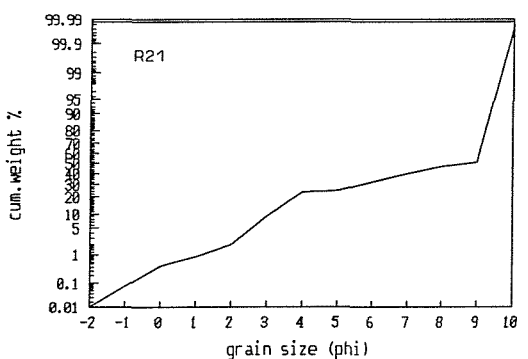
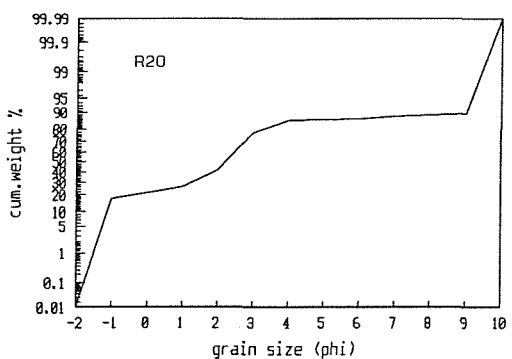
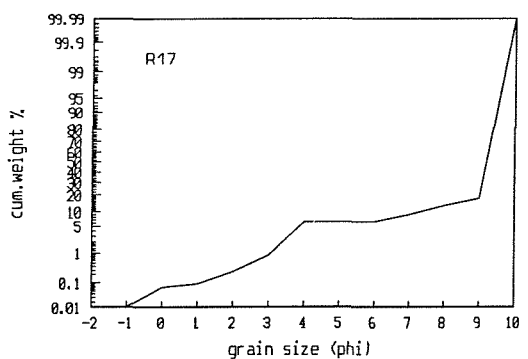
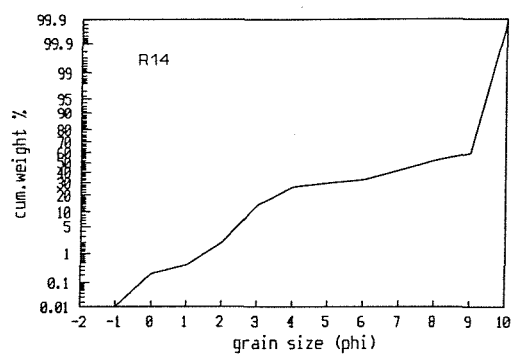
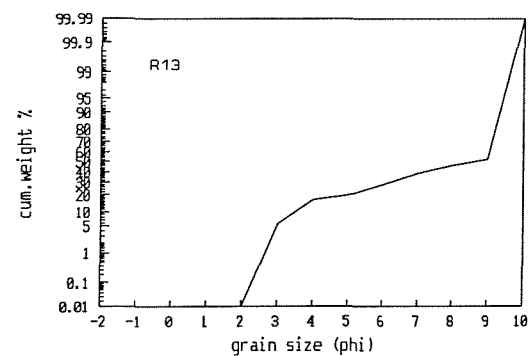
Diameter in (ϕ), finer than	Diameter in Microns, finer than	Size classes	Withdrawal depth (cm)	Elapsed time for withdrawal of sample in Hours (h), Minutes (m), and Seconds (s)					
				18°	19°	20°	21°	22°	23°
4	62.5	silt clay	20	20s	20s	20s	20s	20s	20s
4.5	44.2		20	2m 0s	1m 57s	1m 54s	1m 51s	1m 49s	1m 46s
				restir					
5	31.2		10	2m 0s	1m 57s	1m 54s	1m 51s	1m 49s	1m 46s
5.5	22.1		10	4m 0s	3m 54s	3m 48s	3m 42s	3m 37s	3m 32s
6	15.6		10	8m 0s	7m 48s	7m 36s	7m 25s	7m 15s	7m 5s
7	7.8		10	31m 59s	31m 11s	30m 26s	29m 41s	28m 59s	28m 18s
8	3.9		5	63m 58s	62m 22s	60m 51s	59m 23s	57m 58s	56m 36s
9	1.95		5	4h 16m	4h 9m	4h 3m	3h 58m	3h 52m	3h 46m
10	0.98		5	17h 3m	16h 38m	16h 14m	15h 50m	15h 28m	15h 6m
11	0.49		5	68h 14m	66h 32m	64h 54m	63h 20m	61h 50m	60h 23m

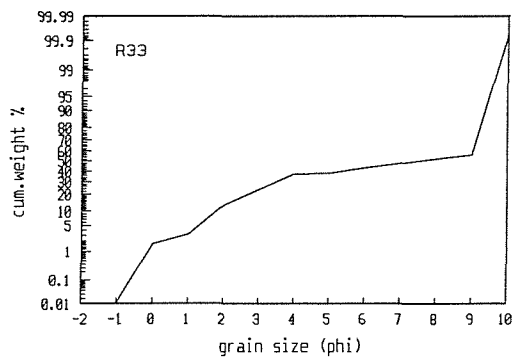
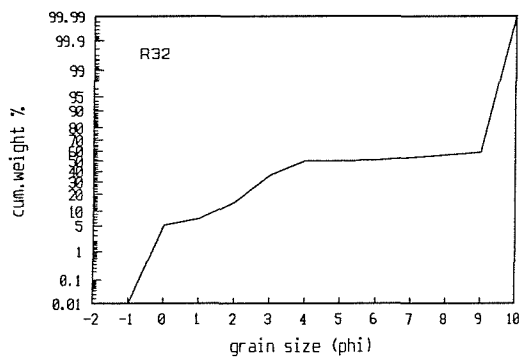
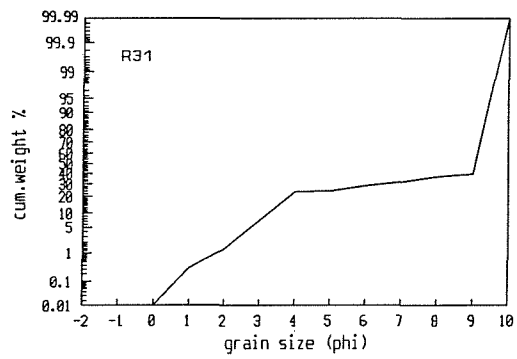
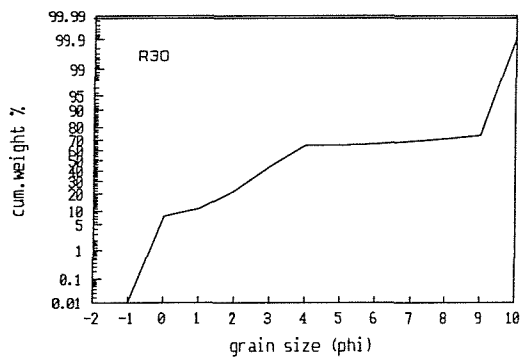
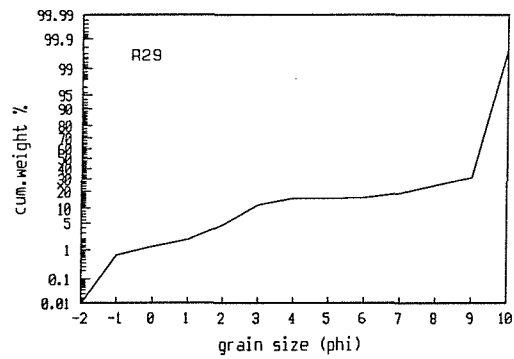
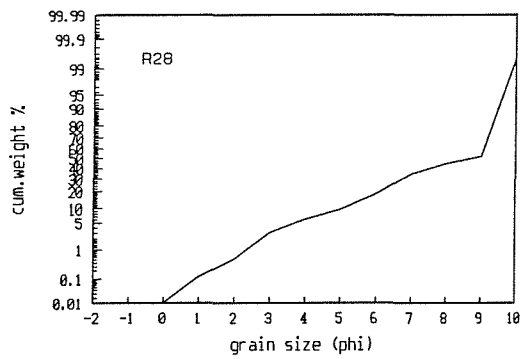
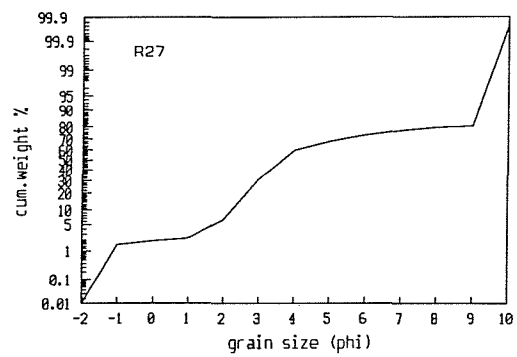
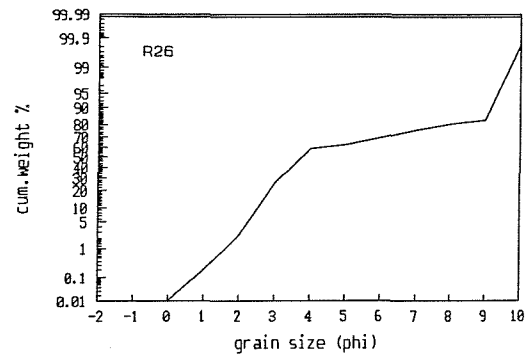
B2. CUMULATIVE CURVES

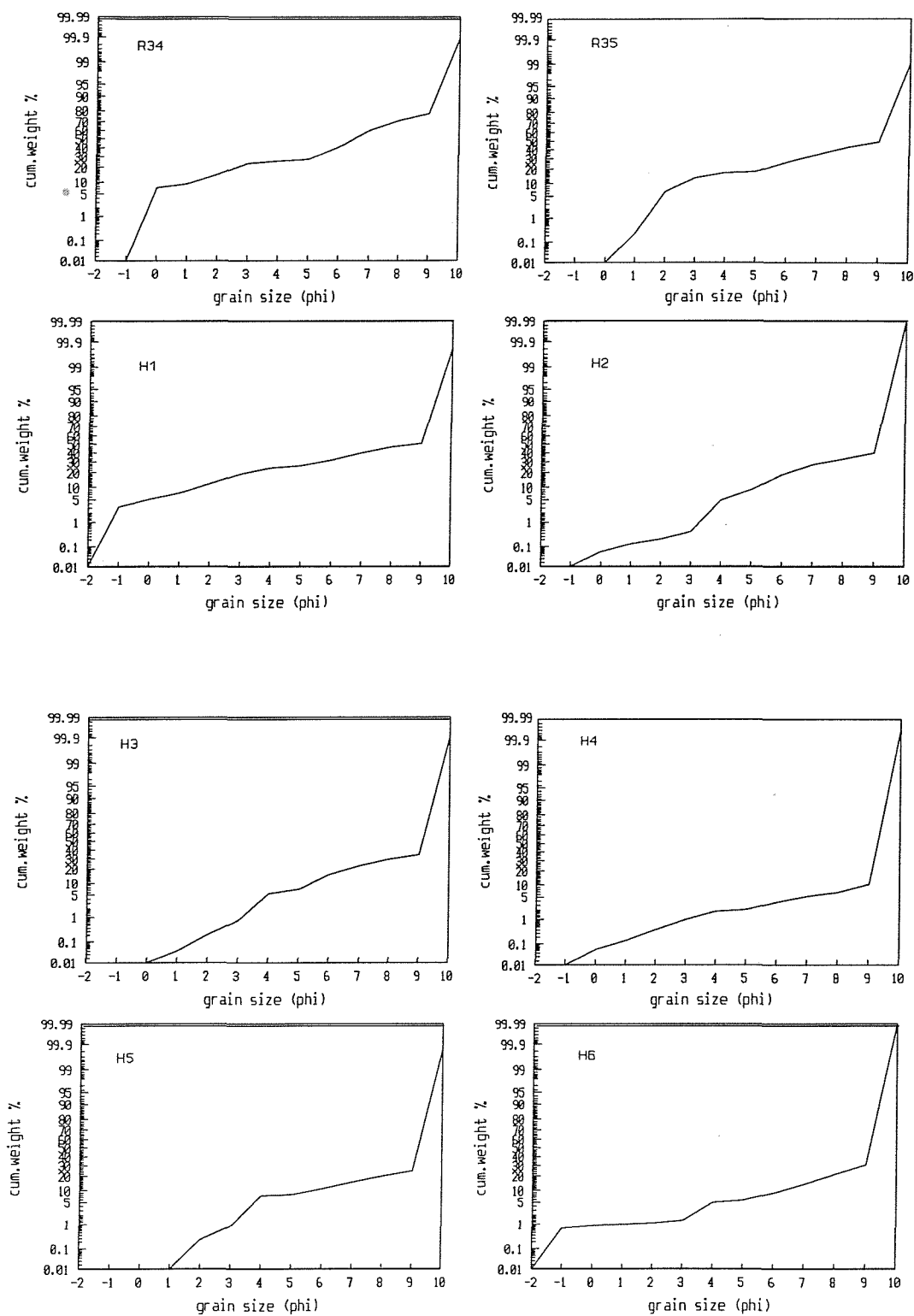
Cumulative curves of all samples displayed in this section were used to derive grain size textural parameters (Section 5.1.3). Curves were plotted on a probability ordinate scale (Muller, 1967; Dyer, 1986; and McManus, 1988). The grain sizes in ϕ corresponding to specified percentile values were read directly from these curves, and entered into the formulae (Chapter 5, Table 5.2) in order to calculate the various grain size textural parameters.

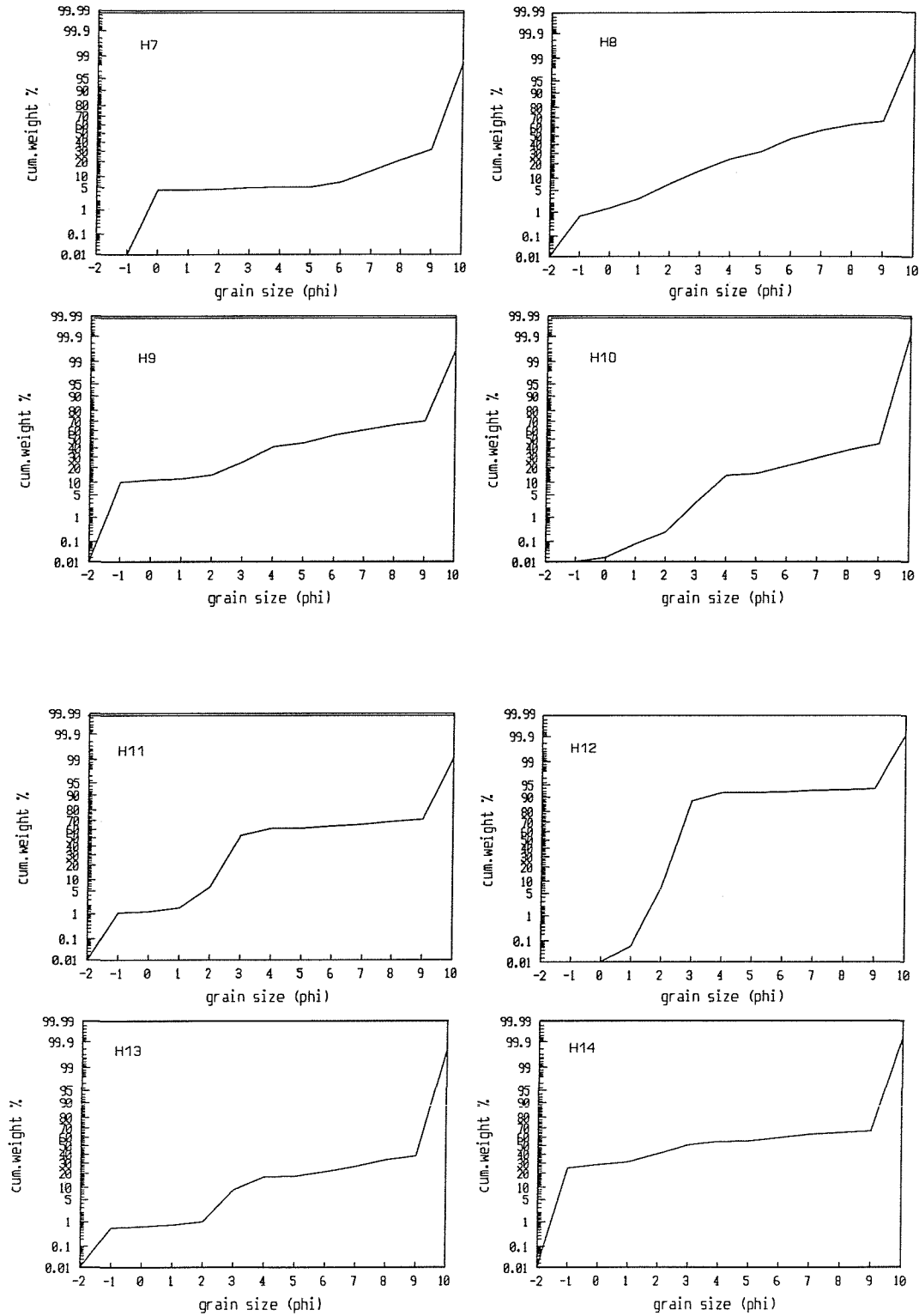


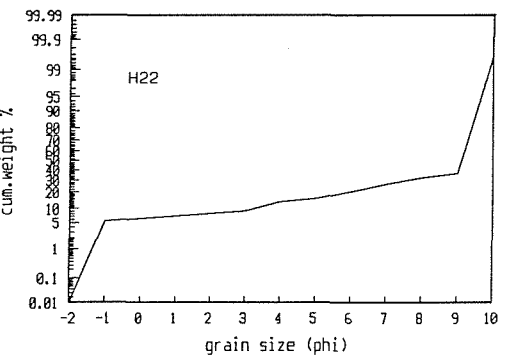
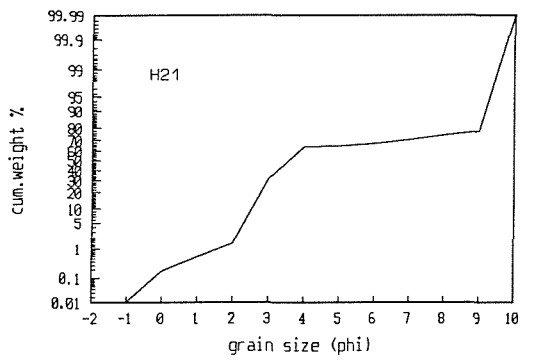
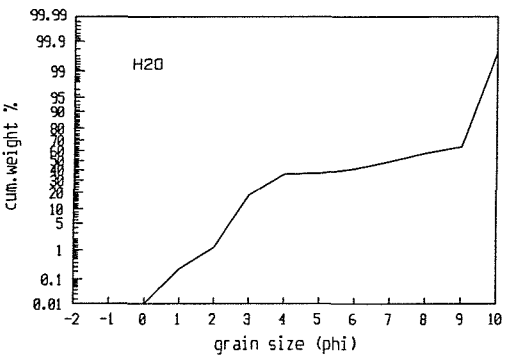
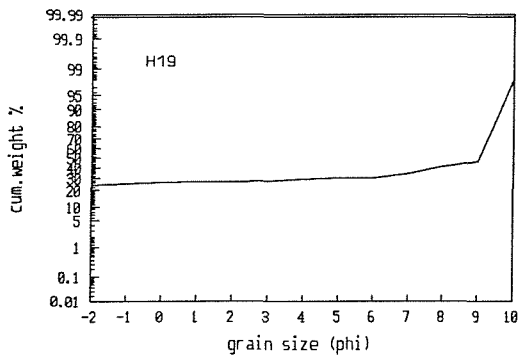
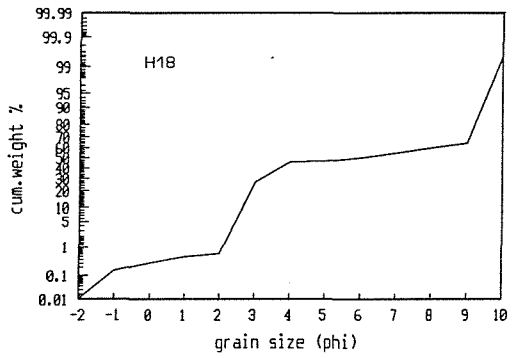
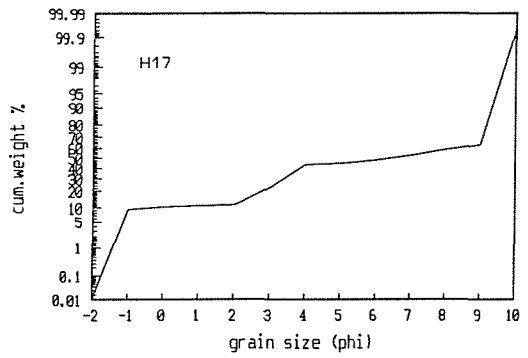
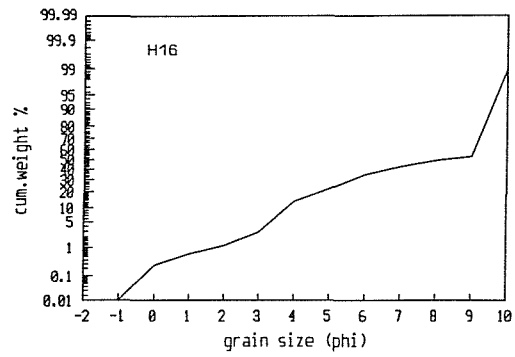
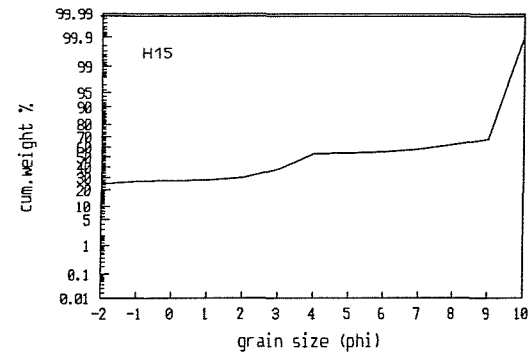


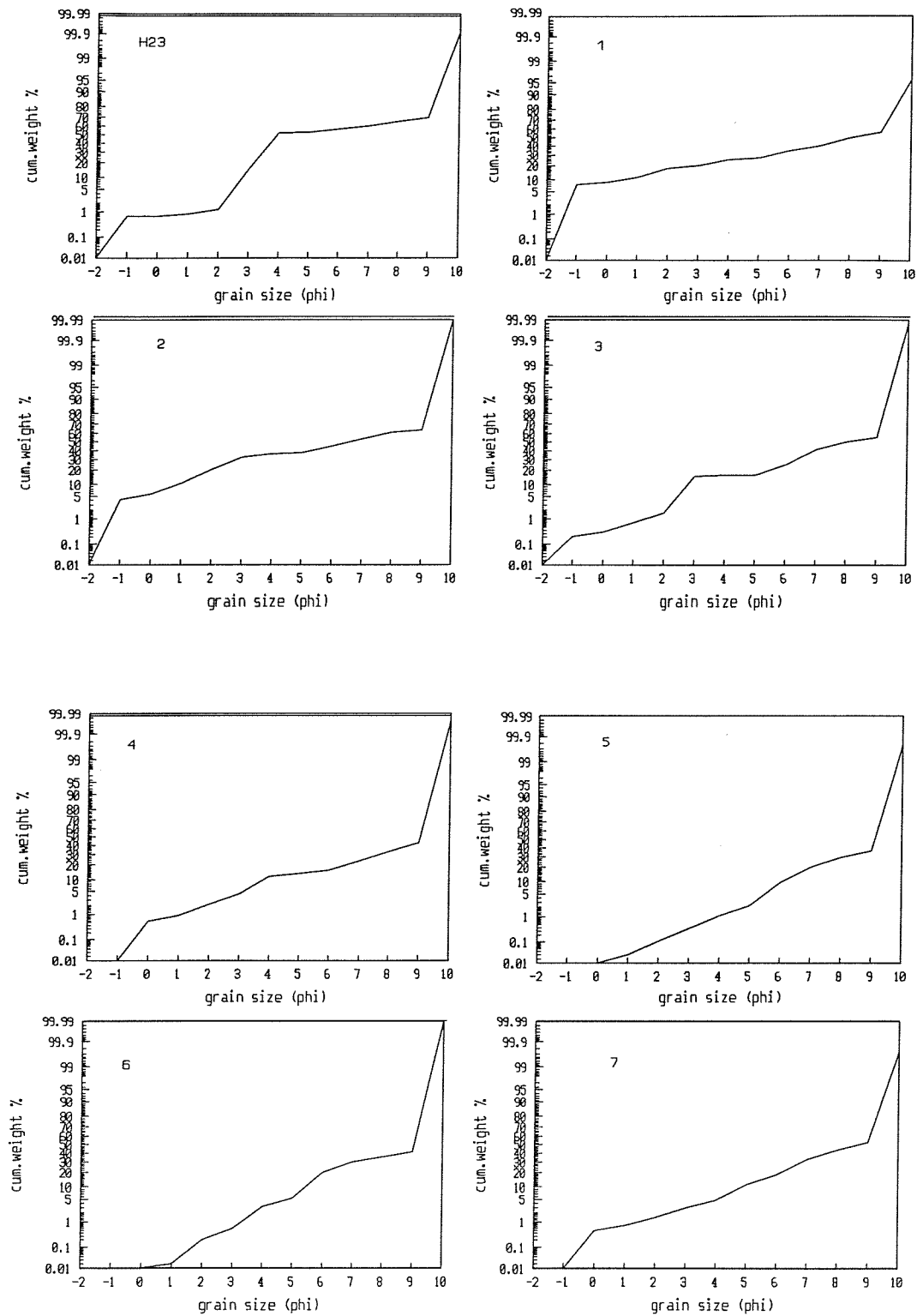


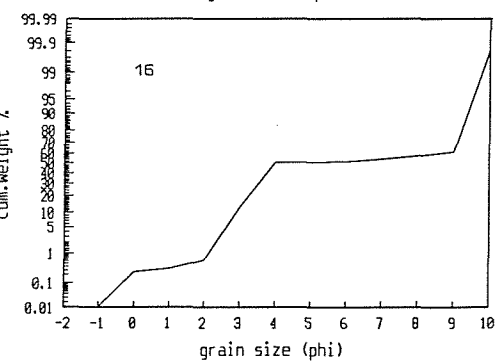
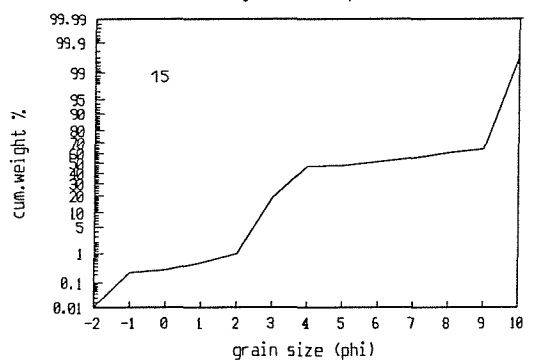
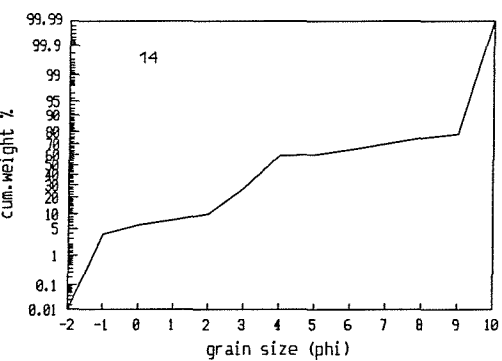
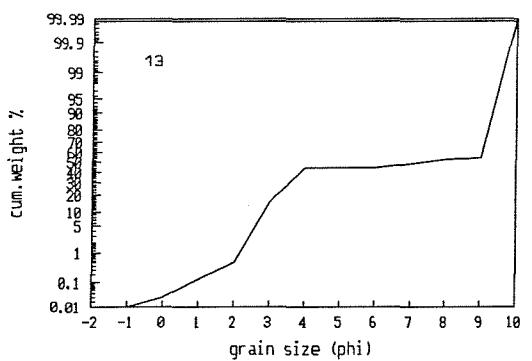
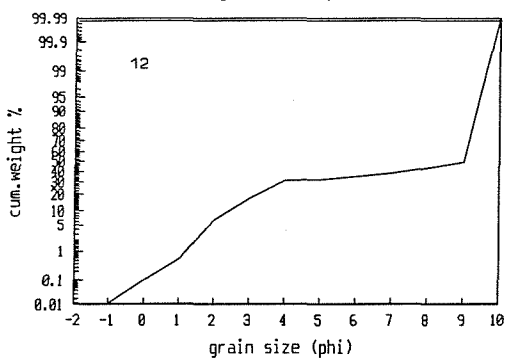
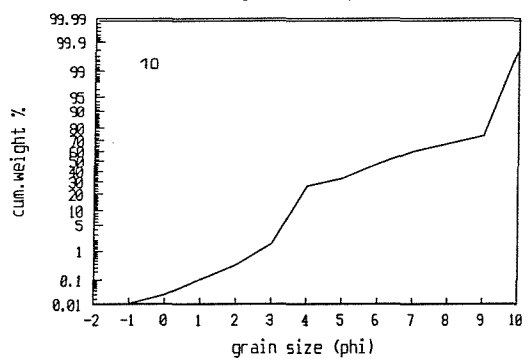
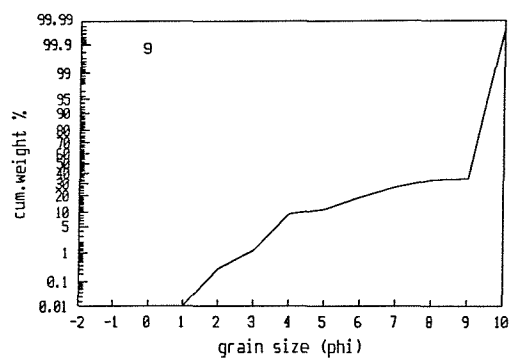
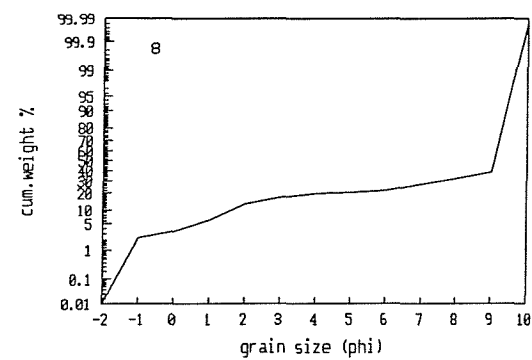


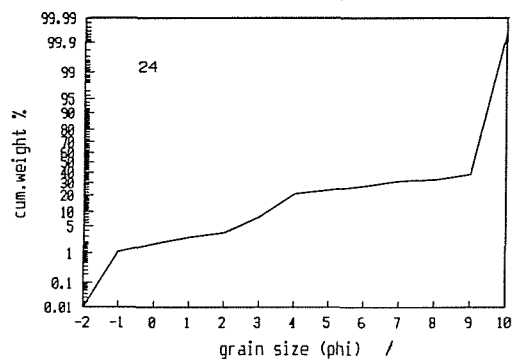
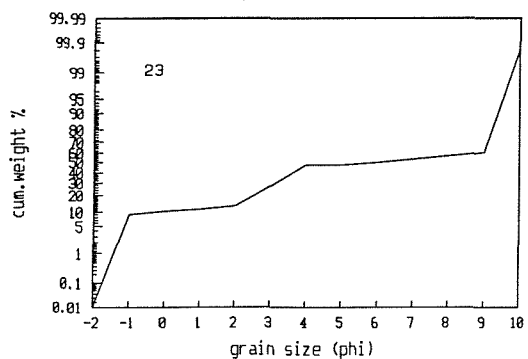
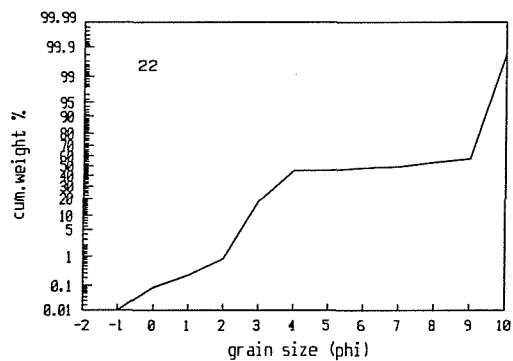
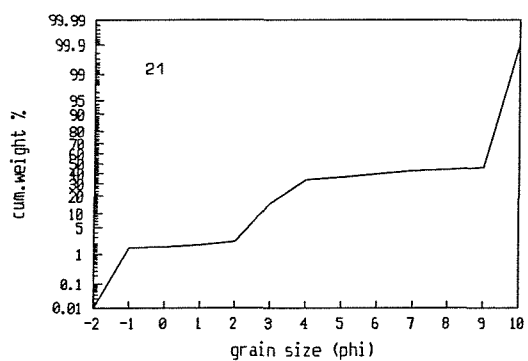
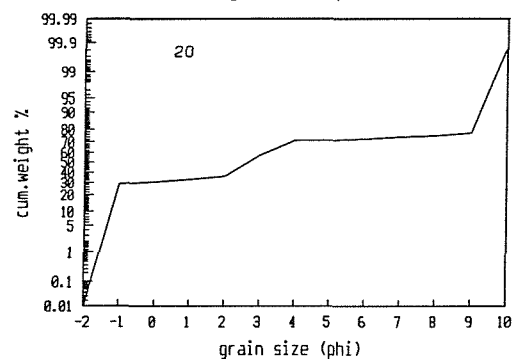
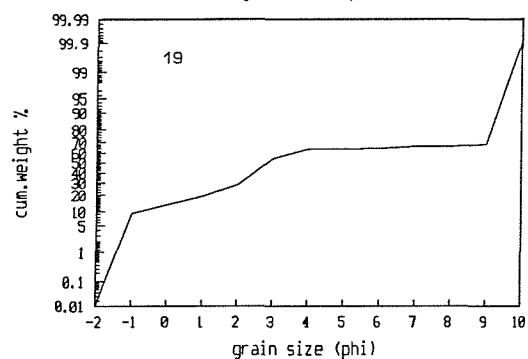
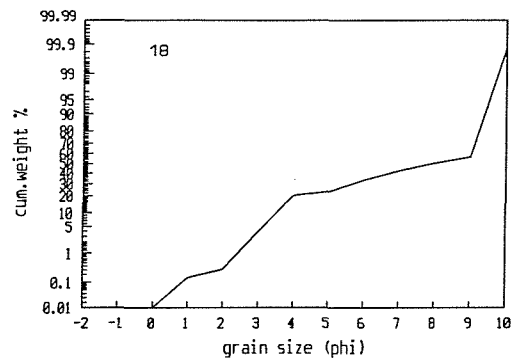
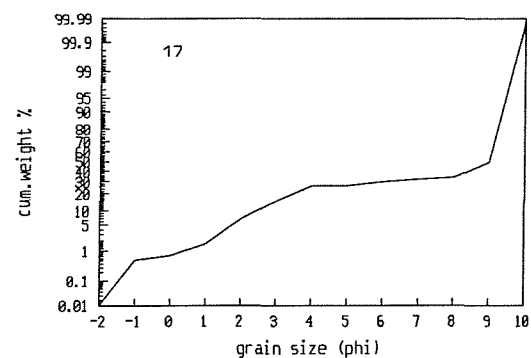


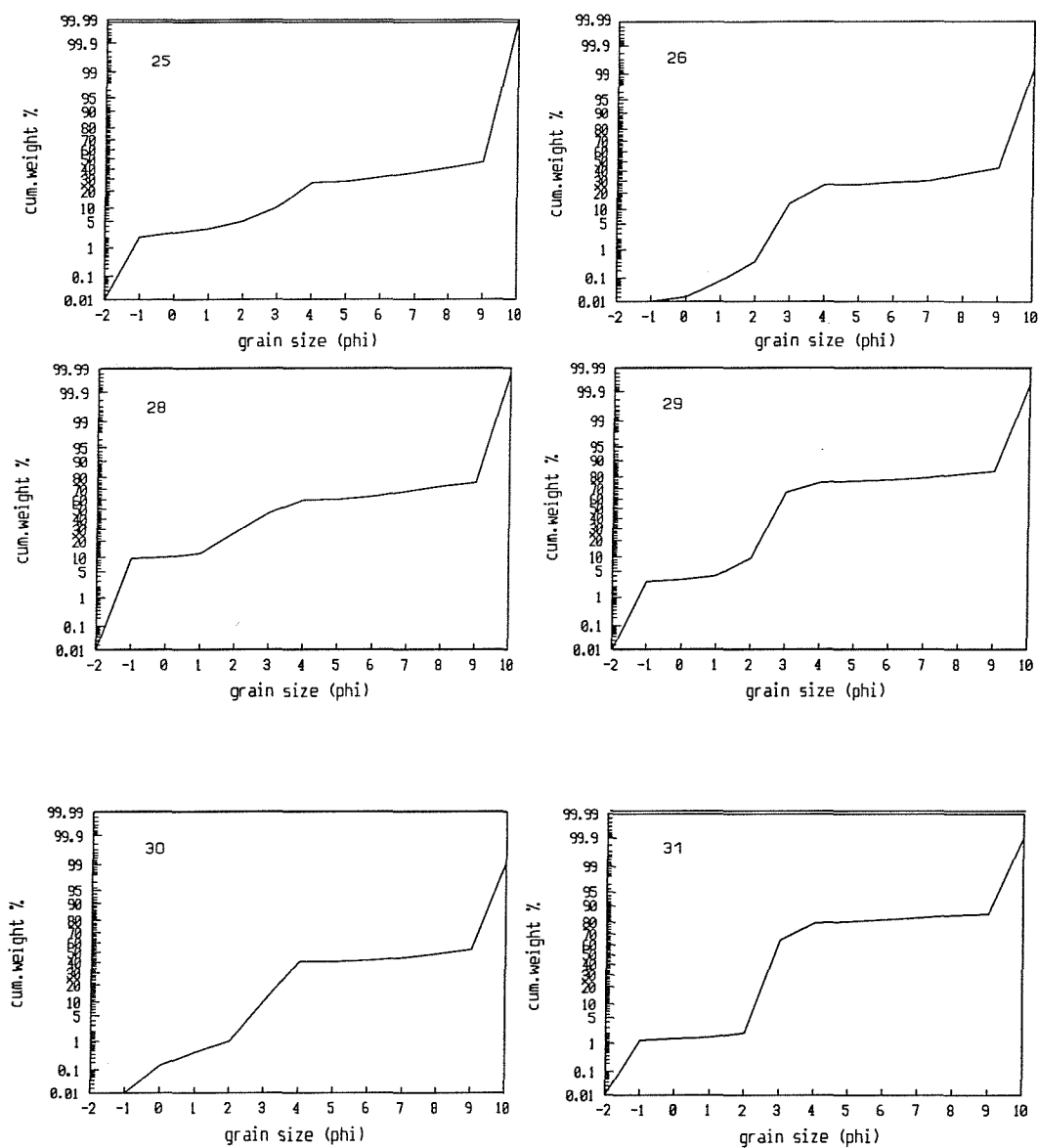












B3. CHEMICAL DATA TABLES

Table B3 : Total and 'sum' metal concentrations for all the samples (for sample locations, see Figure 4.1).

Sample No	Al (ppm)		Co (ppm)		Cu (ppm)		Cr (ppm)		Fe (ppm)		Pb (ppm)		Mn (ppm)		Ni (ppm)		Zn (ppm)	
	total	sum	total	sum	total	sum	total	sum	total	sum	total	sum	total	sum	total	sum	total	sum
H1	53,000	76,000	20	29	86	120	70	78	41,000	48,000	250	330	160	200	48	68	250	330
H2	75,000	99,000	26	35	34	45	57	71	54,000	66,000	77	88	270	240	53	66	130	160
H3	91,000	110,000	34	40	40	52	140	160	69,000	77,000	75	96	540	470	94	110	220	240
H4	83,000	110,000	31	37	58	66	64	79	57,000	62,000	84	93	300	230	60	77	160	190
H5	55,000	100,000	19	36	18	39	57	81	39,000	66,000	41	67	230	250	43	72	95	150
H6	74,000	110,000	23	36	29	49	64	84	41,000	57,000	60	80	240	210	50	70	120	170
H7	77,000	88,000	26	36	31	47	63	73	53,000	61,000	77	74	250	210	54	65	130	150
H8	48,000	58,000	14	19	100	88	49	62	25,000	32,000	140	190	220	220	40	50	180	210
H9	33,000	45,000	10	18	29	50	38	40	22,000	25,000	37	63	160	180	29	41	77	120
H10	64,000	94,000	23	30	26	41	64	75	49,000	47,000	56	74	270	200	48	62	120	160
H11	49,000	45,000	9	11	21	24	41	36	28,000	32,000	62	74	140	120	17	24	150	110
H13	29,000	83,000	7	22	8	19	23	72	23,000	52,000	50	74	140	200	13	44	59	150
H15	42,000	45,000	17	20	74	96	62	49	32,000	31,000	69	58	160	140	30	34	170	160
H16	43,000	76,000	15	27	27	56	51	82	31,000	42,000	60	120	150	150	35	62	93	90
H17	47,000	58,000	14	17	20	26	38	47	38,000	42,000	58	83	160	140	27	33	100	120
H18	54,000	55,000	17	14	25	31	61	56	43,000	50,000	32	76	180	160	32	30	130	120
H20	40,000	58,000	12	14	13	22	36	49	33,000	42,000	19	83	130	150	25	31	91	110
H21	49,000	41,000	11	12	19	24	30	41	30,000	32,000	63	54	120	120	21	23	93	91
H22	81,000	80,000	37	36	61	81	82	81	68,000	54,000	150	190	130	130	76	76	230	260
H23	42,000	41,000	21	22	20	25	52	53	44,000	42,000	45	46	180	130	27	28	77	72

R1	20,000	13,000	7	4	33	54	19	9	14,000	5,300	51	67	49	25	9	6	77	57
R2	47,000	35,000	20	15	20	27	50	32	38,000	32,000	300	310	170	120	33	23	95	87
R3	47,000	26,000	19	3	76	47	36	22	38,000	24,000	62	50	150	93	31	20	160	96
R4	41,000	45,000	19	19	150	230	40	49	86,000	97,000	330	530	250	260	41	56	370	550
R5	53,000	61,000	24	18	22	29	50	43	41,000	38,000	55	61	150	160	39	44	120	150
R6	72,000	80,000	27	35	13	22	60	75	52,000	51,000	43	56	200	190	40	54	99	140
R7	65,000	84,000	25	28	5	15	57	68	53,000	46,000	26	40	290	320	46	64	76	140
R9	76,000	85,000	32	39	17	26	63	75	56,000	53,000	42	53	220	200	56	71	110	170
R10	63,000	89,000	23	24	3	18	50	62	39,000	41,000	30	35	240	180	46	69	74	140
R11	62,000	83,000	21	32	15	43	86	100	38,000	46,000	52	67	140	210	49	85	120	170
R12	43,000	67,000	18	25	16	30	36	59	34,000	39,000	49	65	170	170	30	38	96	140
R13	32,000	51,000	18	20	48	57	45	52	35,000	34,000	74	130	180	190	36	31	190	260
R14	71,000	78,000	23	21	64	73	95	90	64,000	68,000	44	85	280	260	48	46	190	140
R17	91,000	110,000		44	17	20	110	150	40,000	46,000	34	29	500	500	30	99	100	120
R21	34,000	11,000	26	8	130	72	55	79	39,000	12,000	220	75	390	130	51	15	330	100
R23		50,000	12	16	95	76	43	31	36,000	35,000	180	200	220	220	29	35	280	240
R24	22,000	33,000	25	18	94	130	39	48	18,000	9,800	97	160	180	51	46	39	180	200
R25	78,000	86,000	24	21	66	75	77	94	60,000	65,000	120	87	350	340	45	52	200	220
R26	30,000	41,000	16	25	26	50	61	74	31,000	40,000	54	70	140	150	23	34	100	140
R27	43,000	44,000	21	17	47	49	60	40	38,000	31,000	72	76	160	120	28	25	190	170
R28	68,000	76,000	42	39	75	76	81	75	71,000	68,000	120	130	380	400	64	61	240	250
R29	72,000	83,000	22	24	61	73	90	90	62,000	62,000	62	100	300	230	41	49	190	250
R30	27,000	36,000	13	19	10	21	49	53	21,000	24,000	53	52	150	100	28	41	110	120
R31	52,000	76,000	19	28	6	27	51	53	38,000	36,000	23	34	320	280	45	60	64	140

R32	40,000	50,000	13	23	36	16	37	41	29,000	42,000	29	40	280	320	33	47	68	94
R33	41,000	68,000	14	25	58	38	44	56	27,000	40,000	52	86	250	370	37	58	95	160
R34	63,000	71,000	21	27	56	60	77	64	50,000	54,000	99	100	290	260	52	58	180	180
R35	63,000	70,000	18	37	21	33	43	75	48,000	80,000	58	53	280	250	39	54	120	110
1	48,000	56,000	21	29	10	13	44	65	46,000	53,000	31	36	190	190	31	39	64	73
2	60,000	60,000	28	22	7	11	57	50	37,000	36,000	35	43	180	170	41	35	78	86
3	63,000	72,000	31	36	10	12	49	65	53,000	66,000	41	45	370	360	50	54	91	120
4	67,000	83,000	30	31	48	71	96	120	42,000	50,000	80	79	420	300	70	92	150	190
5	95,000	89,000	24	22	62	61	78	78	63,000	61,000	97	95	430	320	53	51	200	180
6	77,000	83,000	32	36	46	51	110	110	56,000	60,000	68	68	480	440	70	85	170	180
7	69,000	82,000	21	21	61	66	69	66	53,000	55,000	46	47	360	340	45	47	160	180
8	50,000	76,000	22	33	40	74	71	108	51,000	58,000	76	82	370	300	58	83	190	210
9	62,000	82,000	18	19	26	34	53	61	51,000	55,000	60	78	300	270	37	43	130	140
10	44,000	55,000	17	24	18	33	74	66	23,000	41,000	51	57	240	250	39	52	100	130
12	51,000	74,000	23	35	30	38	74	100	35,000	51,000	51	55	260	250	52	74	100	170
13	42,000	54,000	12	30	15	21	39	56	35,000	52,000	72	53	230	190	24	40	90	86
14	35,000	34,000	12	13	7	11	22	31	34,000	40,000	36	53	180	120	17	21	76	69
15	48,000	51,000	22	26	17	26	54	44	47,000	47,000	64	60	260	200	31	34	96	86
16	44,000	49,000	18	29	16	26	60	66	36,000	38,000	51	36	250	230	39	54	100	110
17	40,000	73,000	16	40	18	27	57	110	43,000	62,000	43	57	260	260	36	77	94	180
18	62,000	63,000	17	32	22	28	52	65	44,000	59,000	87	62	250	240	34	44	130	110
19	32,000	38,000	20	39	15	20	53	59	43,000	110,000		59	220	230	30	40	120	230
20	31,000	29,000	9	11	15	13	25	23	29,000	34,000	69	63	180	180	18	17	83	79
21	49,000	71,000	21	30	21	30	75	100	19,000	47,000	52	41	220	190	49	69	92	150

22	38,000	53,000	18	29	13	20	45	50	42,000	52,000	43	49	220	200	26	39	65	83
23	48,000	52,000	22	16	16	19	54	43	51,000	45,000	50	66	250	240	33	32	87	130
25	61,000	67,000	29	37	21	27	59	70	61,000	71,000	59	72	290	280	43	52	100	130
26	42,000	71,000	13	17	14	22	30	57	34,000	54,000	52	71	190	200	27	39	93	130
28	52,000	39,000	15	11	16	16	28	34	35,000	37,000	55	70	180	150	30	23	110	89
29	9,000	22,000	8	10	9	10	14	17	29,000	34,000	7	34	110	140	13	15	32	70
30	37,000	53,000	12	16	14	18	35	54	35,000	46,000	64	70	200	200	23	31	82	110
31	16,000	23,000	7	7	6	7	12	16	28,000	27,000	10	56	130	120	10	12	48	43

Table B4 : Metal concentrations in various size fractions.

Sample No	Co (ppm)			Cu (ppm)			Cr (pm)			Pb (ppm)			Ni (ppm)			Zn (ppm)		
	sand	silt	clay	sand	silt	clay	sand	silt	clay	sand	silt	clay	sand	silt	clay	sand	silt	clay
H1	5	22	41	77	85	150	18	75	110	110	230	490	25	52	96	150	250	460
H2	1	25	39	47	37	48	0	69	77	63	77	94	34	54	74	130	120	140
H3	15	31	44	220	31	47	38	110	180	64	80	100	33	75	130	200	180	260
H4	0	26	36	0	54	68	0	69	81	58	83	95	37	56	80	120	160	190
H5	5	16	40	90	18	37	24	51	91	23	39	76	17	36	83	51	81	170
H6	0	17	42	110	19	52	13	50	96	23	45	90	23	39	80	57	93	200
H7	4	19	38	130	24	44	11	50	83	68	54	79	19	44	74	80	110	170
H8	6	17	32	160	57	74	36	55	87	200	150	210	26	45	72	190	180	270
H9	7	14	28	45	21	80	9	47	76	26	47	130	16	34	80	35	100	250
H10	2	20	35	48	24	46	18	50	97	35	52	92	14	44	79	32	110	200
H11	2	17	30	4	32	64	0	63	110	26	86	170	2	34	68	18	170	290
H13	2	16	30	7	15	24	0	50	98	4	52	100	0	28	61	12	91	210
H15	3	24	44	55	94	160	7	75	100	39	90	79	3	42	77	76	190	300
H16	7	21	38	48	38	73	11	55	92	68	83	160	19	46	87	110	160	300
H17	3	22	30	11	34	41	1	70	90	26	85	150	1	45	63	13	170	220
H18	3	14	27	10	19	62	0	40	130	48	28	130	1	28	68	10	110	250
H20	4	15	23	11	20	33	9	50	84	64	69	110	5	33	54	26	120	190
H21	4	18	31	7	31	66	13	57	110	30	69	110	2	35	72	27	140	240
H22	21	25	32	140	45	79	45	44	70	240	110	200	55	57	87	350	190	270
H23	8	21	45	10	22	50	11	69	110	19	45	91	4	30	67	12	80	170

R1	0	35	41	53	64	71	0	71	97	54	120	210	0	54	63	40	210	220
R2	3	22	43	25	19	38	7	49	91	430	70	120	4	35	70	46	110	190
R3	1	26	33	24	69	130	3	55	83	29	78	120	0	43	90	38	180	290
R4	11	23	33	180	150	320	33	65	72	460	320	680	29	45	100	360	350	880
R5	1	30	39	10	26	56	0	72	90	21	65	110	0	49	100	20	140	310
R6	4	20	48	44	13	25	3	56	97	25	42	69	2	29	77	21	77	190
R7	4	27	32	29	13	14	0	56	89	15	42	42	11	50	83	12	110	190
R9	4	27	34	32	19	26	6	51	120	15	44	63	14	50	88	23	130	210
R10	5	25	26	60	13	14	6	67	89	4	36	39	12	51	78	19	120	160
R11	9	27	42	80	24	33	25	100	130	16	61	87	7	69	120	63	140	210
R12	5	29	36	30	23	30	7	59	91	30	59	87	2	49	59	35	130	200
R13	9	20	22	86	43	56	16	53	64	45	87	180	11	43	30	100	210	340
R14	6	27	26	16	96	92	16	120	120	28	120	99	8	65	56	25	91	230
R17	10	40	47	26	21	19	15	100	160	5	24	31	7	66	110	25	110	130
R19	6	16	20	82	85	290	10	42	72	64	160	470	9	34	51	72	240	750
R21	9	30		180	130		16	56		96	220		14	49		130	330	
R22	10	19	23	190	180	180	12	78	120	400	280	250	24	52	63	300	320	320
R23	10	17	24	55	99	94	2	66	70	210	200	200	19	40	52	220	250	250
R24	9	31	39	150	130	84	13	110	120	140	210	200	21	92	69	150	340	270
R25	7	16	23	170	50	81	12	57	110	130	100	78	12	34	59	310	180	230
R26	4	44	69	19	62	130	33	100	170	22	100	180	0	56	110	26	200	390
R27	1	35	47	11	74	130	3	92	95	24	110	190	0	49	72	30	250	480
R28	1	31	50	11	52	100	0	59	98	34	94	160	0	47	82	21	200	330
R29	10	22	27	36	64	83	1	74	110	99	97	100	16	48	57	290	210	250

R30	9	27	40	6	33	51	15	93	130	33	65	95	11	62	100	49	210	250
R31	8	22	37	78	13	11	7	37	73	13	34	42	16	47	79	34	98	190
R32	2	8	47	4	4	32	6	25	45	15	18	72	14	23	88	25	42	180
R33	8	18	38	25	30	50	13	50	93	68	54	110	24	42	90	39	120	260
R34	11	26	43	26	63	85	19	63	110	66	110	130	28	58	86	77	200	250
R35	7	32	51	47	22	34	6	69	100	18	56	62	6	46	75	13	98	140
1	5	24	47	8	14	16	0	49	110	16	41	45	4	33	65	3	66	120
2	3	19	43	6	13	15	0	39	100	17	45	66	0	27	72	6	61	180
3	1	31	50	9	10	14	0	64	87	19	43	54	0	51	74	16	99	170
4	8	32	35	34	69	78	17	110	140	25	87	86	6	95	110	46	210	210
5	5	20	23	34	51	66	0	66	85	550	83	93	0	42	55	0	160	190
6	0	33	39	2	44	57	16	100	130	22	70	69	0	75	94	24	170	200
7	4	20	22	75	65	66	0	57	80	110	46	40	6	42	54	170	180	180
8	13	24	41	54	46	85	23	81	140	46	61	97	21	55	110	160	140	240
9	4	11	24	57	16	38	8	41	75	50	52	92	5	24	54	28	98	180
10	9	16	47	10	16	74	10	63	120	22	46	100	2	34	120	37	91	250
11	4	16	25	7	25	46	7	68	100	27	66	99	3	32	57	17	130	220
12	6	36	51	17	36	50	15	98	160	11	53	79	2	110	110	44	170	230
13	9	29	50	9	25	32	9	77	95	25	63	77	7	43	70	15	110	150
14	6	21	26	8	12	19	0	51	95	54	38	63	4	31	56	31	63	170
15	7	28	48	26	24	27	4	53	90	26	93	88	5	45	67	19	130	150
16	6	30	56	19	21	35	11	81	130	8	38	71	0	62	120	18	110	210
17	8	31	54	21	27	34	8	88	160	16	50	74	0	66	110	39	140	250
18	7	26	46	26	24	33	4	58	98	22	58	82	6	37	67	22	99	150

19	32	42	53	10	33	40	13	100	140	41	74	92	12	85	89	180	170	330
20	6	13	26	6	18	34	0	38	89	53	57	97	3	27	57	36	110	200
21	3	36	45	26	27	33	13	99	150	11	54	58	2	71	110	28	200	210
22	11	30	48	13	23	26	2	74	93	22	66	73	7	46	70	31	110	130
23	9	13	26	10	16	30	6	46	84	43	77	91	9	27	60	72	100	210
25	14	28	50	14	20	35	10	69	99	30	62	94	13	40	74	56	99	180
26	2	10	25	2	15	32	0	34	88	22	59	96	2	22	58	14	75	200
28	4	16	25	8	19	33	1	47	100	51	63	120	3	34	61	32	110	200
29	5	10	33	3	14	39	4	38	65	3	59	160	6	18	59	31	83	290
30	4	11	27	7	17	27	4	40	99	30	60	110	3	23	56	27	82	190
31	3	12	30	2	17	30	0	38	92	45	25	140	2	25	58	7	91	220

Table B4 (continued) : Metal concentrations in various size fractions.

Sample No	Mn (ppm)			Al (ppm)			Fe (ppm)		
	sand	silt	clay	sand	silt	clay	sand	silt	clay
H1	170	220	200	9,000	60,000	120,000	17,000	39,000	67,000
H2	28	300	230	34,000	100,000	100,000	10,000	43,000	80,000
H3	130	480	480	31,000	83,000	120,000	38,000	67,000	84,000
H4	0	340	230	0	77,000	120,000	17,000	59,000	63,000
H5	68	270	270	19,000	54,000	120,000	12,000	33,000	76,000
H6	0	330	200	15,000	53,000	120,000	14,000	39,000	63,000
H7	13	280	210	9,000	55,000	100,000	7,000	47,000	70,000
H8	96	280	250	13,000	48,000	100,000	8,000	37,000	44,000
H9	69	260	260	10,000	39,000	97,000	8,000	21,000	50,000
H10	38	220	220	14,000	62,000	120,000	8,000	44,000	57,000
H11	39	280	230	4,000	51,000	130,000	4,000	52,000	84,000
H13	52	300	220	5,000	48,000	120,000	7,000	52,000	64,000
H15	72	250	200	8,000	53,000	98,000	3,000	50,000	67,000
H16	54	230	180	16,000	56,000	110,000	8,000	38,000	57,000
H17	38	250	210	9,000	70,000	110,000	11,000	58,000	71,000
H18	41	250	270	9,000	45,000	120,000	11,000	40,000	100,000
H20	74	220	170	8,000	49,000	110,000	14,000	52,000	61,000
H21	52	250	230	10,000	58,000	120,000	13,000	51,000	73,000
H22	97	130	140	35,000	57,000	97,000	55,000	42,000	57,000
H23	73	250	180	10,000	42,000	92,000	14,000	47,000	84,000

R1	10	190	150	3,000	93,000	110,000	0	56,000	56,000
R2	62	250	220	6,000	52,000	100,000	17,000	39,000	67,000
R3	40	250	250	2,000	50,000	110,000	6,000	58,000	83,000
R4	290	300	260	6,000	50,000	110,000	99,000	72,000	99,000
R5	20	200	230	300	71,000	140,000	2,000	55,000	79,000
R6	60	240	180	11,000	43,000	110,000	9,000	52,000	56,000
R7	28	450	260	3,000	63,000	110,000	0	53,000	47,000
R9	23	260	220	6,000	65,000	100,000	1,000	53,000	64,000
R10	23	290	180	10,000	70,000	100,000	3,000	50,000	44,000
R11	0	380	260	15,000	67,000	110,000	8,000	32,000	64,000
R12	71	270	210	8,000	60,000	100,000	15,000	50,000	52,000
R13	81	230	200	11,000	45,000	66,000	16,000	37,000	38,000
R14	62	410	290	15,000	82,000	110,000	25,000	84,000	84,000
R17	68	440	540	12,000	81,000	120,000	4,000	43,000	49,000
R19	61	150	230	10,000	24,000	44,000	3,000	21,000	36,000
R21	130	400		11,000	36,000		10,000	40,000	
R22	130	330	270	6,000	57,000	100,000	12,000	67,000	64,000
R23	160	320	250	4,000	54,000	110,000	10,000	52,000	58,000
R24	0	460	0	5,000	76,000	96,000	5,000	36,000	10,000
R25	210	350	330	56,000	52,000	99,000	23,000	49,000	71,000
R26	71	280	230	8,000	62,000	120,000	4,000	65,000	120,000
R27	41	240	230	11,000	65,000	120,000	2,000	56,000	88,000
R28	77	440	430	7,000	61,000	99,000	0	58,000	87,000
R29	180	280	240	6,000	73,000	100,000	23,000	63,000	70,000

R30	0	400	270	7,000	61,000	94,000	3,000	60,000	64,000
R31	110	430	310	7,000	55,000	110,000	12,000	43,000	44,000
R32	240	270	430	2,000	25,000	110,000	21,000	22,000	68,000
R33	330	430	370	3,000	54,000	120,000	7,000	38,000	68,000
R34	120	330	270	6,000	77,000	120,000	22,000	58,000	76,000
R35	140	320	260	3,000	62,000	96,000	10,000	65,000	110,000
1	53	300	200	1,000	47,000	94,000	4,000	71,000	69,000
2	31	250	240	2,000	38,000	130,000	1,000	54,000	56,000
3	43	440	410	3,000	66,000	98,000	0	64,000	89,000
4	0	450	310	12,000	78,000	97,000	11,000	51,000	57,000
5	280	380	290	0	67,000	100,000	0	52,000	66,000
6	0	540	410	6,000	70,000	94,000	0	52,000	67,000
7	170	420	290	5,000	73,000	98,000	2,000	57,000	58,000
8	150	380	330	11,000	54,000	98,000	42,000	42,000	66,000
9	44	320	280	15,000	34,000	110,000	10,000	38,000	67,000
10	0	390	270	13,000	40,000	110,000	4,000	36,000	76,000
11	51	340	280	9,000		98,000	17,000	49,000	76,000
12	83	380	310	6,000	71,000	110,000	10,000	66,000	70,000
13	76	360	260	9,000	59,000	96,000	16,000	58,000	85,000
14	16	310	260	8,000	42,000	96,000	16,000	65,000	80,000
15	88	390	290	7,000	63,000	100,000	14,000	70,000	79,000
16	94	330	380	6,000	60,000	100,000	7,000	42,000	75,000
17	83	360	350	3,000	65,000	100,000	3,000	43,000	87,000
18	64	340	250	9,000	55,000	93,000	17,000	55,000	80,000

19	210	320	270	5,000	80,000	96,000	123,000	84,000	74,000
20	1100	320	270	5,000	47,000	96,000	21,000	38,000	72,000
21	40	320	260	10,000	69,000	110,000	14,000	55,000	66,000
22	92	370	270	8,000	67,000	95,000	20,000	69,000	80,000
23	160	340	310	12,000	44,000	99,000	27,000	38,000	68,000
25	120	450	300	9,000	52,000	98,000	31,000	65,000	91,000
26	48	260	250	3,000	43,000	110,000	11,000	33,000	78,000
28	55	330	280	7,000	51,000	100,000	15,000	44,000	80,000
29	76	300	360	3,000	30,000	110,000	18,000	31,000	110,000
30	79	390	250	10,000	34,000	94,000	17,000	38,000	72,000
31	57	360	280	7,000	43,000	100,000	13,000	47,000	94,000

Table B5 : Metal concentrations in various geochemical phases.

Core X1	Al ppm	Co ppm	Cr ppm	Cu ppm	Fe ppm	Mn ppm	Ni ppm	Pb ppm	Zn ppm
cm	Reducible Phase								
0-1	14,000	10	34	70	35,000	254	30	51	115
1-2	13,000	10	29	62	34,000	234	26	52	115
2-3	14,000	10	26	58	35,000	233	24	49	114
3-4	14,000	12	35	65	39,000	264	29	57	127
4-5	13,000	9	30	60	29,000	196	26	48	110
5-6	14,000	12	35	64	36,000	258	28	59	123
6-7	14,000	12	42	82	40,000	251	30	62	144
7-8	13,000	10	32	69	36,000	262	26	53	121
8-9	15,000	10	37	54	31,000	234	26	50	107
9-10	16,000	11	32	68	33,000	262	30	54	122
10-11	16,000	10	39	97	30,000	243	26	53	124
11-12	17,000	10	37	100	33,000	262	8	55	134
12-13	7,000	4	16	48	13,000	107	15	24	82
13-14	17,000	11	42	66	35,000	259	31	55	122
14-15	16,000	11	43	65	33,000	264	27	54	117
Organic Phase									
0-1	2,000			7	3,000	5	6	2	4
1-2	2,000		1	9	5,000	17	5	2	7
2-3	3,000		2	8	6,000	16	5	2	13
3-4	2,000		1	9	7,000	21	7	3	8
4-5	772			5	4,000	6	7	1	8
5-6	834			5	3,000	0	4		4
6-7	282			6	4,000	21	4		3
7-8	950			7	4,000	6	5	1	5
8-9	335			3	2,000	0	3		2
9-10	469			4	3,000	5	4		2
10-11	103			6	4,000	12	5		2

APPENDICES

11-12	0			5	2,000	9	5		1
12-13	0			2	305	0	2	1	0
13-14	397			4	2,000	18	5		4
14-15	1,000			6	3,000	12	4	2	3

Residual Phase

0-1	44,000	8	25	2	6,000	18	16	8	18
1-2	45,000	10	26	3	5,000	47	17	9	14
2-3	43,000	11	26	4	5,000	18	16	0	15
3-4	48,000	13	32	4	5,000	33	21	10	23
4-5	36,000	7	17	2	5,000	16	14	5	15
5-6	45,000	9	20	2	6,000	18	16	8	14
6-7	49,000	10	29	5	7,000	11	20	10	20
7-8	49,000	8	23	2	6,000	9	18	6	17
8-9	44,000	7	16	3	5,000	26	17	8	13
9-10	46,000	10	23	4	5,000	21	16	8	13
10-11	43,000	9	24	4	7,000	9	17	8	12
11-12	42,000	8	17	3	6,000	10	14	10	12
12-13	36,000	5	12	2	6,000	0	14	3	12
13-14	43,000	8	20	2	6,000	16	16	9	13
14-15	46,000	11	21	2	5,000	14	18	8	13

Core X5	Al ppm	Co ppm	Cr ppm	Cu ppm	Fe ppm	Mn ppm	Ni ppm	Pb ppm	Zn ppm
cm	Reducible Phase								
0-1	5,000	15	17	5	43,000	160	16	21	72
1-2	5,000	13	19	6	39,000	160	14	21	66
2-3	7,000	15	24	7	40,000	160	15	22	80
3-4	9,000	17	35	8	52,000	210	19	28	78
4-5	11,000	16	38	10	34,000	230	23	31	88
5-6	0	11	0	2	10,000	180	15	36	51
6-7	0	11	0	1	13,000	130	13	18	34
7-8	7,000	12	17	3	25,000	110	15	16	41
8-9	0	12	0	1	3,000	180	20	25	26
9-10	4,000	6	11	2	12,000	60	10	9	67
Organic Phase									
0-1	0	0	0	0	300	0	3	3	0
1-2	0	0	0	1	930	1	1	2	1
2-3	57	1	0	0	240	0	2	2	0
3-4	0	1	0	0	3,000	2	4	4	1
4-5	630	2	0	0	580	0	4	5	1
5-6	890	3	0	5	4,000	16	5	6	10
6-7	820	2	0	1	3,000	10	4	3	8
7-8	0	1	0	0	210	0	2	3	0
8-9	530	2	0	1	2,000	9	5	6	7
9-10	730	2	0	2	2,000	11	4	3	10
Residual Phase									
0-1	9,000	2	5	1	2,000	7	3	3	5
1-2	13,000	3	7	1	2,000	7	5	3	4
2-3	15,000	3	12	2	2,000	10	4	3	5
3-4	21,000	4	8	0	4,000	3	5	4	4
4-5	21,000	5	7	1	3,000	10	6	4	5
5-6	32,000	10	39	6	20,000	42	16	10	24
6-7	23,000	7	22	3	16,000	36	11	7	19
7-8	15,000	3	6	1	2,000	10	5	1	4
8-9	22,000	5	15	2	19,000	39	11	7	19
9-10	25,000	7	24	3	16,000	44	11	7	23